

Max-Planck-Institut für Kolloid- und Grenzflächenforschung
Abteilung für Kolloidchemie

Novel Poly(*N*-substituted glycine)s:
Synthesis, post-modification, and physical
properties

Dissertation

zur Erlangung des akademischen Grades

„doctor rerum naturalium“

(Dr. rer. nat.)

in der Wissenschaftsdisziplin „Polymer- und Kolloidchemie“

eingereicht an der

Mathematisch-Naturwissenschaftlichen Fakultät

der Universität Potsdam

von

Joshua W. Robinson

Potsdam, Januar 2013

This work is licensed under a Creative Commons License:
Attribution - Share Alike 3.0 Germany
To view a copy of this license visit
<http://creativecommons.org/licenses/by-sa/3.0/de/>

Published online at the
Institutional Repository of the University of Potsdam:
URL <http://opus.kobv.de/ubp/volltexte/2013/6478/>
URN [urn:nbn:de:kobv:517-opus-64789](http://nbn-resolving.org/urn:nbn:de:kobv:517-opus-64789)
<http://nbn-resolving.org/urn:nbn:de:kobv:517-opus-64789>

Statement of Independent Work

The following dissertation work was conducted between October 2010 to October 2012 at the Max Planck Institute of Colloids and Interfaces in the Colloid Chemistry department under the supervision of Dr. Helmut Schlaad. The presented work was completed independently and is of reasonable scientific value.

Joshua W. Robinson
Potsdam-Golm

Referees:

PD. Dr. Helmut Schlaad (MPIKG)

Prof. Dr. Andreas Taubert (University of Potsdam)

Prof. Dr. Michael Meier (Karlsruhe Institute of Technology)

Defense:

18th of March, 2013

Awarded:

magna cum laude

ABSTRACT

NOVEL POLY (*N*-SUBSTITUTED GLYCINE)S: SYNTHESIS, POST-MODIFICATION, AND PHYSICAL PROPERTIES

Joshua W. Robinson

Max Planck Institute of Colloids and Interfaces
Department of Colloid Chemistry

Various synthetic approaches were explored towards the preparation of poly(*N*-substituted glycine) homo/co-polymers (a.k.a. polypeptoids). In particular, monomers that would facilitate in the preparation of bio-relevant polymers via either chain- or step-growth polymerization were targeted. A 3-step synthetic approach towards *N*-substituted glycine *N*-carboxyanhydrides (NNCA) was implemented, or developed, and optimized allowing for an efficient gram scale preparation of the aforementioned monomer (chain-growth). After exploring several solvents and various conditions, a reproducible and efficient ring-opening polymerization (ROP) of NNCA was developed in benzonitrile (PhCN). However, achieving molecular weights greater than 7 kDa required longer reaction times (>4 weeks) and sub-sequentially allowed for undesirable competing side reactions to occur (*eg.* zwitterion monomer mechanisms). A bulk-polymerization strategy provided molecular weights up to 11 kDa within 24 hours but suffered from low monomer conversions (ca. 25%). Likewise, a preliminary study towards alcohol promoted ROP of NNCA suffered from impurities and a suspected alternative activated monomer mechanism (AAMM) providing poor inclusion of the initiator and leading to multi-modal dispersed polymeric systems. The post-modification of poly(*N*-allyl glycine) via thiol-ene photo-addition was observed to be quantitative, with the utilization of photo-initiators, and facilitated in the first glyco-peptoid prepared under environmentally benign conditions. Furthermore, poly(*N*-allyl glycine) demonstrated thermo-responsive behavior and could be prepared as a semi-crystalline bio-relevant polymer from solution (*ie.* annealing).

Initial efforts in preparing these polymers via standard poly-condensation protocols were insufficient (step-growth). However, a thermally induced side-product, diallyl diketopiperazine (DKP), afforded the opportunity to explore photo-induced thiol-ene and acyclic diene metathesis (ADMET) polymerizations. Thiol-ene polymerization readily led to low molecular weight polymers (<2.5 kDa), that were insoluble in most solvents except heated amide solvents (*ie.* DMF), whereas ADMET polymerization, with diallyl DKP, was unsuccessful due to a suspected 6 member complexation/deactivation state of the catalyst. This understanding prompted the preparation of elongated DKPs most notably dibutenyl DKP. SEC data supports the aforementioned understanding but requires further optimization studies in both the preparation of the DKP monomers and following ADMET polymerization.

This work was supported by NMR, GC-MS, FT-IR, SEC-IR, and MALDI-ToF MS characterization. Polymer properties were measured by UV-Vis, TGA, and DSC.

Keywords: peptoid, α -amino acid *N*-carboxyanhydride, thermo-responsive, bio-relevant polymers, polyglycine

ACKNOWLEDGEMENTS

I first and foremost would like to thank all the teachers/instructors/professors that have guided my education towards the cumulative knowledge and skill-set that I currently possess. Their patience, professionalism, and diligence are just as much an accreditation to this degree as the many efforts and hours I put forth. In particular, I would like to recognize the wonderful mentors throughout my research experience: Dr. Michael Ketterer provided me with my first opportunity in a research laboratory as a bachelor student at NAU; Dr. Steven L. Castle raised the bar and provided me with a professional level understanding of research as I worked towards my Master of Science at BYU; and Dr. Helmut Schlaad for his guidance towards my first scientific publications and dissertation work at the MPIKG. In addition, I would like to recognize a few of the many junior scientists who have contributed to my research efforts, over the years, including Dr. Ma Bing, Dr. Banerjee, Dr. Hiro Urakami, and Dr. Junpeng Zhao. I would also like to express my appreciation to the many junior scientists/students that I have shared ideas and laboratory space with. More recently, this would include Ms. Clara Valverde Serrano, Ms. Ina Dambowsky, Mr. Kai Krannig, and Mr. Christian Secker. I especially would like to thank the support I received from the technicians including Mrs. Marlies Gräwert (SEC), Mr. Olaf Niemeyer (NMR), Mrs. Sylvia Pirok (EA), Mrs. Irina Shekova (TGA), Ms. Nora Fiedler (supplies), and Mrs. Ines Below-Lutz (supplies). I especially would like to thank Ms. Jessica Brandt for all the wonderful support she provided over these last 3 years. She truly is the heart of the laboratory. In addition I would like to recognize Dr. Steffen Weidner for his kind contribution towards MALDI-ToF MS measurements. Finally, I would like to thank the Max Planck Society for their research support and all the amazing scientists that I have had the opportunity to meet throughout their Ph.D. program.

I would like to apologize to my family for all the years of neglect, and time lost, while I explored intellectual curiosities and my place in this world. In the following years I hope to rectify this and demonstrate that the sacrifices over these many years were not in vain. Thank you for your patience and love.

Table of Contents

Title Page	i
Statement of Independent Work	ii
ABSTRACT	iii
ACKNOWLEDGEMENTS	iv
List of Abbreviations	viii
1. Introduction	1
1.2 How to define these systems	2
1.3 Polymeric systems with amides in the side-chain.....	3
<i>1.3.1 Polynorbornenes and related structures</i>	4
<i>1.3.2 Polyacrylamides</i>	4
<i>1.3.3 Poly(2-oxazoline)s</i>	5
1.4 Polymeric systems with amides in the backbone	6
<i>1.4.1 Polypeptides and related structures</i>	6
<i>1.4.2 Polypeptoids</i>	7
<i>1.4.3 Glycopeptides</i>	8
<i>1.4.4 Significant material properties</i>	9
1.5 Objectives of dissertation	10
2. Theory and Methodology	11
2.1 ROP with NCAs	11
<i>2.1.1 ROP of NNCA</i> s.....	14
2.2 Thiol-ene/yne addition.....	15
2.3 Thermo-responsive behavior	16
2.4 Analytical Methods	18
<i>2.4.1 Thermo-analysis</i>	18
<i>2.4.2 NMR</i>	19
<i>2.4.3 SEC</i>	20
<i>2.4.4 MALDI-ToF MS</i>	22
3. Results and Discussion.....	24
3.1 Polypeptoid via Chain-Growth Polymerizations.....	24
<i>3.1.1 NNCA Preparation</i>	24
<i>3.1.1.1 Summary of NNCA Preparation</i>	30

3.1.2 Benzylamine Initiated ROP.....	30
3.1.3 Anionic/Promoted ROP Investigations.....	41
3.1.4 Summary of Nucleophilic ROP of NNCAs.....	50
3.1.5 Post-Modification of Functional Polypeptoids.....	51
3.1.6 Thermal and Solution Properties.....	56
3.1.7 Thermo-Responsive Behavior.....	60
3.2 Polypeptoids via Step-Growth Polymerizations.....	61
3.2.1 Diketopiperazine (DKP).....	62
3.2.2 ADMet attempts with <i>N,N'</i> -dibutenyl DKP.....	66
4. Summary of Results.....	68
5. Outlook and Perspective.....	70
5.1 Outlook.....	70
5.2 Perspective.....	71
6. Experimental Procedures.....	74
6.1 Materials.....	74
6.2 Analytical Instrumentation and Methods.....	74
6.2.1 Gas chromatography mass spectrometry (GC-MS).....	74
6.2.2 Melting point apparatus.....	74
6.2.3 Nuclear magnetic resonance (NMR) spectroscopy.....	75
6.2.4 Fourier transform infrared (FT-IR) spectroscopy.....	75
6.2.5 Size exclusion chromatography (SEC).....	75
6.2.6 Matrix-assisted laser desorption/ionization time-of-flight mass spectrometry (MALDI-ToF MS)....	75
6.2.7 Thermal analysis (DSC and TGA).....	76
6.2.8 Turbidimetry.....	76
6.3 Synthetic Procedures.....	76
6.3.1 Monomer Synthesis.....	76
6.3.2 Pathway B.....	76
6.3.3 Cyclic Diene Monomer.....	79
6.3.4 Preparation of poly(<i>N</i> -allyl/propargyl glycine) (PNAG _n).....	81
6.3.5 Modification of PNAG via thiol-ene photo-addition.....	83
6.3.6 Promoted ROP.....	85
6.3.7 Preparation of polydiketopiperazine.....	86

7. Bibliography and Notes..... 88
Appendix: Supporting Spectra..... 98

List of Abbreviations

AAMM	alternative activated monomer mechanism
ACN	acetonitrile
ADME	absorption distribution metabolism excretion
ADM _{et}	acyclic-diene metathesis
a.k.a	also known as
AIBN	azobisisobutyronitrile
AMM	activated monomer mechanism
BEMP	2- <i>tert</i> -butylimino-2-diethylamino-1,3-dimethylperhydro-1,3,2-diazaphosphorine
Bn	benzyl
BnNH ₂	benzyl amine
Boc	<i>tert</i> -butoxycarbonyl
<i>ca.</i>	<i>circa</i> (approximate)
Cbz	benzyloxycarbonyl
CD	circular dichroism
CROP	cationic ring-opening polymerization
Da	Dalton(s)
DBU	1,8-diazabicyclo[5.4.0]undecene
DIA	diisopropylamine
DMA	<i>N,N</i> -dimethyl acetamide
DMAP	4-(dimethylamino)pyridine
DMF	<i>N,N</i> -dimethyl formamide
DMPA	2,2-dimethoxy-2-phenyl-acetophenone
DNPC	bis(2,4-dinitrophenyl)carbonate
DSC	differential scanning calorimetry
<i>eg.</i>	<i>exempli gratia</i> (for example)
eq.	equivalence(s)
<i>etc.</i>	<i>et cetera</i> (and the rest)
FDA	Federal Drug Administration
g	gram(s)
HEMP	hydroxy-4'-(2-hydroxyethoxy)-2-methylpropiophenone

Hz	hertz
<i>ie.</i>	<i>id est</i> (that is)
LCST	lower critical solution temperature
M	moles/liter
MALDI-ToF	matrix assisted laser desorption/ionization time of flight
mg	milligram(s)
mL	milliliter(s)
L	liter(s)
mol	mole(s)
MS	mass spectrometry
NAM	normal amine mechanism
NCA	<i>N</i> -carboxyanhydride
n.d.	not determined/detected
NEt ₃	triethylamine
nm	nanometer(s)
NMBA	<i>N</i> -methylbenzamide
NMP	1-methyl-2-pyrrolidinone
NNCA	<i>N</i> -substituted glycine <i>N</i> -carboxyanhydride
PEG	poly(ethylene glycol)
PEO-OH	poly(ethylene oxide) alcohol
PEO-NH ₂	poly(ethylene oxide) amine
PhCN	benzyl nitrile
PHPMA	poly(<i>N</i> -(2-hydroxypropyl)methacrylamide)
PNiPAAm	poly(<i>N</i> -isopropyl acrylamide)
PNiPOx	poly(<i>N</i> -isopropyl oxazoline)
ppm	part per million
RAFT	radical addition-fragmentation chain-transfer
RI	refractive index
RIP	redox-initiated polymerization
r.t.	room temperature
SEC	size exclusion chromatography
<i>t</i> -BuP ₄	1- <i>tert</i> -butyl-2,2,4,4,4-pentakis(dimethylamino)-2λ ⁵ ,4λ ⁵ -catenadi(phosphazene)

$t\text{-BuP}_4$	1- <i>tert</i> -butyl-4,4,4-tris(dimethylamino)-2,2-bis[tris(dimethylamino)-phosphoranylidenamino]-2 λ^5 ,4 λ^5 -catenadi(phosphazene)
TFA	trifluoroacetic acid
TGA	thermo-gravimetical analysis
TLC	thin layer chromatography
UCST	upper critical solution temperature
UV	ultra-violet
<i>via</i>	(way, path)
ZMM	zwitterion monomer mechanism
ZSM	zwitterion solvent mechanism
α	alpha
β	beta
Δ	Delta (change)
γ	gamma
μ	micro
ω	omega
π	pi
\AA	angstrom
\bar{n}	average degree of polymerization
T_{cp}	cloud point temperature
J	coupling constant
T_c	crystallinity transition temperature
D	dispersity
H	enthalpy
S	entropy
G	Gibbs' free energy
T_g	glass transition temperature
T_m	melting transition temperature
\bar{M}_n	number average molecular weight
\bar{M}_w	weight average molecular weight

1. Introduction

1.1 Origins of biopolymers and biomaterials

The so called “Big Bang Theory” suggests that the known universe began as a singularity event approximately 13.7 billion years ago. A consequence of this event was the formation of hydrogen which fused to construct helium followed by further fusions leading to many of the other elements. This finite matter, with infinitive density, from a single point of origin expanded and cooled into stars and galaxies. Supernova occurrences facilitated in the further diversification of matter distributed throughout the galaxies. Included in this matter were lighter elements such as oxygen, nitrogen, and carbon which collected on nearby planets. One planet, Earth, accumulated high enough concentrations of these elements, or primitive matter, and approximately 3.9 billion years ago, with the appropriate temperature and atmospheric conditions, this matter led to the development of amino acids and other biomolecules. The first biopolymers were constructed from the combination of these biomolecules and led to the development of colloidal assemblies inside this “Primordial Soup” recipe. The origins of life grew out of this biomolecule cocktail and progressed over the next 3 billion years into the complex and diverse organisms found throughout Earth’s ecosystem.

Organisms from single cell (*eg. bacteria, Archaea, etc.*) to multi-cell (*eg. plants, animals, etc.*) systems behave as bio-factories producing a plethora of biomolecules and biopolymers. The latter can be classified into 3 main categories: polynucleosides, peptides/proteins, and polysaccharides. An organism’s reproduction (diversification), function (behavior), and survival (armament) depend on the production of sequence and architecturally controlled biopolymers. In addition, the three dimensional orientation and stimuli-responsive behavior of these systems facilitate in transportation, communication, and mechanical integrity both internally and externally. Higher order structures typically lead to self-assembled macromolecular structures with additional functions or improved mechanical strength. For example, peptides with secondary structures often assemble into tertiary or quaternary systems allowing for functional behavior such as enzymatic processes (*eg. DNA polymerase, hydrolase, etc.*) or oxygen transport (*eg. hemoglobin, myoglobin, etc.*). Furthermore, supramolecular aggregation of keratin or chitin is responsible for the mechanical strength of fingernails or exoskeletons, respectively. Often, these biomaterials include smaller molecules or inorganic compounds entangled or coordinated within their assemble structures (*ie. composite materials*).

Consumption of biopolymers by heterotrophs has been occurring since their evolution as an organism (600 million years) whereas the utilization of naturally-derived biomaterials is more of a recent (2000 years) phenomenon brought about due to the challenges surgeons faced in tissue repair work.¹ The slow development of modified and synthetic biomaterials may be contributed to the lack of previous knowledge and understanding of these evolved chemical systems. It was not until Friederich Wöhler (1828) demonstrated the preparation of urea in a laboratory setting that the scientific community accepted the premise that biomolecules (organic molecules) could be synthesized outside living systems or until Hermann Staudinger (1922) proposed that polymers were covalently linked smaller molecules (he coined macromolecules) which facilitated in a new subdiscipline of chemistry, polymer science. With these and other milestone discoveries, a plethora of organic molecules and macromolecules were synthesized including the peptides developed by Emil Fischer (1901) once again illustrating the possibility of preparing living matter inside a beaker. However, the advancement of the preparation of polynucleotides and polypeptides was seen much later after the development of sequencing analysis techniques and corresponding synthetic strategies (>1953). In fact, only recently the first polycarbohydrate was successfully sequenced by Robert Linhardt's laboratory (2011) illustrating the infancy of the biopolymer and biomaterial field.²

1.2 How to define these systems

A “biopolymer” is defined as a polymeric material produced by a living system and corresponds to the 3 previously described categories. This limits the use of the terminology to either utilizing isolated materials from living systems or the exact synthetic replication of the biologically prepared polymer. Due to the difficulties associated with preparing uniformly dispersed biopolymers, polymer scientists typically prepare bioinspired, biohybrid, biomimetic, or biorelevant polymeric systems. These polymeric materials allow for a non-intrusive interface with biological systems (*ie.* biocompatible), may have higher order structures resembling tertiary and quaternary structures, or undergo mechanical or conformational changes upon introducing an external stimulus. The term “biomaterial” may include many of these aforementioned properties but also is used in a broader context to include any matter, surface, and construct that interacts with biological systems. Overall, the three main tiers are biocompatibility, function, and mechanical properties.

Exploitation of these properties allow for application development such as extracellular matrices, drug delivery devices and encapsulating agents, sensors, bio-separation devices, and water retardant adhesives. Each of these applications requires specific properties/functions that are

directly influenced by the design of the polymeric system. In general, all of these materials should be biocompatible or biologically inert when employed. For example, poly(ethylene glycol) (PEG), the current “gold standard” approved by the FDA, has frequently been utilized as an encapsulating agent and drug conjugate which in turn may be accredited to its bio-compatibility and solubility in physiological environments that prevents accumulation via excretion. Notably, degradation of PEG has been limited to bacteria and dehydrogenase (oxidative enzymatic process) and therefore is generally considered to be an inert synthetic polymeric material.³ However, due to PEG’s relatively simple architecture (a polyether) other desirable material properties such as stimuli-responsive behavior and crystallinity are difficult to achieve without chemically altering the repeating unit (*i.e.* adding a methyl group) or copolymerization strategies (*e.g.* the utilization of a more complex polymer system either as a PEG-block or as the backbone with PEG as a side chain).⁴ Contrarily, polymers with esters (*eg.* poly(lactic acid), polycaprolactone, *etc.*) or amides (*e.g.* polyacrylamide, poly(2-oxazoline), and peptides) as the main constituent of the side chain or backbone have demonstrated either or both crystalline and stimuli-responsive characteristics. In particular, poly(L-lactic acid) has crystallinity properties whereas poly(*N*-isopropyl acrylamide) (PNiPAAm) undergoes a phase transition, in aqueous environments, when an external stimuli is applied.⁵ Poly(2-*isopropyl*-2-oxazoline) (PiPOx), a constitutional isomer of PNiPAAm where the nitrogen of the amide is within the backbone, has both crystallinity and stimuli-responsive behavior.⁶ Overall, these material properties, related to stereo-control and/or polar functional groups (*i.e.* esters and amides), have readily lead to the design of biomaterials with applications as sutures, extracellular matrices, and biosensors.

1.3 Polymeric systems with amides in the side-chain

As previously eluded to, polyamides, where the amide component is comprised in the side-chain, have demonstrated properties suitable for a number of applications. These polymeric materials have, in many cases, desirable biocompatibility, stimuli-responsive behavior, and mechanical properties that facilitated in their utility in various biomedical applications. The design of these systems includes either a synthetic non-biologically relevant amide or oligomeric peptides as side chains. The exterior location facilitates in a greater interaction with the surrounding medium whereas the synthetic backbone provides mechanical durability. However, the stable backbone prevents biodegradation making these systems “non-ideal” as drug delivery or tissue growth scaffolds.

1.3.1 Polynorbornenes and related structures

Controlled polymerization of strained bicyclic systems (*ie.* norbornenes) via metathesis, with functional tolerant catalysts, has provided a platform for producing biomimetic synthetic polymers. The norbornene monomer can readily be modified in the *exo/endo* positions with a myriad of biologically tolerant or functional chains. This has facilitated in the preparation of polynorbornenes with pendant elastin-like side chains which in turn have been demonstrated to be stimuli-responsive and support cell proliferation.⁷ Furthermore, various other peptide side-chain polynorbornenes have been described in the literature where only a few are illustrated in Figure 1.

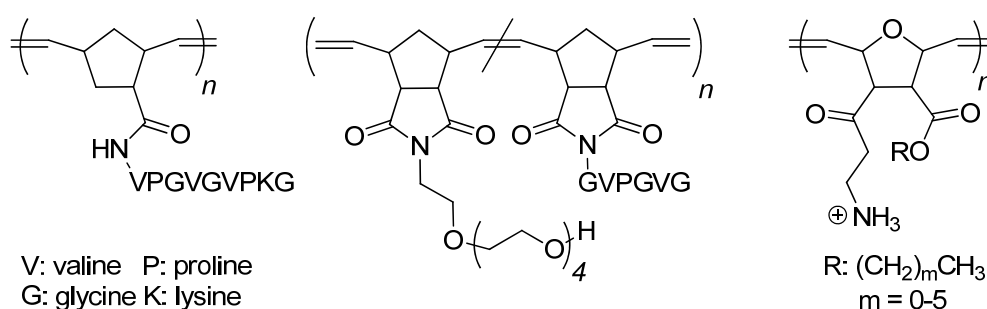


Figure 1. Examples of polynorbornenes with peptide like side chains.

1.3.2 Polyacrylamides

Polyacrylamides were introduced in the late 1950s and currently have become one of the dominating bio-relevant polymers seen in the literature. The simple preparation, biocompatibility, and thermo-responsive properties have been the main contributing factors to this advancement. The introduction of reversible addition-fragmentation chain-transfer (RAFT), atom transfer radical (ATRP), and cerium (IV) redox-initiated polymerizations (RIP) have contributed to higher molecular weights (>100 kDa) and fairly narrow distributions of the homo/co-polyacrylamide chains ($\mathcal{D} = 1.01\text{--}1.40$) expanding their potential as biomaterials.⁸ The polyacrylamides' thermo-responsive properties have led to the design of micelles, hydrogels, surfaces, and bioconjugates with “intelligent on-off systems”.⁵ Furthermore, these bio-related properties facilitated in a number of patents related to biomaterial applications. For example, polyacrylamides have been developed and utilized throughout Europe and China for the last 15 years as implants for reconstructive surgery and soft tissue augmentation.⁹ Thermally controlled biological cell detachment, via poly(*N*-isopropyl acrylamide) coated-surfaces, has attracted attention as a tissue growth scaffolds.¹⁰ Furthermore, polyacrylamides have found their way into polymer therapeutics and are currently undergoing clinical trials as a polymer-conjugate drug delivery systems.¹¹

1.3.3 Poly(2-oxazolines)

Polyoxazolines are structural isomers of polyacrylamides and synthetic polypeptides (Figure 2). They were first introduced back in the 1960s but have suffered from poor industry inclusion, presumably due to the higher associated costs in production. However, in recent years they have acquired greater attention and the generation of patents related to various applications has risen. They are typically prepared by cationic ring opening polymerization (CROP) and undergo a phase transition in aqueous solutions when heated above their respective cloud points.⁶ These physical similarities to the polyacrylamides, as well as their structural similarities, have led to a number of publications attempting to elucidate the differences between these polymeric systems and determine what advantages one system may have over the other one. For example, PNiPAAm (32 °C)⁸ and PiPOx (36 °C)¹² have lower critical solution temperatures (LCST) within or near the average physiological temperature range of homo-sapiens (36.1–37.2 °C). However, these synthetic polyanamides have recently been described as undergoing two separate phase transition pathways (coil-to-globular vs. extended-dehydration).¹³ In addition, PiPOx may form stable crystalline precipitates from warm aqueous solutions via a nucleation growth mechanism occurring in the polymeric rich phase.¹⁴ It is unclear how these differences may be exploited for biomedical applications but the similar biocompatibilities between these two systems have led to complementary application investigations.¹² Once again, the synthetic backbone does not permit biodegradation. Notably, this limitation has been overcome by designing multiblock copolymers with biologically cleavable linkers (*eg.* ester, carbonate, disulfide, hydrazone, urethane, *etc.*) facilitating in targeted polymeric degradation (<45 kDa or <3.5 nm) which allows for renal filtration.¹⁵ Currently this approach has been utilized in the design of acrylamide copolymer conjugates (*eg.* poly(*N*-[2-hydroxypropyl] methacrylamide-*b*-*N*-[Gly-Phe-Leu-Gly-doxorubicin] methacrylamide; PK1 (FCE28068)) as drug carriers. Although the inclusion of such degradable bonds is intuitively more challenging for polymers prepared via CROP, such hydrolytically sensitive linkages have been extended to the polyoxazolines.¹²

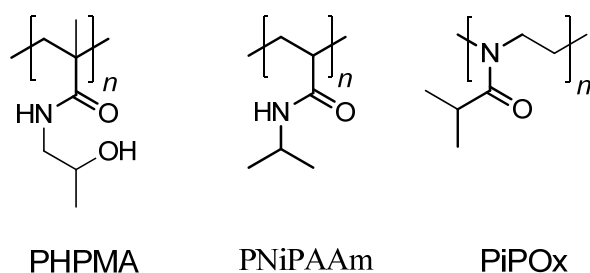


Figure 2. Examples of the commonly investigated polyacrylamides and poly(2-oxaline)s.

1.4 Polymeric systems with amides in the backbone

The non-biodegradability of the aforementioned polymeric systems has hindered the development of drug delivery and tissue growth scaffolds (extracellular matrices) for biomedical applications. Although biodegradable linkers afford the opportunity to break these multicomponent systems into smaller, water soluble, units (allowing for renal excretion), bioaccumulation of these foreign (xenobiotic) synthetic polymers is still a concern. An approach to overcome this limitation is to utilize, or design, polymeric materials primarily composed of hydrolytically cleavable bonds within the backbone. This may be achieved by isolating and/or modifying natural polymers (*eg.* dextran, hyaluronic acid, chitosan, collagen, *etc.*) or the synthesis of polyesters, polycarbonates, poly(urethane)s, and polyamides (*eg.* nylon, polypeptides, *etc.*).^{11, 16} Although each of these degradable materials deserves further consideration, I will limit the focus of this discussion to bio-relevant, degradable, polyamides as they pertain to the main topic of this thesis.

1.4.1 Polypeptides and related structures

The supramolecular assembly of biopolymers, with or without mineral deposits, facilitates in the production of structural and mechanical features found throughout animals. In particular, fibril collagen (*ie.* a protein or natural polypeptides with quaternary structures) can be found in connective tissues (composed with cells), cartilage (assembled with proteoglycan and elastin fibers), and bone (composite material with hydroxyapatite). These properties and the inherent biocompatibility attributed to the first biomaterial investigations with collagen.^{16b} In addition mobile proteins may be utilized for transporting (*eg.* hemoglobin) and/or signaling (*eg.* peptide/protein hormones) between cells. Once again, these natural polypeptides have been harvested from living matter for a myriad of biomedical treatments (*eg.* transfusions, hormone therapy). Even with the intrinsic value of cultivating materials from living systems, the disadvantages include damage to the host, low-abundances, limited inter-organism compatibility, and limited diversity. Contrarily,

synthetic biomaterials promise lower costs, abundant materials, reduced organism rejection, and versatile material composition.

One of the first polyamides synthetically made was nylon by Wallace Carothers (1935) who, at the time, was working for Dupont. Although this silk-substitute is generally utilized as a commodity material, it has been explored for biomedical applications as well.¹⁷ Synthetic polypeptides (*ie.* chains of α -amino acids) and peptidomimetic polymers (*ie.* side-chain and/or backbone derivatives of amino acids)¹⁸ have been mainly prepared as therapeutic agents or drug delivery systems (*eg.* drug conjugates, micelles, dendrimers, *etc.*).^{11, 15, 16b} Peptide therapeutics require sequence and molecular weight control (*ie.* precise, uniformly dispersed, molecular weights) whereas drug delivery systems allow for more ambiguity (*ie.* homo/co-polymers with varying molecular weights, non-uniform dispersion). Synthetic control is guaranteed via solid phase (bio-organic chemistry) or microorganisms (bio-engineering) approaches whereas solution phase synthesis (polymer chemistry) allows for a convenient way to prepare synthetic polyamides.¹⁹ Solution phase polymerization is accomplished either in a step-growth or chain-growth fashion where the latter is favored due to the level of control which allows for copolymer designs. In particular, nucleophilic (*ie.* primary amines, alkoxides, and carbenes) ring opening polymerization (ROP) of α/β -amino *N*-carboxyanhydrides (NCA) lead to well-defined polyamides (*ie.* polypeptides or *pseudo*-peptidomimetic polymers; see Theory and Methodology for mechanistic pathway). In as much, a variety of homo/co-polypeptides and related polymers have been prepared and investigated for properties needed for biomedical applications. Such studies included mechanic strength, thermo-analysis, and stimuli-responsive behaviors. In addition the adsorption, distribution, metabolism, and excretion (ADME) pathways were explored. However, only a limited number of polypeptides have demonstrated the desirable properties needed for biomaterials.^{16b} In part, this has been attributed to the poor bio-distribution of these polypeptides caused by proteolysis. Approaches to overcome this limitation include conjugation or encapsulation with synthetic polymers, such as PEG, or designing derivatives of polypeptides. Both of these techniques suppress enzymatic degradation by preventing the amide backbone from fitting in the active pocket of enzymes.

1.4.2 Polypeptoids

Peptoids, regioisomers of common peptides or sequence specific *N*-substituted glycine oligomers, were originally explored as peptidomimetics for peptide therapeutics that demonstrated

desirable biological activity but suffered from poor pharmacokinetics caused in part by *in vivo* proteolysis.²⁰ A peptide-peptoid hybrid, where select amino acids were replaced by their regioisomer, demonstrated resistance to enzymatic degradation.²¹ Continued research has led to the diversification of the structure, developed alongside fundamental and application based investigations, to include non-sequence specific *N*-substituted glycine macromolecules as uniformly or nonuniformly dispersed homo-/co-polymers. Application based investigations have included DNA drag tags,²² nanosheets,²³ cell permeation labels,²⁴ and calcium carbonate mineralization.²⁵ Whereas fundamental research provided insight into foldamers,²⁶ self-assembly,²⁷ surface influences,²⁸ and tunable crystallinity.²⁹ To date, the majority of these investigations were carried out with sequence controlled mono-dispersed peptoids. Due to their intrinsic biocompatibility and resistance to enzymatic degradation, an increasing trend in the “biopolymer” community has been to investigate the feasibility of nonuniformly dispersed peptoids as potential biomaterials.³⁰

Owing to their bio-organic roots, peptoids were traditionally prepared by solid phase utilizing an atypical submonomer technique.^{20, 31} Although the current solid phase synthetic approach affords sequence control and produces material on the gram scale,³² achieving high molecular weight peptoids has been limited to chain-chain coupling procedures.³³ Interestingly, a solution phase submonomer approach, that included intermediate roto-evaporation of the volatiles, was designed but still suffered greatly to limitations in chain length.³⁴ Polymer scientists utilized metal-mediated alternating copolymerization of carbon monoxide and imines³⁵ or ring opening polymerization (ROP) of α -amino acid *N*-carboxyanhydrides (NCAs).³⁶ The latter afforded well defined polymers allowing for copolymerization strategies. Previously, these techniques were adapted by Kricheldorf *et al.* for *N*-methyl glycine (a.k.a. sarcosine) during their extensive investigations into the active monomer and zwitterion mechanisms of *N*-unsubstituted NCAs (Figure 3).³⁷ Zhang *et al.* described the first bottom up approach of *N*-substituted NCAs that were polymerized via an *N*-heterocyclic carbene (NHC).³⁸ More recently, Luxenhofer *et al.* provided a detailed report of a series of peptoid homo- and block-copolymers.³⁹ Likewise, Schlaad *et al.* described a separate approach for the synthesis of poly(*N*-allyl glycine) homopeptoids.⁴⁰

1.4.3 Glycopeptides

Glycopeptides are of great interest in the biomedical field due to their potential as smart therapeutics, biosensors, and tissue engineering scaffolds. The inherit chirality of the sugars allow for specific receptor recognition and binding. In as much, a plethora of materials containing

carbohydrates as modified materials, copolymer systems, or as the side chains of either synthetic or peptide based biopolymers have been designed. In particular, our group has focused on the latter by the post-modification of synthetic or peptide based biopolymers via thiol-ene photoaddition. Prior to joining the Schlaad group, they were investigating the synthesis of poly(α -allyl glycine) and its post-modification which facilitated in the production of glycopeptides. One of the main difficulties that they were having was in achieving reasonable to high molecular weights. They attributed these challenges to the poor solubility of polypeptides caused by hydrogen bonding and possible higher order structures (eg. β -sheets). To overcome this, they utilized macroinitiators (ie. PEO-NH₂) to increase solubility and molecular weight. As an alternative, we decided to target the regioisomer, poly(*N*-allyl glycine), based on the understanding that the removal of hydrogen bonding would readily lead to higher molecular weights and the lack of amide hydrogen would also reduce competing side reactions such as the AMM and therefore produce well-defined biopolymers. Likewise, we targeted poly(*N*-propargyl glycine) which hypothetically should have facilitated in a higher carbohydrate ratio. In addition we recognized that these poly(*N*-substituted glycine) systems have structural similarities to other bio-inspired polymers such as the polyacrylamides and poly(2-oxazoline)s and therefore would have similar stimuli responsive and material properties such as thermoresponsive behavior and thermoprocessing character. In as much, we expanded our investigations to include poly(*N*-alkyl glycine)s that are unable to be post-modified towards glycopeptides.

1.4.4 Significant material properties

The fundamental understanding of crystallinity and stimuli-responsive behavior is a prerequisite for the sophisticated design of biopolymers that encompass properties necessary for specific applications. For example, the structural order of a polymer (ie. crystallinity) is largely responsible for the hardness, density, transparency, and diffusion properties of the bulk material. In addition, polymers are more accurately described as being semi-crystalline as in there are local structural ordered states throughout the polymer but suffer from polymer dynamics (ie. global conformational properties) which causes defects in the overall structural organization. Crystallinity can be experimentally measured by X-ray diffraction or more commonly by calorimetric techniques. The latter facilitates in a convenient route towards determining the ordered state of most polymeric systems. On the other hand, measuring the phase transition behavior (via ultra-violet or infrared turbidimetry) of polymers while changing the environmental conditions by an

external stimuli (*eg.* temperature, pH, light, magnetic or electric field, ionic factors, biological molecules, *etc.*) affords information on how a polymeric system may respond in similar environments. From a biomedical standpoint, pH and temperature are the most interesting external-stimuli parameters to investigate. Generally speaking, these particular phase transitions of a polymeric solution are driven by chemical (pH) and/or physical (temperature) interactions between the polymer and aqueous environment, where the enthalpy of solvation is altered by changing the ionic character (*ie.* cationic or anionic) of the solute or entropy of the solution. Notably, the hydrophilic and hydrophobic character (*ie.* the ratio and position of polar and non-polar units) influences the initial solvating potential of the polymer. Therefore, we rationalized that structural isomers of PNiPAAM, PiPOx, polyleucine (PLeu), and poly*is*leucine (PIIle) would exhibit stimuli-responsive behavior and, in ordered structures, crystallinity phenomena.

1.5 Objectives of dissertation

We were interested in investigating poly(*N*-substituted glycine)s for biomaterial properties such as thermo-responsive behavior, thermo-processability (crystallinity), and solubility. In particular, we wanted to demonstrate the aqueous solubility of these polymers and develop a post-modification strategy for functional (*ie.* alkene and alkyne) polypeptoids. To achieve these initial objectives we had to synthesize a series of side-chain polypeptoids by following a published synthetic route for alkyl derivatives and develop our own efficient pathway towards functional derivatives. Furthermore, we wanted to be able to control the chemical composition, molecular weights, and distributions. To achieve these goals we had to understand the following theories (*ie.* mechanisms and physical behavior) and utilize the appropriate methods (*ie.* equipment and instrumentation).

2. Theory and Methodology

2.1 ROP with NCAs

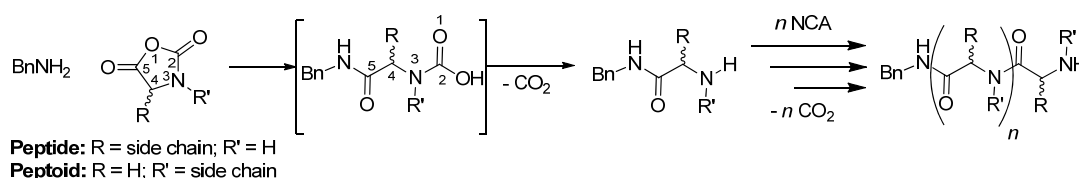
Ring opening polymerization (ROP) with α -amino acid *N*-carboxyanhydrides (NCA) can be achieved by utilizing nucleophilic initiators such as amines, alcohols, and carbenes (Figure 3). Transition metals (*eg.* Co, Ni) have also been demonstrated to lead towards “living” polymerization via an insertion, ring-addition, and ring-contraction catalytic mechanism (Figure 4). Primary amines such as benzylamine (BnNH₂) and hexylamine (HexNH₂) are commonly utilized due to their high initiator efficiency. Silyl amines have been demonstrated to increase the level of “control” of polymerization by reducing chain termination and transfer pathways. Suppression of alternative pathways also may be achieved by utilizing an ammonium chloride as the initiator and propagating species. Contrarily, secondary and tertiary amines produce polypeptides with large molecular weight distributions due to poor initiator efficiency or promotion of the activated monomer mechanism (AMM). Likewise, alcohols treated with strong bases (*eg.* butyl lithium, NaH, *etc.*) promote the AMM for NCAs. In general, reagents that have competing basic tendencies, in respect to their nucleophilic character, readily initiated ROP via an AMM pathway. Although carbenes have an inherit basic character, they have been utilized for *N*-substituted glycine NCAs suggesting that the AMM may be suppressed via substitution of the amide.

The normal amine mechanism (NAM) is a bimolecular reaction that occurs between a nucleophile (*eg.* primary amines, propagating amine) and a NCA monomer (*ie.* α -amino acid or *N*-substituted glycine). Ideally, nucleophilic attack occurs at the 5 position, carbonyl, and passes through a tetrahedral intermediate. Reformation of the carbonyl favors the ring opening, or anhydride cleavage, producing a temporary carbamate which readily undergoes decarboxylation into the propagating amine (*ie.* 1° α -amino acid or 2° *N*-substituted glycine). In an ideal system, the newly produced nucleophiles continue the cycle until the consumption of the monomer is complete (as illustrated in Figure 3, NAM). In a non-ideal system (*ie.* reality) competing reaction pathways, early termination, and chain-end transfers influences the reactivity and composition of the polypeptide.^{36b, 41}

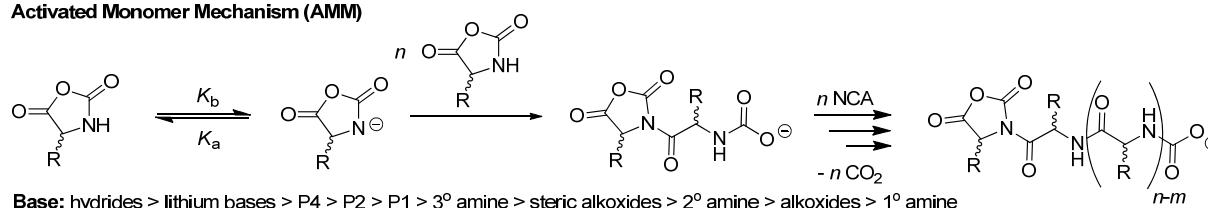
The activated monomer mechanism (AMM) is initiated by first deprotonating the strained amide in the cyclic anhydride by a reasonable base followed by nucleophilic attack to a neighboring NCA which causes the anhydride ring to open (Figure 3). This active dimer reacts with additional monomers either by propagation or chain-monomer transfers. Notably, the active sites on the α -

and ω -terminus may facilitate in a step-growth pathway and lead to multi-modal molecular weight distributions. In addition, intra-chain-end coupling may occur leading to cyclic polyamides. Likewise, the zwitterion monomer mechanism (ZMM) and zwitterion solvent mechanism (ZSM) may produce cyclic polyamides during propagation and termination steps. However, the initiation for these two is slightly different than the AMM. Initiation occurs via the electron rich carbonyl moiety. If the amide is secondary (2°), rearrangement/migration may occur with this bond. Furthermore, ZMM and ZSM may be suppressed at low temperatures whereas the AMM is thermodynamically independent. The majority of these undesirable initiation and/or propagating pathways have extensively been investigated and proposed by Kricheldorf.^{36a, 37, 42}

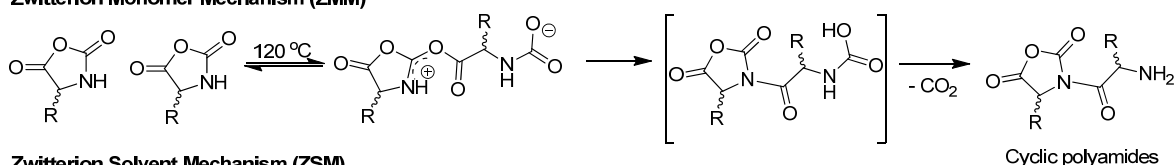
Normal Amine Mechanism (NAM)



Activated Monomer Mechanism (AMM)



Zwitterion Monomer Mechanism (ZMM)



Zwitterion Solvent Mechanism (ZSM)

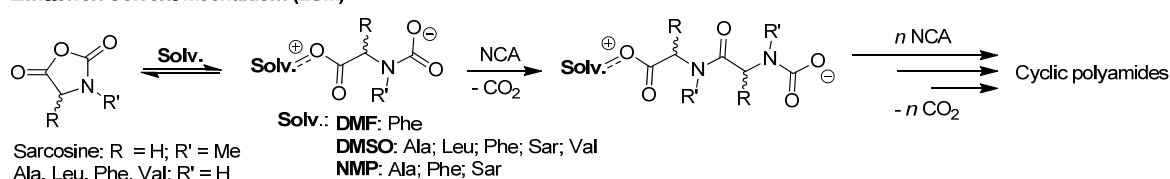


Figure 3. Known mechanism pathways towards polypeptides: normal amine mechanism (NAM); activated monomer mechanism (AMM); zwitterion monomer mechanism (ZMM); and zwitterion solvent mechanism (ZSM). The latter 3 reaction pathways compete with the NAM, desirable, pathway and lead to ill-defined systems. Note: many alternative polypeptide structures are created under the undesirable mechanism pathways and for simplicity only one is illustrated here.

Various approaches have been devised in an attempt to suppress these alternative mechanisms. Examples include the substitution of the amide with protecting groups, investigations towards initiator efficiency, and controlling the initiation and propagation pathways. Placing a protecting group on the amide of the NCA suppresses the AMM and increases the solubility of the propagating polymer via the removal of the hydrogen. However, preparing NCAs with protecting groups was challenging and worse the electron withdrawing nature of the majority of protecting groups, as well as the increased sterics, impeded propagation. Interestingly, investigations with silyl protecting groups (with lower electron withdrawing properties) inadvertently confirmed a common rearrangement of NCAs to an α -isocyanato carboxylic acid providing insight into a common terminating species (*ie.* hydantoic acid).⁴¹ Alternatively, nucleophilic attack to the 2 position, carbonyl, of the NCA has also been proposed for this observation, found in the composition of polypeptides. Sterics and electronic features on both the nucleophile and NCA influence the approach and addition sequence. In as much, several studies investigating these properties between various initiators and NCAs (in various solvents) has been conducted where primary amines, such as hexyl- and benzyl-amine, demonstrated the most versatile and highest initiator efficiencies. Although such initiators favor nucleophilic attack to the 5 position at or below room temperature (r.t.), they inherently maintain basic properties which, combined with impurities, do not suppress other competing pathways (*ie.* AMM).

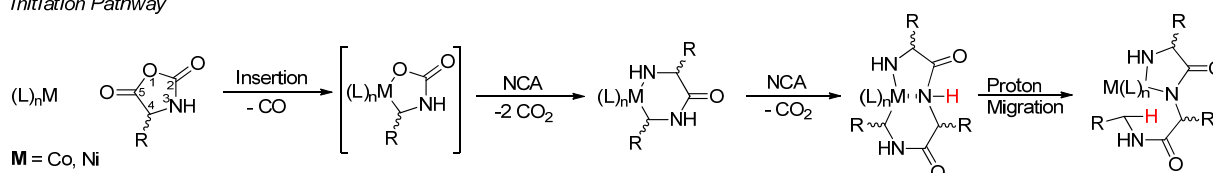
The mediation of amine initiators or propagating species via transition metals, silanes, or halogenated acid additives affords kinetic and/or thermodynamic controlled polymerizations (Figure 4). These techniques suppress the AMM and, in some situations, terminating and transfer reaction pathways. Deming and co-workers were the first to introduce a kinetic and thermodynamic controlled (“living”) polymerization technique for the ROP of α -amino acid NCAs which included the insertion of a transition metal (*ie.* Co or Ni) followed by carbonmonoxide (CO) release to form the initiator.⁴³ Then propagation would proceed via a ring addition followed by ring contraction cycle. The migration of the transition metal complex along the polymer chain throughout the propagation cycle suppresses termination and transfer pathways as well as increases the affinity to coordinate to monomers. This is cleverly achieved by reducing the basicity of the propagating amine (suppressing the AMM and chain-transfer pathways) and directing the approach of the monomer (suppressing termination pathways) via alignment with the transition metal’s *d* orbitals. Likewise, silylamines coordinate with the carbonyl of α -amino acid NCAs and undergoes an insertion and migration pathway throughout the propagation cycle.⁴⁴ However, suppression of

Chapter 2: Theory and Methodology

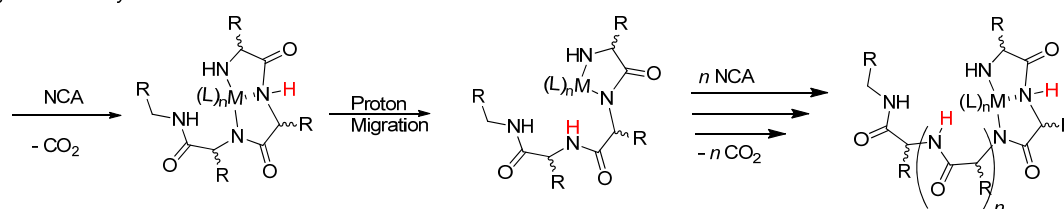
termination and chain-transfer pathways has not been demonstrated for this latter approach. In a similar fashion, ammonium mediated ROP of α -amino acid NCAs suppresses the AMM by reducing the number of statistical amines in solution while keeping the amide protonated thereby reducing the basicity of the initiator and propagating species.⁴⁵ However, the slow propagation requires the reaction mixture to be heated increasing the opportunity for other side reactions to occur (eg. ZMM, α -isocyanato carboxylic acid).

Transition Metal Mediated

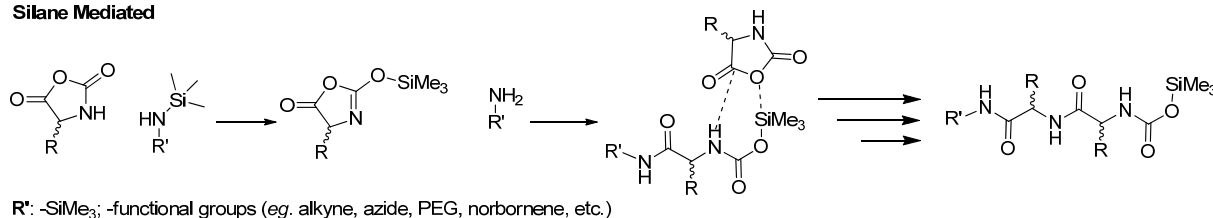
Initiation Pathway



Propagation Pathway



Silane Mediated



Ammonium Mediated

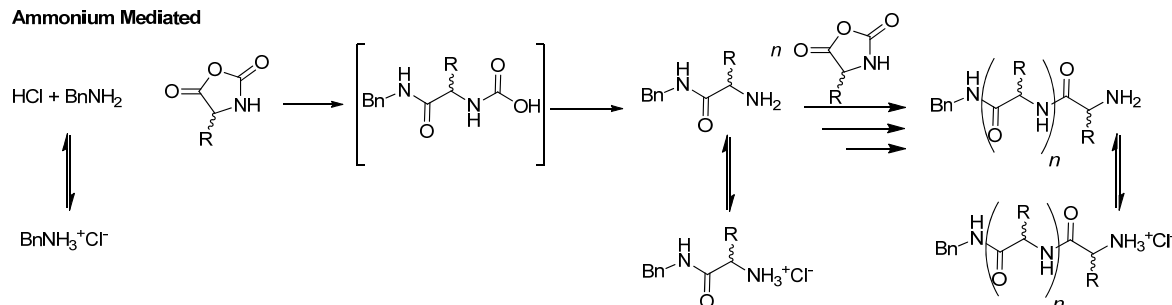


Figure 4. Controlled ROP of NCAs via transition metal, silane, and ammonium mediation.

2.1.1 ROP of NNCA_s

At the beginning of this dissertation work, there were only a few publications describing the ring opening polymerization (ROP) of *N*-substituted glycine *N*-carboxyanhydrides (NNCA) towards

polypeptoids. Prior to 2010, NNCA were primarily utilized for bimolecular kinetic and mechanism studies (pioneering work by Ballard and Bamford, 1958)⁴⁶ or investigations into the polymerization mechanisms of α -amino acid NCAs (extensive studies by Kricheldorf, 1980-2008).^{36a} The latter studies were primarily conducted with *N*-methyl glycine NCAs (a.k.a. sarcosine, commonly found in multicellular organisms). Noteworthy, Okada and coworkers demonstrated the controlled propagation of sarcosine NNCA from ammonium chitosan towards chitosan-*graft*-polysarcosine providing improved solubility (2006) for this modified biopolymer.⁴⁷ Zhang and coworkers were the first to publish the synthesis of alkyl (*ie.* *n*butyl and methyl) side-chain *cyclic*-polypeptoids utilizing a *N*-heterocyclic carbene (NHC) as the initiator (α - and ω -terminus).^{38a} Overall, these earlier publications support the suppression of the AMM and suggest a level of kinetic control may be achieved towards the ROP of NNCA following the NAM.

2.2 Thiol-ene/yne addition

Thiols (*ie.* R-S-H) hold great significance in biology and organic chemistry. For example, disulfide bonds play a vital role in stabilizing folded proteins thereby influencing function and mechanical properties. In organic chemistry, the thiols' heteroatom and *d* orbital properties have been exploited towards covalent bond formations. In particular, the nucleophilic (*ie.* Michael addition) and radical addition of thiols to unsaturated systems (*ie.* olefins with or without conjugation) have proven to be the most successful coupling reactions. Noteworthy, the electronic properties of the thiol and olefin (*ie.* neighboring donating or withdrawing groups) influences which of the aforementioned mechanistic pathways the coupling reaction will occur. For example, nucleophilic additions are favored with electron rich thiols and electron poor olefins where the opposite electronic conditions favor radical additions. However, the conditions of the reaction (*eg.* temperature, reagents, solvents, pH, *etc.*) play a more significant role towards the coupling reaction mechanism. The radical addition of thiols to alkenes and alkynes are illustrated in Figure 5 and described below.

The radical addition of thiols to unsaturated bonds occurs by an initiation, propagation, and termination sequence.⁴⁸ The initiation, or formation of the thiol radical, may be induced by direct (*ie.* photon) or indirect (*ie.* radical transfer) means. Ultra-violet (UV) light sources induces a homolytic bond cleavage to occur between the sulfur and hydrogen producing a temporary thiyl radical (*ie.* R-S \cdot).⁴⁹ Radical initiators/additives that are thermally sensitive (*ie.* AIBN) or photosensitive (*ie.* DMPA) will create a thiyl radical by hydrogen abstraction. In either case, a

neighboring π system (*ie.* alkene or alkyne) radically combines to the thiyl radical regioselectively (preference for terminal addition or least substituted carbon) producing a carbon-sulfide bond and carbon radical. The newly formed radical may propagate the addition cycle by abstracting hydrogen from a neighboring thiol, subsequently reacting with another π system. For alkenes this undergoes a single cycle pathway whereas alkynes under-take a two cycle pathway with the 2nd thiol addition occurring internally at the electronically rich carbon.⁵⁰ Termination occurs either through radical-radical recombination (*ie.* R-S-S-R or R-CH₂-CH₂-R) or reduction (*ie.* R=CH₂-R) pathways. Intuitively, this implies that greater than stoichiometric quantities of the thiol are required to suppress undesirable carbon-carbon recombination or reduction pathways. However, an excess amount of thiols requires additional purification and increases cost. In particular, thio-sugars are expensive and are commercially limited. Therefore, investigations towards the post-modification of functional side-arm polypeptoids via photo-addition of thiols to alkenes and alkynes required methodology studies as described in Chapter 3: Results and Discussion.

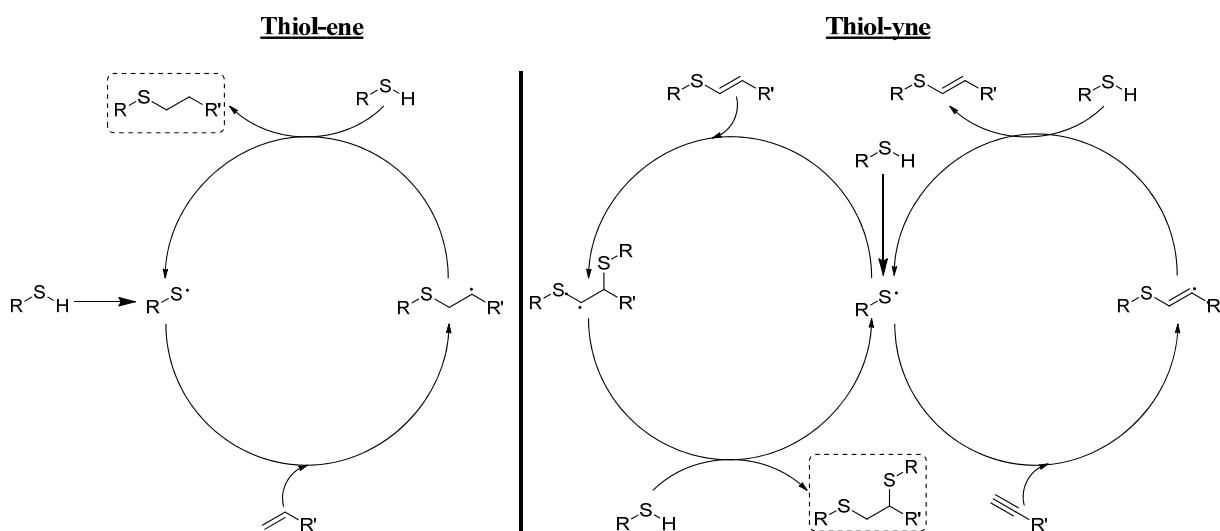


Figure 5. Thiol-ene and thiol-yne radical addition cycles.

2.3 Thermo-responsive behavior

A polymeric material that undergoes conformation or mechanical changes, via an external stimulus (*eg.* magnetic field, pH, temperature, *etc.*), may be utilized for biomedical applications including biosensors, drug delivery, and tissue engineering. In particular, pH and temperature responsive polymeric materials are commonly investigated. As described earlier, we were interested

in polymers that undergo a phase transition, in aqueous environments, as a response to changes in temperature. In particular we expected poly(*N*-substituted glycine) homopolymers to have thermo-responsive properties comparable to their synthetic structural isomers, polyacrylamides and poly(2-oxazoline)s, but with enhanced bio-relevancy (*ie.* greater similarities to peptides).⁸ The next few paragraphs will provide the reader with the appropriate terminology and fundamental knowledge required towards understanding thermo-responsive properties and how they relate to this dissertation.

The majority of thermo-responsive materials may be classified as either having an upper or lower critical solution temperature (UCST or LCST, respectively). These expressions describe the route towards dissolution or phase separation of polymers. For example, UCST describes not only the temperature at which the biphasic region (*ie.* dissolution/phase separation) of a polymer-solution occurs but it also indicates that solubility increases with temperature; or in other words polymer-solvent interactions are favored as polymer and solvent entropies increase. The opposite trend is observed for LCST phase diagrams; solubility increases at lower temperatures (*ie.* solvent and polymer entropies decrease while polymer-solvent interactions increase). A few polymer-solvent systems have both an LCST and UCST phase diagram. Related to this dissertation, PNiPAAm and PiPOx demonstrate LCST behaviors at or near the physiological temperature range of homo-sapiens albeit the turbidity measurements are typically conducted in pure water.^{5,12}

In general, a homogeneous sample (*ie.* light passes through sample without obstruction/refraction) of polymer in water is prepared below favorable mixing temperatures at a particular concentration and subjected to increases in temperature through the demixing phase. As the polymer-water mixture separates, colloidal particles form impeding the transmittance of light where the change is recorded by the turbidity instrument. The point at which turbidity or phase separation is considered to be of significance is called the cloud point temperature (T_{cp}). In the literature, the T_{cp} is typically defined either as the inflection point of the sigmoidal turbidity plot or as the percentage of transmittance lost during increased turbidity. The ambiguity here naturally does not always allow for direct comparisons which may be a moot point when considering that preparation of the sample, sharp to broad transitions, and various instruments may play a greater role in the lack of comparability. For example, a sample that undergoes a sharp phase transition (*ie.* <1 °C) would not have a significant variance between the inflection point and a transmittance decrease of 20% whereas a broad phase transition (*ie.* >1 °C) could have a difference as high as 10 °C. However, sharp-reversible-phase transitions are desirable for biomedical applications. In any

case, the T_{cp} is assumed to be the point at which mixing/demixing energies are infinitesimally measurable (*ie.* $\Delta G \approx 0$, Equation 1). Therefore, the T_{cp} s of various concentrations of the same sample (*eg.* \bar{M}_n , D , composition) may be plotted on a graph (Temperature vs. Concentration) allowing for the critical solution temperature phase diagram to be visualized and calculated.⁵¹

$$\Delta G_{mix} = \Delta H_{mix} - T\Delta S_{mix} \quad \text{Equation. 1}$$

2.4 Analytical Methods

2.4.1 Thermo-analysis

Thermo-analysis via differential scanning calorimetry (DSC) and thermo-gravimetric analysis (TGA) provide insight into the processability and robustness of the material. These routine measurements afford an opportunity to identify new materials that may have comparable mechanical properties to well-known materials thereby suggesting potential applications. For example, polymeric materials with a high degree of crystallinity fractions ($\geq 76\%$), glass transition temperatures (T_g) equal or greater than 170 °C, and thermally stable until 400 °C reasonably may have applications similar to Kevlar™.⁵² However, it is unlikely that a high cost polymeric material, as described in this dissertation, will be utilized as a commodity polymer.

Differential scanning calorimetry (DSC) measurements are conducted under an inert atmosphere in an insulated chamber. There are two pans (*ie.* sample and reference) placed on two separate heaters. The heat flow is regulated by sensors and computer programs enabling matched temperatures between the pans as well as monitoring the amount of heat added or removed throughout the measurement. The amorphous regions of the polymeric material are tolerant towards the heat flow until the heat capacity of the material is reached in which point the polymer becomes more pliable and the overall heat capacity changes. This change is observed on the endotherm and is denoted as the glass transition temperature (T_g). If the polymeric sample is completely amorphous, no further change will be observed until decomposition occurs (*ie.* bond cleavage). However, if regions of the polymeric material can align into an order or crystalline state above the T_g , then an exothermic peak related to the crystallization transition temperature (T_c) will be observed followed, a little later, by an endothermic peak related to the melting transition temperature (T_m) of these crystalline regions. Once again, no further peaks should be observed past the T_m until decomposition. Notably, thermo-stability of the polymeric material is analyzed prior to these measurements, via TGA, to avoid decomposition within the DSC device.⁵³

Thermo-gravimetric analysis (TGA) measures mass loss over a temperature range which provides information about the stability of the polymeric material. A polymer sample is placed on a mass scale inside an insulated oven, which may be flushed with an inert gas (*eg.* nitrogen), and heated until no further mass loss is detectable. It is common to detect separate mass losses associated to solvents/impurities and molecular stability variances (*eg.* weak bonds vs. strong bonds throughout the macromolecule). Overall, TGA and DSC are reliable thermo-analysis techniques that provide significant polymer property information.

2.4.2 NMR

Nuclear magnetic resonance (NMR) spectroscopy is a powerful organic molecule characterization technique. NMR provides insight into chemical composition by probing the nucleus of an atom's spin state. However, this technique is limited to odd numbered nuclei (*eg.* ^1H , ^{13}C , ^{15}N , ^{31}P , *etc.*) and their relative natural abundances. In addition, NMR measurements require a homogeneous sample which may be achieved either by dissolution or high-speed gyration (*ie.* solid-phase NMR). Furthermore, the interpretation of the spectra requires extensive education and training towards shifting patterns, impurity identification, connectivity (*ie.* J couplings and/or 2D NMR techniques), unique electronic environments (*eg.* aromatic shielding effects), and *etc.* Even with these challenges NMR techniques have facilitated in the identification and verification of millions of organic molecules, small and large.⁵⁴

The identification, or chemical composition analysis, of polymers includes some unique considerations. For starters, it is important to recognize that polymers are macromolecules that may be uniformly or nonuniformly distributed. The fore-mentioned are biopolymers, bioengineered synthetic peptides, or solid phase prepared peptides. These polymers include sequence specificity in the backbone which have unique and/or similar chemical environments and register on $^1\text{H}/^{13}\text{C}$ NMR spectra as several peaks making identification challenging. In addition, some of these peaks may overlap, depending on chemical similarity, and skew integration calculations. Contrarily, nonuniformed distributed polymers (*ie.* synthetic polymers) have a relatively simple backbone made up of anywhere between one to few variations in the repeating units affording readily identifiable chemical shifts/environments. However, due to the abundances of macromolecules with individual molecular weights and different levels of heterogeneity/solubility, the chemical environments are observed to be slightly different by NMR spectroscopy causing a broadening effect. This may lead to peak overlap, skewed integration calculations, and poor connectivity

determination. However, choosing an α/ω -terminus with a unique shifting pattern to the backbone minimizes calculation errors associated to the average degree of polymerization (\bar{n}). Notably, poor removal/purification of unincorporated terminus units may skew calculations. Therefore NMR spectroscopy analysis of synthetic polymers cannot stand alone and needs to be combined with molecular weight analytical techniques to verify polymer architecture.

2.4.3 SEC

Size exclusion chromatography (SEC), also known as gel permeation chromatography (GPC), fractionates samples by hydrodynamic volume. Separation is driven by the diffusion of dissolved macromolecules into swollen porous material (*ie.* particles or microgel) with slightly different porosity dimensions. Diffusion is governed by the hydrodynamic radius of the individual macromolecules, porosity of the individual material, and internal concentration of the corresponding pores. To promote physical, while suppressing chemical, driven separation, it is important to choose a mobile phase that swells the porous material and dissolves the macromolecules while choosing a stationary phase that has minimal chemical interactions (*eg.* London dispersion forces) with the solute. If these ideal conditions are achieved then fractionalization would occur as follows.

Imagine that we synthesized three separate polymer chains with relative molar masses and solvated hydrodynamic radii of small (*S*), medium (*M*), and large (*L*). The nonuniformly dispersed sample is loaded onto a column with swollen pore sizes between small to large (P_s – P_L). As the sample is pushed through the column, *S*, *M*, and *L* polymers are diffused into P_L until an equilibrium is reached between these pores and surrounding solvent (a.k.a. dead volume). Likewise, *S* and *M* polymers are diffused into P_M and/or P_s . Due to the concentration reaching equilibrium between the pores and the dead volume space, the initial concentration of *M* and *S* polymers, in respect to *L*, has decreased in the dead volume space where polymer *S* has decreased by the greatest value. As the concentration of the dead volume decreases with the forward movement of the mobile phase, the polymers are diffused out of the pores. This equilibrium driven diffusion process continues throughout the duration of the column and causes the polymer fractions to separate. Intrinsically, this means that the polymer *S* spends more time, statistically, diffused in the pores than *M* or *L*. Likewise, polymer *M* spends more time than *L*. The effect of this is that polymer fraction *L* leaves the column first followed by polymer fraction *M* and finally polymer fraction *S*. The elution of these fraction volumes are typically monitored by ultra-violet

(UV) and refractive index (RI) detectors where the data is plotted as curves (Intensity vs. Elution Volume). Depending on how similar the hydrodynamic radii of these polymer fractions are and the resolution of the column, mono- to multi-modal curves may be observed/plotted. The elution volume is dependent on the hydrodynamic radius of the polymer and not its chemical composition. Therefore two separate polymer samples with the same or similar solvated hydrodynamic radii will have the same elution volume regardless of respective molar masses. In as much, absolute molar mass calculations are limited to calibration curves derived from polymers with the same chemical composition allowing for the same polymer swelling dynamics or tandem SEC instruments with single-/multi-angle static light scattering (S/MALS) and/or viscosity detectors. Otherwise, molar mass to elution volume calibration curves provide a relative or apparent molar mass value. More precisely, an infinitesimal point on a calibration curve in respect to molar mass represents an infinitesimal point of the elution volume in respect to the sample. The height or intensity of this infinitesimal point represents the number of macromolecules at that particular molar mass in relationship to the other molar masses detected in the volume fraction. The probability (x_i) of choosing one macromolecule (M_i) from this nonuniformed dispersed fraction volume is equal to the corresponding intensity (n_i) divided by the total/sum of intensities (Equation 2). The number average molecular weight (\bar{M}_n), or statistically referred to as the mean molecular weight, can be calculated by summing up the product of multiplying the probability by its corresponding molecular weight.⁵¹

$$x_i = \frac{n_i}{\sum_i n_i}; \bar{M}_n = \sum_i x_i M_i \quad \text{Equation 2}$$

Likewise, the weight average molecular weight (\bar{M}_w), or statistically referred to as the 2nd moment about the mean, can be calculated by summing up the product of multiplying the probability of isolating a monomer (in_i) of a given chain by its corresponding molecular weight (Equation 3).

$$w_i = \frac{in_i}{\sum_i in_i}; \bar{M}_w = \sum_i w_i M_i \quad \text{Equation 3}$$

Finally, the degree of dispersion, dispersity (\mathcal{D}), of these molecules can be calculated by dividing the weight by the number average molecular weights (Equation 4).

$$\mathcal{D} = \frac{\bar{M}_w}{\bar{M}_n} \quad \text{Equation 4}$$

Experimentally, when $\mathcal{D} = 1.00$ the system is described to be uniformly dispersed but when $\mathcal{D} > 1.00$ it is called non-uniformly dispersed. However, properly describing a uniformly dispersed system requires more absolute analytical instrumentation. For example, the so called mono-

(uniform)-dispersed PEO, utilized in drug delivery systems, has a SEC $D = 1.00$ whereas gel electrophoresis techniques and mass spectrometry describe a *near*-mono or non-uniform dispersed system. Even with this and other limitations (*eg.* exclusion/permeation limits) SEC has many advantages that out way the disadvantages and is a routine measurement towards achieving apparent \bar{M}_n and reliable D for new polymer systems.⁵⁵

2.4.4 MALDI-ToF MS

Matrix assisted laser desorption/ionization time-of-flight mass spectrometry (MALDI-ToF MS) is an absolute instrumental technique that identifies the molar mass(es) of macromolecules. Like any time of flight mass spectrometer, individual molar masses are ionized and accelerated towards the detector reaching a max velocity related to the mass to charge (m/z) capacity. Separation of various masses occurs during the flight and individual ionized molecular masses are recorded. However, the high intensity ionization approaches cause macromolecules to readily fragment or rearrange requiring “soft” ionization approaches. In MALDI-ToF MS, ionization is accomplished indirectly by transferring ionization from a smaller molecule that readily ionizes at lower intensities to the neighboring macromolecules. The “matrix” is a crystalline mixture of optical absorption molecules (*eg.* dithranol), transfer molecules (*eg.* sodium acetate), and analyte (*ie.* macromolecule). Typically this mixture is loaded onto a sample plate where the volatile organics are removed by evaporation at room temperature. The remaining residue is irradiated by a laser under vacuum where the majority of the energy is absorbed and ionized by the small molecules which transfers to the neighboring macromolecules via an alkali metal (*eg.* sodium, potassium) or proton association. Once again, this charged macromolecule species accelerates towards the detector. Notably, even with these “soft” ionization techniques a statistical portion of the macromolecules may fragment or rearrange. Resolution of ionized macromolecules may be improved by lengthening the flight path via ion reflection induced by a strong electronic field (linear to reflection mode). Although fragmented macromolecules are separated out by this approach, the signal of the ionized macromolecules is also reduced.

The corresponding spectra illustrate peaks associated to the molar masses of these macromolecules with their respective ionizing compound. Notably, a high resolution spectra will illustrate isotopes of these macromolecules where the data is commonly smoothed (*ie.* average of isotope peaks) prior to \bar{M}_n and \bar{M}_w calculations. In addition, MALDI-ToF mass spectra afford an opportunity to verify the mass of the repeating unit (Δm), average degree of polymerization (\bar{n}), and

calculate the suspected α -/ ω -terminus moieties. However, \bar{M}_w and D calculations may be skewed due to averaging peaks and underrepresented macromolecules (*ie.* longer chains) via the lack of effective ionization. In addition, the matrix may show biases or react undesirably with the macromolecule influencing the detection of the appropriate macromolecules. Furthermore, the residue on a sample plate is rarely homogeneously spread out on the surface requiring multiple irradiations in various spots with different intensities.⁵⁶

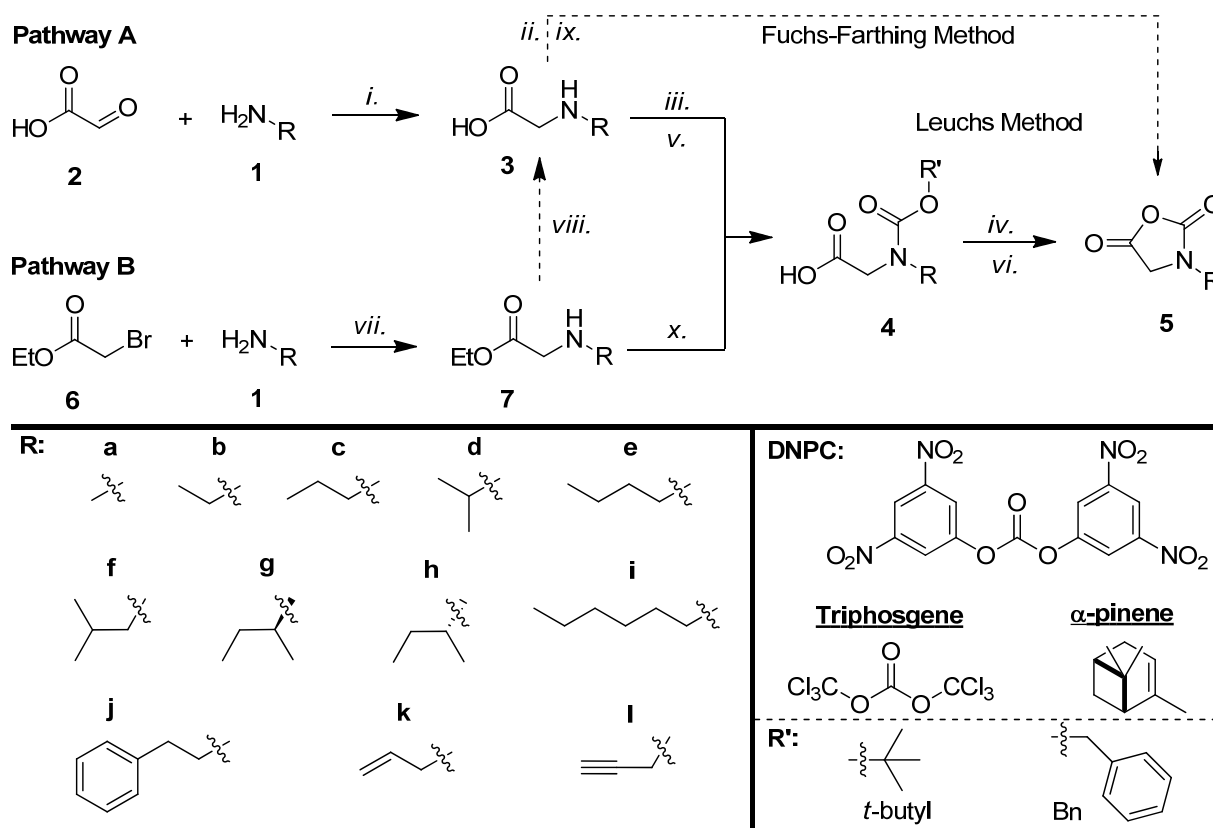
3. Results and Discussion

3.1 Polypeptoid via Chain-Growth Polymerizations

Polypeptoids are essentially derivatives of polyglycines where the nitrogen of the amide is substituted with functional groups (*eg.* alkyl, aryl, ether, alkene, alkyne, etc.). As described in Chapter 1, the three main synthetic approaches are solid phase, bioengineering, and solution phase. We chose to focus our efforts on the latter due to our group's interests and experience in bio-inspired polymers as potential materials. We explored amine initiated ring-opening polymerization (ROP) via an amino acid *N*-carboxyanhydride (NCA) and various step growth polymerizations. The chain-growth polymerization technique facilitated in well-defined polypeptoids and was utilized towards copolymerization strategies. Therefore, the cornerstone of our approach was dependent on an efficient synthesis of the monomers described below.

3.1.1 NNCA Preparation

The synthesis of *N*-substituted glycine NCAs (NNCA) can be achieved either by addition to a preformed monomer or the preparation of its previous constituent (prior to cyclization). The notion of creating a stock compound that could be readily modified prior to polymerization is attractive but was demonstrated to be too unstable for long term storage and suffered from competition of ROP via the active monomer mechanism (AMM).^{36a} The direct mono-alkylation of α -amino acids (*eg.* glycine) prior to cyclization would be an alternative solution that would facilitate in the facile synthesis of a myriad of NNCA. Current literature has shown great strides in the selective mono *N*-alkylation of primary amines through enzyme mediated addition/substitution,⁵⁷ metal mediated substitution,⁵⁸ *in situ* reduction of an imine intermediate,⁵⁹ and an 5-oxazolidinone route.⁶⁰ However, many of these methods suffer from over alkylation or are limited in scope to a selected few primary/secondary amines. Further developments in the mono-alkylation of α -amino acids would be a prerequisite for our investigations. Alternatively, the syntheses of *N*-substituted glycine derivatives from primary amines and acetyl analogues offer a facile synthesis of a diverse library of glycine derivatives via a plethora of commercially available amines.



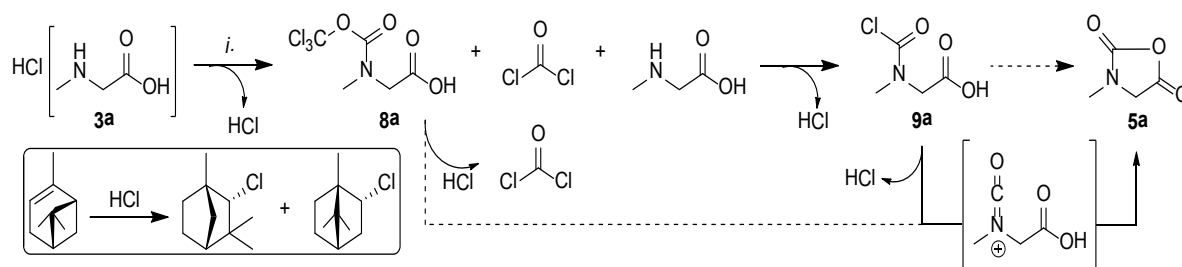
Scheme 1. Synthetic pathways towards *N*-substituted *N*-carboxyanhydrides. (i) (a) CH_2Cl_2 , (b) HCl , H_2O , Δ ; (ii) triphosgene, α -pinene, THF, Δ ; (iii) Boc_2O , NEt_3 , H_2O ; (iv) PCl_3 , CH_2Cl_2 , 0°C ; (v) benzyl chloroformate, NaOH , toluene, 0°C ; (vi) acetyl chloride, acetic anhydride, Δ ; (vii) NEt_3 , THF, 0°C ; (viii) LiOH , $t\text{-BuOH}:\text{H}_2\text{O}$, 0°C ; (ix) DNPC, THF, Δ ; (x) (a) Boc_2O , dioxane, (b) NaOH , MeOH .

Zhang *et al.* was the first to propose a bottom-up approach towards NNCAs (Scheme 1; Pathway A; step i, iii, iv).^{38a} This pathway included a one-pot monocarboxymethylation of primary amines (step i), quantitative addition of *tert*-butyloxycarbonyl (Boc) (step iii), and an acyl halide induced cyclization (a.k.a. Leuchs' method; step iv). Altogether, the synthetic pathway described by the group was effective towards the preparation of *N*-alkyl glycine NCAs. Our initial efforts supported step i as an efficient path towards the preparation of *N*-alkyl glycines (**3f**, **g/h**, **i**, and **j**) whereas sub-sequential attempts at the *N*-allyl glycine derivative (**3k**) resulted in low yields (<10%). Reviewing the original work by Tomkinson *et al.* suggested that only yields up to 25% were possible for the allyl species.⁶¹ Investigations of the intermediate illustrated that the low yields were a result of refluxing the crude mixture in aqueous hydrochloric acid (HCl). Suspecting that this was caused

by a trans-addition to the alkene (*ie.* hydrolysis or hydro-chlorination) we attempted to overcome this limitation by exploring various conditions such as replacing HCl with acetic acid or citrus acid, more mild acids. Unfortunately, we did not observe any improvements.

Further literature screening provided the answer to our problem. A bimolecular substitution reaction (S_N2), between allylamine (**1k**) and α -bromo ethylacetate (**6**), was proposed by Liskamp *et al.*⁶² The synthesis was simple and the purification via flash chromatography was fairly straightforward (Scheme 1; Pathway B; step vii). To reduce cost, the 2 equivalence of allyl amine was reduced to 1 and substituted first with di-isopropyl amine (DIA) and later triethylamine (Et₃N). This simple modification afforded us with a modest yielding first step (ca. 70%) and the opportunity to produce *N*-allyl glycine ethanoate (**7k**) on the multi-gram scale (<40 g). Likewise, *N*-propargyl glycine ethanoate (**7l**) was successfully prepared (ca. 70%; see Appendix: A1–A2) although a small portion (9%) was lost to the competing bis-substituted by-product (*ie.* over alkylation). The quantitative saponification of **7k** to **3k** was accomplished under standard conditions (step viii). Satisfied that we now had a mild, efficient, and versatile route towards functionally substituted glycine derivatives, we attempted cyclization.

Fuchs-Farthing method is a one-pot cyclization approach that utilizes amino acids and phosphene equivalents. In particular, our group previously prepared racemic α -allyl glycine NCA from its α -amino acid precursor and triphosgene (step *ii*).⁶³ Our initial attempt at preparing *N*-allyl glycine NCA (**5k**), via this aforementioned pathway, was unsuccessful. Unsure if the failure was caused by trans-addition or some other unknown circumstance, we made several more attempts with *N*-methyl glycine (**3a**; a.k.a. sarcosine), a simple and commercially available glycine derivative. After several attempts, which included changing conditions such as temperature and equivalences of triphosgene and α -pinene, to prepare NNCA **5a**, we suspected that the alkyl was somehow influencing the cyclization. A closer look of the cyclization mechanism provided some enlightenment.



Scheme 2. Cyclization mechanism pathway with sarcosine (**3a**). (i) $\frac{1}{2}$ eq. triphosgene, 2 eq. α -pinene, THF, Δ .

Investigations by Mantovani *et al.* suggest that the generation of phosgene from triphosgene occurs after the formation of a tetrahedral intermediate (rate limiting step) where the phosgene was consumed instantly by the nearest nucleophile.⁶⁴ Therefore, combining triphosgene and sarcosine should have produced HCl, (1,1,1-trichloromethyl carbamate)-*N*-methyl glycine (diphosgene species) (**8a**), and (chlorocarbamate)-*N*-methyl glycine (**9a**) in the first stage (Scheme 2). Ideally, the latter should have readily undergone cyclization and released hydrochloric acid (HCl). Note that the HCl species released throughout this reaction was expected to be either sequestered by the α -pinene or removed via streaming argon. The diphosgene species (**8a**) was detected by crude ¹H-NMR and GC-MS but the chlorocarbamate (**9a**) was not. Naturally, the latter intermediate would be unstable and difficult to detect by the aforementioned techniques. Cyclization could occur either through a 2nd tetrahedral or immonium cation pathway. In any case, the energy barrier would be substantially higher during the 2nd stage than the 1st stage because of ring strain. Although a 2nd tetrahedral intermediate would be afflicted with increased steric-hindrance whereas formation of the immonium cation intermediate would be influenced by the stability of the leaving group (*ie.* chlorine or trichloromethyl oxide). Notably, α -isocyanato carboxylic acid moieties (imine relatives) have been reported in the literature as a common occurrence when *N*-unsubstituted α -amino acid NCAs were treated with bases or trimethylchlorosilane.^{36b, 41}

Suspecting that the energy barrier of this immonium cation intermediate was impeding cyclization, we decided to explore bis(2,4-dinitrophenyl)carbonate (DNPC), with a larger and more stable leaving group, as an alternative cyclic-transformation reagent (Scheme 1; step ix).⁶⁵ Glycine derivatives **3a** and **3k** were treated with DNPC in THF and refluxed over 8 hours. Conversions >70% were determined via ¹H-NMR (by monitoring the α -methylene peaks shifts) over the duration of the reaction. The successful preparation of **5a** and **5k** support our understanding that the rate limiting step of the 2nd stage was the formation of the immonium cation. Noteworthy,

Luxenhofer and coworkers were able to prepare **5a** via triphosgene (1/3 equivalence) under conditions not explored in our laboratory.³⁹ However, they report utilizing a different strategy for longer and branched alkyl groups.

In general, Leuchs' method of preparing NCAs included the formation of a carbamate ester and halogenation of the carboxylic acid which in turn induced cyclization.^{36a} This required two additional synthetic steps from the amino acid derivative but provided an efficient alternative to the Fuchs-Farthing method. Owing to the advancements in protection group designs, a number of carbamate esters can readily be produced quantitatively. In particular Zhang's and Luxenhofer's protocols included the addition of *tert*-butyloxycarbonyl (Boc) and carboxybenzyl (Cbz), respectively (Scheme 1; Pathway A; step iii and v).^{30, 38b} Likewise, we incorporated a Boc group in our synthetic efforts for **4k** and **4l** (Pathway B; step x). This was a modified one-pot-two-reaction approach first described by Liskamp which afforded us with material on the gram scale at yields >90% (**4l**: A3–A4).⁶²

An important feature in choosing which carbamate ester to utilize is the cyclization conditions and subsequent purification. Our rationale for choosing the Boc carbamate ester was due to Zhang's published protocol which utilized phosphorous trichloride at reduced temperatures (0 °C) to induce cyclization (step iv).^{38a} This would allow us to minimize hydrochlorination of the π systems (*ie.* alkene and alkyne) during the experiment. Contrarily, Luxenhofer's cyclization route included refluxing the *N*-alkyl pre-monomers in acetic anhydride with acetyl chloride (step vi).³⁹ Notably, they took advantage of the thermal stability of the Cbz-*N*-alkyl glycine derivatives and NNCA's whereas Boc groups are known to be thermally labile and *N*-unsubstituted α -amino acid NCA's readily undergo thermally induced bimolecular reactions.

Monomer purification plays a vital role in the degree of polymerization, molecular weight distribution, and architecture. Common impurities from the monomer synthesis include *N*-chloroformyl amino acid chlorides, HCl, α -isocyanato carboxylic acid chlorides, cyclic oligomers, and halogen byproducts (*ie.* *tert*-butylmethyl chloride, benzyl chloride, *etc.*). It is imperative to remove all these electrophiles for a nucleophilic initiated ring opening polymerization. These impurities/electrophiles lead to low initiator efficiency, chain termination, and chain transfer. Over the last 100 years, NCAs have frequently been purified by liquid-liquid extraction and recrystallization techniques. Sublimation and the use of adsorbent materials (*ie.* activated carbon) are less commonly reported. Choosing which technique to utilize greatly depends on the NCA and

monomer preparation procedure. For example, induced cyclization via PCl_3 with the Boc carbamate auxiliary would produce byproducts that should be soluble in H_2O or volatile enough to remove by vacuum but the newly formed NCA is at risk of being removed or reactive with the H_2O . Therefore, each NCA had to go through a series of trials and errors to determine the best purification procedure for that particular monomer. The purification of the monomer turned out to be the most time consuming and cumbersome component of the project. Our earlier efforts determined that the best results were achieved with the use of activated charcoal followed by recrystallization strategies (eg. **5a**→ CH_2Cl_2 /heptanes; **5f**→EtOAc/heptanes; **5l**→ Et_2O). Notably, many of these early ‘pure’ NCAs had a yellow hue to the crystal powder but no impurity was detected via NMR, FT-IR, or GC-MS. In particular, an intense yellow color was observed for monomers prepared with DNPC, presumably due to the 2,4-dinitrophenol byproduct (detectable by GC-MS), even after several recrystallization attempts which typically lead to loss of the monomer. These difficulties and the expense of the DNPC (ca. \$45 or €35 per gram) encouraged us to continue our investigations with the Leuchs’ method towards NNCA.

Our early attempts with the ROP of these *N*-substituted glycine NCAs produced mix results (discussed in the polymerization section). The lack of reproducibility and control of the monomer/initiator feed ratio suggested early chain terminations and/or chain transfers. Naturally, we suspected the purity of the monomers and investigated additional approaches to improve their purity. Deming and Kramer published successful purification of hydrophobic α -amino acid NCAs via flash chromatography.⁶⁶ The byproducts were much more polar and presumably would stick to the silica gel. Brief communications with Kramer suggested that their strategy was to utilize the difference in hydrophobic and hydrophilic nature of the NCAs and byproducts, respectively. We envisioned that this purification approach would be transferrable to our NNCA targets. Unfortunately, our *N*-allyl glycine NCA monomers were never recovered after being loaded onto the silica gel. (Purification with γ -benzyl L-glutamate NCA by Kai Krannig confirmed that we had prepared the silica gel and solvents as described by Kramer.) Further investigations with two-dimensional thin layer chromatography (2D TLC) supported our suspicions that the *N*-substituted glycine NCAs readily degrade on silica gel.

While pursuing higher monomer purity, Luxenhofer *et al.* released a publication disclosing the use of vacuum distillation for their *N*-alkyl glycine NCA targets. Due to their high yields, purity, and success in the subsequent co-polymerization of these monomers, we immediately adopted this technique and were pleased to see that vacuum distillation was applicable to most of the NNCA

(**5b–e** and **k**) whereas sublimation produced pure **5a** (A5–A7) and **5l** (A11–A13) as white powders with yields >70%. Interestingly, our initial efforts towards distilling **5k** at 120 °C, without vacuum, resulted in the collection of 1,4-diallylpiperazine-2,5-dione (DKP **13k**: A14–A16) as a white crystalline powder (ca. 30%) inside the water cooled condenser and small amounts of **5k** (6%: A8–A10). In addition, there appeared to be a yellow residue remaining in the initial flask and the majority of the monomers had increased stability allowing for longer storage times. Furthermore, improved purification allowed for reproducible, and therefore reliable, polymerizations.

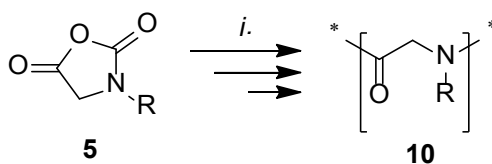
3.1.1.1 Summary of NNCA Preparation

In summary, the 3 step synthesis described by Zhang and Luxenhofer allowed for facile preparation of *N*-alkyl glycine NCAs (**5b–e**) (Scheme 1; Pathway A; Step i, iii/v, iv/vi) with modest overall yields (25–45%). Our synthesis of functional *N*-substituted glycine NCAs (**5k** and **l**) that combined Liskamp, Zhang, and Luxenhofer procedures resulted in pure monomer at the gram scale with modest yields (36–58%) (Pathway B; Step vii, x, iv: see Chapter 6: Experimental Procedures). Noteworthy, Zhang *et al.* proposed an alternative route towards *N*-(R)/(S)-1-phenylethane glycine NCAs that closely resembles this aforementioned approach.⁶⁷ A direct one-pot strategy from *N*-substituted glycine derivatives via DNPC treatment resulted in successful cyclization but was discontinued due to expense and challenges in purification (Step ix). Vacuum distillation or sublimation proved to be the superior purification technique for these *N*-substituted monomers due to scope of application and efficiency. Monomers **5f–j** were no longer being targeted due to the data released by the aforementioned authors. Likewise, monomers **5b–e** were prepared by Christian Secker and explicitly discussed in his Master of Science thesis,⁶⁸ as well as in a recent publication submission, and therefore will not be described in this dissertation.

3.1.2 Benzylamine Initiated ROP

Benzyl amine (BnNH₂) was utilized as the initiator for two main reasons: 1) this initiator was demonstrated to have high initiator efficiency (>80%) for α -amino acid NCA ROP; and 2) end group detection (α -terminus) should readily be observed by NMR and SEC (UV detection). Our initial attempts towards ring opening polymerization (ROP) of *N*-substituted glycine NCAs lead to high dispersity values (\mathcal{D} > 1.2) and low molecular weights (\bar{M}_n < 2000 g/mol, apparent). Utilizing *N*-methylglycine NCA as a model monomer, we saw slight improvements as recrystallization techniques improved. By employing low pressure and temperature techniques,⁶⁹ we observed a

significant improvement and were able to obtain polymers with $D < 1.2$ and closer to targeted molecular weights, albeit low molecular weight polymers were being targeted. However, we noticed a significant difference in polymerization when utilizing 1,4-dioxane or DMF as the solvent. To explore this we screened several solvents including 1–2% w/w of DMF, 1,4-dioxane, NMP, and CH_2Cl_2 (Table 1; **AP76**, **75**, **72**, **73**). These reactions were initiated ($[\text{M}]_0/[\text{I}]_0 = 40$) at low temperatures (-70 to 10 °C, depending on melting point of solvents) followed by reduction in pressure. The results indicated that low D values (< 1.1) were achievable when polymerizations were conducted in DMF or CH_2Cl_2 , where the latter halogen solvent produced molecular weights closer to the targeted value. In as much, we utilized these conditions towards the preparation of poly(*N*-allyl/propargyl/methyl glycine) homo- and co-polymers (Scheme 3).



Scheme 3. BnNH_2 initiated ROP of NCA **5a**, **k**, and/or **l**. (i) BnNH_2 , monomer, solvent, reduced pressure.

We initially began with exploring the homo-polymerization towards poly(*N*-allyl glycine) (PNAG) and poly(*N*-propargyl glycine) (PNPG) from their oil and crystalline monomers, respectively. While targeting relatively low monomer-initiator feed ratios ($[\text{M}]_0/[\text{I}]_0 = 40$ and 50) at concentrations as high as 10% w/w in CH_2Cl_2 , we observed quantitative conversions as determined by the consumption of the monomer by GC-MS monitoring (**AP80** and **AP130**). Notably, the end group (α/ω terminus) analysis by $^1\text{H-NMR}$, utilizing the benzyl peaks and backbone integration, suggested lower average degrees of polymerization ($\bar{n} = 33$ and 47 , respectively) than originally targeted. Accrediting these lower values to the overlapping benzyl and CHCl_3 peaks, we submitted **AP80** for quantitative analysis by MALDI-ToF MS. A Poisson distribution confirmed a well-defined PNAG material with an \bar{n} of 28 (M_p : $m/z = 2888.9$, $[(\text{C}_7\text{H}_8\text{NO})(\text{C}_5\text{H}_7\text{NO})_{28}(\text{C}_2\text{H}_3\text{O})]^- [\text{Na}]$) suggesting either early chain termination, chain transfer agents, or experimental error (*eg.* improper delivery of the initiator). We further investigated higher molecular weights ($[\text{M}]_0/[\text{I}]_0 = 150$) and observed similar limitations in the \bar{n} (**AP106** = 47 ; **AP109** = 32) even when consumption of the

monomer was confirmed by GC-MS. Careful MALDI-ToF MS analysis did not reveal an early termination product (*ie.* α -isocyanate ω -terminus) but did support well-defined polypeptoid architectures and $\mathcal{D} = 1.02$ – 1.03 . We therefore prepared a new solution of BnNH_2 in DMF (0.1 M) and targeted random and block copolymers.

Table 1. Molecular characterization of BnNH₂ initiated ROP from recrystallized *N*-R glycine NCAs obtained under different reaction conditions (*eg.* solvent).

Sample	R	Solvent	[M] ₀ / [I] ₀	\bar{M}_n^A (kg/mol)	\mathcal{D}^A	\bar{n}^B	\bar{M}_n^C (kg/mol)	\mathcal{D}^C	\bar{n}^C	Y ^D (%)
AP76	Me	Dioxane	40	4.41	1.42	38 ^G	–	–	–	33 ^E
AP75	Me	NMP	40	2.44	1.10	50 ^G	–	–	–	26 ^E
AP72	Me	DMF	40	2.46	1.05	29 ^G	–	–	–	18 ^E
AP73	Me	CH ₂ Cl ₂	40	3.34	1.06	30 ^G	–	–	–	18 ^E
AP80	Allyl	CH ₂ Cl ₂	40	2.34	1.17	33; 7 ^G	2.97 ^J	1.02	28	54 ^{FL}
AP130	Propargyl	CH ₂ Cl ₂	50	4.31 28.7	1.15 1.09	47 ^I	–	–	–	84 ^F
AP106	Allyl	CH ₂ Cl ₂	150	6.36	1.04	23 ^H	4.67 ^K	1.02	47	49 ^F
AP109	Propargyl	CH ₂ Cl ₂	150	4.18 20.8	1.09 1.09	12 ^H	3.20 ^J	1.03	32	23 ^F
AP107	(allyl)(propargyl)	CH ₂ Cl ₂	150	5.85 22.1	1.06 1.04	10 ^H	4.45 ^K	1.01	45	18 ^F
AP108	(allyl)(propargyl)	CH ₂ Cl ₂	150	4.93 19.4	1.06 1.04	29 ^H	n.d.	n.d.	n.d.	14 ^F
AP129	(Me)(propargyl)	CH ₂ Cl ₂	100	3.90 20.0	1.11 1.04	19 ^G	–	–	–	36 ^F

^AApparent number-average molecular weight (\bar{M}_n) and dispersity (\mathcal{D}), as determined by size exclusion chromatography (SEC), eluent: NMP + 0.5 wt% LiBr, 70 °C, stationary phase: PSS-GRAM, calibration: PS; ^BAverage number of repeat units, as determined by ¹H-NMR end group analysis; ^CMatrix-(DCTB)-assisted laser desorption/ionization time of flight mass spectrometry (MALDI-ToF MS) \bar{M}_n values are reported: the center peak with highest intensity was utilized to determine average degree of polymerization (\bar{n}) and residual mass; ^DGravimetric yield; Purification of the polymer was achieved by ^EDialysis: 1 kDa regenerated cellulose membrane against H₂O or THF; and/or ^Fprecipitation into Et₂O; ^GD₂O; ^HCDCl₃; ^IDMF-d₇; ^JReflector mode; ^KLinear mode; ^L2 steps: cyclization and polymerization.

We initially targeted poly[(*N*-allyl)-*r*-(*N*-propargyl) glycine] (**AP107**) and poly[(*N*-allyl)-*b*-(*N*-propargyl) glycine] (**AP108**) for the purpose of exploring orthogonal post-modification strategies. We targeted poly[(*N*-methyl)-*r*-(*N*-propargyl) glycine] (**AP129**) in hopes of increasing solubility for post-modification investigation in aqueous mediums. We targeted reasonable chain lengths ($[M]_0/[I]_0 = 150$ and 100 , respectively) and obtained a 1:1 incorporation for **AP107** and 2:1 for **AP108** (allyl:propargyl, $^1\text{H-NMR}$ analysis). Presumably due to gelation, a low average degree of polymerization ($\bar{n} = 19$) and incorporation was achieved for **AP129**. Interestingly, this sample did demonstrate improved solubility in H_2O with a bluish hue. In addition, we detected two peaks by refractive index (RI) during size exclusion chromatography (SEC) for the *N*-propargyl containing polypeptoids typically separated by 4 to 5 magnitudes for the co- and homo-polymers. Zhang *et al.* observed a similar phenomenon during their investigations of cyclic poly[(*N*-(*n*)butyl)-*r*-(*N*-propargyl) glycine] materials and attributed these findings to suspected aggregation.⁷⁰ Naturally, this suggests that the SEC conditions (NMP eluent, polyester gel) was not ideal for *N*-propargyl polypeptoids allowing for adsorption competition.

In addition to suspecting the solvent, CH_2Cl_2 , as a transfer agent, we began to question the purity of our monomers. Although we never detected impurities via NMR or GC-MS, we commonly observed a yellow tint to the monomer material and “spontaneous” reactivity after a fair number of recrystallizations. As described in the earlier section (NCA preparation) we investigated alternative purification strategies for these monomers. During these purification investigations, Luxenhofer *et al.* published the synthesis of *N*-alkyl side chain polypeptoids both as homo- and co-polymers.³⁹ In particular, they disclosed a facile purification strategy for their monomers utilizing vacuum distillation. Although distillation is a common purification tool in the laboratory, it was overlooked on many occasions due to previous reports that described α -amino acid NCAs as undergoing thermally induced ROP via a suspected zwitterion initiation mechanism as well as the scale required for distillation (>1 g).^{37c} In respect to Luxenhofer’s success with distillation and our need to produce large batches of functional material that would undergo post-modification screening, we adapted this procedure towards our efforts and discovered monomers without discoloration and increased stability towards storage, albeit *N*-allyl glycine NCA remained sensitive to environmental conditions. With this efficient and reproducible purification technique for our monomers, we returned our attention towards choosing an appropriate solvent.

We reinvestigated CH_2Cl_2 as a solvent candidate with our pure *N*-allyl glycine monomers and observed similar low molecular weight limits as before. The data suggests that low degrees of

polymerization targets ($[M]_0/[I]_0 = 20$ or 30) readily led to full conversions over a 2 to 4 day time span (Table 2). Contrarily, longer chain targets ($[M]_0/[I]_0 = 100$) appeared to reach an upper limit near $\bar{n} \approx 46$ around week 2. Full consumption of the monomer by week 3 and cyclic dimer products were detected by GC-MS. Likewise, we screened *N,N*-dimethylacetamide (DMA) and benzonitrile (PhCN) as possible substitutes and observed an upper limit of $\bar{n} \approx 33$ and 81 , respectively. Notably, GC-MS detected trace amounts of the monomer up to 30 days prior to termination via acetic anhydride suggesting significant stability in these solvents over CH_2Cl_2 . Overall, this solvent study appears to suggest that CH_2Cl_2 behaves as a transfer agent and promotes competing side reactions whereas PhCN supports polymerization presumably by a coulombic-cationic-interaction with the propagating species, essentially a Lewis acid/base interaction.

Table 2. Molecular characterization of BnNH₂ initiated ROP from distilled *N*-R glycine NCAs obtained under different reaction conditions (eg. solvent).

Sample	R	Solvent	[M] ₀ /[I] ₀	\bar{M}_n^A (kg/mol)	\mathcal{D}^A	\bar{n}^B	\bar{M}_n^C (kg/mol)	\mathcal{D}^C	\bar{n}^C	Y ^D (%)
AP159	allyl	CH ₂ Cl ₂	20	1.22	1.16	16	n.d.	n.d.	n.d.	72 ^F
AP164	allyl	CH ₂ Cl ₂	30	2.44	1.12	21	n.d.	n.d.	n.d.	84 ^F
AP162	allyl	CH ₂ Cl ₂	100	5.97	1.10	46	n.d.	n.d.	n.d.	100 ^F
AP144	allyl	DMA	100	2.17	1.23	33	n.d.	n.d.	n.d.	36 ^E
AP163	allyl	PhCN	100	4.15	1.10	81	–	–	–	59 ^F
AP182A	allyl	PhCN	20	2.05	1.07	18	2.28	1.01	20	100 ^F
BP25.25	allyl	PhCN	25	3.78	1.05	21	2.63	1.02	24	95 ^F
BP25.50	allyl	PhCN	50	6.90	1.04	35	4.51	1.01	44	91 ^F
BP25.75	allyl	PhCN	75	10.1	1.03	45	6.63	1.01	68	86 ^F
BP35.25	propargyl	PhCN	25	3.14	1.05	21	2.07	1.02	21	94 ^F
BP35.50	propargyl	PhCN	50	5.43	1.04	37	3.80	1.02	39	94 ^F
BP35.75	propargyl	PhCN	75	9.88	1.04	51	6.46	1.01	67	94 ^F
AP167A	allyl	C ₇ H ₁₆ ^G	400	10.3	1.10	94	n.d.	n.d.	n.d.	85 ^J
AP167B	allyl	C ₇ H ₁₆ ^H	400	23.5	1.33	101	n.d.	n.d.	n.d.	100 ^J
AP167C	allyl	C ₇ H ₁₆ ^I	400	28.9	1.39	108	n.d.	n.d.	n.d.	100 ^J
AP182D	allyl	C ₇ H ₁₆ ^G	100	9.52	1.03	46	7.84	1.01	80	100 ^J
AP182C	allyl	PhCN/C ₇ H ₁₆ ^G	400	24.2	1.04	49	n.d.	n.d.	n.d.	79 ^J

^AApparent number-average molecular weight (\bar{M}_n) and dispersity (\mathcal{D}), as determined by size exclusion chromatography (SEC), eluent: NMP + 0.5 wt% LiBr, 70 °C, stationary phase: PSS-GRAM, calibration: PS; ^BAverage number degree of polymerization, as determined by ¹H-NMR end group analysis in DMF-d₇; ^CMatrix-(DCTB)-assisted laser desorption/ionization time of flight mass spectrometry (MALDI-ToF MS) \bar{M}_n values are reported utilizing linear mode: the center peak with highest intensity was utilized to determine \bar{n} and residual mass; ^DGravimetric yield; Purification of the polymer was achieved by ^EDialysis: 1 kDa regenerated cellulose membrane against THF and/or ^Fredissolved in THF and precipitated in heptanes; BnNH₂/NMP (1.0 M) was injected into ^Gthe high stirring reaction solution, ^Hstagnant heptanes layer; ^Ior directly into the monomer; ^Jcrude yield contains monomer.

These refined conditions were applied to a series of PNAG (**10k**) and PNPG (**10l**) homopolymers (**AP182A–BP35.75**; Exemplarily: see A20–A34 and A35–A44 for characterization and thermal analysis data of **BP25.50** and **BP35.50**, respectively). We targeted low to “high” molecular weights ($[M]_0/[I]_0 = 20, 25, 50, \text{ and } 75$) which would proceed to completion within 2 weeks. We observed well-defined polymers ($D = 1.03\text{--}1.07$) where the architectures were confirmed by MALDI-ToF MS analysis with \bar{M}_n s ranging from 2.1 to 6.6 kg/mol. Exemplarily, **BP25.75**'s (10k) corresponding $^1\text{H-NMR}$ (DMF- d_7) and MALDI-ToF MS (Linear mode; DCTB matrix) spectra are shown in Figure 6. As illustrated, boxes F and G are assigned to the alkene, A to the aromatic (α -terminus), H to the acetyl group (ω -terminus), and E/B/C/D as overlapping peaks associated to the backbone. The number of repeating units can readily be calculated by summing up the integration associated to the repeating unit and dividing this by the number of hydrogens ($H = 7$). Then take the integration of the aryl group and divide by the number of hydrogens associated to this end group ($H = 5$). Finally, divide the repeating unit adjusted integration by the end group adjusted integration to receive the average number of repeating units ($\bar{n} = 45$). $^1\text{H-NMR}$ analysis provided an in house facile calculation of the overall success of these polymerizations but for quantitative molecular weights and end group analysis, samples were submitted for MALDI-ToF MS measurements and analyzed as follows: the center peak ($m/z = 6771.7$) was subtracted by the sodium mass (23.00 Da) and then divided by the repeating unit mass ($\text{C}_5\text{H}_7\text{NO} = 97.05$ Da) to provide the approximate average repeating units including residue mass fraction (69.53). Subtracting the whole number (68) allowed for the determination of the residue mass fraction (1.53) and multiplying this by the repeating unit mass (97.05 Da) provides the end-group mass (148.49 Da) which corresponds to expected values (BnNH/Ac, $\text{C}_9\text{H}_{11}\text{NO} = 149.08$). Finally, the repeating unit mass was confirmed by the calculation of the average distance between the peaks ($\Delta m = 97.1$ Da). Notably, the values for \bar{n} , calculated by $^1\text{H-NMR}$, were always lower than the calculated values from MALDI-ToF MS analysis. We originally attributed this to poor solubility of the material in D_2O , overlapping of the residue peaks of CDCl_3 or THF- d_6 , and/or the associated error (ca. 10%) with NMR integration calculations. In hindsight we suspect that the purification process (precipitation into petroleum ethers at room temperatures) of these polymers was not sufficient in removing the unincorporated initiator species (BnNHAc) and therefore influenced the calculations towards lower than true \bar{n} values. Contrarily, this purification technique was efficient in removing excess acetic anhydride (terminating agent) and PhCN (solvent residue).

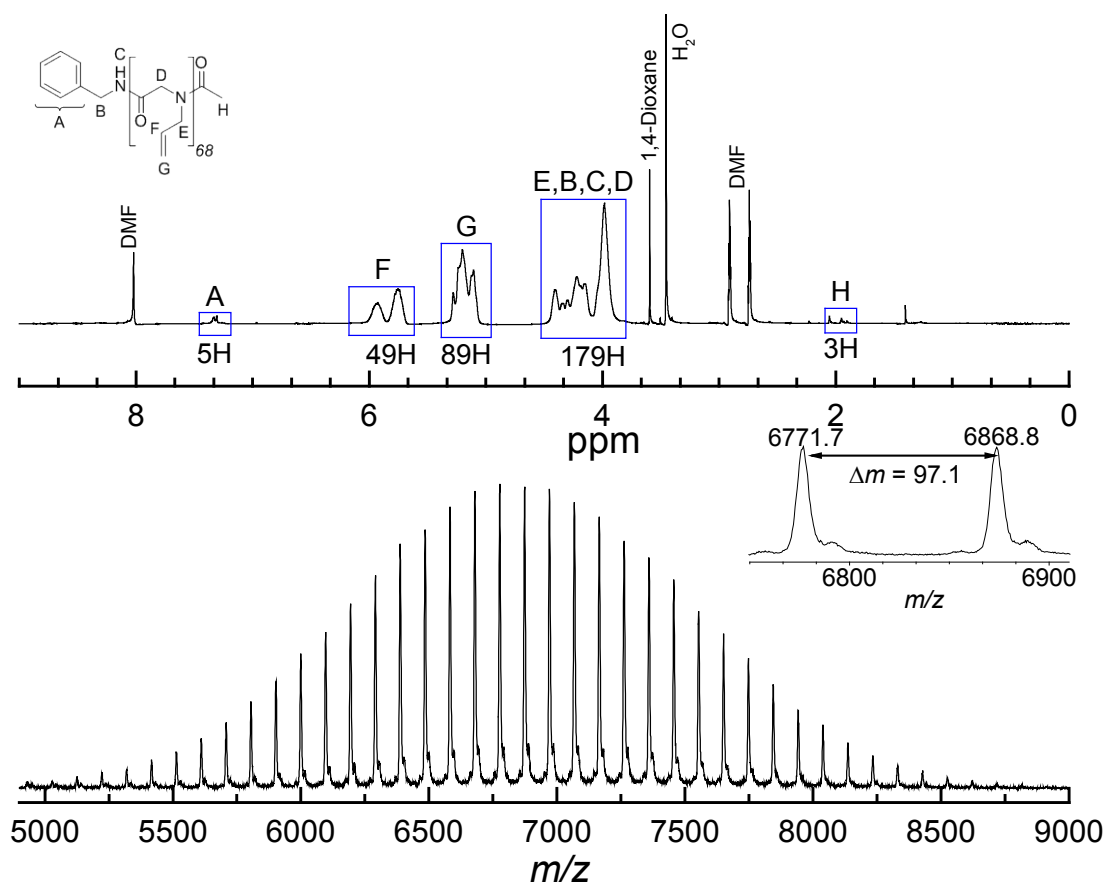


Figure 6. Exemplarily ¹H-NMR (top) and MALDI-ToF MS (bottom) of 10k (BP25.75).

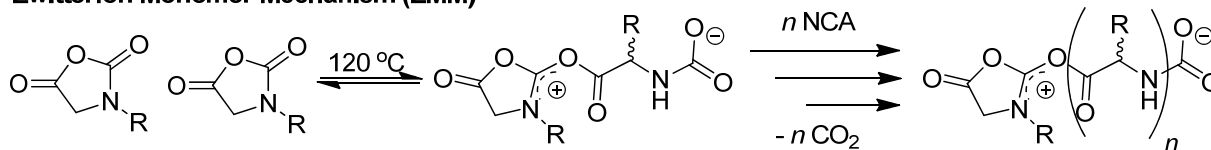
As previously mentioned, the monomers appeared to have a greater stability when distillation/sublimation was utilized as the purification technique. In fact, *N*-propargyl and *N*-methyl glycine NCAs were commonly transferred from the sublimation apparatus to reaction/storage flasks while being exposed to the environment for short durations. This seemed to hold true for most of the other *N*-alkyl glycine NCAs produced in our laboratory except for *N*-allyl glycine NCA. Once exposed to the environment, the monomer (translucent oil) would react and become a hard plastic like material within 2 hours. To prevent this, the monomer was continuously kept under an inert atmosphere (*ie.* Argon) and stored under heptanes (for 1 or 2 days). One day while stored under these conditions in a round bottom flask with minor scratches in the glass, we observed a truncated plastic material evolve in the center of the flask. Suspecting that the truncated shape was due to carbon dioxide (CO₂) release during a bulk polymerization, the material was dissolved in DMF and submitted for SEC analysis (NMP). Surprisingly, we detected the largest apparent number-average molecular weight ($\bar{M}_n = 21.5$ kg/mol) that we had received so far (Table 1 and 2: $\bar{M}_n = 1.2$ – 10.1 kg/mol). As mentioned in the Introduction, one of our main goals of this project was to prepare

functional polypeptides with greater molecular weights not previously achievable with poly(α -allyl glycine) homopolymers. Although we had already surpassed the molecular weights of the aforementioned project, we wanted to test the upper molecular weight limits for this new material, poly(*N*-allylglycine). Therefore we attempted a series of heterophase/bulk polymerizations in heptanes (Table 2; **AP167A–AP182D**).

We initially considered three approaches towards accomplishing bulk polymerization. The first two were designed to replicate and understand the previous observation. This included the addition of the initiator solution (1.0 M BnNH₂/NMP; ([M]₀/[I]₀ = 400) into a stagnant system by injecting into the heptanes (C₇H₁₆) layer (**AP167B**) or directly into the monomer layer on the bottom of the flask (**AP167C**). The third approach included high stirring in an attempt to create an emulsion between the monomer and heptanes (**AP167A**). Acetic anhydride was injected approximately 6 hours later to terminate the reactive ends at which point the heptanes were decanted off. No further purification was utilized and samples were analyzed as is. GC-MS detected monomer in each of these samples and ¹H-NMR (\bar{n} = 94–108) with SEC (\bar{M}_n = 10.3–28.9 g/mol) supported polymerization. Unfortunately MALDI-ToF MS analysis was not determined (n.d.) from these samples presumably due to their respectively higher polydispersity index values ($D \geq 1.1$). These results suggested that the high stirring reaction conditions readily leads to well-defined polymers with high molecular weights in a relatively short time frame (6 hours versus a month). In addition, we noticed that only 25% of the targeted average degree of polymerization was achieved and hypothesized that this was the point at which the polymer precipitated out of the monomer solution or the ω -terminus became inactive for other unknown reasons. To investigate this further we prepared 2 additional reactions with different monomer/initiator feed ratios ([M]₀/[I]₀ = 100 or 400) and solvent conditions (C₇H₁₆ or PhCN/C₇H₁₆ [7:30 mL], respectively) at room temperature and stirred them on the highest setting. As before, we obtained relatively high molecular weights over a short reaction time but with lower D values (1.03 and 1.04) where **AP182D** was analyzed by MALDI-ToF MS confirming the architecture and appropriate end groups. Unfortunately we were unable to confirm by these results whether the chain growth inhibition was caused by phase separation or ω -terminus deactivation albeit the MALDI-ToF MS spectrum for **AP182D** (A45–A47) does not detect any alternative α/ω -termini. Likewise, end group analysis by ¹H-NMR does not provide any reliable insight between these bulk polymer materials due to poor removal of the initiator species under the prescribed purification strategy.

Due to the success in utilizing atypical conditions for ROP of NCAs we decided to conduct a short investigation of utilizing heat to promote or speed up the kinetics towards polypeptoids. As previously described, we typically initiated these polymerizations at either temperatures below 0 °C or at room temperature (ca. 23 °C). As before, we decided to utilize *N*-methyl glycine NCA as a model monomer for this investigation. The monomers were dissolved in PhCN and prepared in Erlenmeyer flasks (3) under Argon. One reaction was utilized as the control and initiated at room temperature while the other two were heated by either microwave irradiation (345 W) or oil bath (180 °C) prior to initiation ($[M]_0/[I]_0 = 50$). These reactions were monitored by GC-MS and SEC at set intervals (T_0-T_7) over 123.5 minutes (Figure 7). Monomer was still detectable when the reactions were terminated with acetic anhydride and precipitated into EtO. As illustrated in the plotted graph, the reaction at R.T. affords a gradual molecular weight increase between $T_0 = 0$ to $T_7 = 3,010$ g/mol. Contrarily, the heated reactions had detectable molecular weights prior to the addition of the initiator (oil: $T_0 = 3,156$ g/mol; M.W.: $T_0 = 171$ g/mol) supporting Kricheldorf's zwitterion initiation proposal (Scheme 4).^{37a, 37c} Noteworthy, contaminants such as H₂O cannot be ruled out under these reaction conditions and PhCN became discolored at these elevated temperatures suggesting degradation or side reactions. Furthermore, higher molecular weights were achieved within the first ca. 3 minutes and then gradually decreased through the remainder duration of the reaction suggesting slow initiation or transfer reactions. Overall, this short study deterred us from any further investigations towards utilizing elevated temperatures for ROP of NCAs in solution.

Zwitterion Monomer Mechanism (ZMM)



Scheme 4. Proposed zwitterion monomer mechanism that occurs at elevated temperatures leading to a separate competitive polymerization pathway.

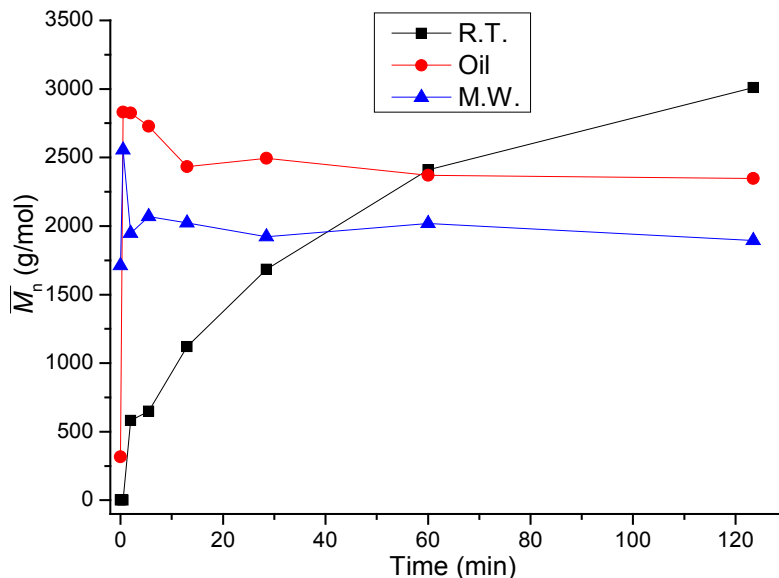


Figure 7. Evolution of apparent molecular weights with time for polymerization of N-methyl glycine at room temperature (R.T.), 180 °C (oil), and under microwave irradiation (M.W.) in PhCN.

3.1.3 Anionic/Promoted ROP Investigations

Anionic ROP of NCAs have previously been explored by several groups utilizing alkoxides, lithium agents, and hindered bases as either coinitors with alcohols or as the α -terminus end group. For α -amino acid NCAs the activated monomer initiation/mechanism led to uncontrolled and ill-defined polypeptides (cyclic and linear). *N*-methylglycine NCA was utilized in many of these studies to confirm/support this alternative initiation by demonstrating the lack of initiation under basic or thermo conditions.^{37-e} We envisioned that this suppression of the AMM could be exploited towards our efforts to achieve higher molecular weights not yet realized with primary amine initiated ROP, as described in the previous section. Exemplarily, Zhang *et al.* has been able to demonstrate in a number of publications successful incorporation of a *N*-heterocyclic carbene (NHC) towards cyclic and, more recently, linear well-defined polypeptoids with molecular weights >10 kg/mol.^{30, 38, 67, 70-71} Such carbenes are notorious for their strong nucleophilic and Bronsted base character which have been exploited towards accelerating the kinetics of other ROPs (*eg.* lactides). In as much, we decided to explore co-initiator/promoter systems towards achieving anionic ROP.

This work began as a collaboration with Junpeng Zhao, a former post-doctoral group member. At the time he was exploring the utilization of “superbases” towards the promotion of ROP of ethylene oxide (EO) to achieve poly(ethylene oxide) (PEO) homo- and co-polymers. Exceptionally, he was able to demonstrate the grafting from PNiPAAm via the amide

deprotonation with 1-*tert*-butyl-4,4,4-tris(dimethylamino)-2,2-bis[tris(dimethylamino)-phosphoranylideneamino]-2 λ^5 ,4 λ^5 -catenadi(phosphazene) (*t*-BuP₄) (Figure 8) which in turn initiated ROP of EO. He was able to achieve a series of brush like copolymers with unique thermoresponsive behavior. In as much, we rationalized that grafting *N*-methyl glycine NCA from PNiPAAm would provide similar/comparable results. Unfortunately, our first attempt at treating a mixture of PNiPAAm and *N*-methyl glycine NCA with *t*-BuP₄ was unsuccessful. The results suggested that ROP did occur but not from the amide side chains. To understand why the grafting from approach may have failed, we turned to a model system with benzamide and *t*-BuP₄.

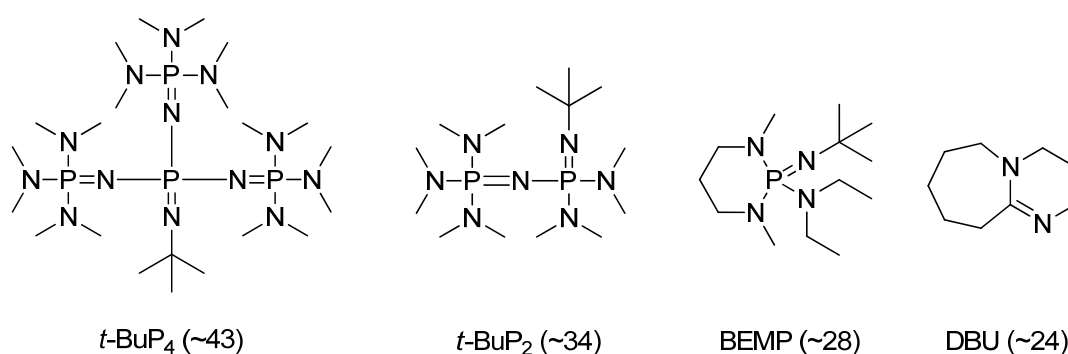


Figure 8. Various ROP promoters. In parenthesis, the approximate pK_a values for the conjugate acids of these Bronsted bases in ACN are listed.

Benzamide was chosen as the α -terminus due to its end group analysis potential either by SEC-UV or ¹H-NMR. In addition, the benzamide should be sterically less hindered than the isopropyl amides found as the side chains of PNiPAAm and therefore improved incorporation (initiator efficiency) was probably achievable. Once again, *t*-BuP₄ was chosen due to Junpeng's previous efforts which demonstrated the activation/deprotonation of such amides as well as the high kinetic inter-bimolecular transfer of the protons by the amide systems and propagating species. We prepared 3 reaction vessels with two of the sealable flasks containing benzamide ([M]₀/[I]₀ = 40) and *N*-methyl glycine NCA (Sar) where the third consisted of only the monomer in THF. Once the reaction solutions were cooled to -75 °C, *t*-BuP₄ (1:1 to benzamide; 1 M in hexanes) was added to one of the initiator and monomer mixtures and to the monomer only solution. The internal pressure was reduced (1.8x10⁻² mbar) and sealed at which point the reaction mixtures were allowed to warm to room temperature. Precipitation was observed for the reactions containing *t*-BuP₄ and the reactions were terminated with acetic anhydride. SEC confirmed polymerization of the reaction vessels treated with *t*-BuP₄ (with and without benzamide; Table 3, **AP74–AP79**). The reaction

solution with initiator and monomer produced a negative result confirming that benzamide by itself does not initiate ROP of *N*-methyl glycine NCA, as expected. Furthermore, GC-MS detected benzamide and monomer in this aforementioned reaction whereas benzamide was only detectable in the reaction not treated with *t*-BuP₄. After dialysis (1 kDa/H₂O), ¹H-NMR analysis (D₂O) confirmed that the benzamide was not incorporated as the α-terminus and it was unclear from the spectrum what the α-terminus may have been. MALDI-ToF MS was unable to provide a reasonable result for further end group analysis. Overall, this study suggested that the coinitiator, *t*-BuP₄, was promoting ROP but not through the benzamide. This was contrarily to our understanding with the EO systems, so we investigated further by NMR studies of the initiator with *t*-BuP₄.

Benzamide proved not to be soluble in THF-d₈, apparently part of the original problem, so *N*-methyl benzamide (NMBA) was utilized for these studies and future polymerization attempts. NMBA and *t*-BuP₄ were prepared in separate NMR tubes with THF-d₈ and measured by ¹H-, ¹³C-, and/or ³¹P-NMR (Figure 9). The NMBA solution was treated with *t*-BuP₄ and immediately measured by ¹H- and ¹³C-NMR (³¹P did not provide any additional insight). We observed the amide peak (7.6 ppm) disappear and a shift in the aromatic region (from 7.4/7.8 to 7.1/8.3 ppm) and concluded successful activation of the initiator. In addition, peaks related to the conjugate acid of *t*-BuP₄ are observable (from 1.2 to 1.3 ppm) supporting this conclusion. Our effort to analyze PNiPAAm with *t*-BuP₄ was thwarted by heterophase separation presumably induced by the hexanes of the *t*-BuP₄ solution; although there were suggestive peaks to support activation of the amide moiety. Satisfied that the coinitiator system was activating the initiator, we returned to our amide initiated ROP of *N*-methyl glycine NCA investigations.

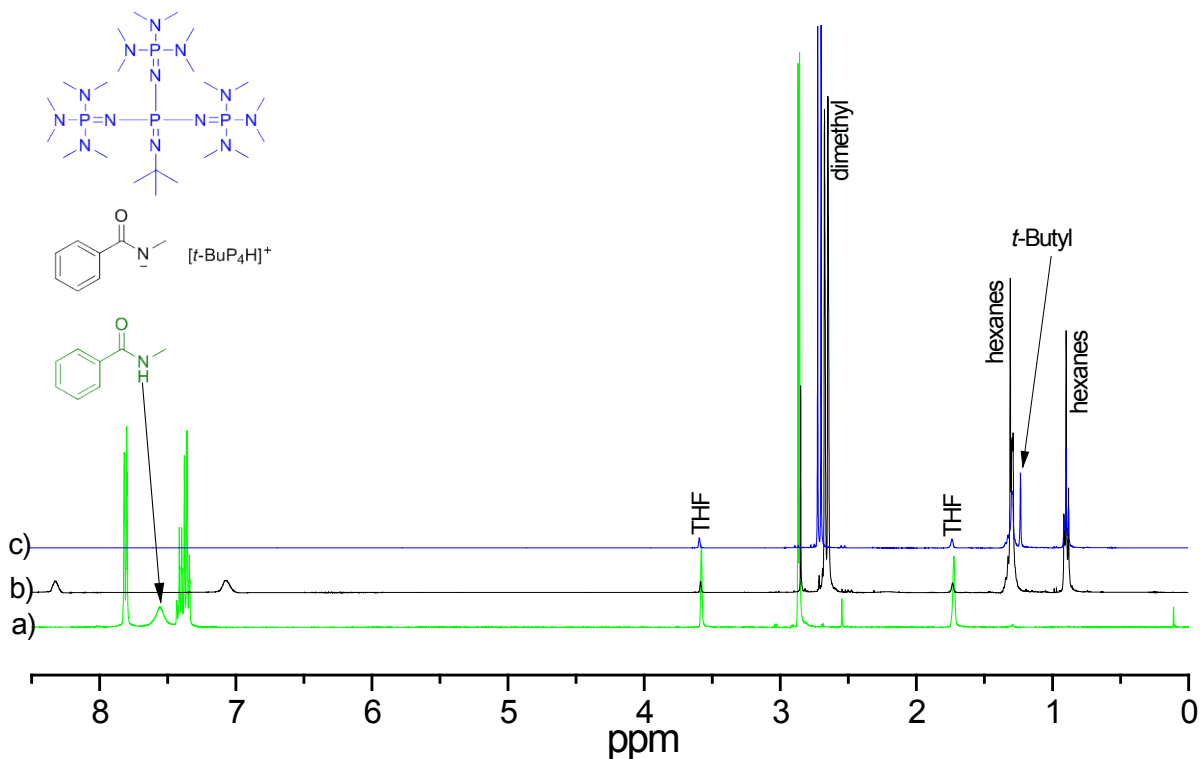


Figure 9. ^1H NMR spectrum of a) *N*-methyl benzamide, b) *N*-methyl benzamide treated with *t*-BuP₄, and c) *t*-BuP₄ overlaid to illustrate chemical shifts related to initiator activation.

To suppress the ROP initiation by possible impurities (NCAs were being purified by recrystallization), the amide moieties (*ie.* NMBA (AP91: A65–A66) and PNiPAAm (AP92)) were treated with *t*-BuP₄ prior to mixing with *N*-methyl glycine NCA. The reactions were monitored by ^1H -NMR (T_0 – T_0) to determine consumption of the monomer (<2 hours). Noteworthy, the α -methylene peaks associated with the NCA and polypeptoid overlapped making it impossible to complete an accurate kinetic study or determine 100% consumption of the monomer. Once again, precipitation was observed within 20 minutes of exposing NCA to the initiator solution. The homopolymer batch was purified by precipitation in Et₂O and washed through an ion exchange column (to remove [t-BuP₄H]⁺) where ^1H -NMR (D₂O) analysis detected trace amounts of the aromatic peaks associated to the α -terminus. Further analysis by GC-MS suggested that the NMBA was not incorporated into the polymer. SEC supported polymerization ($\bar{M}_n = 4.0$ kg/mol; $D = 1.2$) and MALDI-ToF MS analysis provided mix results suggesting some incorporation of the NMBA as well as without but overall was inconclusive (spectrum had a lot of noise). Likewise, the analysis

of the reaction with PNiPAAm (after dialysis purification) suggested some incorporation (slight shift in SEC; \bar{M}_n from 48.0 to 52.5 kg/mol) and a separate low molecular weight polymer (SEC 2nd peak: $\bar{M}_n = 1.64$ kg/mol). We concluded from these results that activated amides were not an efficient initiator for ROP of NCAs either due to steric hinderance or competing/dominating side reactions caused by a slow initiation.

Table 3. Amide or alcohol promoted ROP related results.

Sample	Monomer	Initiator	Promoter	[M] ₀ /[I] ₀	Time (hour)	\bar{M}_n^A (kg/mol)	\bar{M}_w^A (kg/mol)	\bar{D}^A
AP74	Sar ^B	Benzamide	<i>t</i> BuP ₄ ^I	40	36	3.10 ^{K,M}	3.83	1.2
AP78	Sar ^B	Benzamide	–	40	36	n.d.	n.d.	n.d.
AP79	Sar ^B	–	<i>t</i> BuP ₄	40	36	2.49 ^{K,M}	3.16	1.3
AP91	Sar ^B	NMBA	<i>t</i> BuP ₄ ^J	50	12	4.02 ^{K,M}	4.82	1.2
AP92	Sar ^B	PNiPAAm ^F	<i>t</i> BuP ₄ ^J	40	12	1.64 ^{K,M} 52.5 ^{L,M}	2.21 55.0	1.4 1.05
AP92.1	Sar ^B	PEO-OH ^G	<i>t</i> BuP ₄ ^I	40	36	2.11 ^{K,M}	3.53	1.7
AP120	Sar ^D	PEO-OH ^G	<i>t</i> BuP ₂ ^I	70	12	8.95 ^{K,M}	9.54	1.07
AP128	Sar ^D	PEO-OH ^G	<i>t</i> BuP ₂ ^J	70	12	7.26 ^{L,M}	12.5	1.7
AP138 ^c	Sar ^D	PEO-OH ^G	<i>t</i> BuP ₂ ^J	75	36	n.d.	n.d.	n.d.
AP142 ^c	Sar ^D	PEO-OH ^G	<i>t</i> BuP ₂ ^J	75	12	2.27 ^{L,M} 7.07	2.60 7.45	1.1 1.1
BP65	Sar ^D	PEO-OH ^G	<i>t</i> BuP ₂ ^J	70	12	2.04 ^{K,M}	2.42	1.2
BP65	Sar ^D	PEO-OH ^G	BEMP ^J	70	12	1.59 ^{K,M}	2.01	1.3
BP65	Sar ^D	PEO-OH ^G	DBU ^J	70	12	1.56 ^{K,M} 4.19	1.65 4.46	1.06 1.06
AP123	Sar ^D	–	<i>t</i> BuP ₂	70	48	2.66 ^{K,M}	3.41	1.3
AP92.2	Sar ^B	PEO-OH ^G	–	40	36	n.d.	n.d.	n.d.
AP124	Sar ^D	PEO-OH ^G	–	70	48	13.4 ^{K,M}	18.5	1.4
AP125	Sar ^D	PEO-OH ^G	–	70	36	7.26 ^{L,M}	12.5	1.7
AP139 ^c	Sar ^D	PEO-OH ^G	–	75	48	n.d.	n.d.	n.d.
AP140 ^c	Sar ^D	BnNH ₂	–	212	36	5.47 ^{L,M}	6.62	1.2
AP140 ^c	Sar ^D	PEO-NH ₂ ^H	–	84	24	6.46 ^{L,M}	6.94	1.07
AP82	Glu ^C	–	<i>t</i> BuP ₄	40	36	7.36 ^{K,M}	9.39	1.3
AP133	Glu ^B	–	<i>t</i> BuP ₂	70	36	35.0 ^{K,M}	52.4	1.5
AP134	Glu ^B	PEO-OH ^G	–	70	48	n.d.	n.d.	n.d.
AP132	Glu ^B	PEO-OH ^G	<i>t</i> BuP ₂ ^J	70	48	199 ^{K,M}	550	2.8

^aApparent number-average molecular weight (\bar{M}_n), weight-average molecular weight (\bar{M}_w), and dispersity (D), as determined by size exclusion chromatography (SEC), eluent: NMP + 0.5 wt% LiBr, 70 °C, stationary phase: PSS-GRAM, calibration: PS; The monomer was previously purified by either ^bRecrystallization, ^cChromatography, or ^dSublimation; ^eThese reactions were performed in DMA; ^f $\bar{M}_n = 48.0$ kg/mol, $D = 1.11$ (PS); ^g $\bar{M}_n = 3.48$ kg/mol, $D = 1.05$ (PS); ^h $\bar{M}_n = 2.60$ kg/mol, $D = 1.07$ (PS); The promoter/coinitiator was added to either ⁱa mixed solution of initiator and monomer or ^jto the initiator first followed by the addition of the monomer; ^kMeasurement was taken without purification; ^lMeasurement was conducted after dialysis (500-1,000 Da/H₂O).

Alcohols (alkoxy moieties) are attractive initiators and α -terminus units due to their broad abundance in natural products and subsequent cleavable ester bonds. Drug conjugates have frequently been utilized to improve pharmacokinetics and site specificity. They are typically constructed as separate components consisting of an active agent (drug), scaffold carrier (polymer), and targeting agent (receptor binding moiety) which are combined via a myriad of coupling reactions including Diels-Alder, Huisgen, and thiol-ene/yne “click” reactions. Quite often, these conjugated systems utilize designed weak points to release the drug under prescribed conditions. For example, peptide therapeutics were designed with particular amino acid sequences that allowed for enzymatic recognition and subsequent hydrolysis. Likewise, ester groups have been extensively investigated as linkers or hydrolytically cleavable bonds. In as much, we envisioned that an alcohol containing natural product (active agent) could be utilized as an initiator towards the ROP of NNCA (biopolymer) and terminated, or post-modified, with carbohydrates (targeting agent) all in one-pot.

A model system utilizing a primary alcohol, as the initiator, and *N*-methyl glycine NCA (Sar), as the polymer backbone, where acetic anhydride was employed, for convenience, as the ω -terminus was explored. We originally considered utilizing benzyl alcohol as the primary alcohol for these studies but due to the difficulties related to determining the incorporation of the benzamide in our earlier studies we elected to explore PEO-OH ($\bar{M}_n = 3.48$ kg/mol, $D = 1.05$) as a macro-initiator which could readily be monitored by SEC. In addition, we expanded our investigations to include other commonly explored promoters (*ie.* 1-*tert*-butyl-2,2,4,4,4-pentakis(dimethylamino)-2 λ^5 ,4 λ^5 -catenadi(phosphazene) (*t*-BuP₅), 2-*tert*-butylimino-2-diethylamino-1,3-dimethylperhydro-1,3,2-diazaphosphorine (BEMP), and 1,8-diazabicyclo[5.4.0]undecene (DBU); Figure 8) towards alcohol promoted initiated ROPs. Furthermore, three control reactions which included 1) the

monomer and the promoter without initiator (**AP79**, **AP123**), 2) monomer and initiator without the promoter (**AP92.2–AP139**), and 3) *N*-methyl glycine NCA with PEO-NH₂ as the macro-initiator (**AP140**) were exploited to assist in determining the initiator system and efficacy of utilizing these alternative initiator systems (Table 3). Finally, γ -benzyl-L-glutamate NCA (Glu), a common monomer explored in high molecular weight ROPs of NCAs, was utilized for comparison and possible application towards α -amino acid NCAs ROP via promoted alcohol initiation (**AP82–AP132**).

Our initial investigations included combining PEO-OH and *N*-methyl glycine NCA in THF followed by treatment of *t*-BuP₄ or *t*-BuP₂. By SEC, a low \bar{M}_n value (2.1 kg/mol) for *t*-BuP₄ was determined suggesting no inclusion of the macroinitiator whereas a reasonable \bar{M}_n value (8.9 kg/mol) for *t*-BuP₂ was observed. Our control reaction (**AP123**) consisting of PEO-OH and monomer did not lead to any detectable polymerization. Contrarily, monomer treated with *t*-BuP₄ and *t*-BuP₂ readily lead to low \bar{M}_n values of 2.49 and 2.66 kg/mol, respectively. Concerned with the competition of ROP via the promoters, we adjusted the preparation of these polymerizations to include the treatment of the initiator with the promoter prior to the addition of the monomer. In as much, we detected an apparent \bar{M}_n value of 7.26 kg/mol when treated with *t*-BuP₂ (**AP128**). Noteworthy, during these polymerizations in THF we observed precipitation within 1 hour of combining monomer and promoter. In this context, DMA was explored as an alternative solvent which resulted in no detectable (n.d.) polymerization by SEC (**AP138**). Suspecting contamination during the preparation may have caused these unlikely results, we re-prepared the reaction and observed two peaks on the chromatogram of the SEC (**AP142**; Figure 10). The peak associated with the lower M_p value (2.27 kg/mol) was attributed to unincorporated PEO-OH whereas the higher M_p value (7.1 kg/mol) was assumed to include PEO. Analysis by ¹H-NMR, after dialysis, supports inclusion whereas MALDI-ToF MS only detected PEO-OH. The control with PEO-OH and *N*-methyl glycine NCA in DMA produced no detectable polymer within 48 hours. Further injection of BnNH₂ confirmed the stability of the monomer in DMA by producing a polymer with an apparent \bar{M}_n of 5.47 kg/mol. Overall; the polymerizations in DMA did not lead to improvements in molecular weights, via increased solubility, but did increase the opportunity for impurities to be introduced into the reaction mixture.

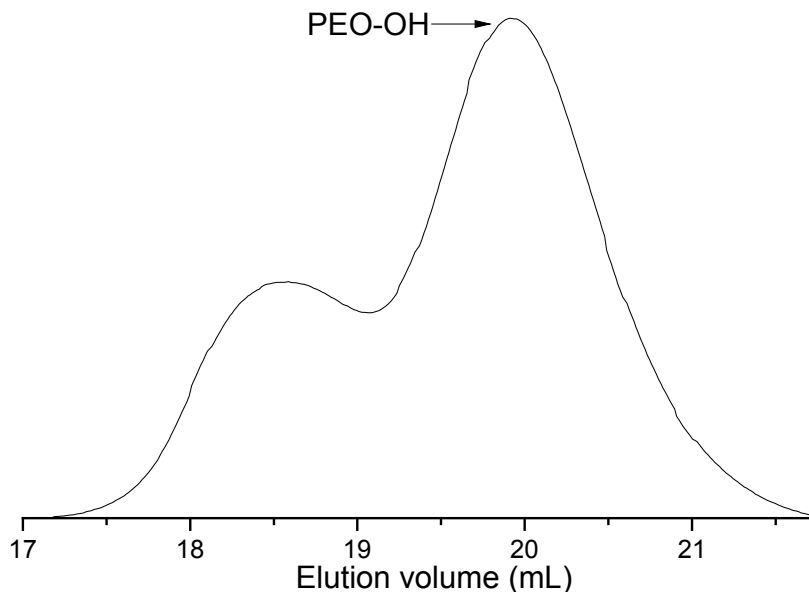


Figure 10. SEC elugram (NMP, RI) of **AP142** after dialysis illustrating unincorporated PEO-OH.

The conditions for the remaining investigations included, ultra-dry, THF as the solvent, sublimated *N*-methyl glycine NCA, and PEO-OH prepared by washing with THF and drying by high vacuum (12 hours). The promoters (when utilized) were used as is from their respective reagent bottles. The screening of PEO-OH treated with *t*-BuP₂ or BEMP produced a polymer with a lower molar mass (2.0 or 1.6 kg/mol) than the macro-initiator once again supporting the lack of control due to a competing initiation process. The promoter DBU resulted in a slight \bar{M}_n increase (from 3.5 to 4.2 kg/mol) as well as a lower \bar{M}_n (1.56 kg/mol) suggesting partial inclusion of the PEO. Significantly, the control with no promoter (**AP124**: A69–A70) produced a polymer with an apparent \bar{M}_n of 13.4 kg/mol which was in contradiction of the previous result, **AP92.2**. An additional control (**AP125**) was conducted and supported this finding that PEO-OH with *sublimated* *N*-methyl glycine NCA readily lead to PEO-b-PNMG without an external promotion. We attribute this finding to the common impurity HCl found associated to recrystallized NCAs which in turn reduces the availability of the electron rich cyclic carbamate from coordinating/deprotonating the PEO-OH and therefore suppressing initiation as observed from sublimated *N*-methyl glycine NCA. Alternatively, PEO-NH₂ (**AP140**: A75–A76) readily led to a polymeric material with a similar \bar{M}_n value (6.5 kg/mol) and reduced \mathcal{D} (1.07). These results indicate that there are no advantages to utilizing PEO with an alcohol over an amine ω -terminus as an initiator except for cost.

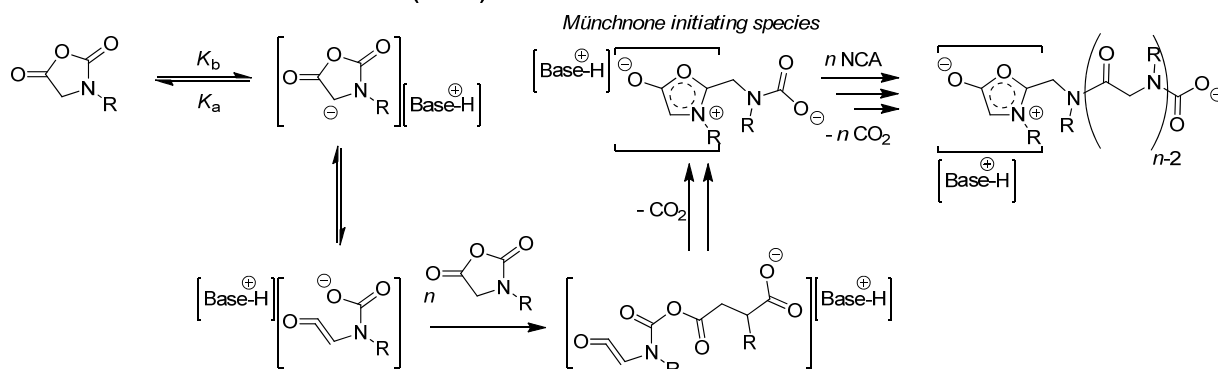
To finalize this anionic/promoted ROP investigation, γ -benzyl-L-glutamate NCA (Glu) was tested under the aforementioned conditions with t -BuP₁ and t -BuP₂. When the monomer was treated with the promoters exclusively, apparent \bar{M}_n values of 7.36 (AP82) and 35.0 (AP133: A73–A74) kg/mol were determined whereas no polymerization was detectable when monomer and PEO-OH was stirred for 48 hours without promoter. When PEO-OH was treated with t -BuP₂ prior to the addition of the monomer, a \bar{M}_n value of 199 kg/mol (AP132: A71–A72) was determined by SEC. Significantly, AP82 was followed by SEC and illustrated that the polymerization goes through a bimodal reaction sequence suggesting two competing mechanisms and once again supporting the AMM as previously described. In the end, these results reconfirm our understanding that anionic/promoted ROP of *N*-unsubstituted α -amino acids NCAs leads to ill-defined systems due to competing mechanisms and undesirable termination sequences warranting our investigations with *N*-substituted glycine NCAs.

3.1.4 Summary of Nucleophilic ROP of NNCAs

Distilled monomers (*N*-allyl/propargyl/methyl glycine NCA) in PhCN initiated with a traditional primary amine (BnNH₂) readily afforded well-defined polymers up to absolute \bar{M}_n s of 6.7 kg/mol and $D < 1.1$. A bulk polymerization strategy with *N*-allyl glycine NCAs afforded polypeptoids with greater apparent \bar{M}_n s up to 28.9 kg/mol over a relatively shorter time frame (½ day versus a month). Further analysis by mass spectrometry suggested that the purification technique of precipitating polymer solution into heptanes was ineffective in removing unincorporated initiator species which affected ¹H-NMR end group analysis overall suppressing the actual degree of polymerization calculations. Likewise, an attempt at creating a calibration curve for SEC utilizing MALDI-ToF MS suggested non-optimal conditions were achieved when NMP was utilized as the eluent. However, the results appear to suggest that quantitative \bar{M}_n s >10 kg/mol are not achievable with allyl or propargyl as the side chain under either solution or bulk polymerization conditions. Further work towards increasing molecular weights, as well as expanding the initiator system, by exploiting the intrinsically suppressed AMM via alcohol promoted ROP of model NCAs illustrated little to modest incorporation of the initiator system (*ie.* NMBA or PEO-OH). In fact, these reactions were plagued by inconsistencies, presumably, created by impurities and competing reaction pathways including a suspected alternative activated monomer mechanism (AAMM, Scheme 5). Recently, Zhang *et al.* proposed that the deprotonation of the α -methylene hydrogen on the NCA would readily react with a nearby monomer and undergo a series of cascade

reactions to produce a so called “Münchnone initiating species”.^{38b} Their work was supported by extensive MALDI-ToF MS analysis and would explain our results that indicated polymerization via an unknown initiator species. Unfortunately, the samples that were sent out for MALDI-ToF MS measurements were not detectable or produced indistinguishable spectra.

Alternative Activated Monomer Mechanism (AAMM)



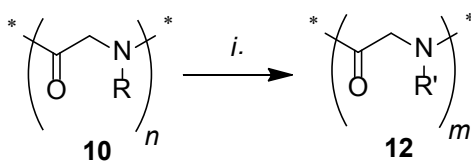
Base: hydrides > lithium bases > P₄ > P₂ > P₁ > 3° amine > steric alkoxides > 2° amine > alkoxides > 1° amine

Scheme 5. Proposed alternative activated monomer mechanism (AAMM) rearrangement to Münchnone initiating species leading to competing polymerization when strong bases were utilized.^{38b}

3.1.5 Post-Modification of Functional Polypeptoids

Once well-defined functional homo- and co-polypeptoids were realized, we set out to fulfill one of the main objectives of this thesis project and that was the preparation of glycopolypeptoids. As previously mentioned, biomaterials with carbohydrate functionality show promise as biosensors, targeting drug carriers, and extracellular matrices. Naturally, this is accredited to the stereospecific receptor recognition nature of the sugar moiety. Utilizing a peptide backbone allows for greater biocompatibility and higher order structures. Polypeptoids, arguably a derivative of polyglycine, maintain the atom economy and chemical sequence that allow for higher order structures while suppressing enzymatic degradation and immunogenic responses. However, due to the lack of the amide hydrogen well-defined secondary structures have not been described for polypeptoids. Instead, *pseudo*-secondary structures (structures that mimic α -helices or β -sheets) have been described for a rare number of polypeptoid variations. These structures are achieved by preparing polypeptoids with orthogonal stereo-groups attached to the amide which in turn governs the organization of the backbone via steric restraints and other non-covalent interactions (*eg.* aromatic

π - π^* stacking). Although enhanced circular dichroism (CD) spectra have been observed for other glyco-*pseudo*-peptide systems (*ie.* functional PiPOxs), this has relatively been unexplored with peptoids. Notably, there are a few examples of glycopeptoids being prepared via solid phase synthesis. Solution phase synthesis of glycopeptides have previously been achieved by two main synthetic approaches: 1) preparation of the glycomonomer followed by polymerization; and 2) post-modification or coupling strategies onto an already preformed bio-relevant polymer backbone. To the best of our knowledge, neither of these strategies have been explored for the preparation of glycopolypeptoids prior to our group's investigations.



Scheme 6. Post-modification of functional polypeptoids via photoaddition of thiol moieties. (i) R'-SH, solvent, $h\nu$.

The preparation of a glycomonomer followed by polymerization is an attractive approach for it allows for tailored inclusion of the sugar moieties by monomer feed ratios. The draw backs include additional protection group steps and in house monomer design and polymerization. Contrarily, post-modified approaches allow for the procurement of the bio-relevant polymer from outside sources and typically include facile/simple coupling strategies that do not require expert knowledge or experience (Scheme 6). In addition, this latter approach allows for the design of one stock bio-relevant polymer systems which can readily be diversified by the screening of several small molecules with the appropriate coupling functional group. The main disadvantage is foreseen in the lack of quantitative addition of the sugar moiety. Due to the advances in “click” chemistry (*eg.* azide-alkyne [3+2], Diels-Alder [4+2] cycloadditions, thiol-ene/yne additions, *etc.*), modular, wide in scope and high yielding, post-modification have been realized. In particular, the post-modification of bio-relevant polymers containing alkene or alkyne functional groups with thiol moieties via chemical or photo radical initiation has been demonstrated to be facile and quantitative under variations conditions for a number of systems. Naturally, these were the main influences towards the rational design that led to the preparation of poly(*N*-allyl/ -propargyl) glycine) homo- and co-polymers as described in the previous section. Furthermore, we did not pursue the

preparation of *N*-glycol glycine NCAs due to the apparent challenges related to a sterically hindered propagating species (2° amine).

We conducted a methodology study to determine the appropriate conditions and time duration required towards the post-modification of PNAG (**10k**) via thiol-ene photo-addition. This initial study included the monitoring of the reaction by ¹H-NMR in DMF-d₇ and the utilization of 1-thioglycerol (racemic), a cheap/commercially available thiol moiety, as a model for glucose. The mixtures were prepared with various equivalences (1.2–5) of thiol to NAG (*API44*) and irradiated by UV-light via a medium pressure mercury lamp; where monitoring by ¹H-NMR measurements were conducted every 60 minutes (T₀–T₇). These investigations suggested that quantitative (>99%) modification of the side arms were readily achieved when excess equivalences (3 and 5) of the thiol moiety was utilized over 6 hours of UV-irradiation (Table 4; **API50.3** and **API50.5**). However, 1.2 to 2 equivalences produced modifications between 58 to >95% (A48) while exposed to UV-irradiation over 2 days (**API48.1.2–API48.1.8** and **API50.2**). Naturally, stoichiometric equivalences between the alkene and thiol was desirable and therefore another good solvating agent, MeOH, was tested with 1.2 equivalences of thiol to alkene (*API64*) and UV-irradiated for 12 hours (**API71**). Unfortunately, a lower degree of modification was observed (36%). We then considered the use of photo-initiators which were known to increase the kinetics of photo-addition by increasing the number of free radicals in a system at any given time. Mixtures of **10k** (*API59*) with 1-thioglycerol (1.2 eq.) were prepared in DMF or CH₂Cl₂ and stirred 10 minutes prior to the addition of 2,2-dimethoxy-2-phenylacetophenone (DMPA) at which point these reactions mixtures were subjected to UV-irradiation for 4 hours (**API77** and **API78**). Quantitative modifications (>95%) of the alkene was observed via ¹H-NMR analysis. Satisfied with these results, we applied the aforementioned conditions towards a higher molecular weight **10k** (*API67C*) and larger amounts of the material (from 25 to 500 mg; *API82A*). High degrees of modifications of 94% and >99% (A49–A52) were observed, respectively (**API80** and **API83A**).

Table 4. Methodology study towards the optimization of post-modification of **10k** (*PNAG*) with 1-thio-glycerol.

Sample	Pre-cursor	[SH] ₀ /[C=C] ₀	Initiator	Solvent	Duration (hour)	<i>m</i> ^a (%)
AP148.1.2	<i>AP144</i>	1.2	–	DMF-d ₇	36	58
AP148.1.4	<i>AP144</i>	1.4	–	DMF-d ₇	36	49
AP148.1.6	<i>AP144</i>	1.6	–	DMF-d ₇	36	57
AP148.1.8	<i>AP144</i>	1.8	–	DMF-d ₇	36	57
AP150.2	<i>AP144</i>	2.0	–	DMF-d ₇	24	>95
AP150.3	<i>AP144</i>	3.0	–	DMF-d ₇	8	>99
AP150.5	<i>AP144</i>	5.0	–	DMF-d ₇	8	>99
AP171	<i>AP164</i>	1.2	–	MeOH ^b	12	36
AP177	<i>AP159</i>	1.2	DMPA	CH ₂ Cl ₂	4	>95
AP178	<i>AP159</i>	1.2	DMPA	DMF	4	>99
AP180	<i>AP167C</i>	1.2	DMPA	DMF	12	94
AP183A	<i>AP182A</i>	1.2	DMPA	DMF	12	>99

^aDegree of modification was determined by ¹H-NMR end group analysis in DMF-d₇; ^btreated with trifluoroacetic acid (TFA).

The post-modification of **10k** (*AP182A*) with 1-thio-β-D-glucose tetraacetate (HS-GlcAc₄) proceeded without incident under the previously prescribed conditions (Table 5, **AP183B**: A54–A58). Exemplarily, the quantitative post-modification was verified by MALDI-ToF MS analysis (Figure 11). As illustrated, the peaks associated to the alkene is no longer detectable by ¹H-NMR whereas MALDI-ToF MS confirms the appropriate mass of the repeating unit ($\Delta m = 461.6$ Da; [C₁₉H₂₇NO₁₀S]⁺ = 461.1 g/mol). Notably, the calculation for the average degree of polymerization (\bar{n}) suggested a lower value than determined for the polymer prior to post-modification (from 20 to 17). In addition, a second homologous series ($\Delta \bar{m} = 461.5$ Da) was detected with mass differences of either –99.3 or +362.1 Da which we are unable to account for. However, these values are within 1 Da of either an NAG repeating unit ([C₅H₈NO]⁺ = 98.1 g/mol) or thio-sugar ([C₁₄H₁₉O₉S]⁺ = 363.1 g/mol) suggesting one additional sugar moiety was attached.

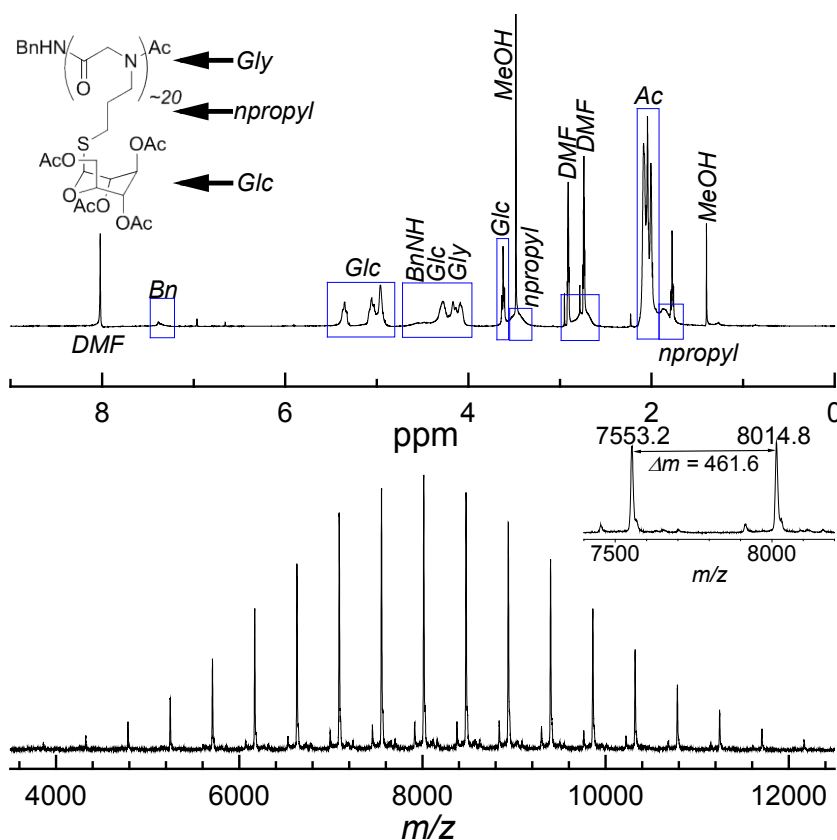


Figure 11. ¹H-NMR (top) and MALDI-ToF MS (bottom) spectra supporting quantitative modification via thiol-ene photoaddition towards glycol-polypeptoid.

The post-modification of **10k** with optically active thiol moieties was extended to the unprotected 1-thio-β-D-glucose (HS-Glc) under benign conditions (*ie.* H₂O). The initial effort included treating the HS-Glc/PNAG (**API82A**) aqueous solution with acetic acid followed by UV-irradiation for ca. 12 hours (**AP184B**). ¹H-NMR analysis suggested a modest conversion of 57%. We then explored a mixed solution of MeOH/H₂O, TFA, HS-Glc, and **API64** (**AP170**). Unfortunately, this resulted in a lower modification of the side arms (41%). For the third attempt, we added hydroxy-4'-(2-hydroxyethoxy)-2-methylpropiophenone (**HEMP**) to an aqueous solution containing TFA, HS-Glc, and **API82A** (**AP184A**: A59–A62). A quantitative modification was observed confirming the efficacy of photo-initiators such as **HEMP** towards the photo-addition of thiol moieties onto water soluble polyamides with alkene side chains. Noteworthy, 1-thioglycerol was ineffective towards the post-modification of PNAG under aqueous conditions.

In an attempt to exploit this suspected aggregation phenomena between the hydrogen accepting backbone of polypeptoids and the hydrogen donating behavior of thioglycerol, we

prepared an optically active thioglycerol ketal as described by Sinibaldi *et al.* which included a 3 step synthetic route starting from *R*- and *S*-solketal.⁷² Unfortunately, our attempts at synthesizing *S*-(2,2-dimethyl-1,3-dioxolan-4-yl)methanethiol (*S*-thioketal) was unsuccessful. However, the preparation of *R*-thioketal resulted in enough material for a preliminary screening towards the post-modification of **10k** (*BP25.25–BP25.75*). Utilizing the aforementioned conditions in DMF with DMPA resulted in moderate modifications between 47–63% (**BP75.25–BP75.75**). Preparing another round of experiments with TFA resulted in modest to quantitative degrees of modification (**BP79.25–BP79.75**: A63–A64). In addition, treating these samples with TFA led to modest levels (2-68%) of de-protection (*ie.* removal of the ketal) suggesting that further work should be focused on a one-pot strategy. On-going investigations towards this one-pot approach are underway.

Table 5. Post-modification of functional polypeptoids with optically active thiol moieties.

Sample	Pre-cursor	Thiol (e.q.)	Initiator	Solvent	Treated	<i>m</i> ^a (%)
AP183B	<i>AP182A</i>	HS-GlcAc ₄	DMPA	DMF	–	>99
AP184B	<i>AP182A</i>	HS-Glc	–	H ₂ O	AcOH	57
AP170	<i>AP164</i>	HS-Glc	–	MeOH/H ₂ O	TFA	41
AP184A	<i>AP182A</i>	HS-Glc	HEMP	H ₂ O	TFA	>99
BP75.25	<i>BP25.25</i>	<i>R</i> -thioketal	DMPA	DMF	–	47
BP75.50	<i>BP25.50</i>	<i>R</i> -thioketal	DMPA	DMF	–	63
BP75.75	<i>BP25.75</i>	<i>R</i> -thioketal	DMPA	DMF	–	54
BP79.25	<i>BP25.25</i>	<i>R</i> -thioketal	DMPA	DMF	TFA	>99
BP79.50	<i>BP25.50</i>	<i>R</i> -thioketal	DMPA	DMF	TFA	84
BP79.75	<i>BP25.75</i>	<i>R</i> -thioketal	DMPA	DMF	TFA	87

^aDegree of modification was determined by ¹H-NMR end group analysis in DMF-d₇.

3.1.6 Thermal and Solution Properties

Poly(*N*-allyl glycine)s (PNAG or **10k**) were soluble in organic solvents such as MeCN, PhCN, DMF, DMA, NMP, MeOH, EtOH, THF, CH₂Cl₂, and CHCl₃. PNAGs solubility was initially limited to ca. 1 mg/mL in H₂O but significantly increased to ca. 20 mg/mL after treatment with MeOH (removed under vacuum). Poly(*N*-propargyl glycine)s (PNPG or **10l**) demonstrated similar solubility to **10k** but was fairly insoluble in EtOH, MeOH, and H₂O. In addition, **10l** was

soluble in 1,4-dioxane and acetone. Copolymers poly(*N*-allyl-*N*-propargyl glycine) (PNANPG) or poly(*N*-methyl-*N*-propargyl glycine) (PNMNPG) had comparable solubility to their homopolymer counterparts. Notably, PNM/PG was soluble in H₂O where the aqueous mixture was light blue. Likewise, thio-glycerol or thio-glucose post-modified **10k** had improved solubility in aqueous media (*ie.* H₂O) but were limited in solubility within organic media to DMF, DMA, NMP, and DMSO. Thio-glucose tetraacetate (HS-GlcAc₄) demonstrated exceptional solubility in most organic solvents and no solubility in alcohols (*ie.* MeOH and EtOH).

PNAGs were thermally stable until 200–320 °C (thermogravimetric analysis, TGA) and had glass transition temperatures (T_g) in the range of 50–70 °C (differential scanning calorimetry, DSC, 2nd heating curves at 20 K/min). No melting or crystallinity transition (T_m or T_c) temperatures were observed in the 2nd or subsequent heating cycles suggesting a non-crystalline material. Recently we observed that poly(*N*-propyl glycine)s were semi-crystalline and that these crystal domains could be erased by MeOH treatment. The significance of this parallel study was in the enhanced solubility of polypeptoids in H₂O. We observed a similar trend with the PNAGs and initially suspected that crystallinity played a significant role in the solubility of this material. Therefore, the 1st endotherms, via DSC, were measured at 1, 10, and 20 K/min with **10k** (Exemplarily: **BP25.50**) after purification (Initial), methanol treatment (Treated), and recrystallization (Annealing) from solution (Figure 12). The DSC detected a small endothermic peak (T_m) at 160 °C for the raw material at a slow heating rate (1 K/min) but observed no such peak for the higher rates (10 or 20 K/min). After treatment with methanol, the same peak was observed for the slow heating rate whereas nothing was detected for the mid-range heating rate (10 K/min). The high heating rate (20 K/min) provided two endothermic peaks at 125 and 160 °C. Notably, while weighing out the freshly treated and freeze dried **10k** material in the aluminum crucible, the material became “wet” in appearance and the morphology changed from a fluffy white material to a more rigid plastic material. Presumably, the material adsorbed H₂O from the environment and underwent a rearrangement/packing orientation which may account for these questionable endothermic peaks. Accordingly, a new sample was prepared without freeze drying and no noticeable exothermic or endothermic peaks above 100 °C were observed (Figure 12, Treated, 20 K/min). Annealing was conducted at 0.5 w/w % at 70 °C for 24 hours in H₂O and after drying was measured by DSC. Endothermic peaks were observed for all three heating rates with sharper and well-defined peaks (T_m at 1 K/min = 157, 163, and 164 °C; 10 K/min = 164 °C; 20 K/min = 158 and 165 °C).

However, our attempts at recrystallization by annealing the bulk material was unsuccessful suggesting that crystallization occurs only by solution phase changes which is contrary to the results described for poly(*N*-propyl glycine)s where recrystallization was observed for both approaches. Naturally, this can be attributed to the relative rotational freedom a linear alkyl chain has over the rigid allyl system.

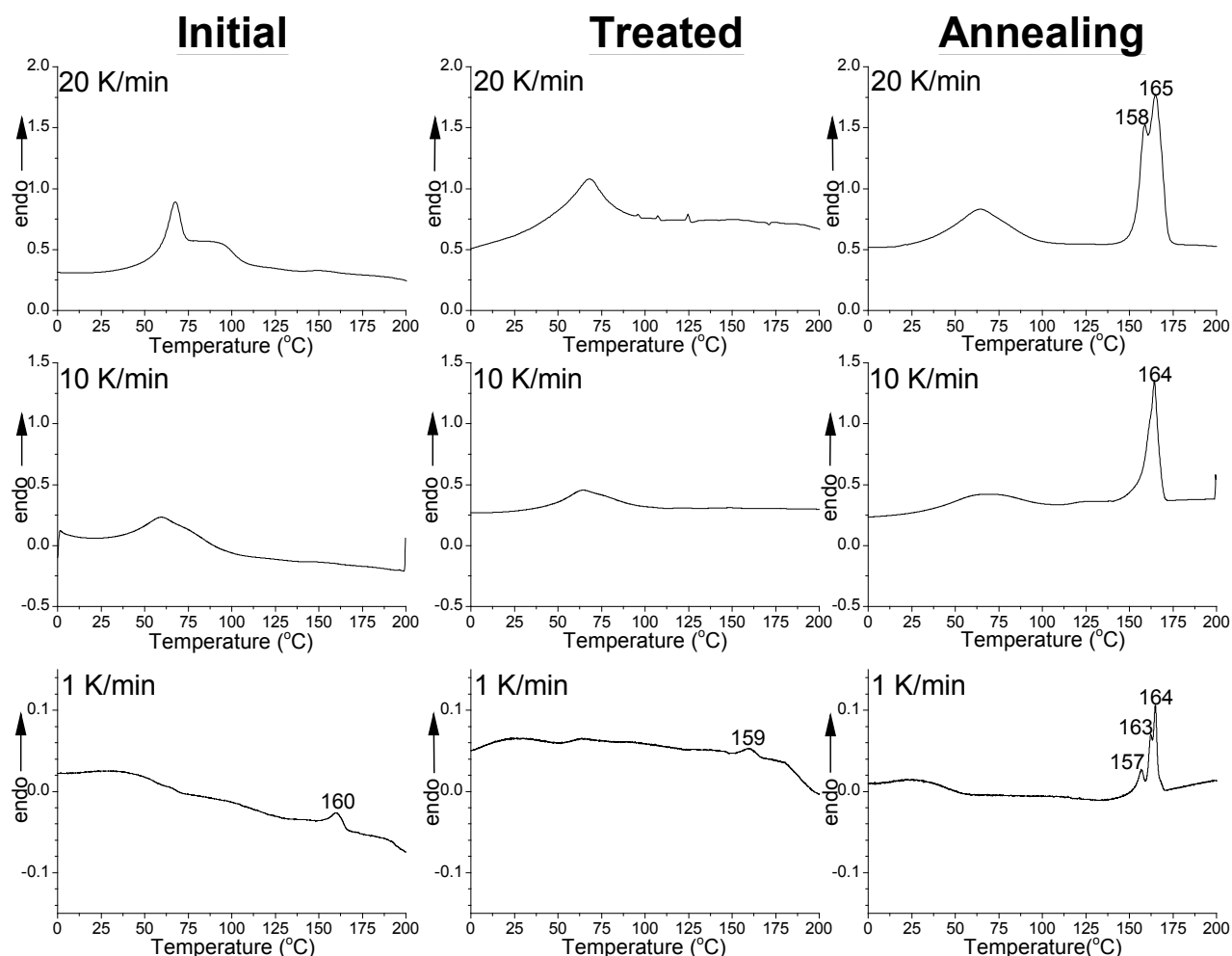


Figure 12. DSC endotherms (1st) were measured at 1, 10, and 20 K/min with **BP25.50** after purification (**Initial**), methanol treatment (**Treated**), and recrystallization (**Annealing**) from solution.

To allow for direct comparison, endotherms were normalized by dividing the heat flow (mW) by the mass of the sample (mg).

PNPGs were thermally stable until 340 °C (TGA, no mass loss) and demonstrated T_g behavior between 79–91 °C (DSC, 2nd heating curves at 20 K/min). A broad exothermic peak was observed in DSC when the samples were heated >200 °C. This peak was fairly reversible when

temperatures were <250 °C. Additional heating led to black material that no longer demonstrated T_g behavior or any other measurable thermo-properties. Exemplarily, the 1st heating curve (10 K/min) is illustrated in Figure 13 for **10l** (**BP35.50**) where an exothermic peak was observed at 238 °C. Further analysis of the material by FT-IR did not provide any additional insight (peaks were broader and weaker but still present). The material was insoluble and could not be measured by ¹H-NMR. Due to this thermally induced chemical reaction, we were unable to determine crystallinity (if any) of the PNPGs and were unable to improve the solubility of this material in aqueous mediums (*ie.* H₂O). Notably, **10l** was not readily soluble in MeOH and was treated with a mixture of this solvent and 1,4-dioxane. Freeze drying was applied to remove these mediums prior to attempts towards dissolution in H₂O. Overall, a conclusion on the poor solubility of the propargyl side chain over the allyl is not well understood. However, the aggregation of the **10l** in NMP (via SEC), post-modified **10k** with glycerol in DMF, and thio-glycerol with **10k** in H₂O suggests a strong affinity of the polyamide backbone towards accepting hydrogen bond donating systems which may lead to the hydrophobic (*ie.* side chains or parts of) components to be predominantly exterior while hydrophilic (*ie.* amide) components remain interior. Presumably, this can be observed by PNAG's poor solubility in H₂O after precipitation in heptanes which would favor hydrophobic components exterior and hydrophilic components interior. The inverse occurred when the PNAGs were treated with MeOH.

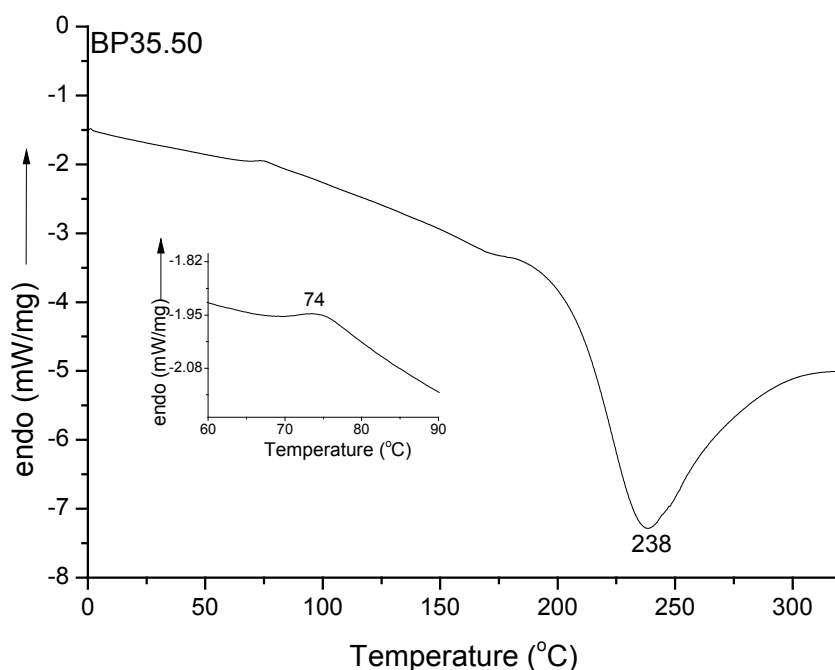


Figure 13. Endotherm of **PNPG₃₉ (BP35.50)** at 20 K/min with an inset to highlight the T_g .

3.1.7 Thermo-Responsive Behavior

As previously indicated, the solubility of PNAGs were dependent on treating the raw material with MeOH. After removing the solvent via vacuum (roto-evaporation followed by high vacuum) at room temperature, it was possible to dissolve in H₂O at concentrations as high as 20 g/L (10 °C). A small sample was analyzed by ¹H-NMR to confirm that the prior vacuum techniques completely removed MeOH and it was not behaving as a plasticizer. Sub-sequentially, portions of the 20 mg/mL solutions of **10k (BP25.50-BP25.75)** were diluted to concentrations of 10, 4.8, 3.4, 2.1, and 1 mg/mL. Transmittance (UV-Vis) was utilized to monitor (continuously) the turbidity (phase transition) of these samples over a preset temperature range. Exemplarily, the heating and cooling curves, with corresponding MALDI-ToF MS spectra, are illustrated in Figure 14.

By MALDI-ToF MS analysis we were able to verify the architecture (*ie.* repeating unit and α/ω -terminus) and confirm the chemical relevance of the samples measured for thermo-responsive behavior. The majority of the results illustrated a fairly narrow hysteresis (≤ 1 °C) supporting “precision” stimuli-responsive behavior. An exception was found for **BP25.50** at 20 g/L where the heating and cooling curves at 0.8 (*ie.* 80%) had a difference of 7 °C. Upon heating, sedimentation was observed frequently for the higher concentrations and stable translucent ribbons, on the lower 1/3 fraction of the cuvette, were observed after the cooling cycle. Furthermore, the highly concentrated (20 g/L) samples were slightly less transparent than H₂O (UV calibration) suggesting an upper concentration limit. The phase transition trend appeared to support a Type I LCST behavior where cloud point temperatures (T_{cp} ; transmittance of 80%) were suppressed with increasing molar masses. For example, the T_{cp} for solutions with a concentration of 4.8 g/L decreased from 44 to 29 °C as \bar{M}_n increased from 2.7 to 6.7 kg/mol, respectively. However, the higher molecular weight T_{cp} appeared to be somewhat independent of concentration ($T_{cp} = 28\text{--}32$ °C for concentrations between 4.8–1.0 g/L). Noteworthy, crystallization could be achieved when samples were heated above 70 °C for ≥ 24 hours.

The post-modification of PNAGs with 1-thioglycerol resulted in material that was non-thermo responsive ($T_{cp} > 100$ °C) at lower molecular weights (< 5 kg/mol). However, higher molecular weights (> 10 kg/mol) appeared to have thermo-responsive behavior that was non-reversible (**AP180: A53**). The formation of these precipitates was attributed to the aggregation behavior between the backbone and diols.

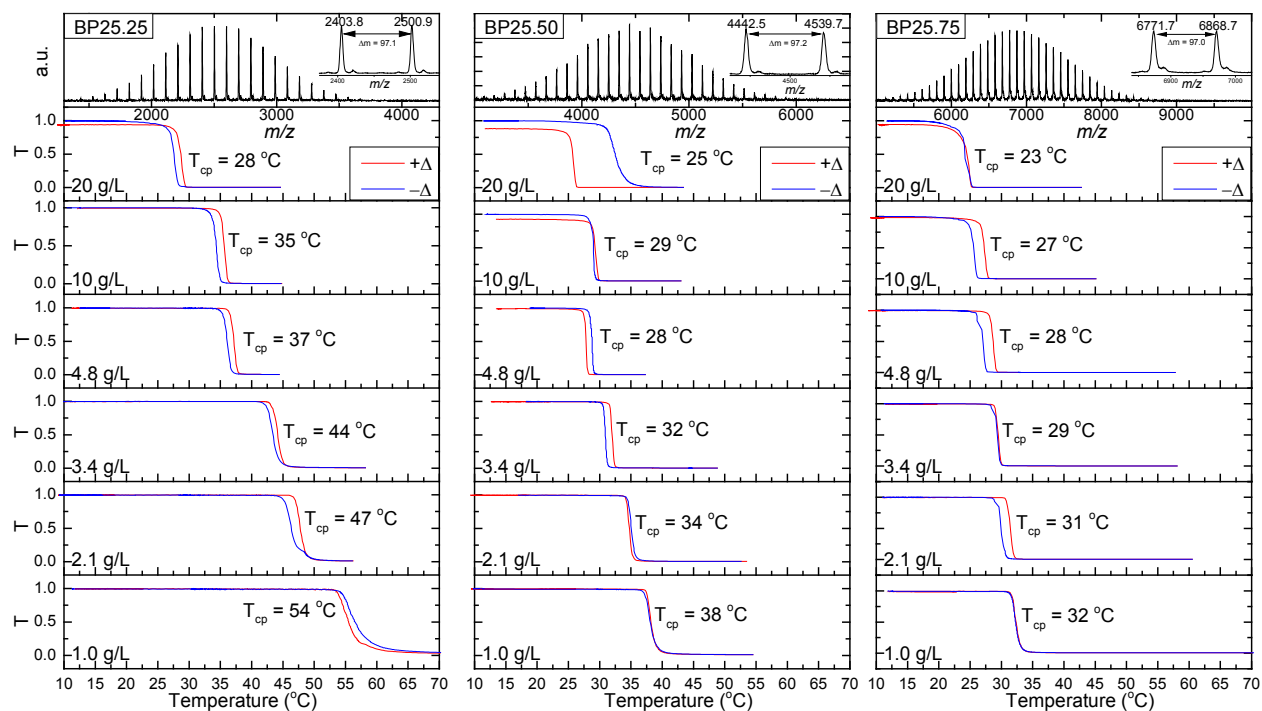


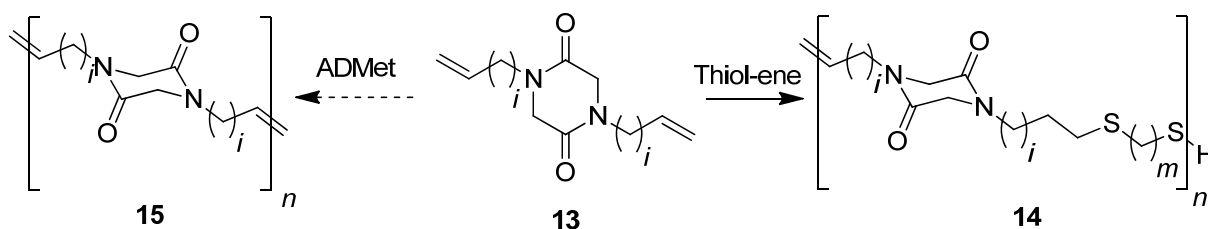
Figure 14. MALDI-ToF MS spectra (top) and turbidity heating (+Δ) and cooling (-Δ) curves (bottom).

3.2 Polypeptoids via Step-Growth Polymerizations

Due to the many challenges related to preparing polypeptoids via ROP of *N*-substituted glycine NCAs, a number of step-growth polymerization routes were considered. The expected higher dispersity values ($\mathcal{D} \geq 2$; ill-defined) typically observed via step-growth polymerization would have not been advantageous towards thermo-responsive investigations (precision stimuli-responsive behavior is dependent on well-defined systems). However, the opportunity to obtain some fundamental data such as solubility, degradation, and thermo-processability was foreseeable. In addition, fractionation could have been employed to achieve lower \mathcal{D} values. The most attractive features of this alternative route included the availability of commercial, high purity, reagents and one pot approaches towards polypeptoids. In general, we explored a number of polycondensation conditions including coupling reagents (*eg.* HOBt/EDC with sarcosine) and halogenating species (*eg.* bromo acetyl bromide with allyl amine) while at room or elevated (via microwave irradiation) temperatures. None of these preliminary studies resulted in any reasonable material to characterize. As further successes were being achieved via ROP of NCAs, we discontinued these parallel investigations. However, an unplanned cyclic alkene dimer (**DKP 13k**: A14–A16) was

prepared during the purification of *N*-allyl glycine NCA (**5k**) and was investigated towards the preparation of poly(diketopiperazines) (PDKP) via ADMet and thiol-ene photo-polymerization.

Our preliminary polymerization investigations included attempts at preparing PDKP via thiol-ene and acyclic-diene metathesis (ADMet) step-growth polymerizations (Scheme 7). Copolymerization of **DKP 13k** and 1,3-propanedithiol yielded polymer **PDKP** (A77–A82) with an apparent molar mass of $\bar{M}_n \approx 2.0$ kg/mol ($D = 2.2$). ADMet polymerization of **DKP 13k** using a 2nd generation Hoveyda-Grubbs catalyst failed, presumably due to a suspected coordination of the amide group to the metal center as described by Masuda *et al.*⁷⁸ They were able to overcome this limitation by extending their side chains by one carbon. In as much, we turned our attention towards understanding and exploiting the synthesis of di-alkene DKPs.

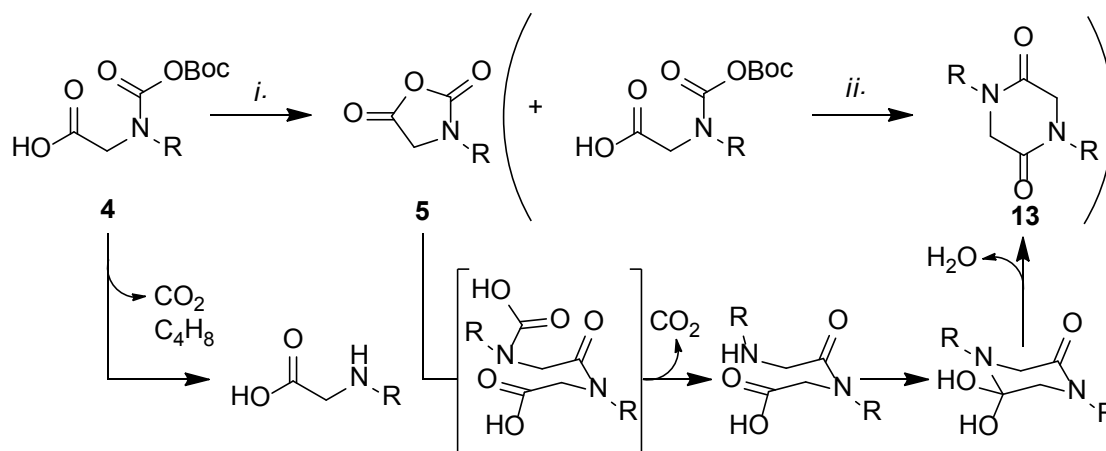


Scheme 7. Step-growth polymerization of DKP via ADMet or thiol-ene addition.

3.2.1 Diketopiperazine (DKP)

In an effort to understand how **DKP 13k** was produced and exploit this for the further development of longer terminal alkenes, we focused our attention on the original conditions that were employed towards the synthesis of NCA **5k**. We considered that the byproducts of cyclization would be HCl, O=PCL₂, and *tert*-butyl chloride. In addition, we considered excess PCL₃ and newly formed **5k** as potential contributing species found in the crude mixture. Byproducts O=PCL₂ and *tert*-butyl chloride were excluded from this investigation due to insolubility or low boiling point, respectively, which facilitated in the removal. Therefore, freshly distilled (vacuum) **5k** was heated (120–150 °C), treated with trifluoroacetic acid (TFA), and PCL₃ separately in 3 separate reaction flasks. Heating led to decomposition and oligomerization whereas treatment with TFA or PCL₃ did not cause any significant change to the monomer until heat was added after 24 hours at which point oligomers and trace amounts of DKP were detected. Considering that an outside contaminate such as water may have some influence, we injected distilled H₂O only to once again detect oligomerization after heating. Suspecting chlorine anions for being responsible for ring opening initiation, we treated **5k** with aluminum trichloride (AlCl₃) and iodine (I₂) but DKP **13k** was not

detected. Finally we explored the labile nature of the Boc group by heating **4k** with and without **5k**. Heating in a sublimation apparatus without **5k** produced non-cyclic dimers and *N*-allyl glycine where the Boc was only observed in trace amounts. The mixture of **4k** and **5k** as the crude cyclic mixture plus heat produced DKP **13k** in low yields (<20%). We therefore concluded that **13k** was being produced by an initial thermally induced decarboxylation of the carbamate Boc moiety which readily reacted with neighboring NCAs therefore forming a dimer intermediate which could undergo another decarboxylation under the acidic conditions initiating cyclization and loss of H₂O (Scheme 8).



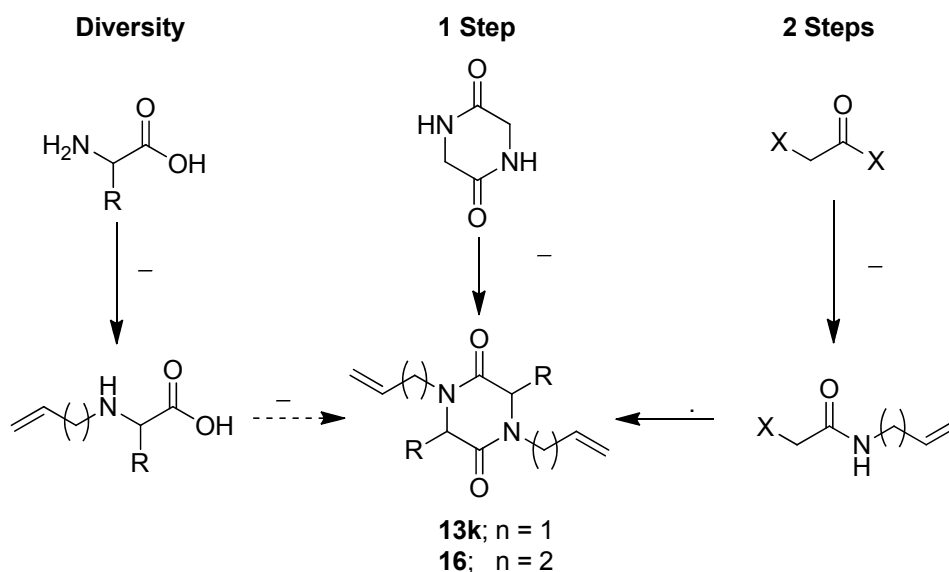
Scheme 8. Initial synthesis of **DKP 13**. Top row: (i) $\frac{1}{2}$ eq. PCl_3 , CH_2Cl_2 (ii) Δ ; Bottom row: proposed mechanism pathway.

We did not attempt to optimize this one-pot approach towards **DKP 13**, instead we opted to investigate three alternative pathways towards **DKPs** that would either increase diversity or shorten the synthetic sequence (Scheme 9). As described previously, mono-addition to the nitrogen of amino acids is a direct way of introducing diversity. In addition, the synthetic route from α -amino acids should allow for stereo-retention. To achieve these goals (diversity and stereo-retention), we attempted to exploit an imine intermediate and metal coordination phenomena towards the mono-addition of alkene chains. When primary amines are exposed to either an aldehyde or ketone an imine is produced (a.k.a. Schiff base). Essentially, this process transforms a strong nucleophile into a weak electrophile which in turn may be treated with strong nucleophiles for addition purposes, hydride donors (*eg.* NaBH_4 , LiBH_4 , LiAlH_4 *etc.*) for reduction, or hydrogenation agents (*eg.* Pd-C, Raney nickel, *etc.*) allowing for the preparation of secondary amines. Corey *et al.* demonstrated the utility of this process in their synthesis of unusual indolozocine tricyclic subunits where the initial step included mono-addition of 3-methyl-2-butenal

to L-tryptophan methyl ester followed by reduction via NaBH_4 treatment.^{59c, 59d} Exceptionally they were able to achieve this without reducing the alkene. Wishing to harness this novel approach, we treated glycine ($\text{R} = \text{H}$) with acrolein ($\text{CH}_2=\text{CH-CHO}$) followed by NaBH_4 (step i). Prior to the addition of the reducing reagent, the imine intermediate was confirmed by $^1\text{H-NMR}$. Unfortunately, the *N*-allyl glycine derivative was not detected or isolated after treatment with NaBH_4 . We suspected that this may have been caused by over reduction due to refluxing the reaction overnight as well as the greater reactivity of a terminal alkene versus the trisubstituted alkene explored by Corey. In an attempt to simplify this approach, we treated glycine with acryloyl chloride and received similarly disappointing results (step ii).

Yamaguchi *et al.* has been able to demonstrate a mono-addition of primary and secondary alcohols to various anilines via a novel pentamethylcyclopentadienyl (Cp^*) iridium catalyst ($[\text{Cp}^*\text{IrCl}_2]_2$). They proposed a catalyst cycle that included the formation of aldehydes/ketones via a hydrogen migration step followed by an *in situ* imine generation which was reduced by hydride addition via the Ir catalyst.^{59a, 59b, 74} When we applied their described conditions between γ -benzyl-L-glutamic acid ($\text{R} = (\text{CH}_2)_2\text{COOCH}_2\text{C}_6\text{H}_5$) and butene-1-ol, we detected the desired product in the reaction mixture but were unable to isolate/purify the product out (step iii). It is important to note that these reactions were being conducted on a screening bases in which we were looking for the most efficient way in creating a versatile route from α -amino acids. Therefore extensive purification efforts were not being employed.

The traditional synthesis of mono-substituted amines included addition of an alkyl halide to a stirring solution of amines (dilute). There was always competition for over alkylation resulting in low yields of the target compound as well as leading to extensive purification efforts. Attempts to overcome this shortcoming included amine protection group approaches and additives that coordinate to secondary amines preferentially over primary amines. The latter provides an *in situ* approach that does not require another synthetic step. Jung *et al.* has proposed cesium as a reasonable additive that leads to the chemoselective addition of alkyls.^{58a} Our efforts with L-glutamic acid ($\text{R} = (\text{CH}_2)_2\text{COOH}$) and 4-bromo-1-butene supported mostly mono-addition in trace quantities (step iv). We attributed the low conversions to the heterophase conditions employed here. In addition, attempts to isolate proved futile.



Scheme 9. Synthetic approaches towards functional DKPs. **Diversity:** (i) R = H, (a) Acrolein, NaOH, MeOH (b) NaBH₄, 0 °C; (ii) R = H, Acryloyl chloride, NEt₃, DMF; (iii) R = (CH₂)₂COOCH₂C₆H₅, [Cp*IrCl₂]₂, NaHCO₃, butene-1-ol, dioxane, Δ; (iv) R = (CH₂)₂COOH, CsOH, 4 Å MS, 4-bromo-1-butene, DMA; (v) MeOPCl₂, NEt₃, 1,3-dimethylimidazolium dimethyl phosphate, toluene, MW Δ; (vi) (a) SOCl₂, MeOH, (b) NEt₃, Δ; **1 Step:** (vii) NaH, *n*Bu₄NI, 4-bromo-1-butene, DMA, 0 °C; (viii) *n*butyl lithium, 4-bromo-1-butene, *n*Bu₄NI, DMA, 0 °C; (ix) BEMP, 4-bromo-1-butene, *n*Bu₄NI, DMF, Δ; **2 Steps:** (x) X = Br, allylamine, K₂CO₃, CH₂Cl₂, Δ; (xi) X = Br, 3-butenylamine hydrochloride, K₂CO₃, CH₂Cl₂, Δ; (xii) X = Br, allylamine, DMAP, K₂CO₃, CH₂Cl₂, Δ; (xiii) X = Cl, allylamine, K₂CO₃, CH₂Cl₂, Δ; (xiv) NaOH, CH₃CN, Δ.

Obviously these initial investigations towards versatile synthesis of functional α -amino acids did not meet expectations. But if high yields were achieved with little difficulty in purification then we would have had an *N*-substituted α -amino acid ready for cyclization. Our approach towards cyclization included two proposed procedures. First off, work by Bräse *et al.* suggested that cyclization could be achieved from *N*-substituted α -amino acid via microwave irradiation in the presence of a chlorinating agent (MeOPCl₂) and ionic liquid (1,3-dimethylimidazolium dimethyl phosphate).⁷⁵ They received high yields with a myriad of α -amino acids (protection groups on side arms) but more relevant to our work was the efficient cyclization of *N*-methyl glycine under these conditions. This of course is why we targeted the direct synthesis of *N*-substituted α -amino acids versus its ester counter-part which in hindsight may have increased solubility and therefore produced better results (step v). If these cyclization conditions did not provide the results we

wanted, then an alternative more traditional approach utilizing strong bases (*eg.* NaOH, KOH, *etc.*) with either the α -amino acid or its ester counter-part would have been explored.⁷⁶ Presumably this would have resulted in epimerization and therefore was only considered as the backup plan (step vi).

In parallel to our mono-addition investigations (**Diversity**; step i-vi), we explored a direct synthetic route from commercially available glycine anhydride (**1 Step**). Our initial efforts began with a traditional approach of utilizing NaH, 4-bromo-1-butene, and *n*Bu₄NI (step vii). An isolated yield of 24% was achieved after this first attempt albeit the product had some minor impurities after flash chromatography (A17). Alongside, we attempted the same reaction utilizing BEMP or lithium *n*butyl as an alternative strong base. Neither of these latter reactions provided detectable quantities of the DKP target.

The final pathway we explored included two synthetic steps that we envisioned would be high yielding (**2 Steps**). This approach was based on work by Shin *et al.* who demonstrated moderate to high yields towards symmetric disubstituted piperazines.⁷⁷ Our initial attempt with allylamine and bromoacetyl bromide produced *N*-allyl 2-bromoamide at a modest yield of 53% (step x; A18). When we applied these conditions to 3-butenylamine hydrochloride we received only 34% of the expected product albeit we were able to recover >50% of 3-butenylamine by liquid-liquid extraction (xi: A19). In an attempt to improve the addition, we repeated the reaction with allylamine and 4-(dimethylamino)pyridine (DMAP) and only recovered 7% of the desired product (xii). Considering that the authors originally utilized chloroacetyl chloride in their studies, we purchased and combined it with 3-butenylamine hydrochloride (xiii). Unfortunately we were unable to recover any of the desired product, *N*-butenylamine 2-chloroamide. We attributed these poor results with the 3-butenylamine hydrochloride to the hetero-phase nature in CH₂Cl₂ (no further attempts were explored). With the material we did receive we attempted homo-annulation and obtained poor yields. We recovered 18% of the diallyl DKP and no dibutenyl DKP. For the latter, instead of DKP we isolated a noticeable amount of acetamide. We concluded from these studies that this may be an attractive alternative but would require further development towards our targeted systems.

3.2.2 ADMet attempts with *N,N'*-dibutenyl DKP

As previously described, we were able to produce a small amount of the dibutenyl DKP monomer and therefore attempted ADMet polymerization. Micro-reactions were prepared in

DMF as the solvent, under argon, with the elongated monomer. After heating to 80 °C, the ruthenium catalyst (2nd generation Hoveyda-Grubbs) was added and the reaction mixture was subjected to reduced pressures. After 1 week, an aliquot was removed and prepared for SEC (NMP/PS). As illustrated in Figure 15, there appeared to be a small change in the hydrodynamic volume of the monomer (blue) to the suspected oligomer (red) suggesting that elongating the alkene allowed for ADMET to proceed forward albeit at a slow rate. However, for this to be a practical approach further optimizations are required and are currently being investigated for both the monomer and polymerization strategies.

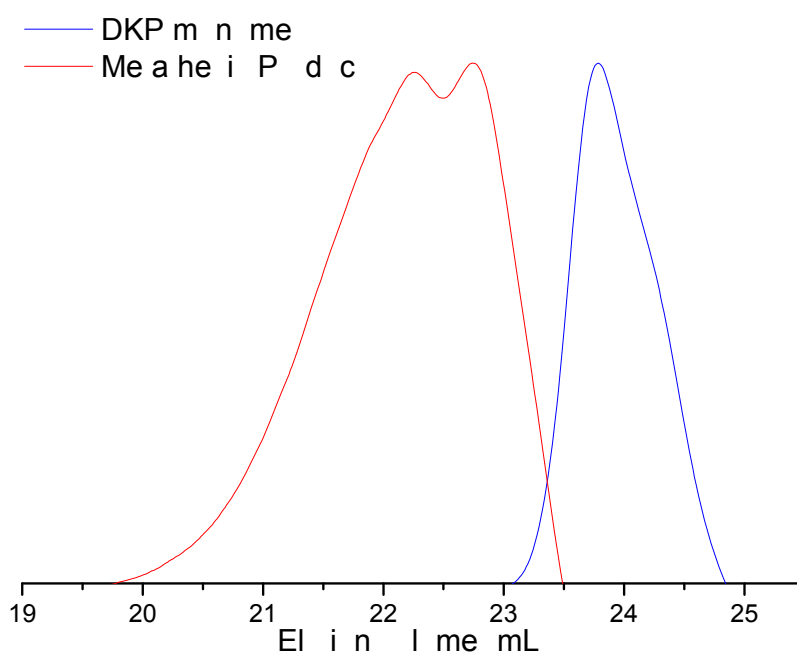


Figure 15. Hydrodynamic volume (NMP, RI) shift from monomer (blue) to oligomer (red).

4. Summary of Results

The preparation of well-defined polypeptoids was achieved through the ring opening polymerization (ROP) of *N*-substituted glycine *N*-carboxyanhydrides (NNCA). The preparation of the NNCA monomers (*N*-allyl and *N*-propargyl) was accomplished by combining strategies from Liskamp, Zhang, and Luxenhofer. Likewise, we observed improved benzyl amine (BnNH₂) initiated ROPs, with controllable monomer/initiator feed ratios ($[M]_0/[I]_0$), in benzonitrile (PhCN) whereas other solvents such as DMF, 1,4-dioxane, and CH₂Cl₂ provided polymeric materials with larger dispersity values (*D*) and lower degrees of polymerization ($\bar{\eta}$). However, molecular weights >6.7 kg/mol were not readily achievable, over 30 days, in PhCN whereas a bulk/heterophase approach provided $\bar{M}_n > 7.8$ kg/mol within 24 hours. Significantly, further investigations towards these heterophase prepared polypeptoids suggest that low *D* = 1.03–1.04 can readily be realized. Overall, these polypeptoid preparation studies supported our objective of overcoming the low molecular weights previously observed for primary amine initiated (BnNH₂, HexNH₂, and PEO-NH₂) ROP of α -allyl glycine NCA towards well-defined poly(*N*-allyl glycine)s.

Promoted alcohol initiated ROP of *N*-methyl glycine NCAs was investigated and provided mixed results suggesting partial to no inclusion of the “initiator”. In general, stronger bases (*ie.* *t*-BuP₄) produced polymers with apparent \bar{M}_n values between 2.1–2.5 kg/mol ($[M]_0/[P]_0 = 40$) with or without PEO-OH suggesting a competing initiation process. Zhang *et al.* recently described a “Münchnone initiating species” as a competing initiation species which is developed *in situ* by the deprotonation of the α -methylene proton. Further investigations with weaker bases (*ie.* *t*-BuP₂, BEMP, and DBU) suggested no additional benefit over macroinitiated ROP via PEO-NH₂ or PEO-OH with sublimated *N*-methyl glycine NCA. However, when γ -benzyl-L-Glu NCA was treated with PEO-OH/*t*-BuP₂ ($[M]_0/[I]_0 = 70$) a polymeric material with an apparent \bar{M}_n of 199 kg/mol was detected by SEC (PS in THF) albeit a bimodal progression was observed.

Poly(*N*-allyl glycine)s (PNAG) underwent facile post-modification via thiol-ene photoaddition allowing for the first published solution phase synthesis of a glyco-peptoid. Prior to this, an extensive ¹H-NMR study was conducted allowing for optimal conditions to be determined including the utilization of photo-initiators which provided glycerol side chains quantitatively (>95%). Further developments in the H₂O solubility of PNAGs facilitated in the preparation of glyco-peptoids under benign conditions, albeit a water soluble photo-initiator (HEMP) was employed to receive quantitative additions. Exemplarily, the quantitative addition of 1-thio- β -D-

glucose tetraacetate (S-GlcAc₄) was confirmed by MALDI-ToF MS analysis. Initial investigations with an optically pure 1-thiol-2*R*-glycerol ketal demonstrated comparable addition when treated with TFA. Notably, modest deprotection of the ketal was observed suggesting preparation of optically active poly(*N*-*propyl*-S-glycerol glycine) could be prepared under a one-pot strategy.

Thermo-analysis suggested that PNAG and poly(*N*-propargyl glycine)s (PNPG) have modest to poor thermal processing potential. Neither of these polymeric systems illustrated crystalline organization after bulk annealing. In addition, PNPG demonstrated thermo-reactivity around 250 °C. However, PNPG and PNAG both demonstrate glass transition temperature (T_g) as high as 91 and 70 °C, respectively. PNAG did demonstrate improved crystallinity when annealing was conducted in H₂O (70 °C) resembling a previous observation for the PiPOx. Likewise, PNAG demonstrated thermo-responsive behavior that was dependent on concentration for low molecular weights (<4.5 kg/mol) suggesting a lower critical solution temperature (LCST) Type I phase transition phenomena. However, higher molecular weights (>6.5 kg/mol) demonstrated a lower dependency on concentrations (<5 g/L) towards cloud point temperatures (T_{cp} = 28–32 °C).

Our attempts at preparing polypeptoids via polycondensation techniques were unsuccessful supporting the additional efforts required in the aforementioned chain growth polymerization approach. However, the diketopiperazine (DKP) by-product, 1,4-diallylpiperazine-2,5-dione (**8k**), readily underwent step growth polymerization via thiol-ene photo-addition. Unfortunately, acyclic diene metathesis (ADMet) was unsuccessful due to a suspected 6 member complexation/deactivation state of the catalyst. A screening effort towards the preparation of simple and diverse DKPs with longer terminal alkene chains, and possible α -methylene functional side chains, indicated that further development and optimization towards the preparation of these monomers will be a prerequisite towards an otherwise relatively unexplored class of bio-relevant polymers. However, the direct preparation of 1,4-dibut-3,3-ene-2,5-dione was achieved and initial investigations suggest ADMet polymerization is feasible for this class of materials.

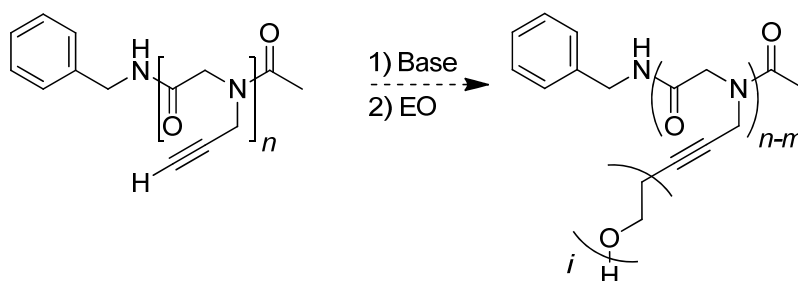
5. Outlook and Perspective

5.1 Outlook

The main objectives of this dissertation project included the increase solubility and molecular weights of poly(*N*-allyl glycine)s, post-modification with simple mercapto moieties (*eg.* thio-glucose, thio-glycerol, *etc.*) and investigations towards their potential material properties (*ie.* semi-crystallinity and thermo-responsive behavior). We targeted and synthesized a regio-isomer of poly(α -allyl glycine)s, poly(*N*-allyl glycine)s, which facilitated in the increased solubility and molecular weights via removal of hydrogen bonding and stereo-influences resulting in secondary structure neutrality. These bio-relevant polymers were demonstrated to undergo quantitative post-modification, in either organic or aqueous media, with thio-glucose and thio-glycerol. We observed that these systems had desirable material properties (*ie.* thermo-responsiveness) and aggregated with hydrogen donating side-chains (*ie.* thio-glycerol/diol). We are now interested in exploiting this suspected self-assembly behavior with chiral hydrogen donating side-chains and in as much began preparing such systems. We envision that further investigations in this area will provide some insight and allow for a comparison study between *N*-substituted and α -side-chain regio-isomers (*ie.* post-modified PNAG vs. poly(α -allyl glycine)). Additional comparative interests include binding, degradation, and biocompatibility studies. Furthermore, we are interested in preparing co-polymers between these systems in an attempt to combine the benefits of both systems including secondary structures and solubility.

We expanded the scope of our objectives throughout this dissertation work to include promoted ROP of NNCA's, thermo-responsive investigations, and step-growth polymerization of DKPs. As previously noted, the promoted ROP of NNCA's was relatively unsuccessful but was explored due to the need for more advanced initiator systems that could allow for fast and controlled polymerizations. So far, the greatest success towards these ends with polypeptoids was achieved by utilizing a *N*-heterocyclic carbene (NHC) as an initiator. This work by Zhang *et al.* demonstrated that the kinetics of the propagation could be increased via the carbamate mechanism and that low dispersity could readily be achieved by an unexpected end-group coordination with the charged heterocyclic. The question still remains, "What other nucleophilic/insertion initiators could be utilized towards controlled ROP of NNCA's?" We suspect catalysts, complimentary to those explored by Deming (*ie.* Ni), and silyl amines could be exploited for polypeptoids towards high molecular weights with low dispersities. Ideally, these initiators should be tolerant towards

functional groups such as the alkene and alkynes discussed throughout this manuscript. Higher molecular weights of PNAG would provide additional insight into the solubility and thermo-responsive limitations in H₂O. The successful thermo-responsive study discussed earlier in this manuscript is limited to relatively low molecular weights (<8.0 kg/mol) and does not provide much insight into applicable systems that typically require molecular weights >45 kg/mol. However, higher molecular weights can readily be achieved by post-modification of functional polypeptoids or ADMet polymerization of the DKPs. In particular, the alkyne hydrogen may readily react with a moderate to strong base (*eg.* *t*BuP₄) to produce an anion which should induce ROP of ethylene oxide (EO) (Scheme 10). This would afford a material with increased H₂O solubility and leave the alkyne in tack facilitating in later modification strategies. Our initial attempt at this was unsuccessful due to precipitation of the polymer in THF after being treated with *t*BuP₄. Alternatively, high molecular weight poly(diketopiperazine)s are foreseeable under ADMet polymerization conditions. In addition, the remaining alkenes could readily be reacted with thiol moieties to change solubility, bioactivity, or physical/mechanical properties via network methodologies. Either of these approaches would facilitate in the preparation of an interesting biomaterial that may be exploited for biomedical applications such as drug delivery or tissue engineering (*ie.* extracellular matrices).



Scheme 10. Proposed grafting from PNPG to achieve greater solubility and molecular weights.

5.2 Perspective

Poly(*N*-substituted glycine)s, or polypeptoids, are an interesting class of bio-relevant polymers and have great potential towards biomedical applications. In relationship to their predecessors, peptoids, these polymers promise to be biocompatible and degradable, but yet enzymatically resistant. Our fundamental investigations illustrate that a number of these polypeptoids (*ie.* *N*-C3 side-chain polypeptoids) undergo a phase transition in response to temperature and have thermo-processability potential (*ie.* T_g , T_m , and T_c). These features would allow for the design of drug delivery systems (*eg.* polymer-drug conjugates, encapsulation, *etc.*) and coated, or composite, biomaterials (*eg.* sutures, ECMs, *etc.*). In addition, the functional side-chain

polypeptoids (*ie.* allyl or propargyl) allow for cross-linking and/or surface modifications facilitating in the design of materials with various mechanical strengths and surfaces with biologically interacting molecules (*eg.* carbohydrates). Due to the “living” behavior of ROP, via the NNCA monomers, more sophisticated copolymers with tunable stimuli-responsive and physical properties are foreseeable.⁷⁸ However, there are many challenges that need to be overcome and further research is required prior to the targeted design of biomaterials.

Achieving molecular weights greater than 40 kDa is required for drug delivery systems and still remains a main challenge in the synthesis of polypeptoids. At this time it is still not well understood why propagation slows down or ceases above 10 kDa. If the propagating end group is being encapsulated by the structure of the polymer, or being terminated by some other means, then the recent development of polymer-polymer conjugates would prove ineffective. However, the post-modification of polypeptoids may readily lead to higher molecular weights. Alternatively, further investigations towards initiators or promoters may contribute or solve these current molecular weight concerns. Notably, Zhang’s investigations with carbene initiator suggest the propagating species favors coordination to electronically poor systems (positively charged) which facilitates in the formation of their cyclic-polypeptoids and higher molecular weight not so easily achieved via amine initiation. Arguably, this observation has similarities to metal-amine and silylamine initiated ROP of α -amino acid *N*-carboxyanhydrides (NCA) where the end-group is managed and activated by the corresponding electron acceptor. Although the current understanding of the mechanisms for these two systems would not permit the formation of linear polymers, it would be interesting to investigate such initiator systems towards the further development of high molecular weight polypeptoids.

The degradation time and pathways of bio-relevant polymers play a vital role in the design and possible applications of biomaterials. One of the main advantages that polypeptoids has over other bio-inspired polymers (*eg.* PEG, PiPAam, PiPOx, polypeptides, *etc.*) is its intrinsic potential to be degradable but resistant to proteolysis. Peptoids have been demonstrated to suppress enzymatic degradation but other degradation pathways have not been explored (albeit the hydrolysis of amides in alkaline solutions is well-known). Therefore degradation studies are a 2nd prerequisite to developing these polymers for biomedical applications. Currently, PEG/PHPMA-drug conjugates are designed with hydrolytically cleavable bonds to facilitate in the degradation and subsequent renal excretion. In addition, the hydrolysis of poly(2-oxazoline) creates polyamines with cytotoxic behaviors and limits their applications. Degradation studies would provide insight into

whether similar designs are warranted for polypeptoid systems or toxic towards cells. Degradation and excretion also prevents bioaccumulation which may cause cell/organ failure through other routes. However, the appropriate degradation rate may provide increased bio-distribution for drugs or increase the efficacy of extracellular matrices (ECM). Therefore it is desirable to design systems that undergo degradation within a prescribed time interval. Once again, the traditional approach, with non-degradable polymers, was to include hydrolytically cleavable polymer-polymer conjugates. Inherently, bio-relevant polymers, with amides in the backbone, provide this opportunity towards degradation. Furthermore, the foreseeable peptide-peptoid copolymers via ROP of NCAs and NNCA would allow for the tailored design of degradable biomaterials.

Although there still remain some challenges related to achieving higher molecular weights and needed degradability studies towards the rationale design of biomaterials, polypeptoids and their hybrids offer a promising future as a complimentary bio-relevant polymeric material. Currently, they are/have capturing/ed the imagination of polymer, bioorganic, and bioengineering scientists worldwide. The fundamental work described throughout this dissertation was driven by the aforementioned potential of these polymers as well as by scientific curiosity. In as much, further investigations (both fundamental and application based) towards these bio-relevant polymers are likely to follow in due course.

6. Experimental Procedures

6.1 Materials

Unless otherwise stated, all reagents were purchased and used as is from commercial sources (Sigma-Aldrich, ACROS, and/or Alfa Aesar). Anhydrous solvents (*ie.* DMF, DMA, and benzonitrile) were either purchased in bottles with a septum over molecular sieves or distilled from a drying agent (*ie.* calcium hydride for CH_2Cl_2 or solid sodium for THF). All other solvents (*eg.* dioxane, EtOAc, MeOH, *etc.*) were used as is from their respective commercial sources. Freshly distilled solvents were stored over activated molecular sieves (3 Å; 3–5 mm beads) and sealed under argon (flowed through a calcium chloride drying tube). Thin layer chromatography (TLC; 0.2 mm silica gel with fluorescent indicator; Polygram® SIL G/UV₂₅₄) plates with visualizing agents (UV, iodine chamber, or KMnO_4 stain) were utilized to monitor the first two synthetic steps of the monomer synthesis. Flash chromatography techniques were utilized with nitrogen pressure to push eluent/sample mixture through silica gel (pore size 60 Å; Fluka). All laboratory equipment was cleaned and oven dried prior to use. The reaction flasks, for polymerization, were prepared by flash drying with a heat gun and reduced pressure (1.2×10^{-2} mbar).

6.2 Analytical Instrumentation and Methods

6.2.1 Gas chromatography mass spectrometry (GC-MS)

An Agilent Technologies GC 6890N MS 5975 equipped with an auto-sampler was utilized for analysis of compounds, purity, and detection of the monomer throughout the polymerization monitoring. Samples were prepared in 2 mL septum-sealed vials at concentrations between 1–10 mg/mL. Enhanced ChemStation® software was utilized for the measuring program and analysis. Monomer measuring program: An aliquot of 1 μL was injected into the heating block (200 °C), split (50:50), and flowed (He; 0.757 bar) through the heated (50–200 °C; 2 minute hold then 8 °C/min) column. After a 2 minute solvent delay, the data was captured (duration of 21.75 minutes) by the aforementioned software and sub-sequentially analyzed.

6.2.2 Melting point apparatus

The power setting of a MEL-TEMP II™ apparatus, produced by Laboratory Devices Inc. (USA), was set to 4 for <100 °C and 5 for 100–200 °C. Samples were measured in open capillary tubes.

Chapter 6: Experimental Procedures

6.2.3 Nuclear magnetic resonance (NMR) spectroscopy

A Bruker DPX-400 MHz instrument was utilized for in house NMR measurements. These measurements were completed at room temperature and the samples were previously prepared in CDCl₃ (sub-monomer to monomer) or DMF-d₇ (polymers) at concentrations of ca. 5 or 25 mg/mL, respectively. Topspin software was utilized for the setup, measurements, and data collection.

The Varian 600 MHz instrument, equipped with an autosampler, was utilized to measure **AP184A-B** (100% and 57% modification) at a separate facility. Samples were prepared in DMF-d₇ (ca. 20 mg/mL) and measured at room temperature. The fid was then transformed into spectra via MestReC© software. The respective deuterated solvent proton peaks (DMF-d₇: 8.02; 162.6)⁷⁹ were identified and used as the internal shifting standard.

6.2.4 Fourier transform infrared (FT-IR) spectroscopy

FT-IR measurements were completed on a Varian 1000 FT-IR, Scimitar series, equipped with an interchangeable sample head. Samples were loaded onto a diamond attenuated total reflectance (ATR) accessory and the Varian Resolutions FTS 1000 software allowed for measurements (transmittance; resolution = 4; 32 scans) and the recording of data.

6.2.5 Size exclusion chromatography (SEC)

SEC with simultaneous UV (270 nm) and RI detection was performed in *N*-methyl-2-pyrrolidone (NMP + 0.5 wt% LiBr) at +70 °C using a column set of two 300 × 8 mm² PSS-GRAM (spherical polyester particles with an average diameter of 7 μm) columns with porosities of 10² and 10³ Å. Solutions containing ca. 0.15 wt % polymer were filtered through 0.45 μm filters; the injected volume was 100 μL; and the flow rate was 0.8 μL/min. Calibration was done with polystyrene standards (Polymer Standards service PSS, Mainz, Germany). The NTeqGPC V6.4 software was used for data recording and handling.

6.2.6 Matrix-assisted laser desorption/ionization time-of-flight mass spectrometry (MALDI-ToF MS)

MALDI-ToF MS was carried out with a Bruker Autoflex III Smartbeam MALDI (Bruker Daltonik), equipped with a laser working at 356 nm. Acceleration voltage was 20 kV and 4 x 500 shots at different places of the spot were recorded. Instrument software (FlexControl) and FlexAnalysis was used for data handling.

Samples were prepared by applying the dried droplet method. 50 μL of matrix (T-2-(3-(4-*t*-Butylphenyl)-2-methyl-2-propenylidene)malononitrile, DCTB, 10 mg/mL in THF) were premixed with 10 μL of sample (2 mg/mL in THF). 1 μL of that mixture was dropped on the target.

6.2.7 Thermal analysis (DSC and TGA)

Differential scanning calorimetry (DSC) was performed on a Netzsch DSC Phoenix[®] under an inert nitrogen atmosphere. The samples were measured at a heating rate of 1, 10, and 20 K/min. Thermogravimetric analysis (TGA) was carried out on a Netzsch TG 209 F1 at 20 K/min under a nitrogen atmosphere.

6.2.8 Turbidimetry

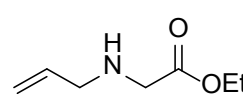
Turbidity measurements were conducted on (i) a turbidimetric photometer (Tepper Analytik TP1-J, Germany) operating at $\lambda = 670$ nm or (ii) a T70+ UV-Visible Spectrometer fitted with a Peltier element (Tresser Instruments, Germany) operating at $\lambda = 660$ nm. Samples were not stirred while heating/cooling rate of 1 $^{\circ}\text{C min}^{-1}$ was applied. The temperature at which in the heating scan transmittance dropped to 80% was taken as the cloud point temperature.

6.3 Synthetic Procedures

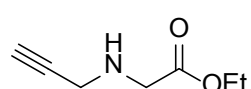
6.3.1 Monomer Synthesis

Pathway A (Chapter 3, Scheme 1) was prepared as described by Luxenhofer³⁹ and reported in Christian Secker's Master Thesis as well as in our publication submission.

6.3.2 Pathway B

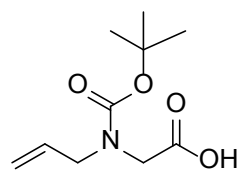
 *Step i.* Ethyl 2-(allylamino)acetate (**7k**). The following procedure was modified from a published procedure described by Liskamp and coworkers.⁶² Allylamine (**1k**, 22 mL; 0.294 mol) and NEt_3 (42 mL; 0.303 mol) were prepared in anhydrous THF (300 mL) and placed under argon. The solution was cooled to 0 $^{\circ}\text{C}$. Ethyl bromoacetate (**6**, 28 mL, 0.255 mol) was dissolved in anhydrous THF (200 mL) and added to the allylamine solution via a dripping funnel (over 30 minutes). White precipitation was observed after the complete addition of **6**. The reaction was stirred for an additional 3–4 hours and then the solvent was removed by roto-vaporization (loss of product was observed below 200 mbar with a water bath set to 40 $^{\circ}\text{C}$). The precipitate was washed with Et_2O (3x50 mL) and filtered off. The filtrate was collected and the solvent was removed by roto-vaporization. The crude oil (55.07 g) was loaded

onto a slurry packed column (1.5 kg of silica gel prepared in Et₂O). Flash chromatography techniques were utilized with Et₂O (5–10 L) as the eluent. Fractions of **7k** were collected ($R_f = 0.09$; KMnO₄ stain) and the solvent was removed by roto-vaporization. A translucent oil (35.45 g) was isolated and analyzed. The yield was adjusted down to 83% due to an observable ether impurity (¹H-NMR analysis). GC-MS detects **7k** ($m/z = 143.1$), with a retention time of 8.5 minutes, and no other peaks (except for solvents). Further analysis correlates with Liskamp and coworkers published data.



Ethyl 2-(prop-2-yn-1-ylamino)acetate (**7l**). Synthesized as previously described.

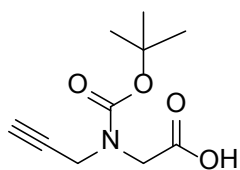
A yellow oil (13.46 g; 76%) was isolated and analyzed. ¹H-NMR (CDCl₃, 400 MHz) δ 4.18 (q, $J = 7.2, 7.2, 6.8$ Hz, 2H), 3.48 (s, 2H), 3.47 (s, 1H), 3.47 (s, 1H)⁸⁰, 2.21 (s, 1H), 1.73 (s, 1H), 1.27 (t, $J = 7.6, 6.4$ Hz, 3H); ¹³C-NMR (CDCl₃, 100 MHz) δ 171.7 (170.2), 81.1 (78.2), 71.8 (73.6), 60.7 (65.7), 49.1 (54.1), 37.5 (43.2), 14.0 (15.1); GC-MS (MSD) $R_t = 9.3$ min; (EI) m/z 141.1 (M⁺, [C₇H₁₀NO₂]⁺ = 141.16 g/mol).



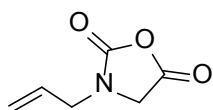
Step ii. 2-(Allyl(*tert*-butoxycarbonyl)amino)acetic acid (**4k**). The following

procedure was modified from a published procedure described by Liskamp and coworkers.⁶² Ethyl 2-(allylamino)acetate (**7k**; 33.00 g; 0.200 mol⁸¹) was dissolved in 1,4-dioxane (500 mL). Boc₂O (44.54 g; 0.204 mol) was added to the stirring solution and the reaction mixture was placed under argon. The reaction was followed by TLC (100% Et₂O; KMnO₄ stain) and the protection was complete within 2–4 hours (R_f change from 0.09 to 0.95). MeOH (300 mL) was poured into the stirring solution. A 4 N NaOH solution (120 mL; 0.48 mol) was added via dripping funnel (ca. 1–2 hours). White precipitation was observed after the complete addition of NaOH. TLC indicated the consumption of the intermediate (Ethyl Boc-*N*-allylglycinoate). The mixture was diluted with H₂O (ca. 300 mL) and 1,4-dioxane was extracted in Et₂O (ca. 3x500 mL). The aqueous layer pH was adjusted to ca. 3 (Litmus paper) with 1 N KHSO₄. Further extractions were carried out with EtOAc (3x150 mL). The collected extracts were dried over MgSO₄ and concentrated down (roto-vaporization) to a white solid. This was re-dissolved in Et₂O and subsequently removed via roto-vaporization (2x). High vacuum was utilized to remove trace amounts of solvents. A white crystalline powder was collected (41.27 g; 96%). Analysis with ¹H-NMR and GC-MS (fragmentation pattern; 16.5 minutes)

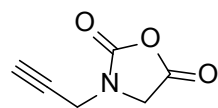
supports product **4k** with no impurities and subsequently matches data presented by Liskamp and coworkers.



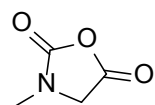
2-((*Tert*-butoxycarbonyl)(prop-2-yn-1-yl)amino)acetic acid (**4l**). Synthetically prepared as described above with a 92% yield. $^1\text{H-NMR}$ (CDCl_3 , 400 MHz) δ 10.37 (bs, 1H), 4.22 (s, 1H), 4.18 (s, 1H), 4.15 (s, 1H), 4.11 (s, 1H), 2.27 (t, J = 2.4, 2.4 Hz, 1H), 1.48 (s, 4.5H), 1.44 (s, 4.5H); $^{13}\text{C-NMR}$ (CDCl_3 , 100 MHz) δ 175.6 (175.3), 154.6 (154.9), 81.4 (78.4), 73.0 (72.8), 47.1 (46.7), 36.6 (37.3), 28.2; GC-MS (MSD) R_t = 8.2 min; (EI) m/z 112.0 (M^+ -Boc, $[\text{C}_5\text{H}_6\text{NO}_2]^+$ = 112.04 g/mol), 57.1 (*t*-butyl, $[\text{C}_4\text{H}_9]^+$ = 57.07 g/mol).



Step iii. 3-Allyloxazolidine-2,5-dione (**5k**). The following procedure was modified from Zhang and Luxenhofer group's reported procedures.^{38a, 39} A reaction flask was oven dried and flushed with argon. Compound **4k** (10.01 g; 0.0465 mol) was added to this flask and dissolved in anhydrous CH_2Cl_2 (350 mL). The stirring solution was cooled to 0 °C. PCl_3 (4.86 mL; 0.0557 mol) was injected slowly (ca. 5 minutes) and the reaction was allowed to stir for 4–5 hours. Volatile organics were removed by a rotovaporizer connected to argon. A Criegee distillation apparatus was flashed dried under vacuum (1.5×10^{-2} mbar). The remaining material was transferred to the distillation round bottom flask utilizing anhydrous THF. Solvents were cryo-condensed away. After leaving on high vacuum for ca. 20 minutes, the distillation flask was placed in an oil bath and well insulated with cotton. The temperature of the oil bath was initially raised to 75 °C. Once the internal thermometer was within 15 degrees of the oil bath, the temperature was slowly raised to 85–90 °C (2.0×10^{-2} mbar).⁸² Boiling point range of product **5k** was 73–88 °C. A translucent oil (3.6 mL; 4.82 g; 73%) was collected. Product **5k** is highly reactive to impurities and must be used immediately or stored under an inert system.⁸³ $^1\text{H-NMR}$ analysis supports product **5k** in 98% purity. $^1\text{H-NMR}$ (DMF-d_7 , 400 MHz) δ 5.98–5.82 (m, 1H), 5.40 (d, J = 16 Hz, 1H), 5.25 (d, J = 10 Hz, 1H), 4.35 (s, 2H), 4.03 (d, J = 6 Hz, 2H); $^{13}\text{C-NMR}$ (DMF-d_7 , 100 MHz) δ 167.9, 153.2, 132.4, 118.6, 49.8, 46.2; FT-IR (crystal) $\tilde{\nu}_{\text{max}}$ 3087, 2985, 2932, 1848, 1763, 1452, 1409, 1272, 1217, 1183, 983, 939, 913, 893, 833, 749, 699, 661, 600, 549 cm^{-1} ; GC-MS (MSD) R_t = 13.0 min; (EI) m/z 141.0 (M^+ , $[\text{C}_6\text{H}_7\text{NO}_3]^+$).

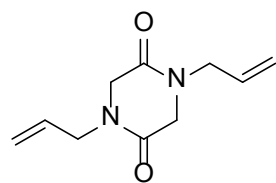


3-(Prop-2-yn-1-yl)oxazolidine-2,5-dione (**5l**). Prepared as described above but sublimation was utilized for purification. White crystalline material (47%) with a melting point of ~ 60 °C. $^1\text{H-NMR}$ (DMF- d_7 , 400 MHz) δ 4.45 (s, 2H), 4.31 (s, 1H), 4.31 (s, 1H), 3.39 (t, $J = 2.8, 2.4$ Hz, 1H), $^{13}\text{C-NMR}$ (DMF- d_7 , 100 MHz) δ 167.2, 152.8, 77.3, 75.9, 49.6, 33.4; FT-IR (crystal) $\tilde{\nu}_{max}$ 3268, 2977, 2938, 2912, 2856, 1847, 1757, 1456, 1437, 1407, 1358, 1300, 1260, 1231, 1192, 1163, 1016, 996, 937, 898, 840, 752, 683, 654 cm^{-1} ; GC-MS (MSD) $R_t = 6.6$ min; (EI) m/z 139.0 (M^+ , $[\text{C}_6\text{H}_5\text{NO}_3]^+$ = 139.02 g/mol), 111.0 ($\text{M}^+ - \text{CO}$, $[\text{C}_5\text{H}_5\text{NO}_2]^+$ = 111.03 g/mol), 67.1 ($\text{M}^+ - \text{COOCO}$, $[\text{C}_4\text{H}_5\text{N}]^+$ = 67.04 g/mol), 39.1 (propargyl, $[\text{C}_3\text{H}_3]^+$ = 39.02).

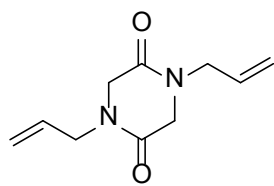


3-Methyloxazolidine-2,5-dione (**5a**). Prepared as described above but purification was accomplished by sublimation. White powder material (60 %) with a melting point of ca. 104 °C. $^1\text{H-NMR}$ (CDCl_3 , 400 MHz) δ 4.12 (s, 2H), 3.05 (s, 3H); $^{13}\text{C-NMR}$ (CDCl_3 , 100 MHz) δ 165.1, 152.3, 50.9, 30.3; FT-IR (crystal) $\tilde{\nu}_{max}$ 2993, 2947, 2917, 1851, 1761, 1654, 1502, 1492, 1443, 1404, 1316, 1277, 1218, 1199, 1062, 983, 905, 837, 748, 690 cm^{-1} ; GC-MS (MSD) $R_t = 5.9$ min; (EI) m/z 115.0 (M^+ , $[\text{C}_4\text{H}_7\text{NO}_3]^+$ = 115.03 g/mol).

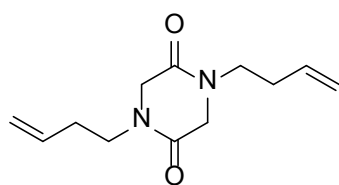
6.3.3 Cyclic Diene Monomer



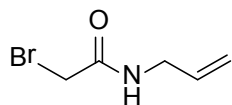
1,4-Diallylpiperazine-2,5-dione (**13k**). Diketopiperazine (DKP) **13** was detected as a side product created during the purification of NCA **5** (previous attempts). Improper insulation/vacuum of a short path distillation caused NCA **5k** to reflux (110–130 °C) in the crude mixture ($\text{O} = \text{PCl}_5$, PCl_5 , HCl , *etc.*) over 3–4 hours. The oil bath temperature was then raised to 140–150 °C and the exterior of the distillation apparatus was heated above 100 °C. NCA **5k** (0.41 g; 6%) and DKP **13k** (2.88 g; 31%) were collected as an oil and white crystalline material (mp = 98 °C), respectively. Noteworthy, Katsu and coworkers observed DKP **13k** as a competing by-product of the cyclization of a tripeptide into the target compound, *N,N',N''*-triallyl-*cyclo*-triglycine.⁸⁴ They did not describe any characterization of DKP **13k**. We herein disclose the full characterization of DKP **13k**. $^1\text{H-NMR}$ (CDCl_3 , 400 MHz) δ 5.76–5.66 (m, 2H), 5.25 (dd, $J = 10, 19$ Hz, 4H), 4.01 (d, $J = 6$ Hz, 4H), 3.94 (s, 4H); $^{13}\text{C-NMR}$ (CDCl_3 , 100 MHz) δ 163.2, 130.8, 119.6, 49.2, 48.2; FT-IR (crystal) $\tilde{\nu}_{max}$ 2976, 2941, 2913, 2862, 2841, 1652, 1486, 1438, 1410, 1334, 1290, 1193, 1138, 1076, 1010, 938, 779, 631 cm^{-1} ; GC-MS (MSD) $R_t = 20.5$ min; (EI) m/z 194.4 (M^+ , $[\text{C}_{10}\text{H}_{14}\text{NO}_2]^+$ = 194.11).



1,4-Diallylpiperazine-2,5-dione (**13k**). Boc-*N*-allyl glycine (**4k**, 1.1700 g, 5.44 mmol) was dissolved in CH_2Cl_2 (50 mL) and cooled to 0 °C under argon. PCl_3 (0.24 mL; 2.75 mmol) was injected and the reaction was allowed to run overnight. Volatile organics were removed by rotovaporization and the crude mixture was heated to 160 °C with an air condenser fixed above the boiling mixture. A white crystalline material began to collect in the condenser (6–12 hrs.). This material was collected by rinsing with MeOH and subsequent removal of volatile organics via rotovaporization. Note that there was additional material still observable in the reaction flask but no further attempt to purify this sample was undertaken. From the condenser, a white material (90.1 mg, 9%) was collected and analyzed by $^1\text{H-NMR}$. Spectroscopy supports DKP **13k**.

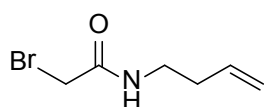


1 Step: 1,4-Di(but-3-en-1-yl)piperazine-2,5-dione.⁸⁵ Suspended glycine anhydride (0.1148 g; 1.006 mmol) in DMA (10 mL) and placed under argon. Added NaH (60 wt %; 0.0972 g; 2.43 mmol) and placed reaction vessel in ice bath (0 °C). After 30 minutes of stirring, 4-bromo-1-butene (0.21 mL; 2.1 mmol) was injected. After 10 minutes, *n*Bu₄NI (0.5 mL of a 0.54 M [DMA]; 0.27 mmol). The reaction was monitored by GC-MS. Additional *n*Bu₄NI (0.5078 g; 1.4 mmol) was injected to attempt to push reaction forward. After 48 hours, reaction mixture was passed through filter and the filtrate was concentrated down by distilling off the solvent under reduced pressures. Crude mixture was loaded onto silica gel prepared in heptanes. Eluent: 30% v/v Acetone/Heptanes afforded a semi-crystalline yellowish material (54.3 mg; 24%). $^1\text{H-NMR}$ (CDCl_3 , 400 MHz) δ 5.81–5.70 (m, 2H), 5.09 (dd, $J = 17, 8$ Hz, 4H), 3.96 (s, 4H), 3.47 (t, $J = 7.2, 7.2$ Hz, 4H), 2.34 (q, $J = 6.8, 7.2, 7.2$ Hz, 4H); GC-MS (MSD) $R_t = 18.6$ min; (EI) m/z 222.2 (M^+ , $[\text{C}_{12}\text{H}_{18}\text{N}_2\text{O}_2] = 222.14$ g/mol).

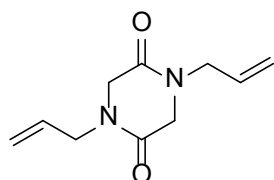


2 Steps:⁷⁷ *N*-allyl-2-bromoacetamide. Allyl amine (**1k**; 3.77 mL; 50.4 mmol) and K_2CO_3 (8.08 g; 58.5 mmol) were combined in CH_2Cl_2 (100 mL). Bromoacetyl bromide (4.82 mL; 55.5 mmol) was injected slowly over 30 minutes and the reaction mixture was stirred overnight. The reaction was heated to reflux for ca. 3 hours and then cooled to room temperature. The reaction mixture was poured into ice water and extracted organics in CH_2Cl_2 . Washed combined extracts with H_2O and then dried extracts with MgSO_4 . The volatile organics were removed by roto-vaporization and impregnated onto silica gel. Once dried, the crude sample was loaded onto a column where silica gel was prepared in heptanes.

Eluent: 20–30% v/v, EtOAc/heptanes. Fraction one was collected and volatile organics were removed by roto-vaporization and then high vacuum. A white crystalline material was collected (4.716 g, 53%). ¹H-NMR (CDCl₃, 400 MHz) δ 6.65 (bs, 1H), 5.88-5.78 (m, 1H), 5.20 (d, J = 22.8 Hz, 1H), 5.17 (d, J = 16 Hz, 1H), 3.91 (d, J = 5.6 Hz, 2H), 3.88 (s, 2H); GC-MS (MSD) R_t = 9.0 min; (EI) m/z 98.1 (M⁺-Br, [C₅H₈NO]⁺ = 98.06 g/mol), 41.1 (allyl, [C₃H₅]⁺ = 41.04 g/mol).

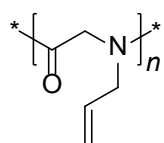


2 Steps:⁷⁷ 2-Bromo-*N*-(but-3-en-1-yl)acetamide. The above procedure was repeated for 3-butenylamine HCl (4.93 g; 45.8 mmol). A transparent oil (2.9667 g; 34%) was collected and analyzed. ¹H-NMR (CDCl₃, 400 MHz) δ 6.54 (bs, 1H), 5.82-5.72 (m, 1H), 5.13 (d, J = 17.2 Hz, 1H), 5.12 (d, J = 9.6 Hz, 1H), 3.87 (s, 2H), 3.37 (q, J = 6.4, 6.0, 6.8 Hz, 2H), 2.33-2.17 (m, 2H); GC-MS (MSD) R_t = 9.0 min; (EI) m/z 150.0, 152.0 (M⁺-allyl, [C₆H₉BrNO]⁺ = 149.95, 151.95 g/mol), 112.1 (M⁺-Br, [C₆H₁₀NO]⁺ = 112.07 g/mol).



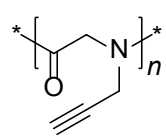
2 Steps:⁷⁷ 1,4-Diallylpiperazine-2,5-dione. A mixture of *N*-allyl-2-bromoacetamide (4.716 g; 26.5 mmol) and KOH (crushed, ca. 3.1 g; 55.2 mmol) was prepared in CH₃CN (132 mL). The reaction mixture was refluxed overnight. Crude reaction was passed through a filter and volatile organics were removed by roto-vaporization. The crude material was redissolved in CH₂Cl₂:iPrOH (10:1) and washed with H₂O. The organic extracts were dried over MgSO₄ and concentrated down to a yellow oil. The crude mixture was loaded onto silica previously prepared in heptanes. Eluent: 15% v/v, Acetone/CH₂Cl₂. Collected fraction and roto-vaporized off volatile organics to collect a yellow material (1.0197 g). This material was then sublimated to receive a white material with slight accents of yellow (0.9565 g, 18%). Analysis by ¹H-NMR and GC-MS matches the previous reported data.

6.3.4 Preparation of poly(*N*-allyl/propargyl glycine) (PNAG_n)

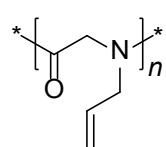


*Homogeneous phase preparation of poly(*N*-allyl/propargyl glycine) homopolymers.* A sealable reaction flask was flashed dried on a Schlenk line. Freshly distilled NCA **5k** (1.834 g; 12.99 mmol) was dissolved in anhydrous THF (ca. 10 mL) and transferred into the reaction flask (under streaming argon). Low vapor volatiles were removed by cryo-condensation and the remaining oil was left on continuous vacuum (1.5x10⁻² mbar) for ca. 30 minutes. Under streaming argon, anhydrous benzonitrile (18 mL, ca. 10% w/w) was transferred into the reaction flask followed by the initiator (a 1.0 M solution of benzylamine in NMP;

$[5\mathbf{k}]_0/[\text{BnNH}_2]_0 = 25, 50, \text{ and } 75$). The pressure was reduced to 2.0×10^{-2} mbar and the reaction flask was resealed. The consumption of the monomer $5\mathbf{k}$ was monitored by GC-MS.⁸⁶ In general, the reaction was complete within 1 week when $\bar{n} < 50$ and 3 weeks when $\bar{n} > 75$. Acetic anhydride was utilized to terminate the end group's activity. The solvent was distilled off (under vacuum) and the crude oil was redissolved in a miniscule amount of THF. The polymers were then precipitated into petroleum ethers. Centrifugation and decantation were utilized in isolating the precipitates. High vacuum was utilized for removing residue solvents. Exemplary example of PNAG when the target \bar{n} was ca. 50: Duration of 4 days; Gravimetric yield = ca. 91%; ¹H-NMR (DMF-d₇, 400 MHz) δ 7.33 (br m, 5H, C₆H₅-), 5.93-5.76 (br, 37H, -CH=), 5.28-5.11 (br, 68H, =CH₂), 4.41-4.15 (br, 69H, allyl[-CH₂-] and initiator overlapping), 3.98 (br, 69H, -CH₂-), 1.95 (m, 3H, -CH₃), $\bar{n} = 35$; ¹³C-NMR (DMF-d₇, 100 MHz) δ 169.9, 169.2, 134.2, 134.0, 117.5, 50.5, 48.4; FT-IR (crystal) $\tilde{\nu}_{\text{max}}$ 3079, 2981, 2921, 1636, 1469, 1404, 1344, 1284, 1212, 1194, 1131, 992, 920, 842, 696, 605 cm⁻¹; SEC (PS): $\bar{M}_n = 6.90$ kg/mol, $D = 1.04$; MALDI-ToF MS (DCTB, linear): $\bar{M}_n = 4.51$ kg/mol, $\bar{M}_w = 4.56$, $\bar{n} = 44$ ($[\text{M}+\text{Na}]^+$, $m/z = 4442.5$, $\text{M} = \text{BnNH-COCH}_2\text{N}(\text{CH}_2\text{CHCH}_2)_n(\text{COCH}_3)$); TGA (20 K/min): 292 °C (11%), 415 °C (67%); DSC (0–200 °C, 10 K/min): $T_g = 66$ °C.



Homogeneous phase preparation of poly(N-propargyl glycine). The aforementioned procedure was utilized with a 1.0 M solution of benzylamine in NMP; ($[5\mathbf{l}]_0/[\text{BnNH}_2]_0 = 25, 50, \text{ and } 75$). Exemplary example of PNPG when the target \bar{n} was ca. 50: Duration of 4 days; Gravimetric yield = ca. 94%; ¹H-NMR (DMF-d₇, 400 MHz) δ 7.36 (br m, 5H, C₆H₅-), 4.82-4.26 (br, 144H, BnNH-, -COCH₂N-, -NCH₂C≡ overlapping), 3.36-3.13 (br m, 40H, ≡CH) 1.95 (br m, 3H, -CH₃), $\bar{n} = 37$; ¹³C-NMR (DMF-d₇, 100 MHz) δ 169.8, 168.8, 79.2, 74.9, 67.4, 47.9, 47.8; FT-IR (crystal) $\tilde{\nu}_{\text{max}}$ 3280, 2979, 1653, 1469, 1437, 1406, 1346, 1284, 1209, 1190, 1119, 1043, 954, 916, 868, 840, 636 cm⁻¹; SEC (PS): $\bar{M}_n = 5.43$ (25.2) kg/mol, $D = 1.04$ (1.05); MALDI-ToF MS (Dithranol, linear): $\bar{M}_n = 3.81$ kg/mol, $\bar{M}_w = 3.89$, $\bar{n} = 39$ ($[\text{M}+\text{Na}]^+$, $m/z = 3880.8$, $\text{M} = \text{BnNH-COCH}_2\text{N}(\text{CH}_2\text{CCH})_n(\text{COCH}_3)$); TGA (20 K/min): 376 °C (56%); DSC (0–250 °C, 10 K/min): $T_g = 94$ °C.



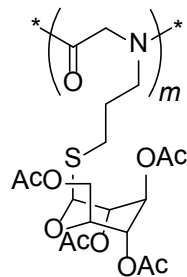
Heterogeneous phase preparation of poly(N-allyl glycine). Exemplary, a flask previously dried and flushed with argon was loaded with NCA $5\mathbf{k}$ (1.096 g; 7.76 mmol) and heptanes (30 mL). Benzonitrile (7 mL) was added and the mixture was stirred on the highest setting to create an emulsion type environment. Benzylamine (1.0 M in NMP; 78 μL ; $[5\mathbf{k}]_0/[\text{BnNH}_2]_0 = 100$) was injected into the stirring mixture. The reaction was

terminated after 12 hours with acetic anhydride (0.1 mL; 1.06 mmol) and continuously stirred for an additional 3-4 hours. Vacuum distillation was utilized to remove volatile organics and the crude mixture was redissolved in THF. This solution was precipitated into heptanes. The precipitates were isolated by centrifugation and decantation procedures. After placing on high vacuum overnight, a white crystalline material was collected and analyzed. Gravimetric yield = ca. 100%; ¹H-NMR (DMF-d₇, 400 MHz) and FT-IR analysis corresponds to previously reported values; SEC (PS): $\bar{M}_n = 9.52$ kg/mol, $D = 1.03$; MALDI-ToF MS (DCTB, linear): $\bar{M}_n = 7.84$ kg/mol, $\bar{M}_w = 7.88$, $\bar{n} = 80$ ($[M+Na]^+$, $m/z = 7842.7$, $M = BnNH-COCH_2N(CH_2CHCH_2)_{80}(COCH_3)$) DSC (−50–250 °C, 10 K/min): $T_g = 67$ °C.

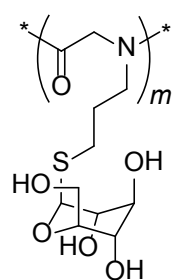
6.3.5 Modification of PNAG via thiol-ene photo-addition

Side chain modification of PNAG_n with 1-thioglycerol. Exemplary, PNAG₈₀ (0.221 g; 2.27 mmol) was dissolved in DMF (2.2 mL) with 1-thioglycerol (0.24 mL; 2.75 mmol) and 2,2-dimethoxy-2-phenylacetophenone (DMPA; 7.3 mg; 0.028 mmol). The round bottom flask was flushed with argon and sealed with a glass stopper. The reaction mixture was then irradiated with UV light for 12 hours. The polymer was precipitated in Et₂O and isolated by centrifugation and decantation. The material was redissolved in MeOH and transferred to a new flask where the volatiles were removed by vacuum. A transparent waxy material (0.468 g; ca. 100%) was collected. ¹H-NMR (DMF-d₇, 400 MHz) δ 7.37 (br m, 5H, C₆H₅-), 4.75-4.61 (br, 38H, -OH), 4.45-4.29 (br, 28H, -CH₂-), 3.71 (br, 16H, -SCH₂CHOHCH₂OH), 3.52-3.45 (br, 83H, -SCH₂CHOHCH₂OH, -NCH₂CH₂CH₂-), 2.74-2.59 (br m, 78H, -SCH₂CHOHCH₂OH, -NCH₂CH₂CH₂-), 1.94-1.81 (br m, 36H, -NCH₂CH₂CH₂-); FT-IR (crystal) $\tilde{\nu}_{max}$ 3354, 2916, 2868, 1756, 1645, 1481, 1429, 1408, 1374, 1339, 1288, 1216, 1151, 1059, 1026, 975, 945, 876, 846, 746, 695, 661 cm⁻¹; SEC (PS): $\bar{M}_n = 5.23$ kg/mol, $D = 1.11$; DSC (−50–250 °C, 10 K/min): $T_g = 22$ °C.

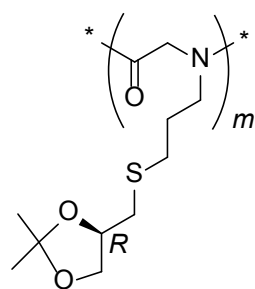
Side chain modification of PNAG_n with 1-thio-β-D-glucose tetraacetate. Exemplarily, PNAG₂₀ (0.240 g; 2.47 mmol) was dissolved in DMF (2.4 mL) and prepared in an Erlenmeyer flask under argon. 1-Thio-β-D-glucose tetraacetate (1.06 g; 2.91 mmol) was added and the mixture was allowed to stir (ca. 20 min). Then DMPA (7.9 mg; 0.03 mmol) was added and the reaction mixture was sealed with a glass stopper and placed under UV irradiation for 12 hours. Reaction



mixture was precipitated into Et₂O and the precipitates were isolated by centrifuge and decantation procedures. A white crystalline material (1.13 g; ca. 99%) was collected. ¹H-NMR confirms product with a conversion of ca. 100%. ¹H-NMR (DMF-d₇, 400 MHz) δ 7.39-7.31 (br m, 5H, C₆H₅-), 5.34 (br t, 16H, Glc), 5.06-4.96 (br, 41H, Glc), 4.56 (br m, 11H, BnNH-), 4.28-4.09 (br, 55H, Glc, Gly), 3.62 (br t, 17H, Glc), 3.45 (br, 39H, *n*propyl), 2.74 (br, 42H, *n*propyl), 2.09-2.01 (br m, 166H, Acetyls), 1.88 (br, 40H, *n*propyl); FT-IR (crystal) $\tilde{\nu}_{max}$ 2946, 1739, 1658, 1429, 1362, 1211, 1027, 906, 832, 746, 679 cm⁻¹; SEC (PS): \bar{M}_n = 5.6 kg/mol, D = 1.05; DSC (-50–250 °C, 10 K/min): T_g = 85 °C.



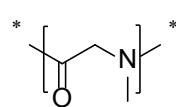
PNAG₂₀ (0.124 g; 1.28 mmol) was dissolved in H₂O (12 mL) and prepared in an Erlenmeyer flask under argon. 1-Thio-β-D-glucose (0.559 g; 2.56 mmol) was added and the mixture was allowed to stir (ca. 20 min). Then 2-hydroxy-4'-(2-hydroxyethoxy)-2-methylpropiophenone (HEMP; 6.8 mg; 0.03 mmol) was added followed by glacial acetic acid (0.8 mL) until the aqueous solution was slightly acidic (Litmus paper). The mixture was then irradiated for 24 hours by UV light. The crude mixture was purified with a dialysis membrane (500 Da) against H₂O. Freeze drying was utilized to remove water. A white material was collected (0.302 g; 75%) and analyzed. ¹H-NMR confirms product with a conversion of ca. 100%. ¹H-NMR (DMF-d₇, 400 MHz) δ 7.37 (br m, 5H, C₆H₅-), 5.15-5.06 (br, 30H, Glc), 4.68-4.28 (br, 43H, *n*propyl, BnNH, Gly), 3.85 (br, 12H, Glc), 3.62-3.21 (br, 80H, Glc), 2.83-2.2.71 (br, 25H, -NCH₂CH₂CH₂-), 2.02-1.86 (br, 21H, -NCH₂CH₂CH₂-); FT-IR (crystal) $\tilde{\nu}_{max}$ 3328, 2895, 1640, 1416, 1344, 1253, 1225, 1022, 876, 828, 683, 558 cm⁻¹; SEC (PS): \bar{M}_n = 5.34 kg/mol, D = 1.07; DSC (-50–250 °C, 10 K/min): T_g = 121 °C.



Exemplarily, PNAG₃₅ (0.1074 g; 1.11 mmol) was dissolved in anhydrous DMF (2 mL). Thiol-glycerol(ketal) (0.1994 g; 1.35 mmol) was added and the solution was stirred for 20 minutes. DMPA (ca. 5 mg) was added and the reaction mixture was irradiated with UV light (ca. 365 nm) for 24 hours. The reaction mixture was split into two parts where **A** was treated with TFA (0.1 mL) and subjected for additional UV irradiation for 24 hours. Sample **B** was precipitated into Et₂O and isolated by centrifugation and decantation. Sample **A** was prepared in the same fashion the following day. ¹H-NMR analysis suggests that sample **A** had improved post-modification (95%) with some loss of the ketal group (68%). Sample **B** illustrated an 84% conversion suggesting the longer duration or *in situ* deprotection of the ketal assisted in thiol-ene

photoaddition. **Sample A:** $^1\text{H-NMR}$ (DMF-d_7 , 400 MHz) δ 7.37 (br m, 5H, C_6H_5 -), 5.15-4.11 (br, 73H, $-\text{OH}$, $-\text{CH}_2$], BnNH -), 3.73 (br, 12H, $-\text{SCH}_2\text{CHORCH}_2\text{OR}$), 3.53 (br, 214H, $-\text{SCH}_2\text{CHORCH}_2\text{OR}$, $-\text{NCH}_2\text{CH}_2\text{CH}_2$ -), 2.84-2.59 (br, 131H, $-\text{SCH}_2\text{CHORCH}_2\text{OR}$, $-\text{NCH}_2\text{CH}_2\text{CH}_2$ -), 1.95 (br, 16H, acetyl), 1.78 (br, 95H, Ketal), 1.36-1.29 (br, 36H, $-\text{NCH}_2\text{CH}_2\text{CH}_2$ -); SEC (PS): $\bar{M}_n = 12.87$ kg/mol, $D = 1.09$.

6.3.6 Promoted ROP



An initiator (*N*-methyl benzamide, PNiPAAm, or PEO-OH) was washed and dried with anhydrous THF and high vacuum techniques. The initiator was redissolved in THF and a promoter (*t*-BuP₁, *t*-BuP₂, BEMP, or DBU) was added to the stirring solution under flowing argon (control reaction A was conducted without initiator; control reaction B was conducted without promoter). The monomer (*N*-methyl glycine NCA or O-benzyl glutamate NCA) was previously dried in the same fashion in a separate flask. After allowing the initiator/promoter solution to stir for ca. 30 minutes, the monomer solution was transferred into this reaction flask. Once sealed, the mixture was cooled with liquid nitrogen so that the reaction pressure could be reduced and then sealed prior to allowing reaction to warm to room temperature. Typically, within 2 hours precipitation was observed but the reaction was allowed to stir for 48 hours prior to termination with acetic anhydride. After 2 hours, methanol was utilized to assist in the transfer of the crude product into a fresh round bottom flask which was utilized to rotatevaporate off the volatile organics. Dialysis (1 kDa regenerated cellulose membranes against H₂O) was utilized to purify these polymers followed by freeze drying. Exemplarily, we illustrate 6 of these reactions to describe the complexity of verifying incorporation of the initiator as well as a suspected activated monomer initiation process.

N-methyl benzamide treated with *t*-BuP₁ and *N*-methyl glycine NCA added. $^1\text{H-NMR}$ (D_2O , 400 MHz) δ 4.49-4.14 (br, 2H, $-\text{CH}_2$), 3.09-2.91 (br, 3H, $-\text{CH}_3$), 2.17-2.03 (br, 0.16H, acetyl); SEC (NMP; PS) $\bar{M}_n = 4.02$ kg/mol, $D = 1.2$.

PEO-OH treated with *t*-BuP₂ and *N*-methyl glycine NCA added. $^1\text{H-NMR}$ (CDCl_3 , 400 MHz) δ 4.24-4.01 (br, 2H, $-\text{CH}_2$), 3.63 (s, 3H, PEO backbone), 3.03-2.93 (br, 3H, $-\text{CH}_3$), 2.12-2.10 (br, 0.17H, acetyl); SEC (NMP; PS) $\bar{M}_n = 7.26$ kg/mol, $D = 1.7$.

PEO-OH and *N*-methyl glycine NCA (**Control B**). ¹H-NMR (CDCl₃, 400 MHz) δ 4.25-4.01 (br, 2H, -CH₂-), 3.63 (s, 1.8H, PEO backbone), 3.04-2.94 (br, 3H, -CH₃), 2.2.50 (br, 0.68H, acetyl); SEC (NMP; PS) \bar{M}_n = 13.4 kg/mol, \bar{D} = 1.4.

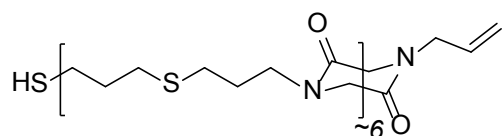
PEO-OH treated with *t*BuP₂ and γ -benzyl glutamic NCA added. ¹H-NMR (CDCl₃, 400 MHz) δ 7.19 (br, 5H, Cbz), 4.97 (br, 2H, Cbz), 3.86 (br, 1H, -CH₂-), 3.58 (s, 3H, PEO backbone), 2.66-1.65 (br, 4H, side chain, amide proton overlapping); SEC (NMP; PS) \bar{M}_n = 199 kg/mol, \bar{D} = 2.8.

γ -Benzyl glutamic NCA treated with *t*BuP₂ (**Control A**). ¹H-NMR (CDCl₃, 400 MHz) δ 8.28 (br, 1H, amide), 7.18 (br, 5H, Cbz), 4.97 (br, 2H, Cbz), 3.86 (br, 1H, -CH₂-), 2.63-2.06 (br, 4H, side chain); SEC (NMP; PS) \bar{M}_n = 35.0 kg/mol, \bar{D} = 1.5.

PEO-NH₂ and *N*-methyl glycine NCA combined. ¹H-NMR (CDCl₃, 400 MHz) δ 4.52-4.16 (br, 2H, -CH₂-), 3.74 (s, 2.2H, PEO backbone), 3.42 (br, 0.04H, -OMe), 3.11-2.94 (br, 3H, -CH₃), 2.20-2.06 (br, 0.14H, acetyl); SEC (NMP; PS) \bar{M}_n = 6.46 kg/mol, \bar{D} = 1.1.

6.3.7 Preparation of polydiketopiperazine

ADMet attempt to make poly(hex-3-ene)diketopiperazine (PHKP). The procedure described by Masuda and coworkers was utilized here with the Hoveyda-Grubbs type II catalyst.⁷³ No polymerization was detected by GPC. GC-MS, TLC, and ¹H-NMR all indicate that the monomer is still present with some other by-products which could be the monomer interacting with the catalyst. Masuda and coworkers described in their publication that a six member deactivation state could form with the Ruthenium catalyst and therefore the methylenes should be elongated until such complexes are not possible.



Thiol-ene step growth synthesis of Poly(dipropylthioether)diketopiperazine (PSKP₆). DKP **8k** (0.510 g; 2.62 mmol) was combined with 1,3-propanedithiol (0.290

g; 2.68 mmol) in an EtOH:H₂O (2.5 mL; 2:0.5) mixture. The reaction solution was then exposed to UV irradiation. Precipitation was observed within 1 hour and the reaction was allowed to stir for an additional 3 hours. The liquids were removed by centrifugation and decantation. The remaining white powder was washed with EtOH (3x) and isolated by the aforementioned technique. High vacuum was utilized to 'dry' the product. Although there was some loss due to a laboratory mishap, we were able to isolate a white powder (**14**; 0.381 g; 24%). ¹H-NMR (DMF-d₇, 400 MHz) δ 6.53-6.43 (m, 1 H), 6.00 (br t, 1.5 H), 4.76 (br s, 23 H), 4.73 (s), 4.67 (s), 4.23 (t, 20 H), 3.36 (t, 22 H),

Chapter 6: Experimental Procedures

3.27 (t, 21 H), 2.60 (q, 32 H), 2.12 (t, 1 H), 2.03 (d, 1.5 H); $^{13}\text{C-NMR}$ (DMF-d₇, 100 MHz) δ 164.6, 132.9, 118.1, 50.5, 47.8, 45.2, 34.5, 34.14, 27.4, 23.4; FT-IR (crystal) $\tilde{\nu}_{max}$ 2912, 1640, 1478, 1438, 1335, 1283, 1216, 1156, 1017, 983, 876, 837, 764, 725 cm^{-1} ; TGA thermally stable until 300 °C; DSC $T_g = 6$ °C.

7. Bibliography and Notes

1. Pandit, A.; Coburn, J. C., Development of Naturally-Derived Biomaterials and Optimization of Their Biomechanical Properties. In *Topics in Tissue Engineering*, Ashammakhi, N.; Reis, R.; Chiellini, E., Eds. UK, 2007; Vol. 3, p 32.
2. (a) Li, L. Y.; Ly, M.; Linhardt, R. J., Proteoglycan sequence. *Mol. Biosyst.* **2012**, *8* (6), 1613-1625; (b) Ly, M.; Leach, F. E.; Laremore, T. N.; Toida, T.; Amster, I. J.; Linhardt, R. J., The proteoglycan bikunin has a defined sequence. *Nat. Chem. Biol.* **2011**, *7*(11), 827-833.
3. Kawai, F., The Biochemistry and Molecular Biology of Xenobiotic Polymer Degradation by Microorganisms. *Biosci. Biotech. Bioch.* **2010**, *74*(9), 1743-1759.
4. Weber, C.; Hoogenboom, R.; Schubert, U. S., Temperature responsive bio-compatible polymers based on poly(ethylene oxide) and poly(2-oxazoline)s. *Prog. Polym. Sci.* **2012**, *37* (5), 686-714.
5. Gil, E. S.; Hudson, S. M., Stimuli-responsive polymers and their bioconjugates. *Prog. Polym. Sci.* **2004**, *29*(12), 1173-1222.
6. Schlaad, H.; Diehl, C.; Gress, A.; Meyer, M.; Demirel, A. L.; Nur, Y.; Bertin, A., Poly(2-oxazoline)s as Smart Bioinspired Polymers. *Macromol. Rapid Comm.* **2010**, *31* (6), 511-525.
7. Sutthasupa, S.; Shiotsuki, M.; Sanda, F., Recent advances in ring-opening metathesis polymerization, and application to synthesis of functional materials. *Polym. J.* **2010**, *42* (12), 905-915.
8. Dimitrov, I.; Trzebicka, B.; Muller, A. H. E.; Dworak, A.; Tsvetanov, C. B., Thermosensitive water-soluble copolymers with doubly responsive reversibly interacting entities. *Prog. Polym. Sci.* **2007**, *32*(11), 1275-1343.
9. Yang, T., Recent Applications of Polyacrylamides as Biomaterials. *Recent Patents on Materials Science* **2008**, *1* (1), 29-40.
10. Cooperstein, M. A.; Canavan, H. E., Biological Cell Detachment from Poly(*N*-isopropyl acrylamide) and Its Applications. *Langmuir* **2010**, *26*(11), 7695-7707.
11. Duncan, R., The dawning era of polymer therapeutics. *Nat. Rev. Drug Discov.* **2003**, *2* (5), 347-360.
12. Sedlacek, O.; Monnery, B. D.; Filippov, S. K.; Hoogenboom, R.; Hruby, M., Poly(2-Oxazoline)s - Are They More Advantageous for Biomedical Applications Than Other Polymers? *Macromol. Rapid Comm.* **2012**, *33*(19), 1648-1662.

13. Katsumoto, Y.; Tsuchiizu, A.; Qiu, X. P.; Winnik, F. M., Dissecting the Mechanism of the Heat-Induced Phase Separation and Crystallization of Poly(2-isopropyl-2-oxazoline) in Water through Vibrational Spectroscopy and Molecular Orbital Calculations. *Macromolecules* **2012**, *45* (8), 3531-3541.
14. Diehl, C.; Cernoch, P.; Zenke, I.; Runge, H.; Pitschke, R.; Hartmann, J.; Tiersch, B.; Schlaad, H., Mechanistic study of the phase separation/crystallization process of poly(2-isopropyl-2-oxazoline) in hot water. *Soft Matter* **2010**, *6* (16), 3784-3788.
15. Larson, N.; Ghandehari, H., Polymeric Conjugates for Drug Delivery. *Chem. Mater* **2012**, *24* (5), 840-853.
16. (a) Li, Y.; Thouas, G. A.; Chen, Q. Z., Biodegradable soft elastomers: synthesis/properties of materials and fabrication of scaffolds. *RSC Adv.* **2012**, *2* (22), 8229-8242; (b) Ulery, B. D.; Nair, L. S.; Laurencin, C. T., Biomedical Applications of Biodegradable Polymers. *J. Polym. Sci. Pol. Phys.* **2011**, *49* (12), 832-864.
17. Armentano, I.; Dottori, M.; Fortunati, E.; Mattioli, S.; Kenny, J. M., Biodegradable polymer matrix nanocomposites for tissue engineering: A review. *Polym. Degrad. Stabil.* **2010**, *95* (11), 2126-2146.
18. Grauer, A.; Konig, B., Peptidomimetics - A Versatile Route to Biologically Active Compounds. *Eur. J. Org. Chem.* **2009**, (30), 5099-5111.
19. Barron, A. E.; Zuckermann, R. N., Bioinspired polymeric materials: in-between proteins and plastics. *Curr. Opin. Chem. Biol.* **1999**, *3* (6), 681-687.
20. Zuckermann, R. N., Peptoid Origins. *Biopolymers* **2011**, *96* (5), 545-555.
21. (a) Miller, S. M.; Simon, R. J.; Ng, S.; Zuckermann, R. N.; Kerr, J. M.; Moos, W. H., Comparison of the Proteolytic Susceptibilities of Homologous L-Amino-Acid, D-Amino-Acid, and N-Substituted Glycine Peptide and Peptoid Oligomers. *Drug Develop. Res.* **1995**, *35* (1), 20-32; (b) Gobbo, M.; Benincasa, M.; Bertoloni, G.; Biondi, B.; Dosselli, R.; Papini, E.; Reddi, E.; Rocchi, R.; Tavano, R.; Gennaro, R., Substitution of the Arginine/Leucine Residues in Apidaecin Ib with Peptoid Residues: Effect on Antimicrobial Activity, Cellular Uptake, and Proteolytic Degradation. *J. Med. Chem.* **2009**, *52* (16), 5197-5206; (c) Kapoor, R.; Eimerman, P. R.; Hardy, J. W.; Cirillo, J. D.; Contag, C. H.; Barron, A. E., Efficacy of Antimicrobial Peptoids against Mycobacterium tuberculosis. *Antimicrob. Agents Ch.* **2011**, *55* (6), 3058-3062.

22. Haynes, R. D.; Meagher, R. J.; Barron, A. E., A Chemically Synthesized Peptoid-Based Drag-Tag Enhances Free-Solution DNA Sequencing by Capillary Electrophoresis. *Biopolymers* **2011**, *96* (5), 702-707.
23. Sani, B.; Kudirka, R.; Cho, A.; Venkateswaran, N.; Olivier, G. K.; Olson, A. M.; Tran, H.; Harada, R. M.; Tan, L.; Zuckermann, R. N., Shaken, Not Stirred: Collapsing a Peptoid Monolayer To Produce Free-Floating, Stable Nanosheets. *J. Am. Chem. Soc.* **2011**, *133* (51), 20808-20815.
24. (a) Hao, G.; Hajibeigi, A.; León-Rodríguez, L. M. D.; Öz, O. K.; Sun, X., Peptoid-based PET imaging of vascular endothelial growth factor receptor (VEGFR) expression. *Am. J. of Nuc. Med. Mol. Imaging* **2011**, *1* (1), 65-75; (b) Dhaliwal, K.; Escher, G.; Unciti-Broceta, A.; McDonald, N.; Simpson, A. J.; Haslett, C.; Bradley, M., Far red and NIR dye-peptoid conjugates for efficient immune cell labelling and tracking in preclinical models. *Med. Chem. Comm.* **2011**, *2* (11), 1050-1053.
25. Chen, C. L.; Qi, J. H.; Zuckermann, R. N.; DeYoreo, J. J., Engineered Biomimetic Polymers as Tunable Agents for Controlling CaCO₃ Mineralization. *J. Am. Chem. Soc.* **2011**, *133* (14), 5214-5217.
26. Fowler, S. A.; Luechapanichkul, R.; Blackwell, H. E., Synthesis and Characterization of Nitroaromatic Peptoids: Fine Tuning Peptoid Secondary Structure through Monomer Position and Functionality. *J. Org. Chem.* **2009**, *74* (4), 1440-1449.
27. (a) Murnen, H. K.; Rosales, A. M.; Jaworski, J. N.; Segalman, R. A.; Zuckermann, R. N., Hierarchical Self-Assembly of a Biomimetic Diblock Copolypeptoid into Homochiral Superhelices. *J. Am. Chem. Soc.* **2010**, *132* (45), 16112-16119; (b) Gelain, F.; Silva, D.; Caprini, A.; Taraballi, F.; Natalello, A.; Villa, O.; Nam, K. T.; Zuckermann, R. N.; Doglia, S. M.; Vescovi, A., BMHP1-Derived Self-Assembling Peptides: Hierarchically Assembled Structures with Self-Healing Propensity and Potential for Tissue Engineering Applications. *ACS Nano* **2011**, *5* (3), 1845-1859.
28. Zoelen, W. v.; Zuckermann, R. N.; Segalman, R. A., Tunable Surface Properties from Sequence-Specific Polypeptoid-Polystyrene Block Copolymer Thin Films. *Macromolecules* **2012**, *45*, 7072-7082.
29. Rosales, A. M.; Murnen, H. K.; Zuckermann, R. N.; Segalman, R. A., Control of Crystallization and Melting Behavior in Sequence Specific Polypeptoids. *Macromolecules* **2010**, *43* (13), 5627-5636.

30. Zhang, D. H.; Lahasky, S. H.; Guo, L.; Lee, C. U.; Lavan, M., Polypeptoid Materials: Current Status and Future Perspectives. *Macromolecules* **2012**, *45* (15), 5833-5841.
31. Culf, A. S.; Ouellette, R. J., Solid-Phase Synthesis of *N*-Substituted Glycine Oligomers (α -Peptoids) and Derivatives. *Molecules* **2010**, *15* (8), 5282-5335.
32. (a) Olivos, H. J.; Alluri, P. G.; Reddy, M. M.; Salony, D.; Kodadek, T., Microwave-assisted solid-phase synthesis of peptoids. *Org. Lett.* **2002**, *4* (23), 4057-4059; (b) Gorske, B. C.; Jewell, S. A.; Guerard, E. J.; Blackwell, H. E., Expedient synthesis and design strategies for new peptoid construction. *Org. Lett.* **2005**, *7* (8), 1521-1524.
33. Murnen, H. K.; Khokhlov, A. R.; Khalatur, P. G.; Segalman, R. A.; Zuckermann, R. N., Impact of Hydrophobic Sequence Patterning on the Coil-to-Globule Transition of Protein-like Polymers. *Macromolecules* **2012**, *45* (12), 5229-5236.
34. Caumes, C.; Hjelmgaard, T.; Remuson, R.; Faure, S.; Taillefumier, C., Highly Convenient Gram-Scale Solution-Phase Peptoid Synthesis and Orthogonal Side-Chain Post-Modification. *Synthesis* **2011**, (2), 257-264.
35. Sun, H. L.; Zhang, H.; Liu, Q. H.; Yu, L.; Zhao, J. G., Metal-catalyzed copolymerization of imines and CO: A non-amino acid route to polypeptides. *Angew. Chem. Int. Edit* **2007**, *46* (32), 6068-6072.
36. (a) Kricheldorf, H. R., Polypeptides and 100 years of chemistry of alpha-amino acid *N*-carboxyanhydrides. *Angew. Chem. Int. Ed.* **2006**, *45* (35), 5752-5784; (b) Hadjichristidis, N.; Iatrou, H.; Pitsikalis, M.; Sakellariou, G., Synthesis of Well-Defined Polypeptide-Based Materials via the Ring-Opening Polymerization of α -Amino Acid *N*-Carboxyanhydrides. *Chem. Rev.* **2009**, *109* (11), 5528-5578.
37. (a) Kricheldorf, H. R.; von Lossow, C.; Schwarz, G., Cyclic polypeptides by solvent-induced polymerizations of α -amino acid *N*-carboxyanhydrides. *Macromolecules* **2005**, *38* (13), 5513-5518; (b) Kricheldorf, H. R.; von Lossow, C.; Schwarz, G., Primary amine-initiated polymerizations of alanine-NCA and sarcosine-NCA. *Macromol. Chem. Physic* **2004**, *205* (7), 918-924; (c) Kricheldorf, H. R.; Von Lossow, C.; Schwarz, G., Imidazole-initiated polymerizations of α -amino acid *N*-carboxyanhydrides - Simultaneous chain-growth and step-growth polymerization. *J. Polym. Sci. Polym. Chem.* **2005**, *43* (22), 5690-5698; (d) Kricheldorf, H. R.; Von Lossow, C.; Schwarz, G., Tertiary amine catalyzed polymerizations of α -amino acid *N*-carboxyanhydrides: The role of cyclization. *J. Polym. Sci. Polym. Chem.* **2006**, *44* (15), 4680-4695; (e) Kricheldorf, H. R.; Lossow,

C. V.; Lomadze, N.; Schwarz, G., Cyclic polypeptides by thermal polymerization of α -amino acid *N*-carboxyanhydrides. *J. Polym. Sci. Polym. Chem.* **2008**, *46* (12), 4012-4020.

38. (a) Guo, L.; Zhang, D. H., Cyclic Poly(α -peptoid)s and Their Block Copolymers from *N*-Heterocyclic Carbene-Mediated Ring-Opening Polymerizations of *N*-Substituted *N*-Carboxylanhydrides. *J. Am. Chem. Soc.* **2009**, *131* (50), 18072-18074; (b) Guo, L.; Lahasky, S. H.; Ghale, K.; Zhang, D. H., *N*-Heterocyclic Carbene-Mediated Zwitterionic Polymerization of *N*-Substituted *N*-Carboxyanhydrides toward Poly(α -peptoid)s: Kinetic, Mechanism, and Architectural Control. *J. Am. Chem. Soc.* **2012**, *134* (22), 9163-9171.

39. Fetsch, C.; Grossmann, A.; Holz, L.; Nawroth, J. F.; Luxenhofer, R., Polypeptoids from *N*-Substituted Glycine *N*-Carboxyanhydrides: Hydrophilic, Hydrophobic, and Amphiphilic Polymers with Poisson Distribution. *Macromolecules* **2011**, *44* (17), 6746-6758.

40. Robinson, J. W.; Schlaad, H., A versatile polypeptoid platform based on *N*-allyl glycine. *Chem. Commun.* **2012**, *48* (63), 7835-7837.

41. Kricheldorf, H. R., *α -Aminoacid-*N*-Carboxy-Anhydrides and Related Heterocycles*. Springer-Verlag: Berlin, 1987.

42. Kricheldorf, H. R.; Von Lossow, C.; Schwarz, G., Primary amine and solvent-induced polymerizations of L- or D,L-phenylalanine *N*-carboxyanhydride. *Macromol. Chem. Phys.* **2005**, *206* (2), 282-290.

43. Deming, T. J., Polypeptide and polypeptide hybrid copolymer synthesis via NCA polymerization. *Adv. Polym. Sci.: Peptide Hybrid Polymers* **2006**, *202*, 1-18.

44. (a) Lu, H.; Bai, Y. G.; Wang, J.; Gabrielson, N. P.; Wang, F.; Lin, Y.; Cheng, J. J., Ring-Opening Polymerization of gamma-(4-Vinylbenzyl)-L-glutamate *N*-Carboxyanhydride for the Synthesis of Functional Polypeptides. *Macromolecules* **2011**, *44* (16), 6237-6240; (b) Lu, H.; Cheng, J. J., *N*-trimethylsilyl amines for controlled ring-opening polymerization of amino acid *N*-carboxyanhydrides and facile end group functionalization of polypeptides. *J. Am. Chem. Soc.* **2008**, *130* (38), 12562-12563.

45. Meyer, M.; Schlaad, H., Poly(2-isopropyl-2-oxazoline)-poly(L-glutamate) block copolymers through ammonium-mediated NCA polymerization. *Macromolecules* **2006**, *39* (11), 3967-3970.

46. Ballard, D. G. H.; Bamford, C. H., Stereochemical Aspects of the Reactions between α -*N*-Carboxy-Amino-Acid Anhydrides and Primary and Secondary Bases. *J. Chem. Soc.* **1958**, (Jan), 355-360.

47. Nakamura, R.; Aoi, K.; Okada, M., Controlled synthesis of a chitosan-based graft copolymer having polysarcosine side chains using the NCA method with a carboxylic acid additive. *Macromol. Rapid Comm.* **2006**, *27* (20), 1725-1732.
48. Northrop, B. H.; Coffey, R. N., Thiol-Ene Click Chemistry: Computational and Kinetic Analysis of the Influence of Alkene Functionality. *J. Am. Chem. Soc.* **2012**, *134* (33), 13804-13817.
49. Nicovich, J. M.; Kreutter, K. D.; Vandijk, C. A.; Wine, P. H., Temperature-Dependent Kinetics Studies of the Reactions $\text{Br}(\text{P}_{3/2}) + \text{H}_2\text{S} \leftrightarrow \text{SH} + \text{HBr}$ and $\text{Br}(\text{P}_{3/2}) + \text{CH}_3\text{SH} \leftrightarrow \text{CH}_3\text{S} + \text{HBr}$ - Heats of Formation of SH and CH_3S Radicals. *J. Phys. Chem. US* **1992**, *96* (6), 2518-2528.
50. (a) Kade, M. J.; Burke, D. J.; Hawker, C. J., The Power of Thiol-ene Chemistry. *J. Polym. Sci. Pol. Chem.* **2010**, *48* (4), 743-750; (b) Fairbanks, B. D.; Sims, E. A.; Anseth, K. S.; Bowman, C. N., Reaction Rates and Mechanisms for Radical, Photoinitiated Addition of Thiols to Alkynes, and Implications for Thiol-Yne Photopolymerizations and Click Reactions. *Macromolecules* **2010**, *43* (9), 4113-4119.
51. Hiemenz, P. C.; Lodge, T., *Polymer Chemistry*. 2nd ed.; CRC Press: Boca Raton, 2007; p xvii, 587 p.
52. Jassal, M.; Ghosh, S., Aramid fibres - An overview. *Indian J. Fibre Text* **2002**, *27* (3), 290-306.
53. Cowie, J. M. G.; Arrighi, V., *Polymers : chemistry and physics of modern materials*. 3rd ed.; CRC Press: Boca Raton, 2008; p 499 p.
54. Silverstein, R. M.; Webster, F. X.; Kiemle, D. J., *Spectrometric identification of organic compounds*. 7th ed.; John Wiley & Sons: Hoboken, NJ, 2005; p x, 502 p.
55. Mori, S.; Barth, H. G., *Size exclusion chromatography*. Springer: Berlin ; New York, 1999; p xiv, 234 p.
56. Barner-Kowollik, C., *Mass spectrometry in polymer chemistry*. Wiley-VCH: Weinheim, 2012; p xv, 483 p.
57. (a) Weiner, B.; Poelarends, G. J.; Janssen, D. B.; Feringa, B. L., Biocatalytic Enantioselective Synthesis of *N*-Substituted Aspartic Acids by Aspartate Ammonia Lyase. *Chem.-Eur. J.* **2008**, *14* (32), 10094-10100; (b) Singh, B.; Lobo, H.; Shankarling, G., Selective *N*-Alkylation of Aromatic Primary Amines Catalyzed by Bio-catalyst or Deep Eutectic Solvent. *Catal. Lett.* **2011**, *141* (1), 178-182.
58. (a) Salvatore, R. N.; Nagle, A. S.; Jung, K. W., Cesium effect: High chemoselectivity in direct *N*-alkylation of amines. *J. Org. Chem.* **2002**, *67* (3), 674-683; (b) Hikawa, H.; Yokoyama, Y.,

Palladium-Catalyzed Mono-*N*-allylation of Unprotected Anthranilic Acids with Allylic Alcohols in Aqueous Media. *J. Org. Chem.* **2011**, *76* (20), 8433-8439; (c) Hikawa, H.; Yokoyama, Y., Palladium-catalyzed mono-*N*-allylation of unprotected amino acids with 1,1-dimethylallyl alcohol in water. *Org. Biomol. Chem.* **2011**, *9* (11), 4044-4050.

59. (a) Fujita, K. I.; Enoki, Y.; Yamaguchi, R., Cp*Ir-catalyzed *N*-alkylation of amines with alcohols. A versatile and atom economical method for the synthesis of amines. *Tetrahedron* **2008**, *64* (8), 1943-1954; (b) Kawahara, R.; Fujita, K.; Yamaguchi, R., *N*-Alkylation of Amines with Alcohols Catalyzed by a Water-Soluble Cp*Iridium Complex: An Efficient Method for the Synthesis of Amines in Aqueous Media. *Adv. Synth. Catal.* **2011**, *353* (7), 1161-1168; (c) Baran, P. S.; Corey, E. J., A short synthetic route to (+)-austamide, (+)-deoxyisoaustamide, and (+)-hydratoaustamide from a common precursor by a novel palladium-mediated indole → dihydroindoloazocine cyclization. *J. Am. Chem. Soc.* **2002**, *124* (27), 7904-7905; (d) Verardo, G.; Geatti, P.; Pol, E.; Giumanini, A. G., Sodium borohydride: A versatile reagent in the reductive *N*-monoalkylation of α -amino acids and α -amino methyl esters. *Can. J. Chem.* **2002**, *80* (7), 779-788; (e) Ikawa, T.; Fujita, Y.; Mizusaki, T.; Betsuin, S.; Takamatsu, H.; Maegawa, T.; Monguchi, Y.; Sajiki, H., Selective *N*-alkylation of amines using nitriles under hydrogenation conditions: facile synthesis of secondary and tertiary amines. *Org. Biomol. Chem.* **2012**, *10* (2), 293-304.

60. Aurelio, L.; Box, J. S.; Brownlee, R. T. C.; Hughes, A. B.; Sleebs, M. M., An efficient synthesis of *N*-methyl amino acids by way of intermediate 5-oxazolidinones. *J. Org. Chem.* **2003**, *68* (7), 2652-2667.

61. Gibbs, T. J. K.; Boomhoff, M.; Tomkinson, N. C. O., A mild and efficient method for the one-pot monocarboxymethylation of primary amines. *Synlett.* **2007**, (10), 1573-1576.

62. Reichwein, J. F.; Liskamp, R. M. J., Synthesis of cyclic dipeptides by ring-closing metathesis. *Eur. J. Org. Chem.* **2000**, (12), 2335-2344.

63. Sun, J.; Schlaad, H., Thiol-Ene Clickable Polypeptides. *Macromolecules* **2010**, *43* (10), 4445-4448.

64. Pasquato, L.; Modena, G.; Cotarca, L.; Delogu, P.; Mantovani, S., Conversion of bis(trichloromethyl) carbonate to phosgene and reactivity of triphosgene, diphosgene, and phosgene with methanol. *J. Org. Chem.* **2000**, *65* (24), 8224-8228.

65. Endo, T.; Sudo, A.; Wang, X.-S.; Kim, H.-K.; Koga, K.; Fujita, Y., Phosgene-Free Synthesis of *N*-Carboxyanhydrides of α -Amino Acids Based on Bisarylcarbonates as Starting Compounds. *J. Polym. Sci. A Polym. Chem.* **2007**, 5365-5369.

66. Kramer, J. R.; Deming, T. J., A general method for purification of α -amino acid-*N*-carboxyanhydrides using flash chromatography. *Biomacromolecules* **2010**, *11*, 3668-3672.
67. Guo, L.; Li, J. H.; Brown, Z.; Ghale, K.; Zhang, D. H., Synthesis and Characterization of Cyclic and Linear Helical Poly(α -peptoid)s by *N*-Heterocyclic Carbene-Mediated Ring-Opening Polymerizations of *N*-Substituted *N*-Carboxyanhydrides. *Biopolymers* **2011**, *96* (5), 596-603.
68. Secker, C. Solubility Investigations of Peptidomimetic N -Alkyl Polyglycines. Free University, Berlin, 2012.
69. (a) Habraken, G. J. M.; Wilsens, K. H. R. M.; Koning, C. E.; Heise, A., Optimization of *N*-carboxyanhydride (NCA) polymerization by variation of reaction temperature and pressure. *Polym. Chem. UK* **2011**, *2* (6), 1322-1330; (b) Habraken, G. J. M.; Peeters, M.; Dietz, C. H. J. T.; Koning, C. E.; Heise, A., How controlled and versatile is *N*-carboxy anhydride (NCA) polymerization at 0 degrees C? Effect of temperature on homo-, block- and graft (co)polymerization. *Polym. Chem.* **2010**, *1* (4), 514-524.
70. Lahasky, S. H.; Serem, W. K.; Guo, L.; Garno, J. C.; Zhang, D. H., Synthesis and Characterization of Cyclic Brush-Like Polymers by *N*-Heterocyclic Carbene-Mediated Zwitterionic Polymerization of *N*-Propargyl *N*-Carboxyanhydride and the Grafting-to Approach. *Macromolecules* **2011**, *44* (23), 9063-9074.
71. (a) Lee, C. U.; Smart, T. P.; Guo, L.; Epps, T. H.; Zhang, D. H., Synthesis and Characterization of Amphiphilic Cyclic Diblock Copolypeptoids from *N*-Heterocyclic Carbene-Mediated Zwitterionic Polymerization of *N*-Substituted *N*-Carboxyanhydride. *Macromolecules* **2011**, *44* (24), 9574-9585; (b) Lahasky, S. H.; Guo, L.; Tang, H.; Zhang, D., Macrocyclic polymer with 'clickable' side-chains: synthesis, characterization and their potential utility towards Janus rings. *Polym. Preprints* **2010**, *51* (1), 620-621.
72. Goubert, M.; Canet, I.; Sinibaldi, M. E., An expedient route to new spiroheterocycles: Synthesis and structural studies. *Eur. J. Org. Chem.* **2006**, (21), 4805-4812.
73. Terada, K.; Berda, E. B.; Wagener, K. B.; Sanda, F.; Masuda, T., ADMET polycondensation of diketopiperazine-based dienes. Polymerization behavior and effect of diketopiperazine on the properties of the formed polymers. *Macromolecules* **2008**, *41* (16), 6041-6046.
74. Yamaguchi, R.; Zhu, M. W.; Kawagoe, S.; Asai, C.; Fujita, K., A New Atom-Economical and Selective Synthesis of Secondary and Tertiary Alkylamines by Means of Cp* Iridium Complex

Catalyzed Multiple *N*-Alkylation of Ammonium Salts with Alcohols without Solvent. *Synthesis-Stuttgart* **2009**, (7), 1220-1223.

75. Jainta, M.; Nieger, M.; Brase, S., Microwave-Assisted Stereoselective One-Pot Synthesis of Symmetrical and Unsymmetrical 2,5-Diketopiperazines from Unprotected Amino Acids. *Eur. J. Org. Chem.* **2008**, (32), 5418-5424.

76. Akerlund, J.; Harmeier, S.; Pumphrey, J.; Timm, D. C.; Brand, J. I., Diketopiperazine-based polymers from common amino acids. *J. Appl. Polym. Sci.* **2000**, 78 (12), 2213-2218.

77. Cho, S. D.; Song, S. Y.; Kim, K. H.; Zhao, B. X.; Ahn, C.; Joo, W. H.; Yoon, Y. J.; Falck, J. R.; Shin, D. S., One-pot synthesis of symmetrical 1,4-disubstituted piperazine-2,5-diones. *B. Korean Chem. Soc.* **2004**, 25 (3), 415-416.

78. Fetsch, C.; Luxenhofer, R., Highly Defined Multiblock Copolypeptoids: Pushing the Limits of Living Nucleophilic Ring-Opening Polymerization. *Macromol. Rapid Comm.* **2012**, 33 (19), 1708-1713.

79. Gottlieb, H. E.; Kotlyar, V.; Nudelman, A., NMR chemical shifts of common laboratory solvents as trace impurities. *J. Org. Chem.* **1997**, 62 (21), 7512-7515.

80. We observed rotamers in the NMR spectrums.

81. Adjusted moles to account for previously mentioned diethyl ether impurity.

82. Slow and careful heating improves the separation of product **5k** (73 °C) from by-product (bp 65 °C).

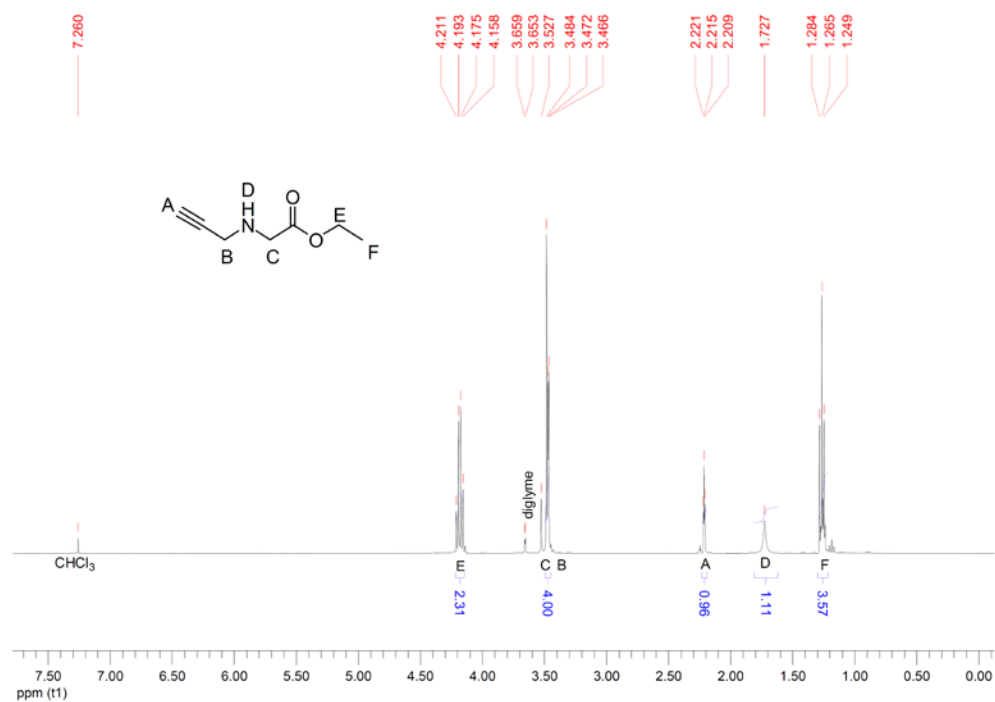
83. *N*-allyl NCA would readily lead to oligomerization, and unknown side products, upon exposure to air contact and/or impurities found in solvents. Interestingly, our investigations with *N*-methyl and *N*-propargyl NCAs indicate a greater stability to ambient conditions. In general, all glassware should be clean and dry. Also, scratched glassware should be avoided, or treated with a silylating agent. We have found that the *N*-allyl NCA can be stored at -20 °C, in a properly prepared flask, under argon and heptanes, for up to 6 months without decomposition. Alternatively, the crude cyclization mixture (CH₂Cl₂, PCl₃, etc.) allows for short term storage (1 month) at 5 °C.

84. Hioki, H.; Kinami, H.; Yoshida, A.; Kojima, A.; Kodama, M.; Takaoka, S.; Ueda, K.; Katsu, T., Synthesis of *N*-substituted cyclic triglycines and their response to metal ions. *Tetrahedron Lett.* **2004**, 45 (5), 1091-1094.

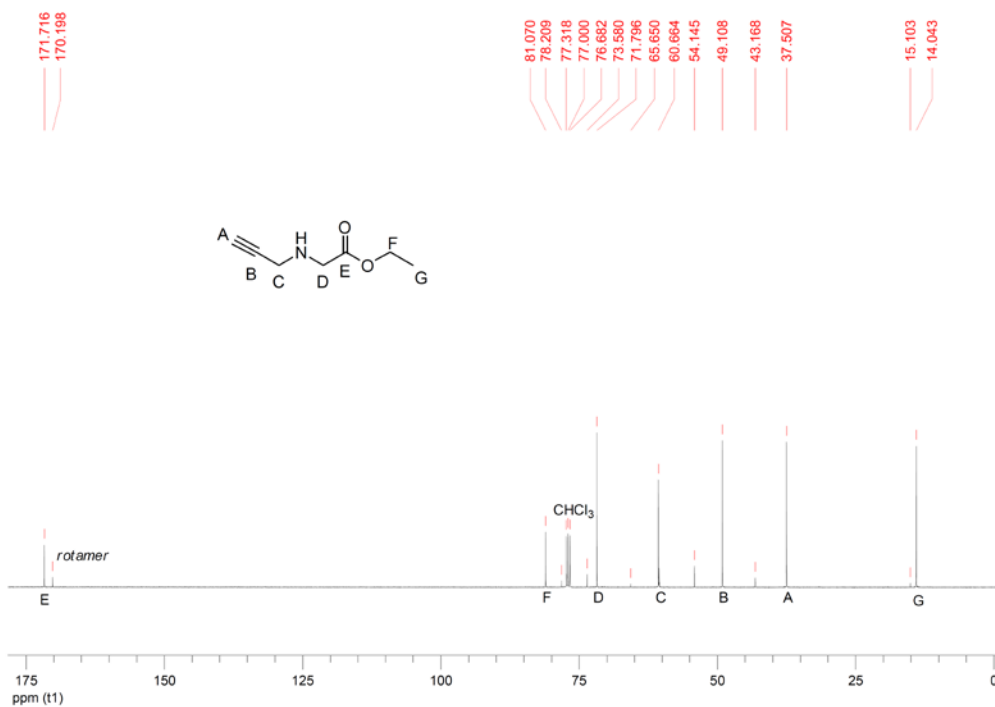
Chapter 7: Bibliography and Notes

85. Dzyuba, E. V.; Kaufmann, L.; Low, N. L.; Meyer, A. K.; Winkler, H. D. F.; Rissanen, K.; Schalley, C. A., CH•••••O Hydrogen Bonds in "Clicked" Diketopiperazine-Based Amide Rotaxanes. *Org. Lett.* **2011**, *13* (18), 4838-4841.
86. The internal pressure of the reaction flask was reduced everytime a sample was taken for analysis.

Appendix: Supporting Spectra

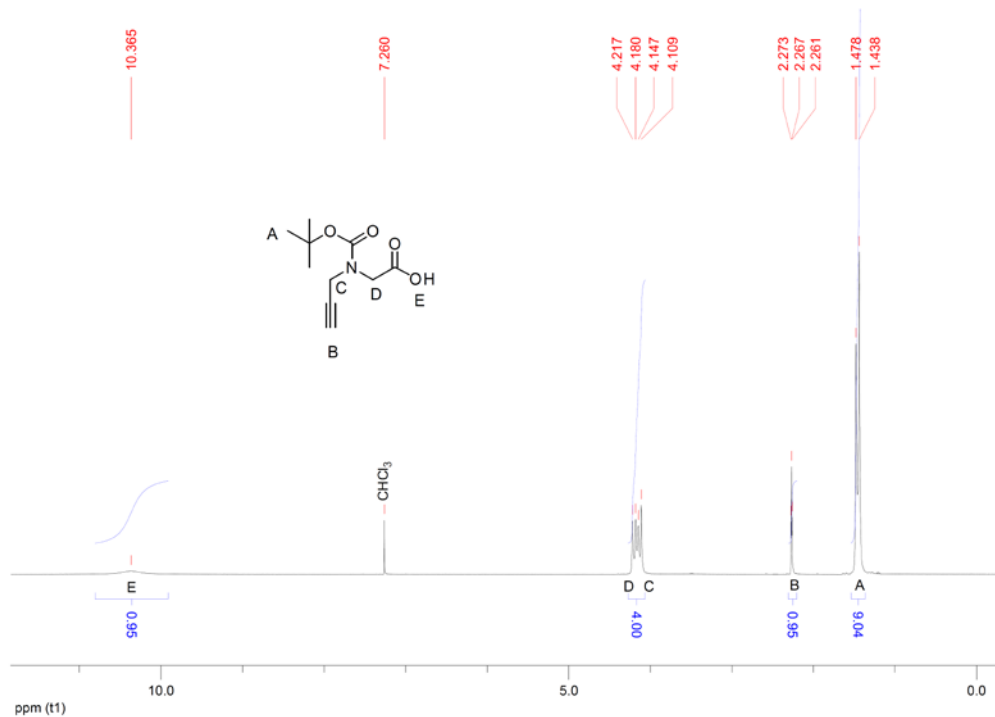


A1. ¹H-NMR spectrum of **7l** in CDCl₃.

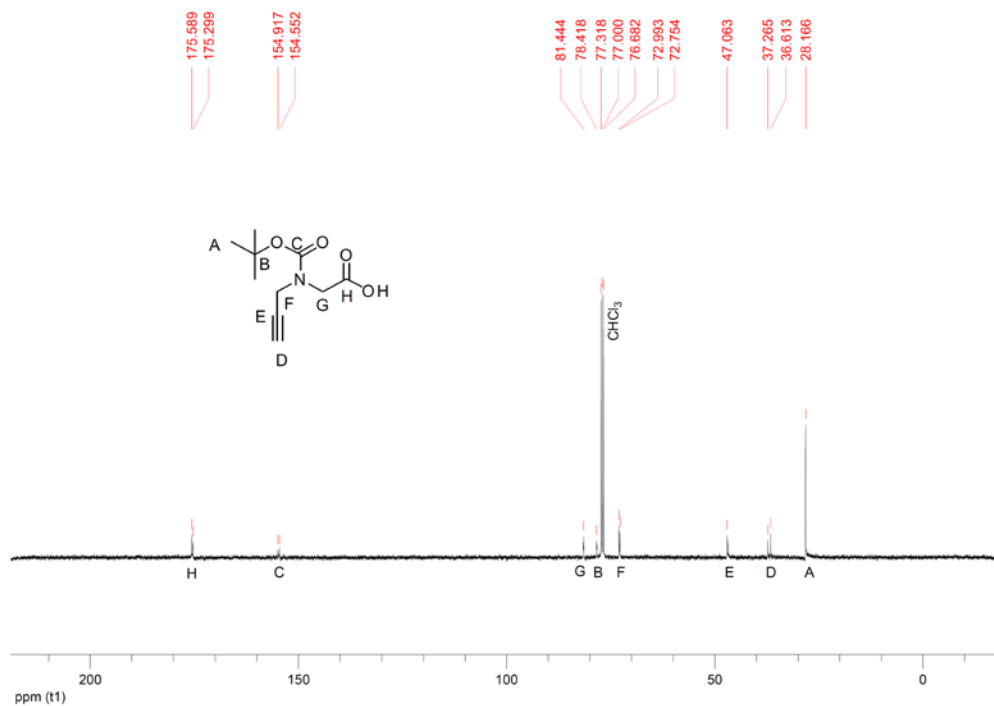


A2. ¹³C-NMR spectrum of **7l** in CDCl₃.

Appendix: Supporting Spectra

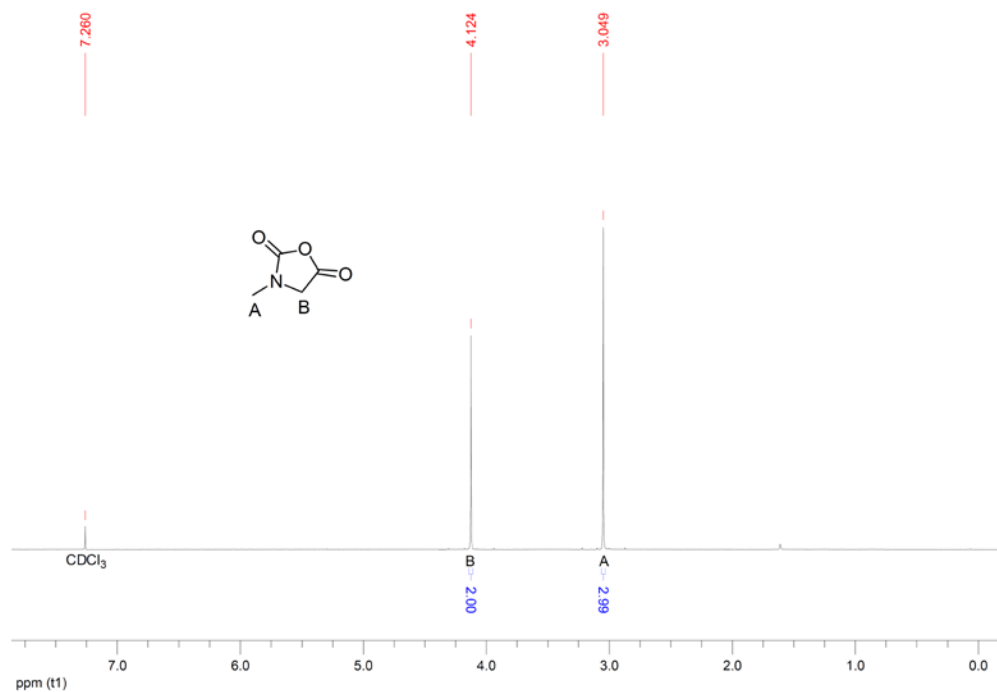


A3. ¹H-NMR spectrum of **4l** in CDCl₃.

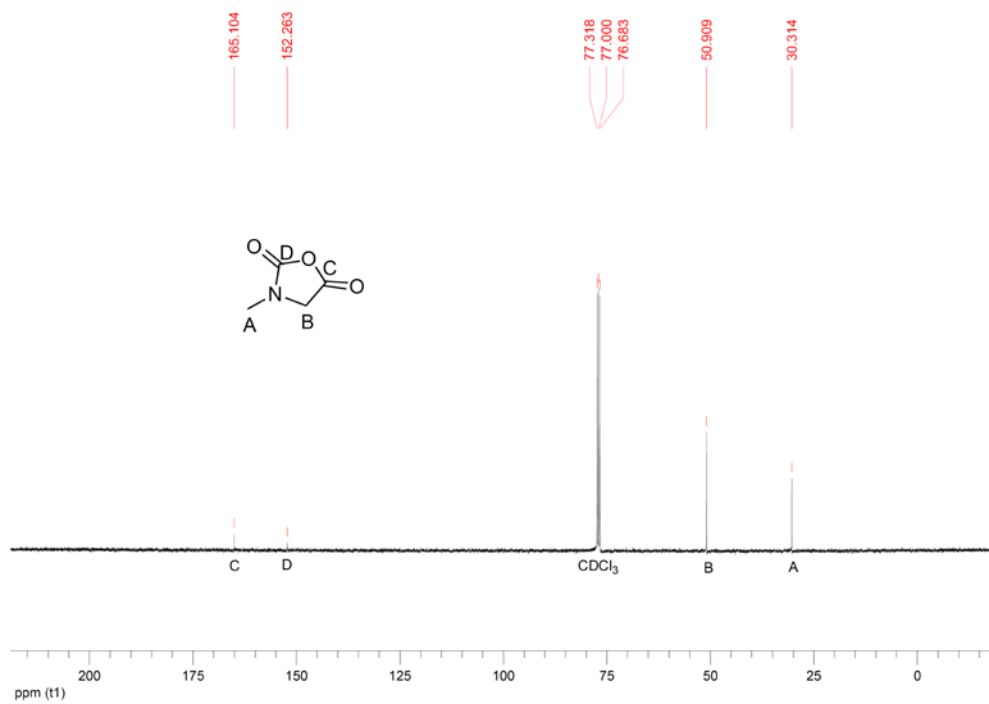


A4. ¹³C-NMR spectrum of **4l** in CDCl₃.

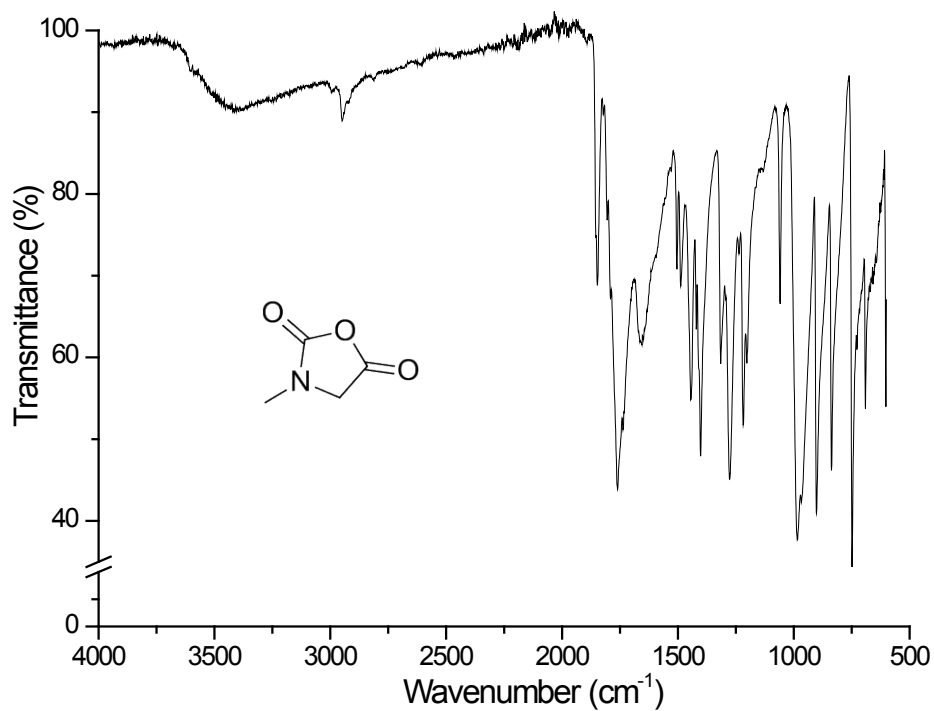
Appendix: Supporting Spectra



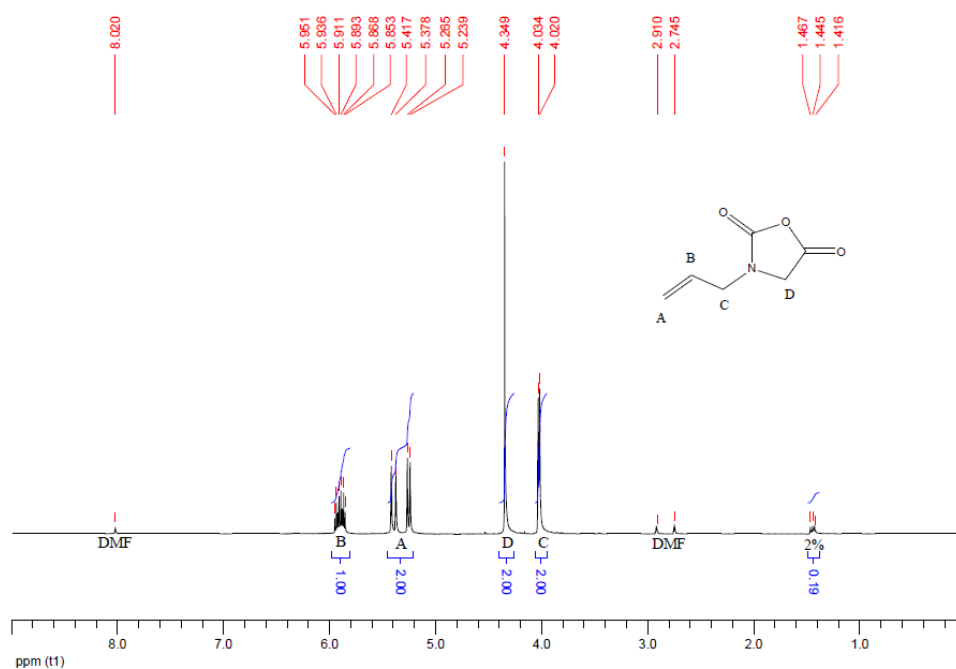
A5. $^1\text{H-NMR}$ spectrum of **5a** in CDCl_3 .



A6. $^{13}\text{C-NMR}$ spectrum of **5a** in CDCl_3 .

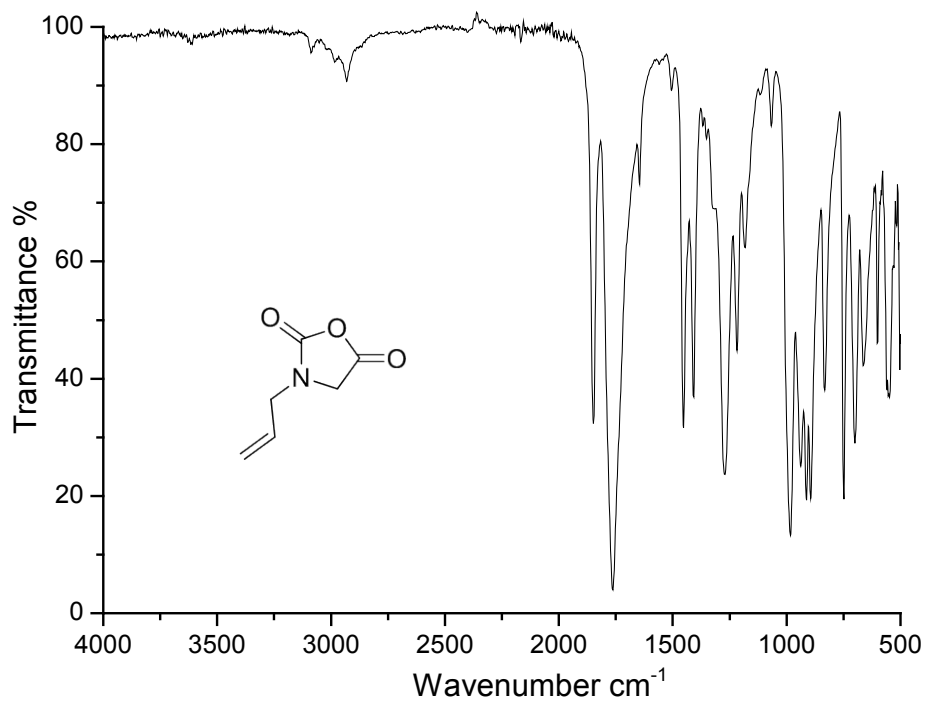
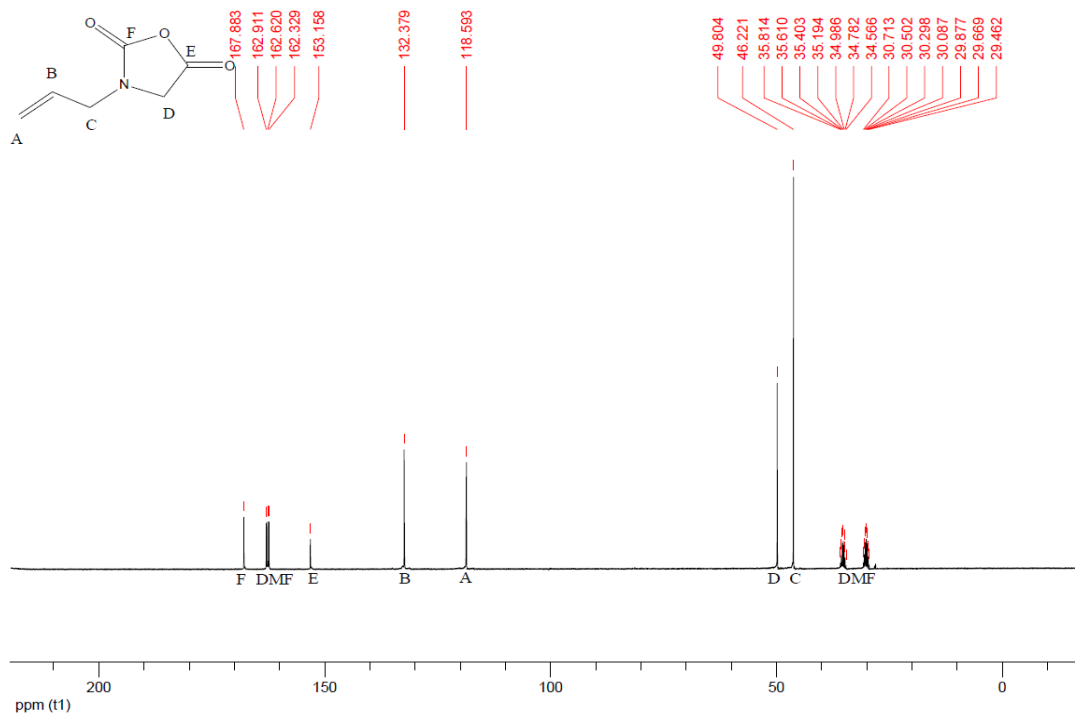


A7. FT-IR spectrum of 5a neat.

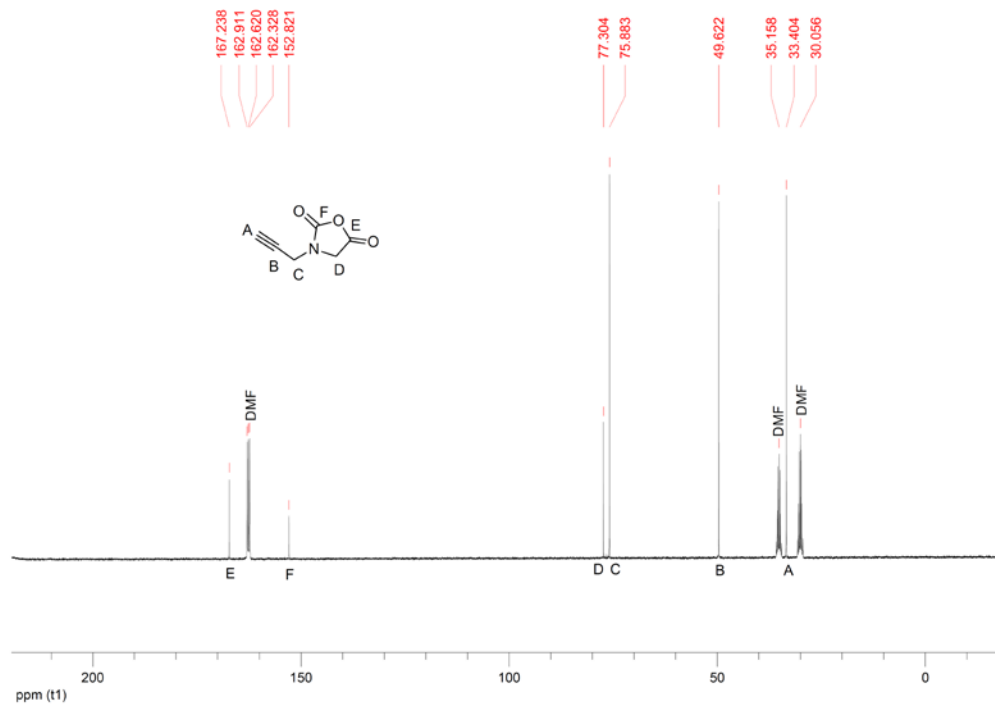


A8. ¹H-NMR spectrum of 5k in DMF-d₇.

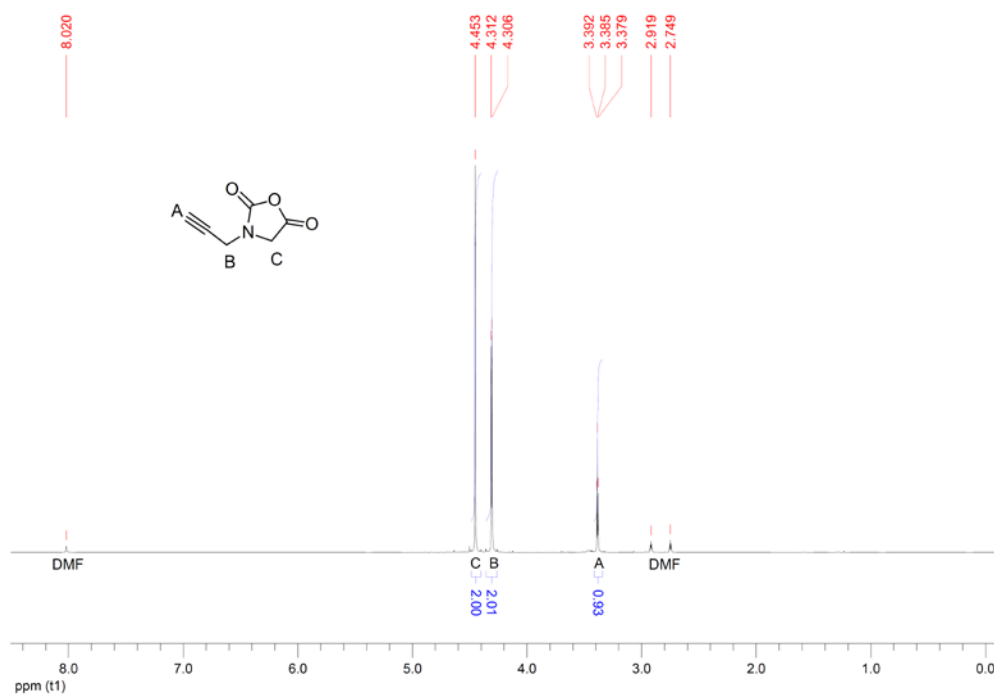
Appendix: Supporting Spectra



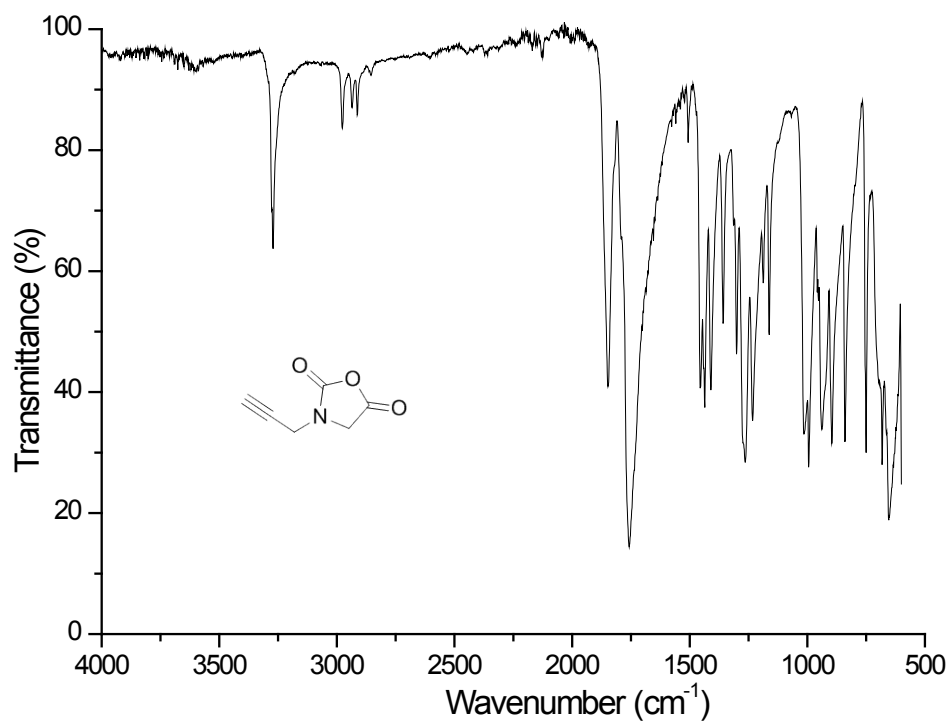
Appendix: Supporting Spectra



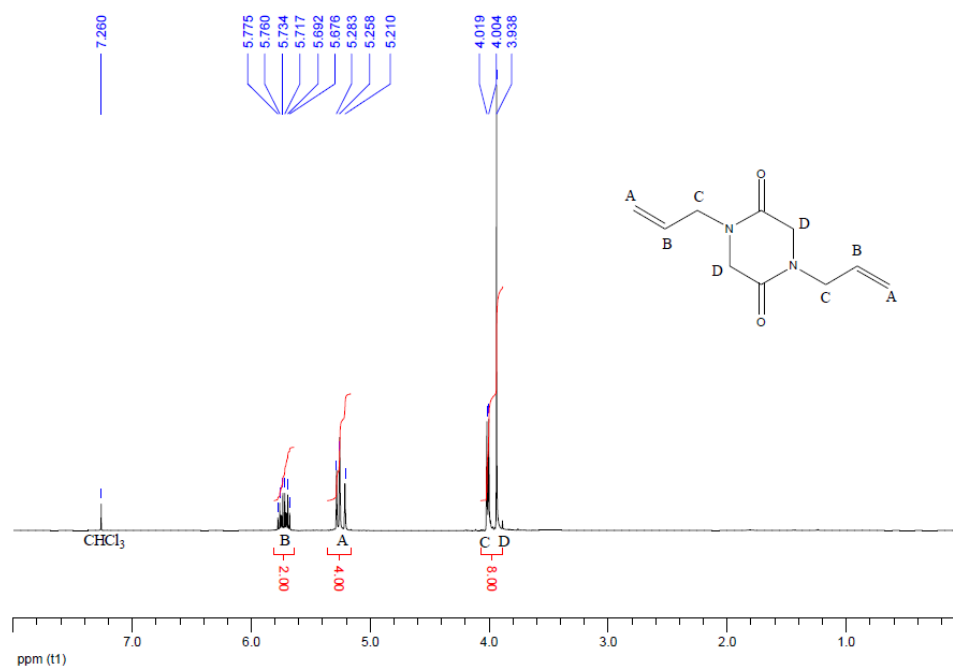
A11. ¹H-NMR spectrum of 51 in DMF-d₇.



A12. ¹³C-NMR spectrum of 51 in DMF-d₇.

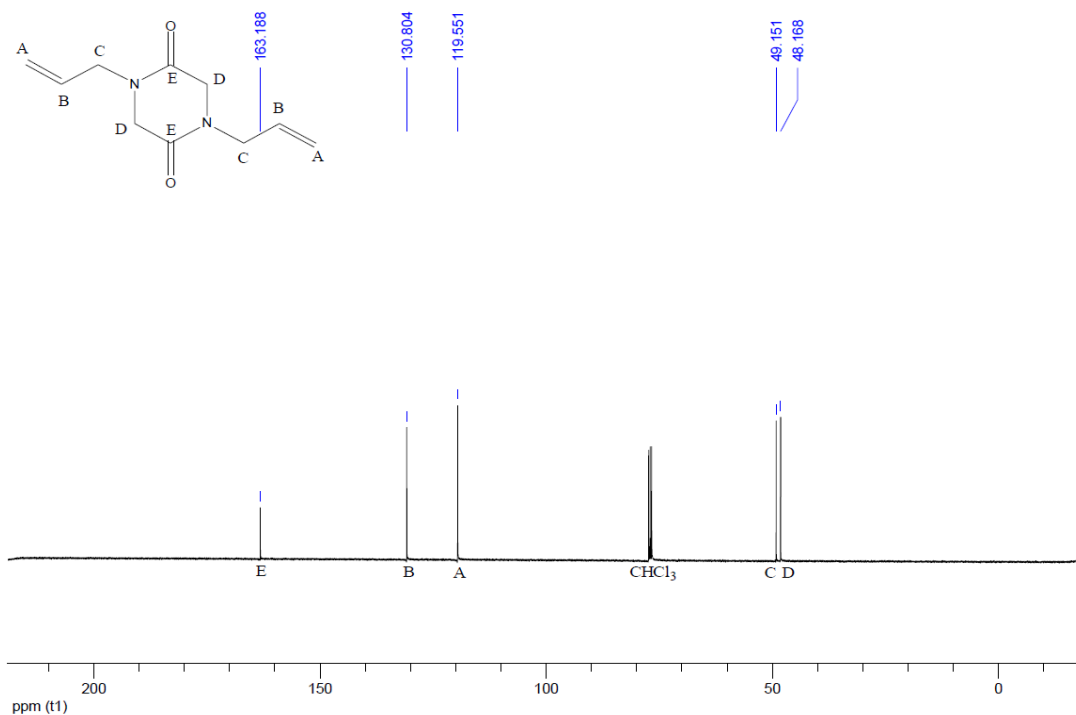


A13. FT-IR spectrum of **5l** neat.

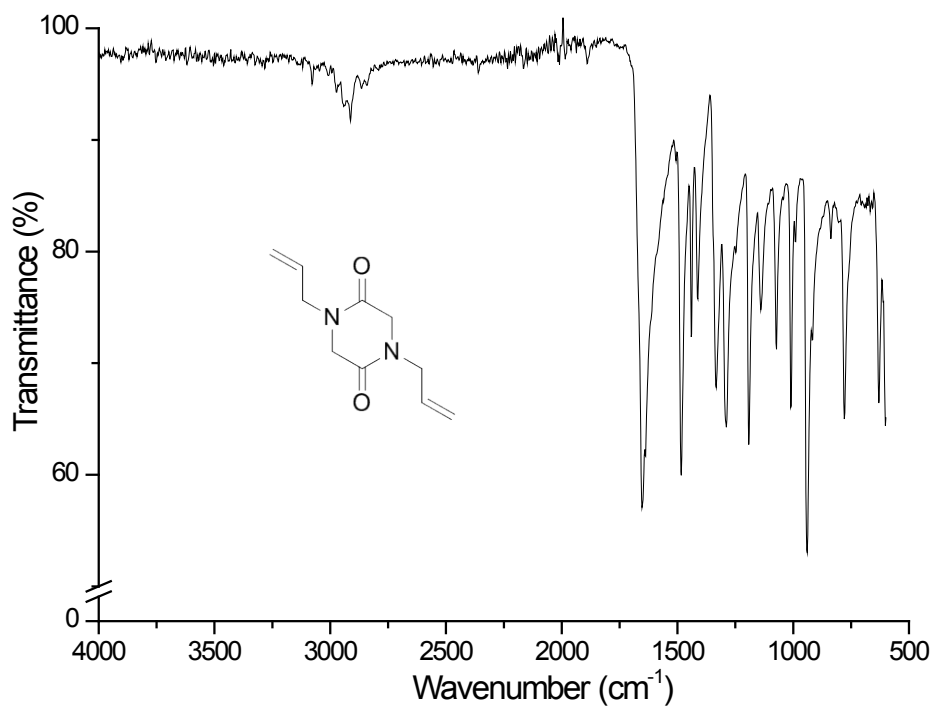


A14. ¹H-NMR spectrum of **DKP 13k** in CDCl₃.

Appendix: Supporting Spectra

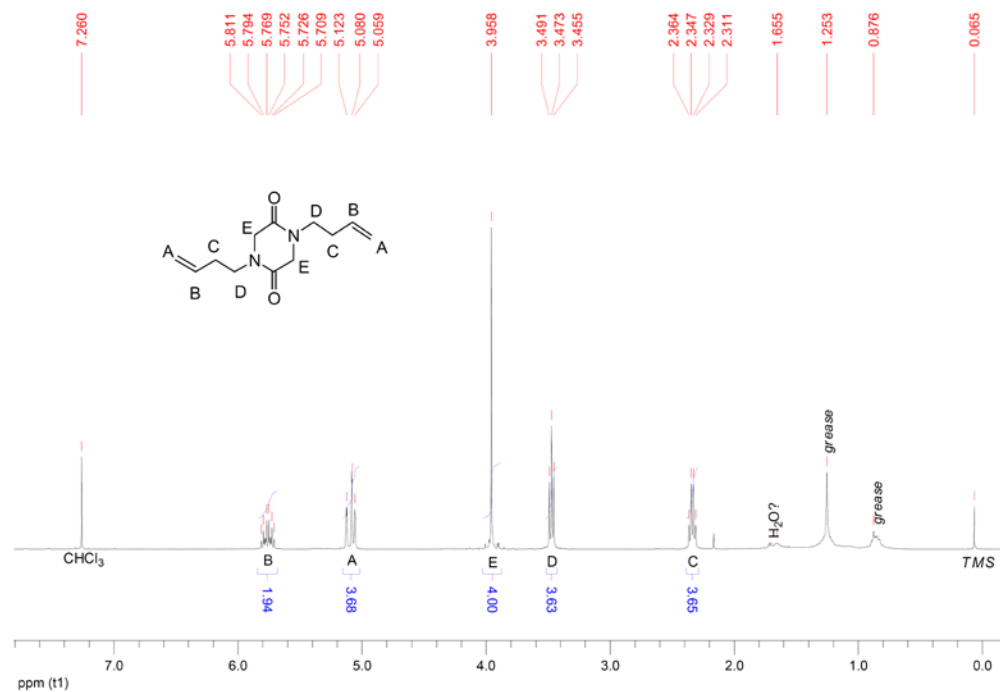


A15. ^{13}C -NMR spectrum of **DKP 13k** in CDCl_3 .

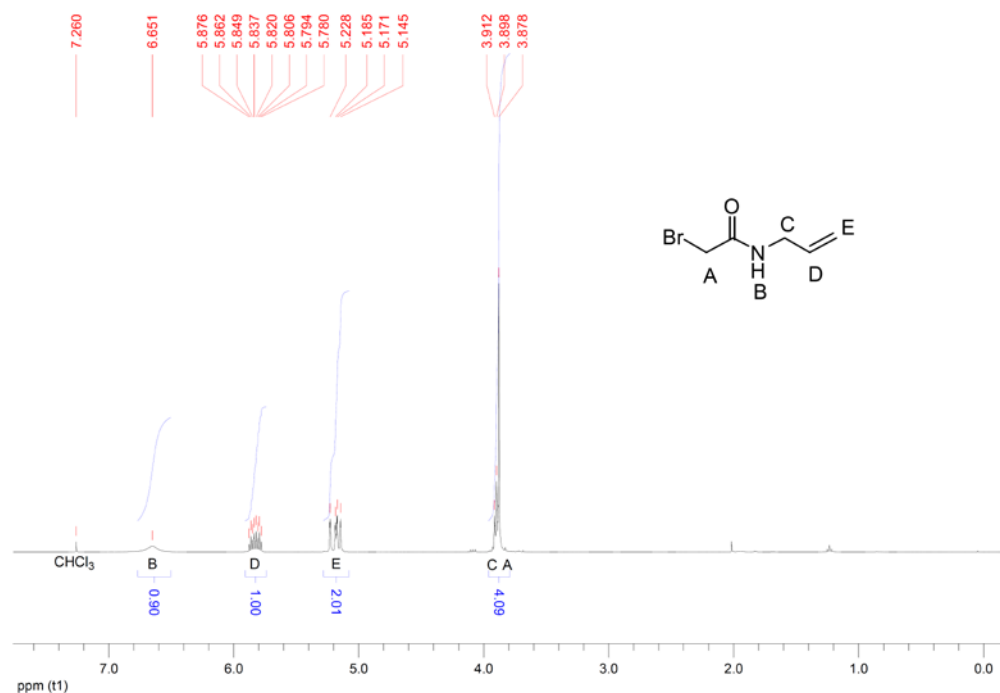


A16. FT-IR spectrum of **DKP 13k** neat.

Appendix: Supporting Spectra

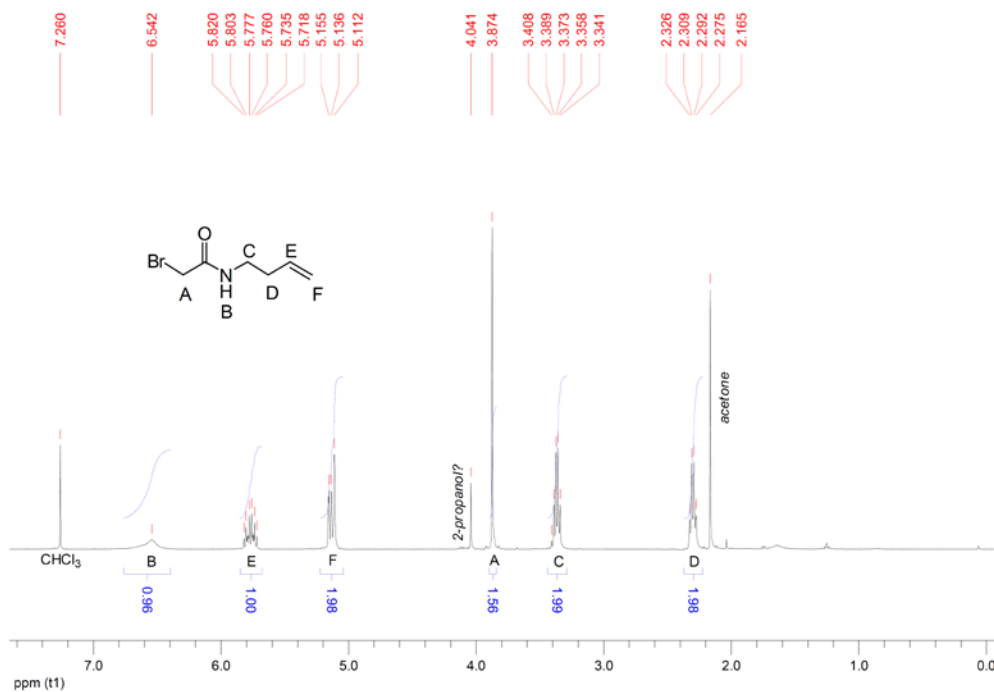


A17. ¹H-NMR spectrum of 1,4-di(but-3-en-1-yl)piperazine-2,5-dione in CDCl₃.

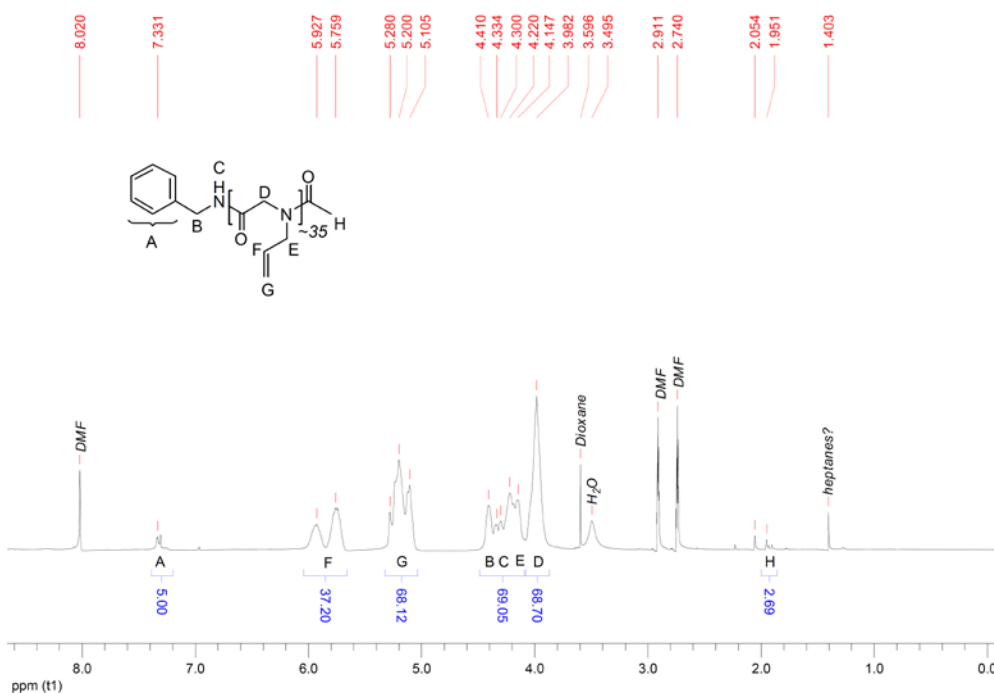


A18. ¹H-NMR spectrum of N-allyl-2-bromoacetamide in CDCl₃.

Appendix: Supporting Spectra

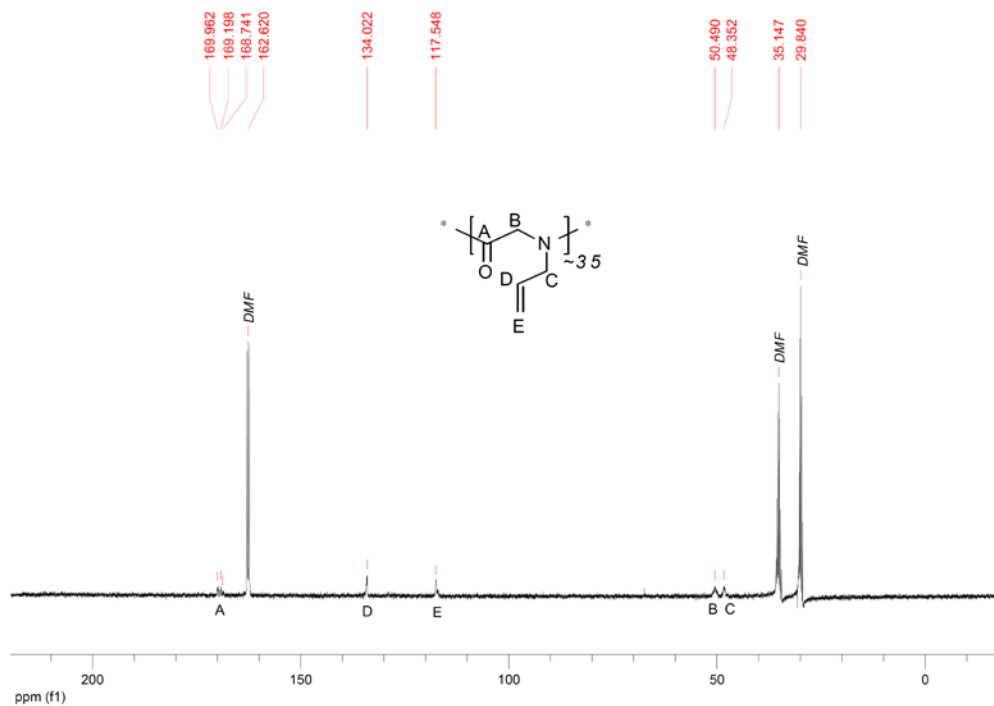


A19. ¹H-NMR spectrum of 2-bromo-*N*-(but-3-en-1-yl)acetamide in CDCl₃.

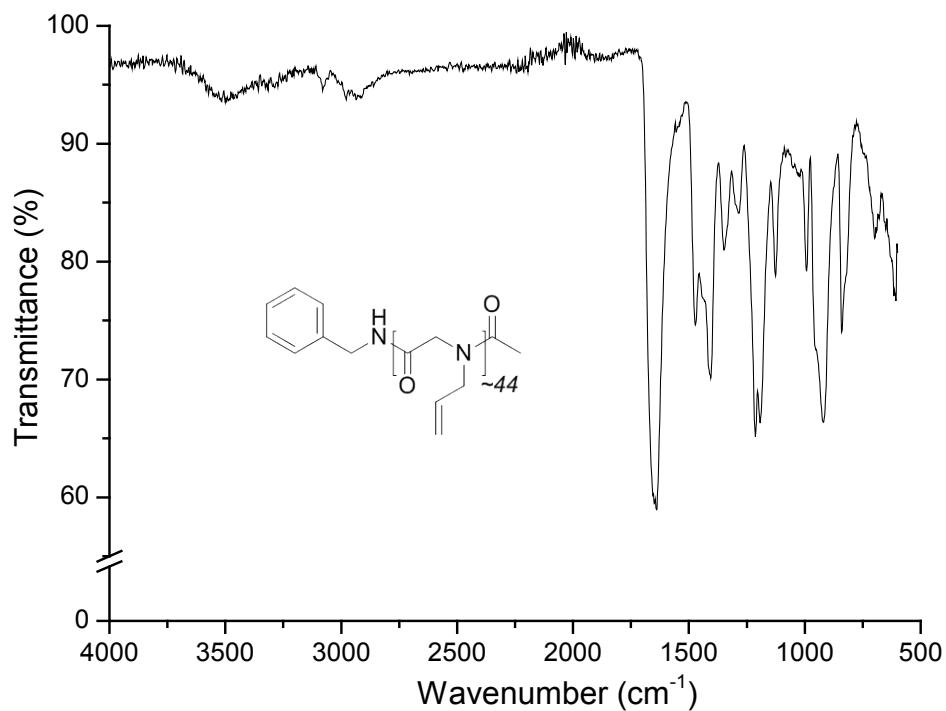


A20. ¹H-NMR spectrum of 10k (BP25.50) in DMF-d₇.

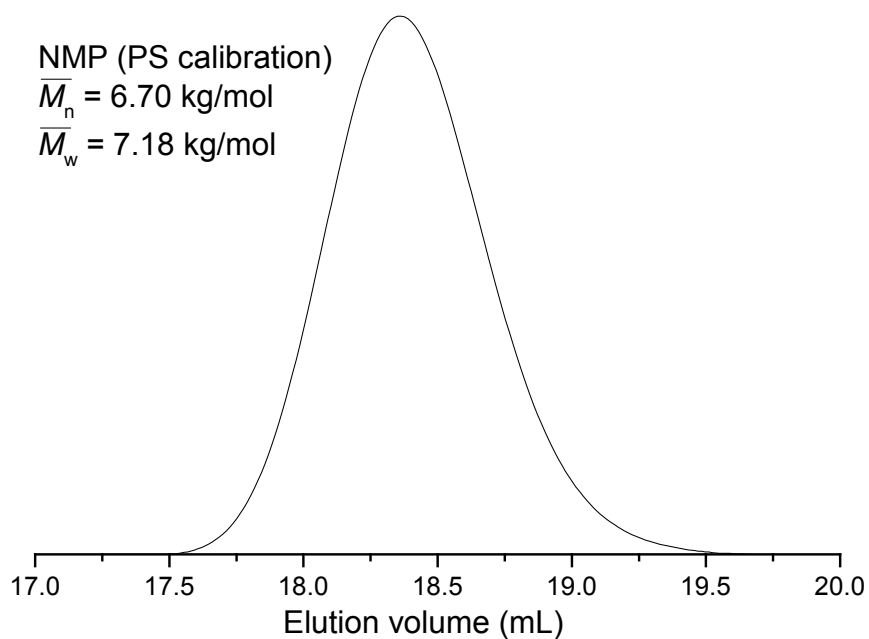
Appendix: Supporting Spectra



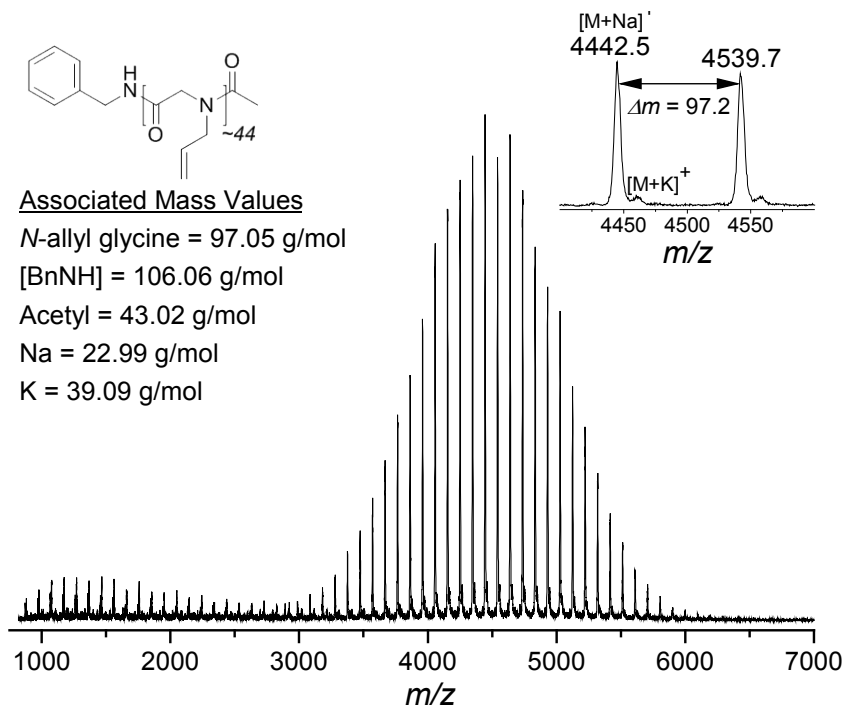
A21. ^{13}C -NMR spectrum of 10k (BP25.50) in DMF-d_2 .



A22. FT-IR spectrum of 10k (BP25.50) neat.

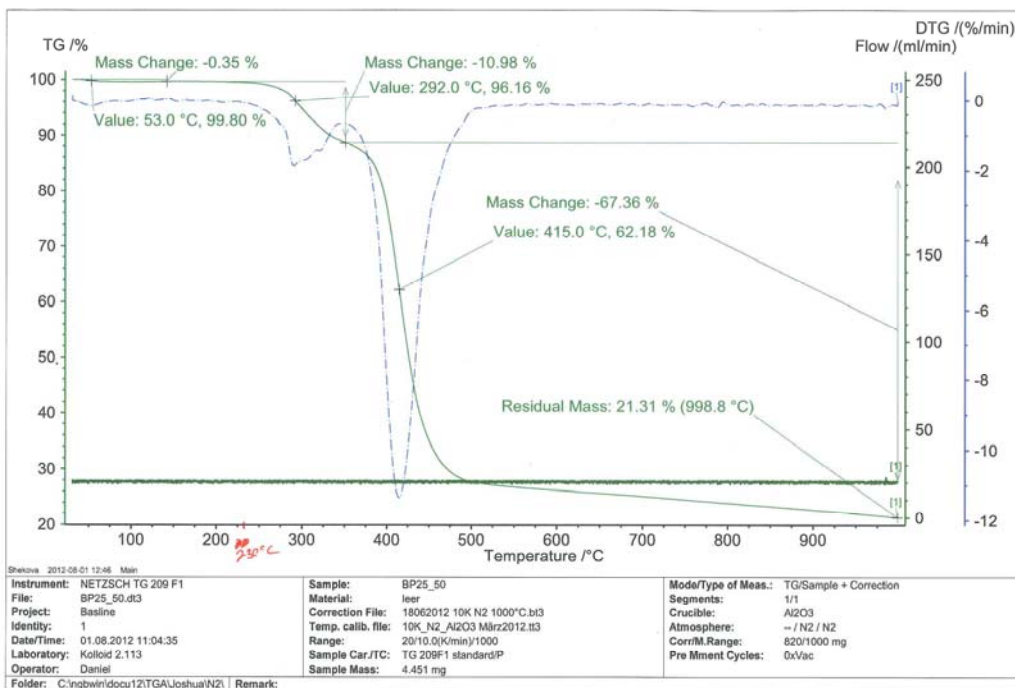


A23. SEC elugram (NMP, RI) of 10k (BP25.50) prepared in DMF.

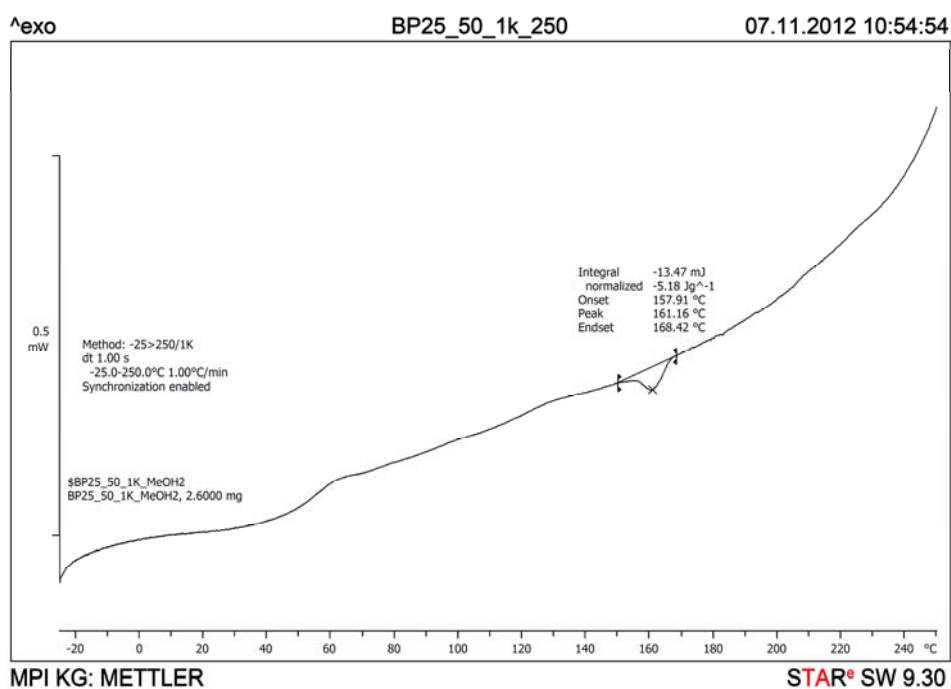


A24. MALDI-ToF MS (linear mode, DCTB/Na⁺) of 10k (BP25.50).

Appendix: Supporting Spectra

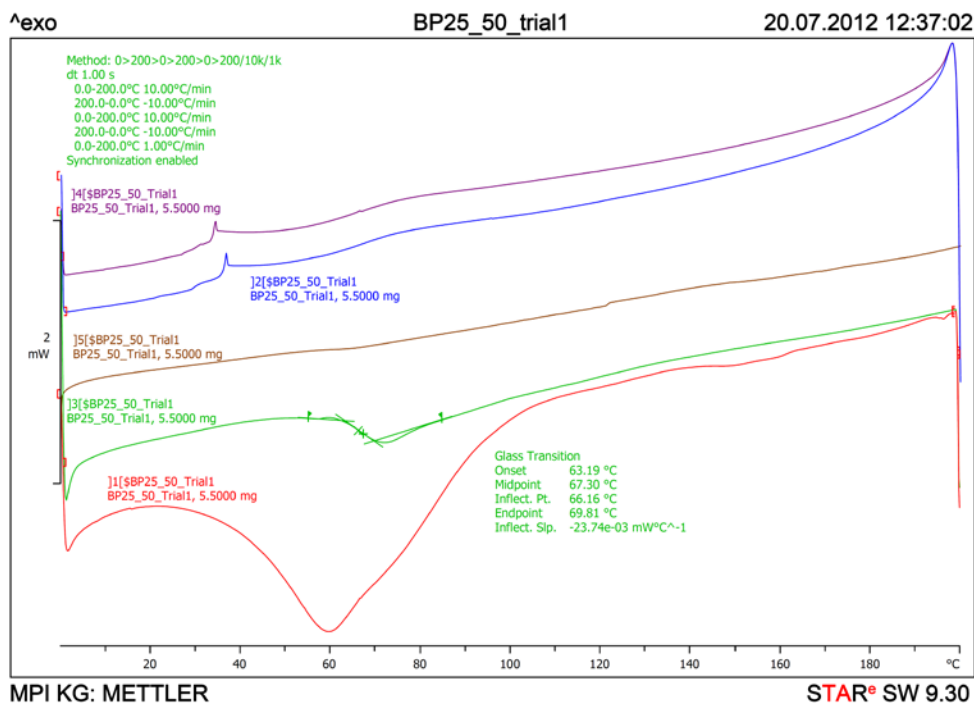


A25. TGA of 10k (BP25.50) neat (20 K/min).

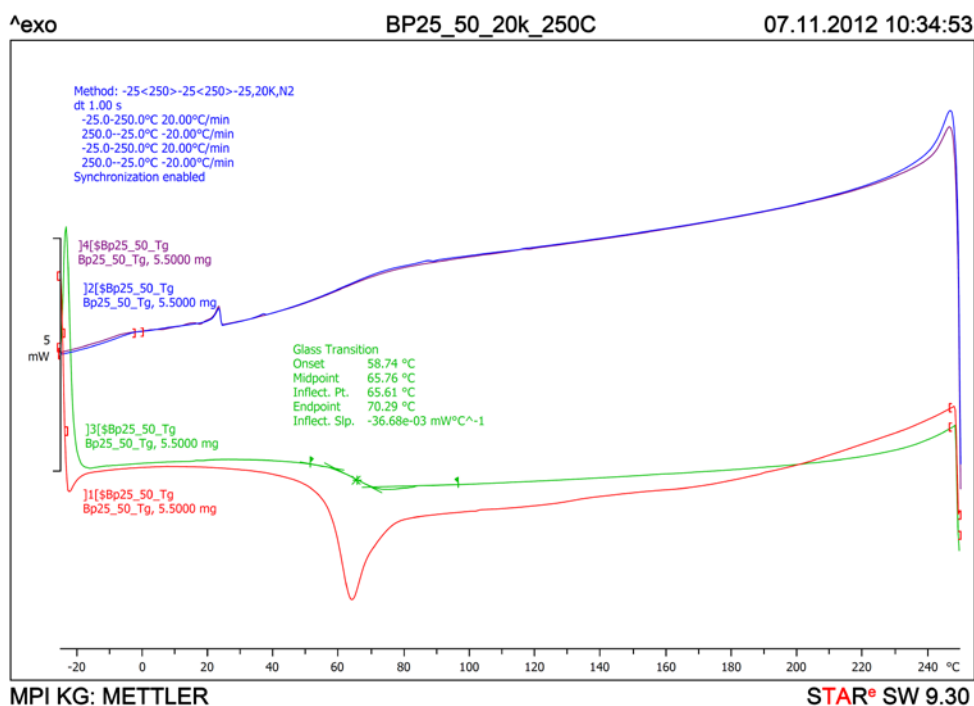


A26. DSC first heating curve of raw 10k (BP25.50) neat (1 K/min).

Appendix: Supporting Spectra

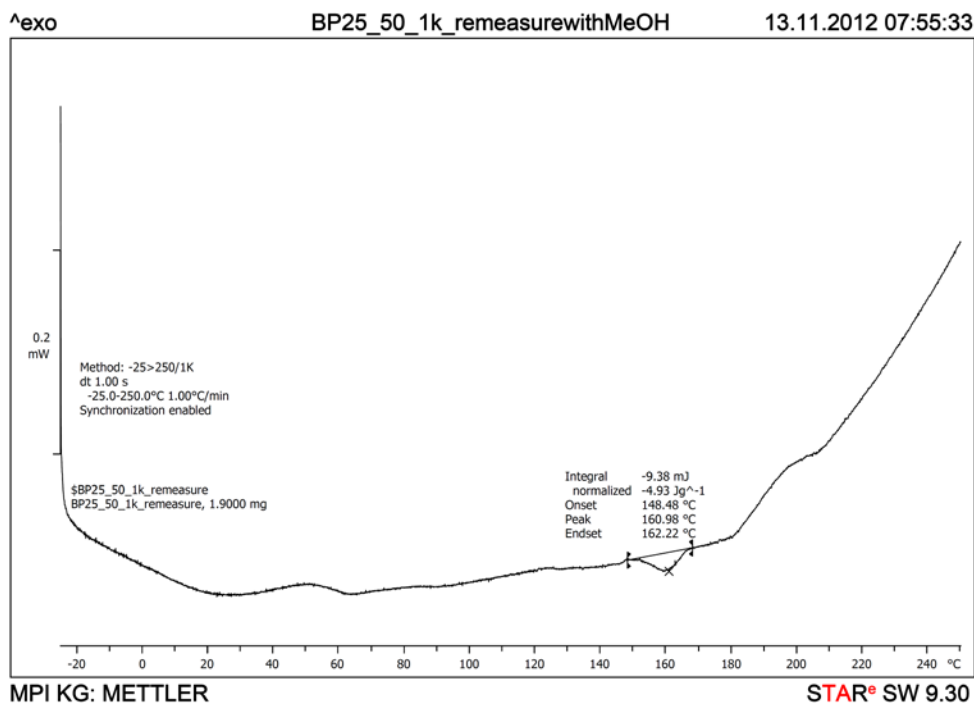


A27. DSC heating/cooling curves of raw 10k (BP25.50) neat (10 K/min).

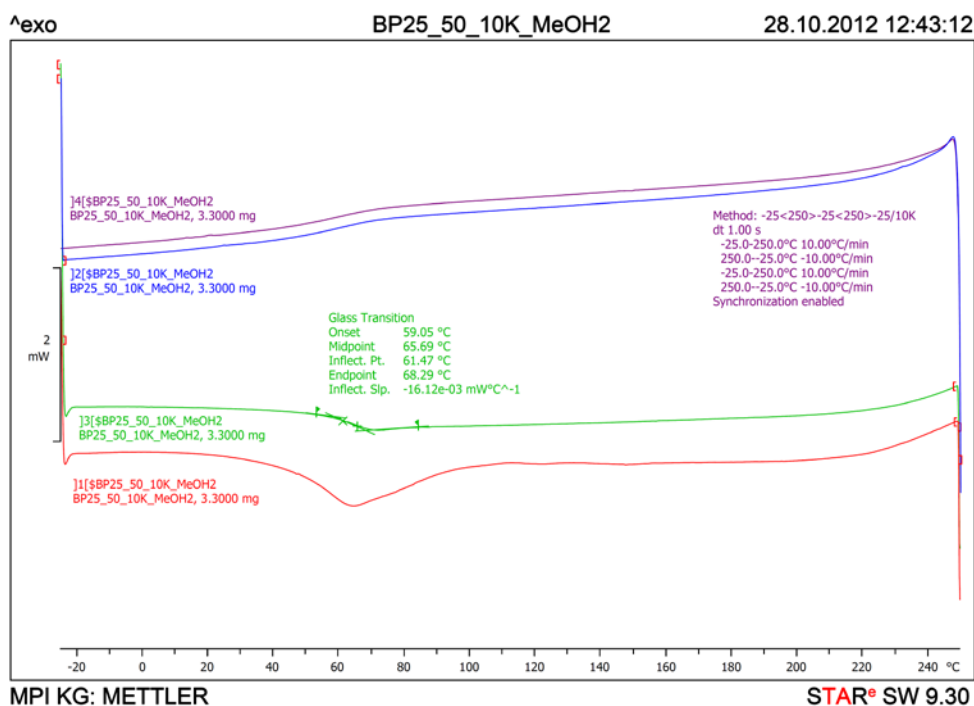


A28. DSC heating/cooling curves of raw 10k (BP25.50) neat (20 K/min).

Appendix: Supporting Spectra

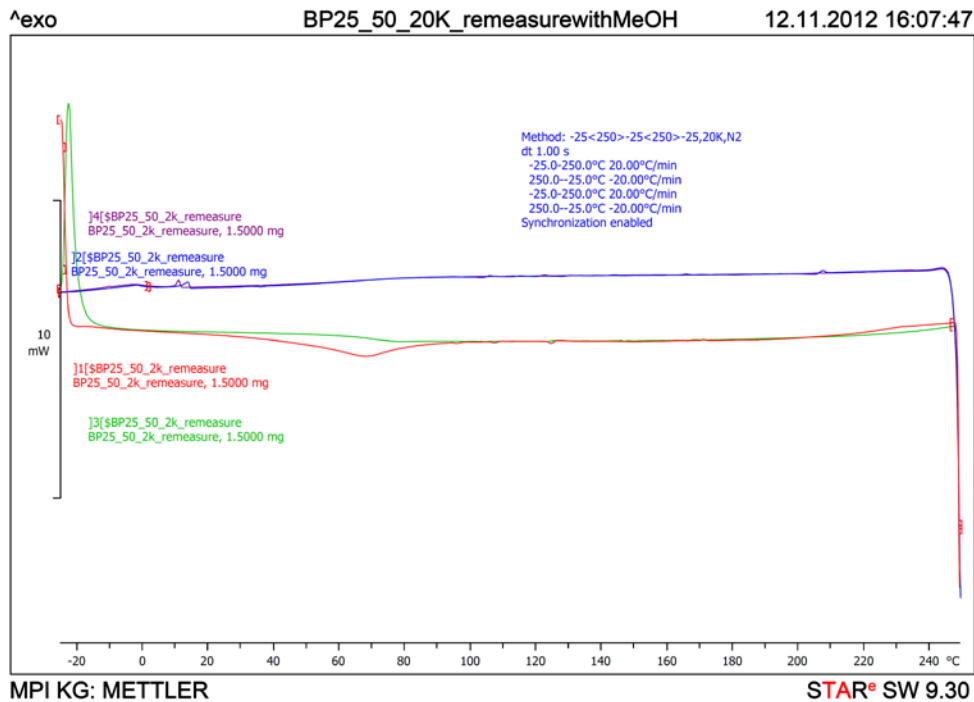


A29. DSC 1st heating curve of treated 10k (BP25.50) neat (1 K/min).

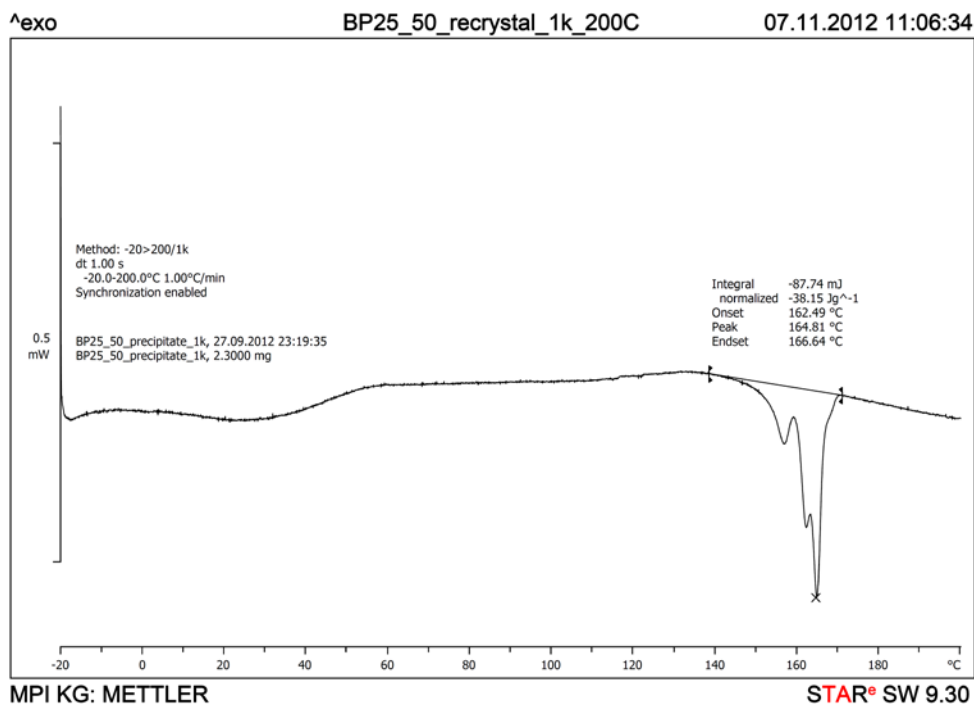


A30. DSC heating/cooling curves of treated 10k (BP25.50) neat (10 K/min).

Appendix: Supporting Spectra

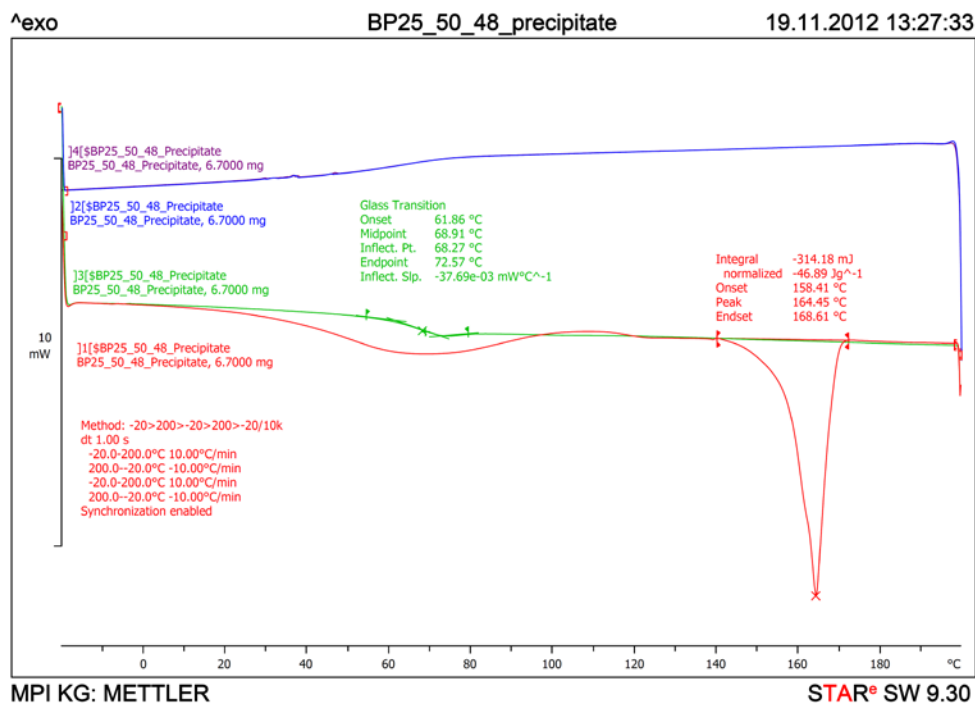


A31. DSC heating/cooling curves of treated 10k (BP25.50) neat (20 K/min).

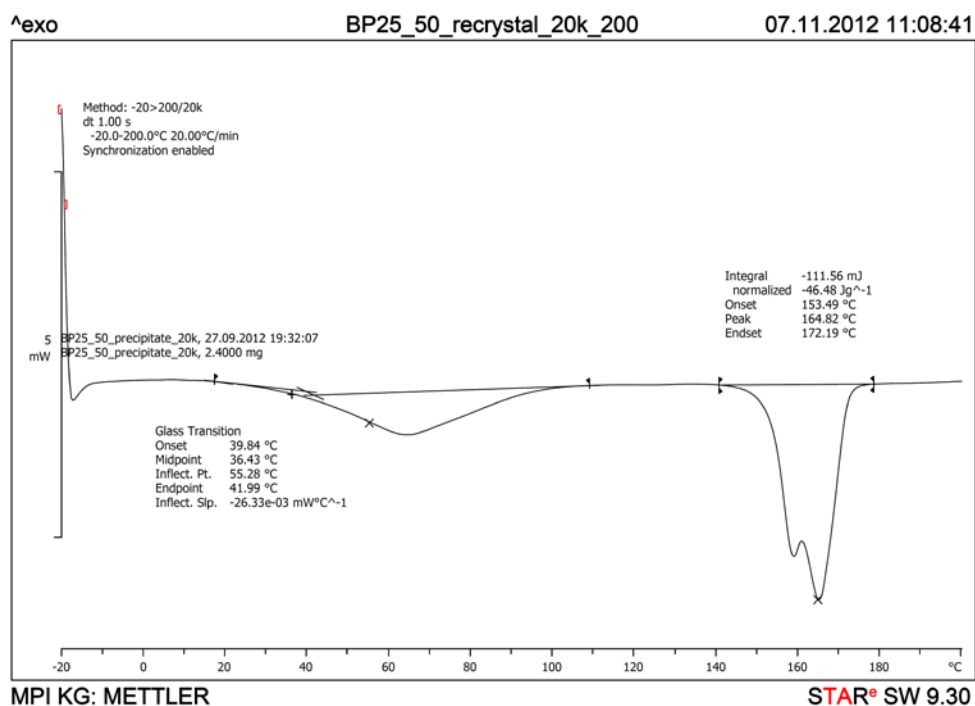


A32. DSC 1st heating curve of solution annealed (ca. 4.8 g/L) 10k (BP25.50) neat (1 K/min).

Appendix: Supporting Spectra

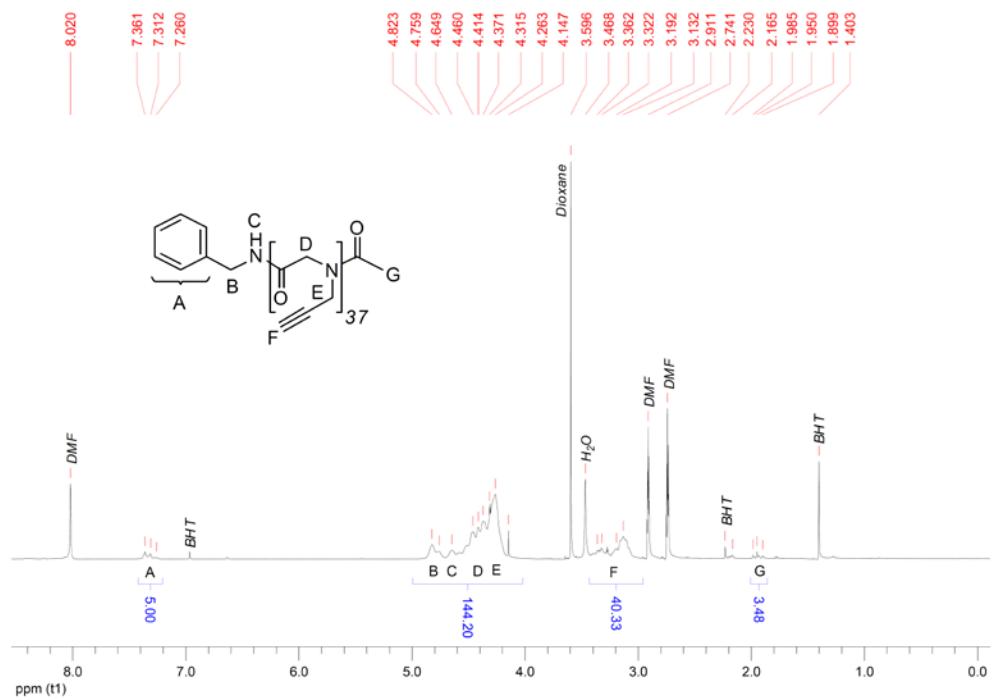


A33. DSC heating/cooling curves of solution annealed (ca. 4.8 g/L) 10k (BP25.50) neat (10 K/min).

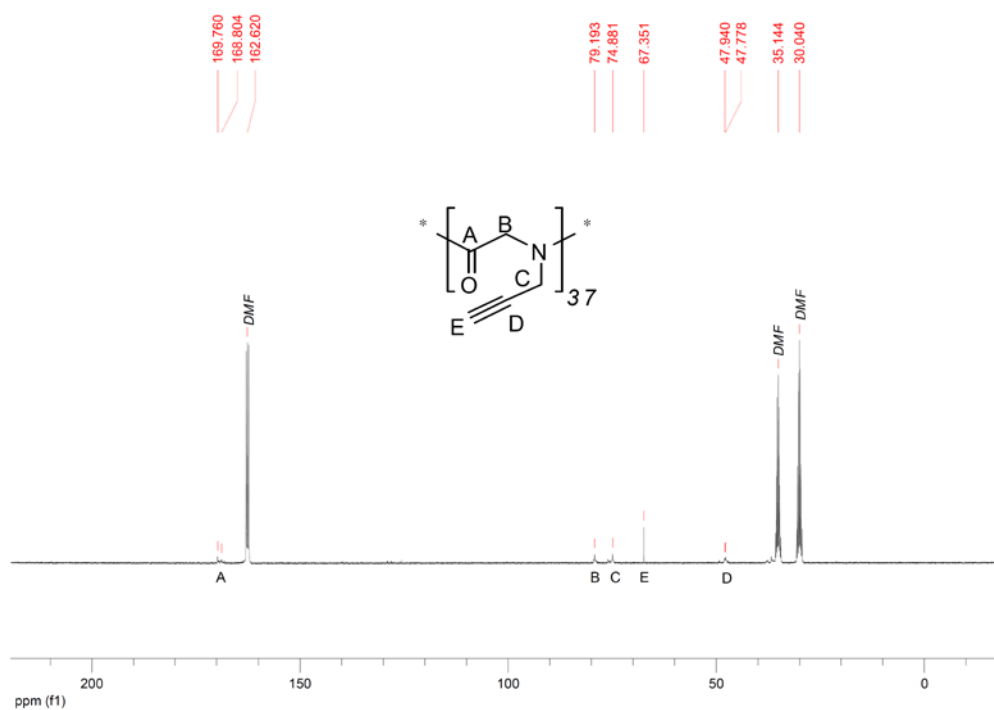


A34. DSC 1st heating curve of solution annealed (ca. 4.8 g/L) 10k (BP25.50) neat (20 K/min).

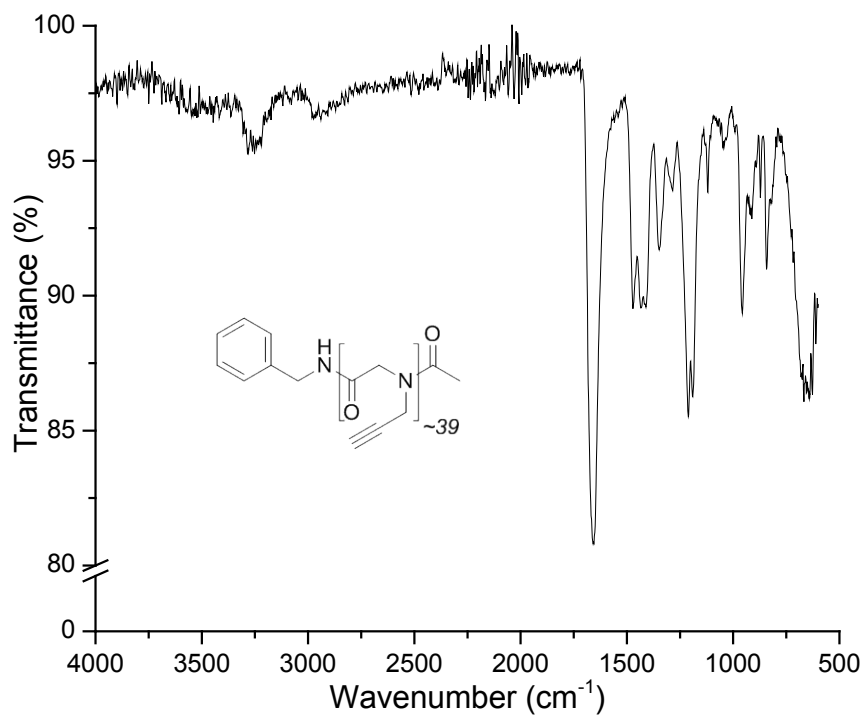
Appendix: Supporting Spectra



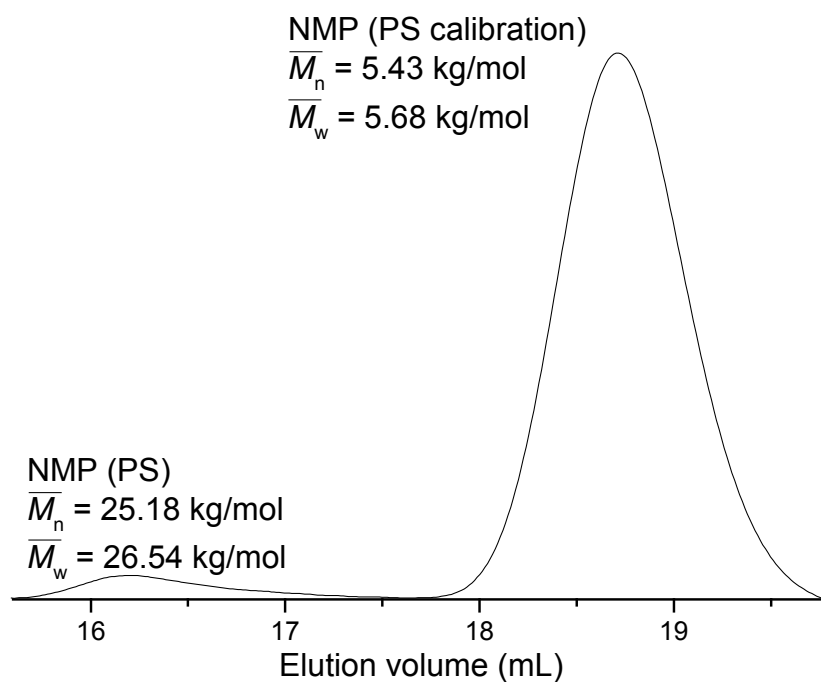
A35. ¹H-NMR spectrum of 101 (BP35.50) in DMF-d₇.



A36. ¹³C-NMR spectrum of 101 (BP35.50) in DMF-d₇.

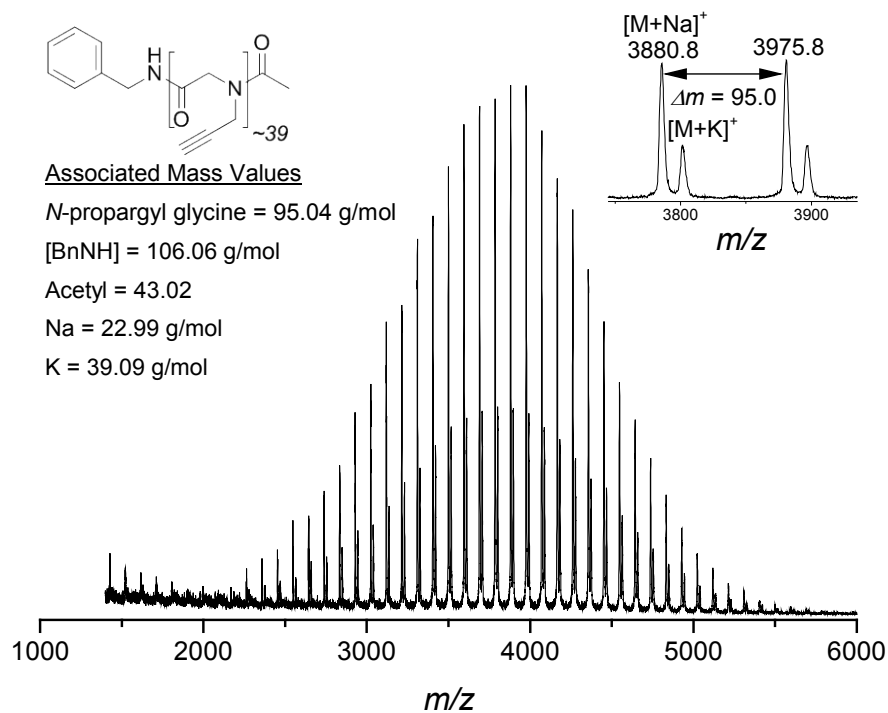


A37. FT-IR spectrum of 10l (BP35.50) neat.

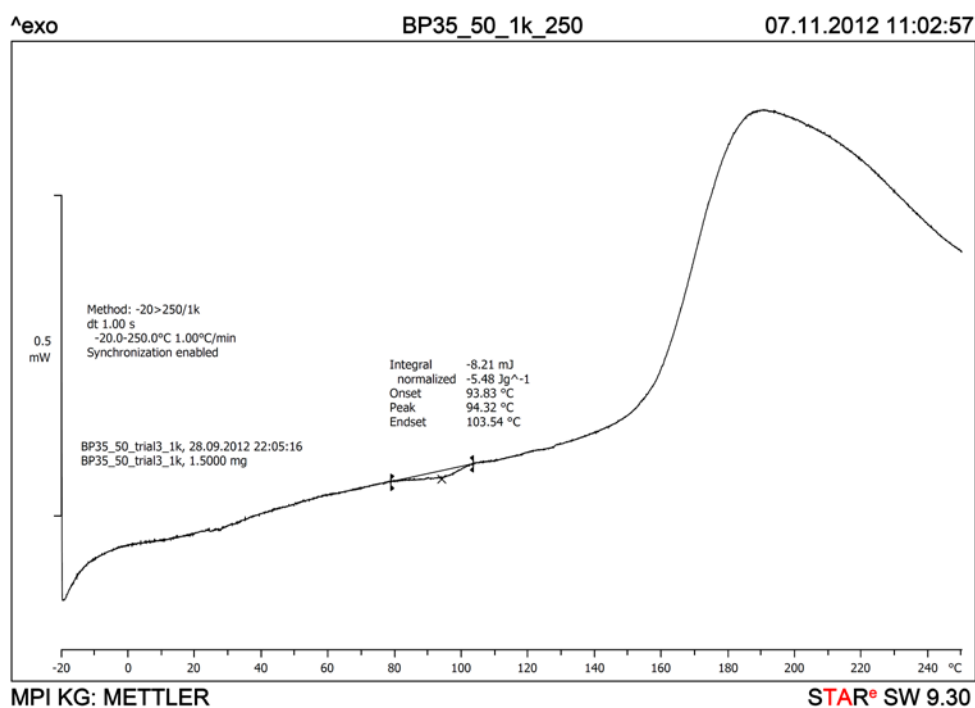


A38. SEC elugram (NMP, RI) of 10l (BP35.50) prepared in DMF.

Appendix: Supporting Spectra

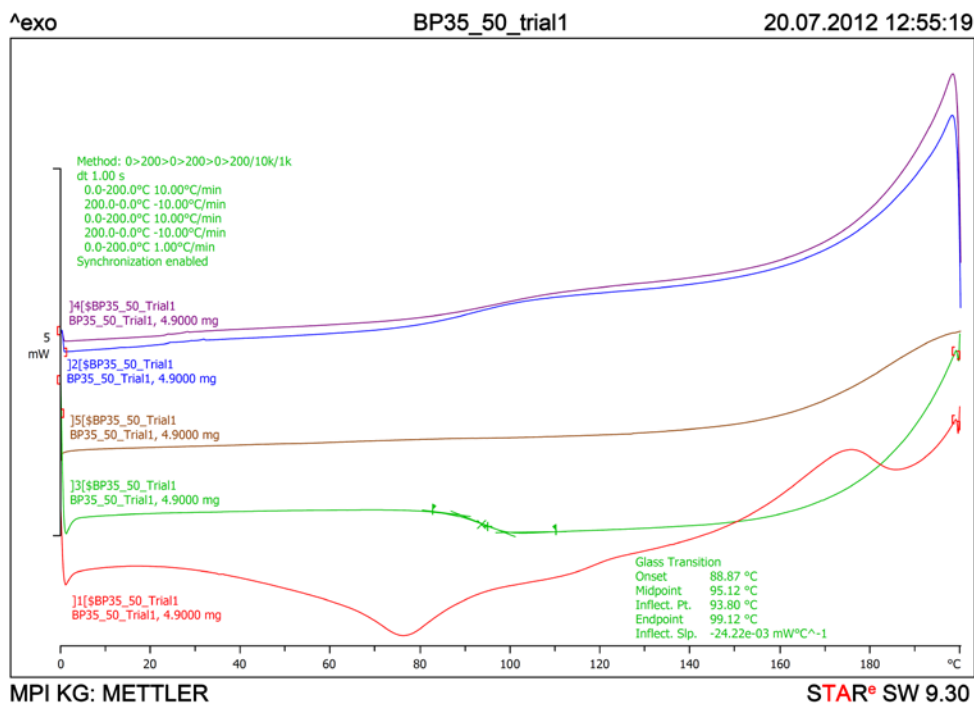


A39. MALDI-ToF MS (linear mode, dithranol and sodium acetate) of 10l (BP35.50).

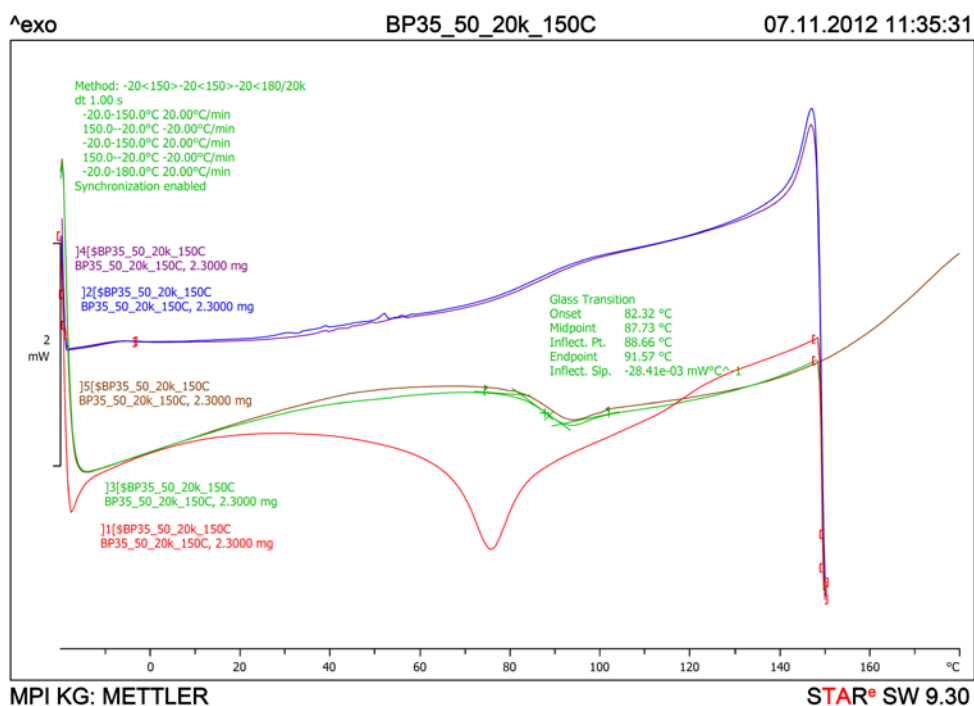


A40. DSC 1st heating curve of raw 10l (BP35.50) neat (1 K/min).

Appendix: Supporting Spectra

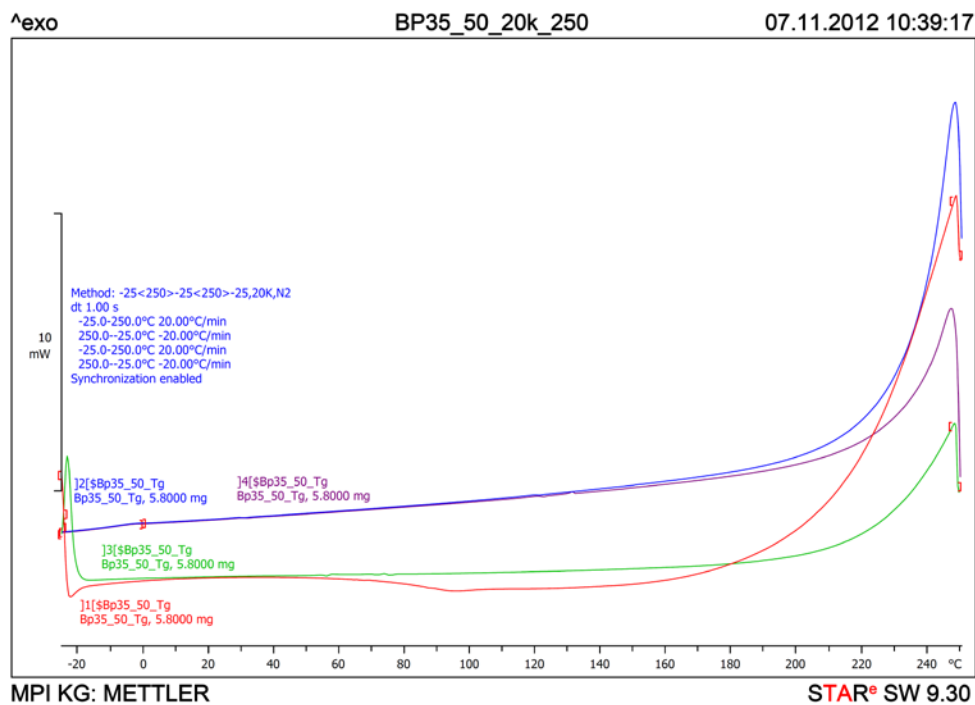


A41. DSC heating/cooling curves of raw 101 (BP35.50) neat (10 K/min).

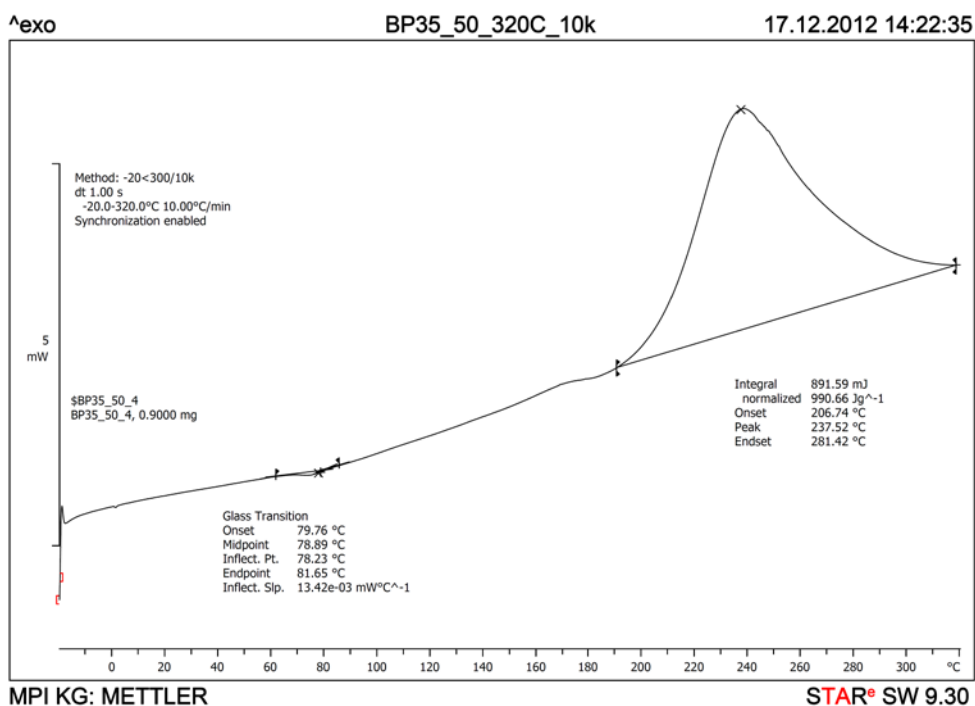


A42. DSC heating/cooling curves of raw 101 (BP35.50) neat (20 K/min).

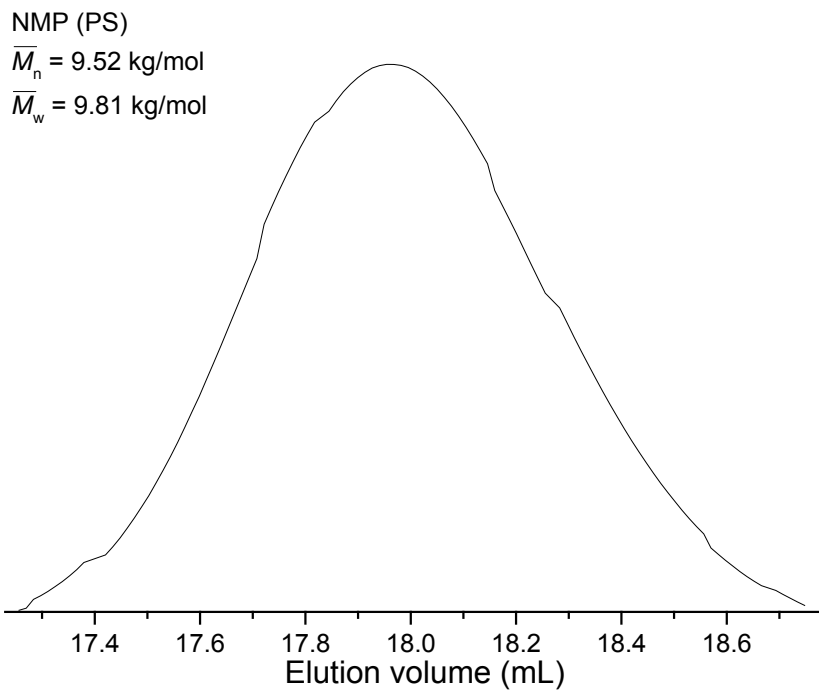
Appendix: Supporting Spectra



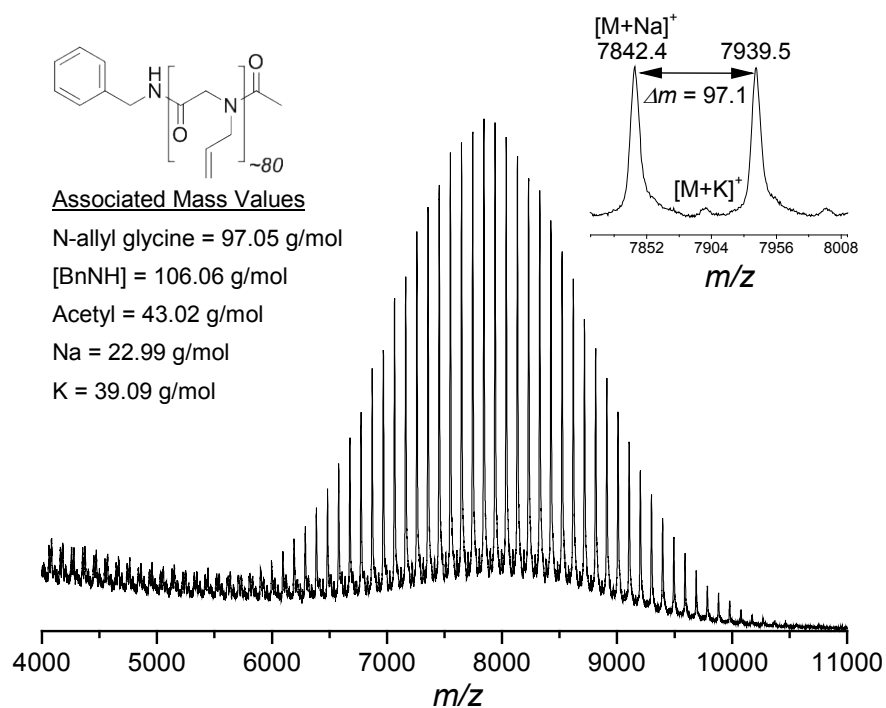
A43. DSC heating/cooling curves of raw 101 (BP35.50) neat (20 K/min up to 250 °C).



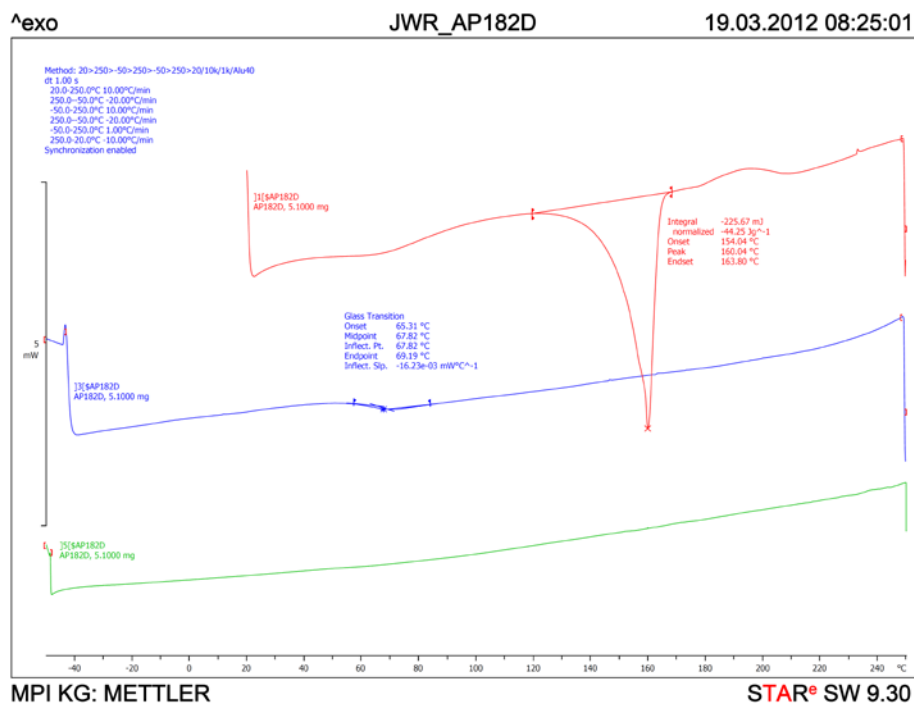
A44. DSC heating/cooling curves of raw 101 (BP35.50) neat (10 K/min up to 320 °C).



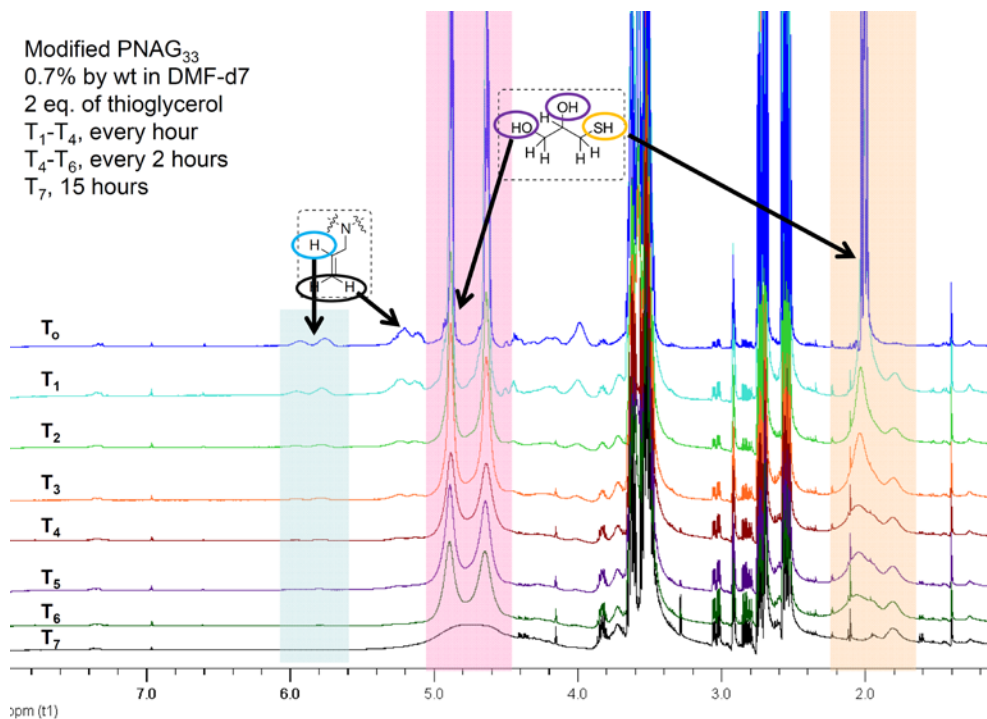
A45. SEC elugram (NMP, RI) of 10k (AP182D) prepared in DMF.



A46. MALDI-ToF MS (linear mode, DCTB and sodium acetate) of 10k (AP182D).

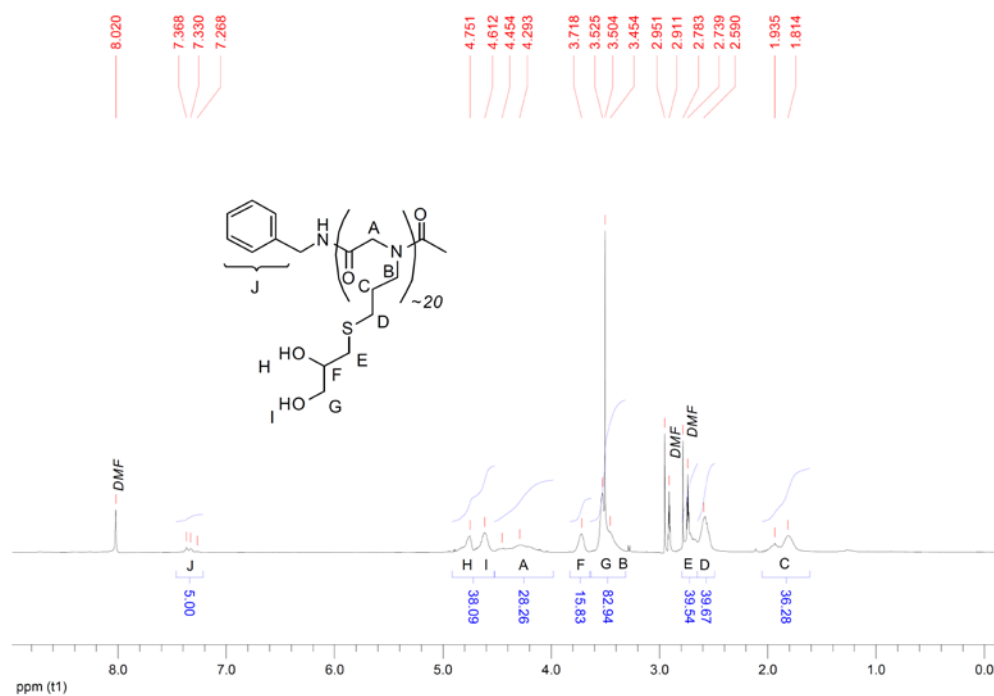


A47. DSC heating curves of raw 10k (AP182D) neat.

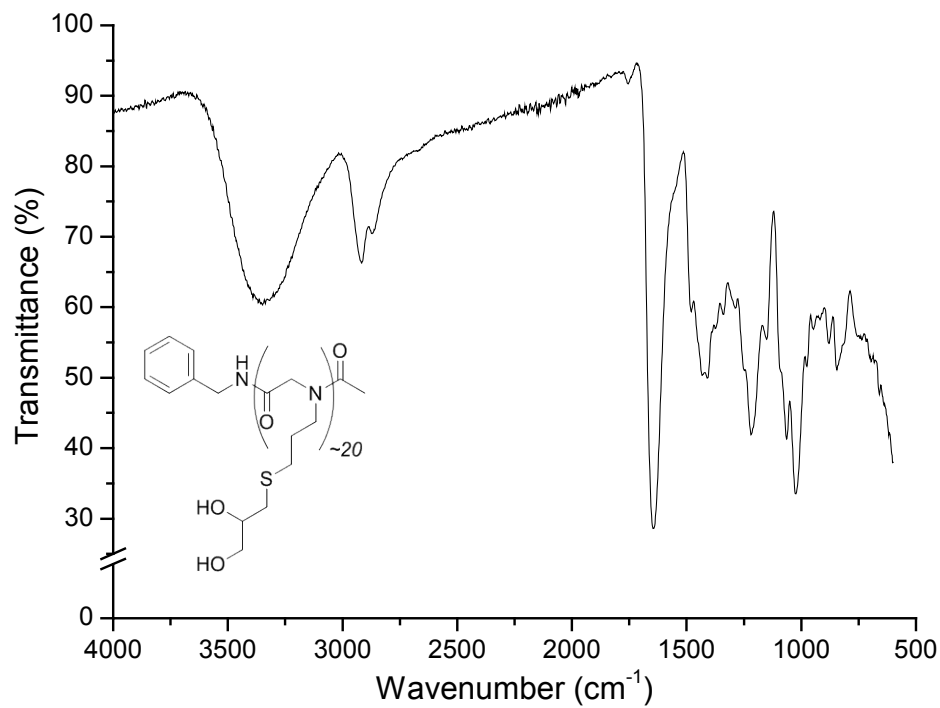


A48. ¹H-NMR model study towards quantitative post-modification of 10k (AP144) in DMF-d₇ (AP150.2).

Appendix: Supporting Spectra



A49. ¹H NMR spectrum of post-modified 10k (AP182A) with thio-glycerol in DMF-d₇ (AP183A).



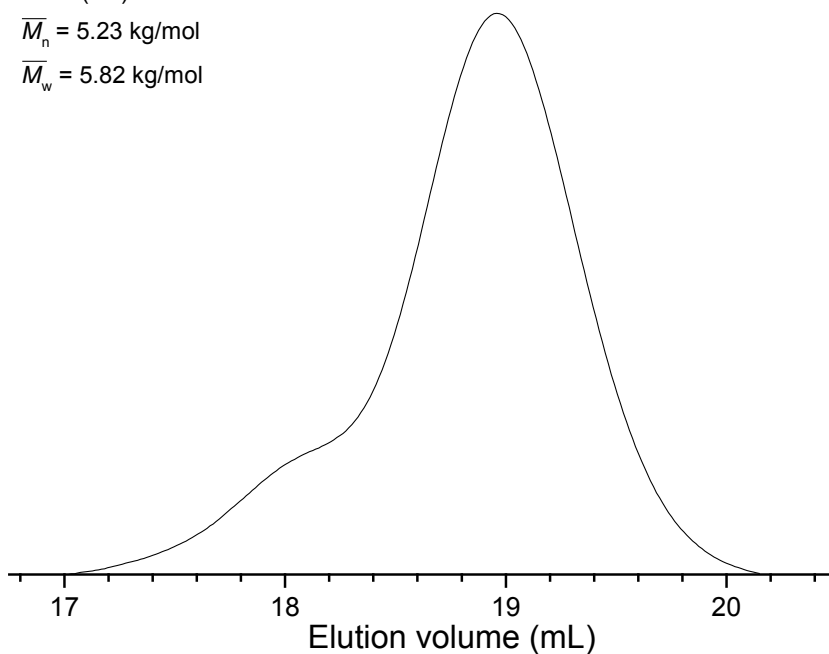
A50. FT-IR spectrum of post-modified 10k (AP182A) with thio-glycerol neat (AP183A).

Appendix: Supporting Spectra

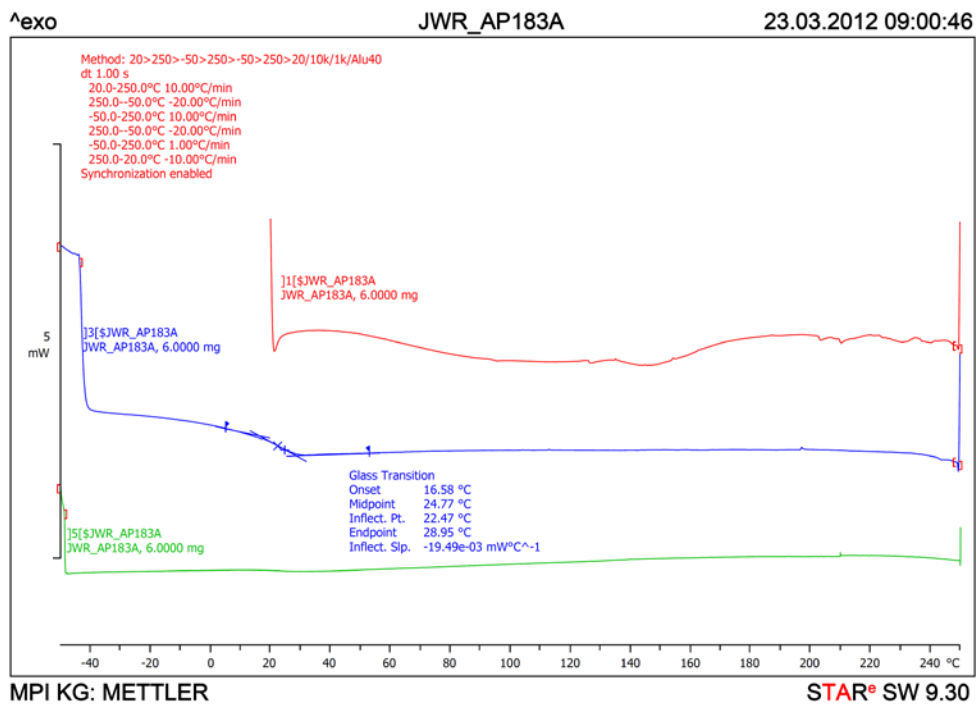
NMP (PS)

$\overline{M}_n = 5.23 \text{ kg/mol}$

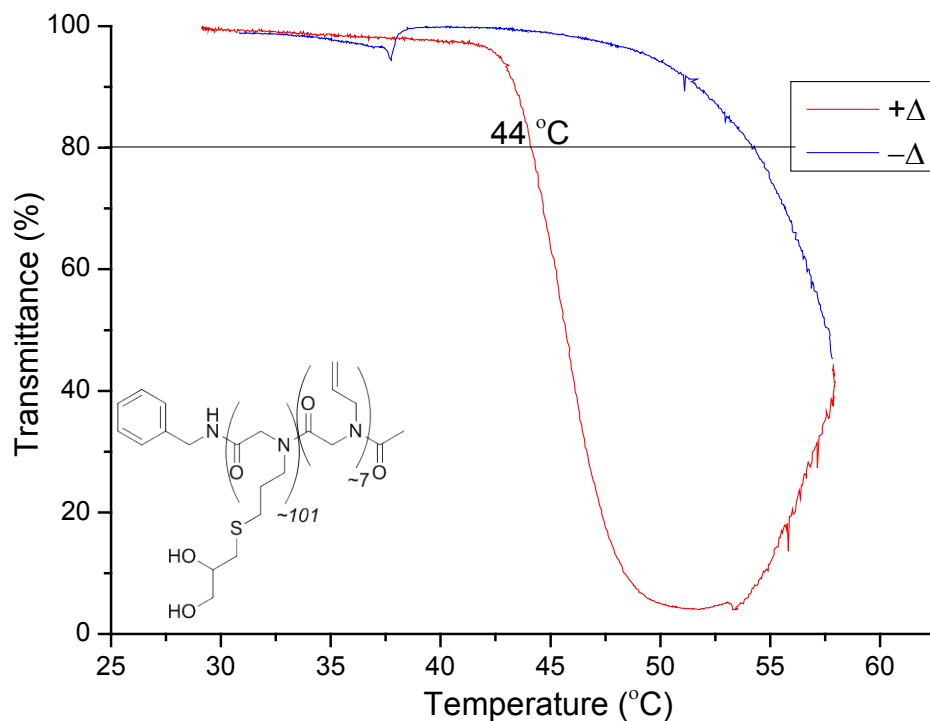
$\overline{M}_w = 5.82 \text{ kg/mol}$



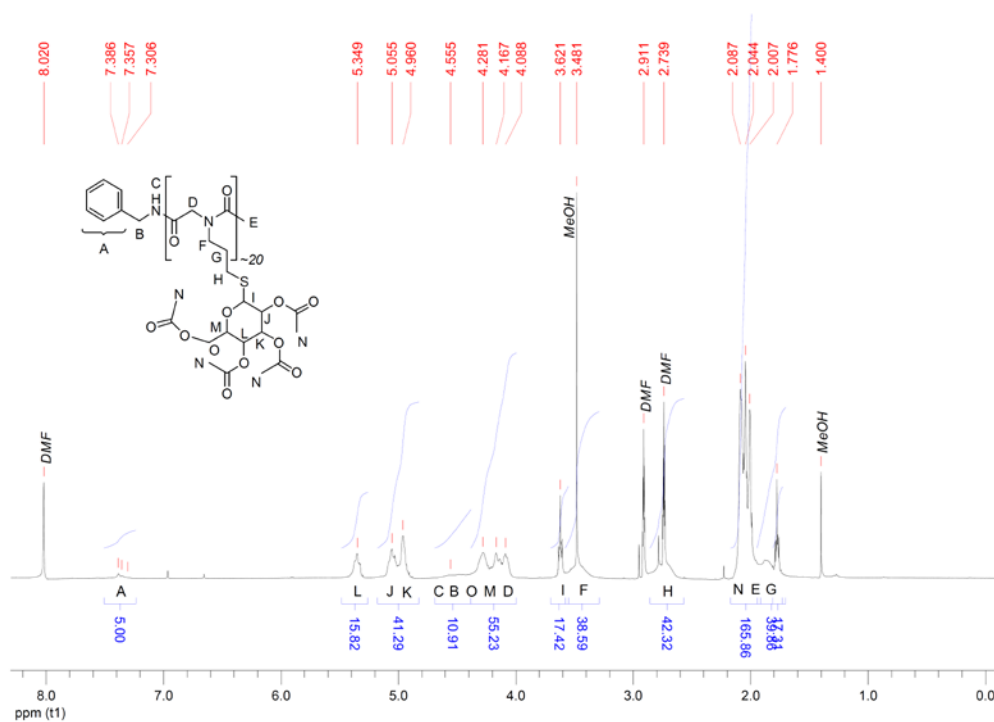
A51. SEC elugram (NMP, RI) of post-modified 10k (*API182A*) with thio-glycerol prepared in DMF (*API183A*).



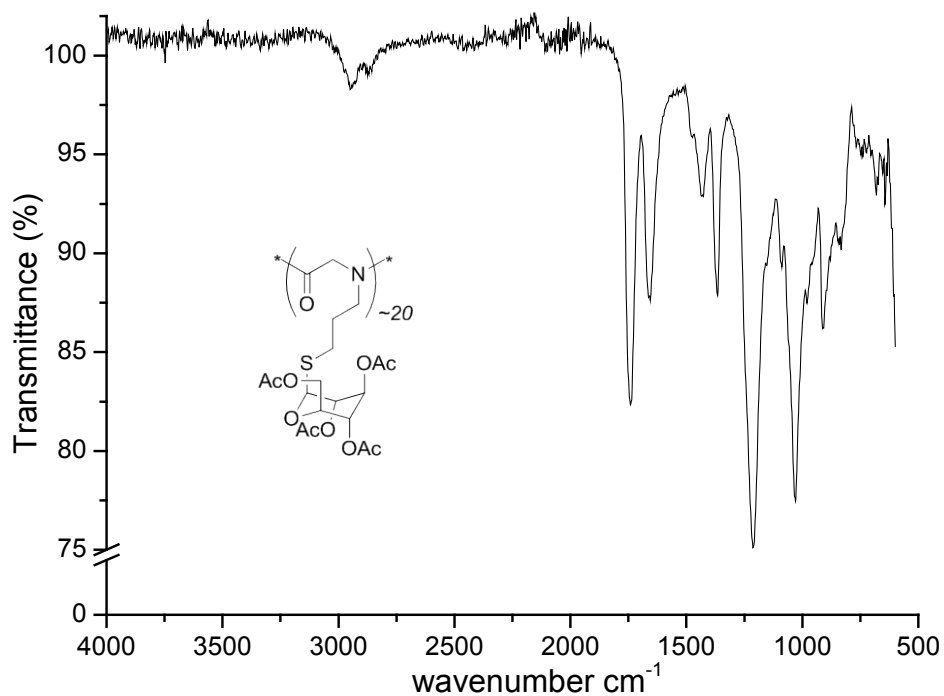
A52. DSC heating curves of post-modified 10k (*API182A*) with thio-glycerol neat (10 K/min) (*API183A*).



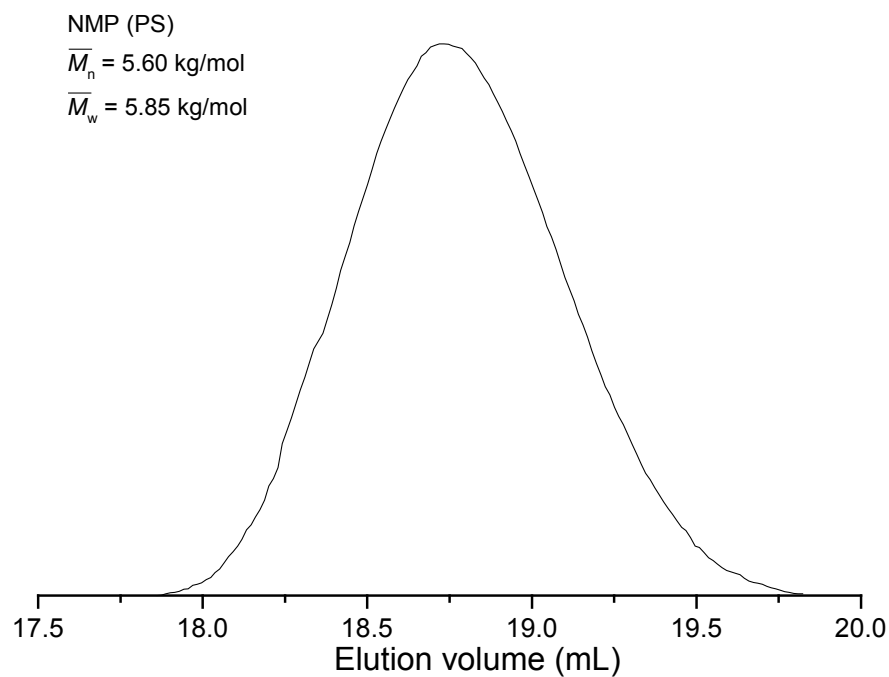
A53. Turbidity curves (1 g/L) of post-modified 10k (AP167C) with thio-glycerol (94%) (AP180).



A54. ¹H-NMR spectrum of post-modified 10k (AP182A) with HS-GlcAc₄ in DMF-d₇ (AP183B).

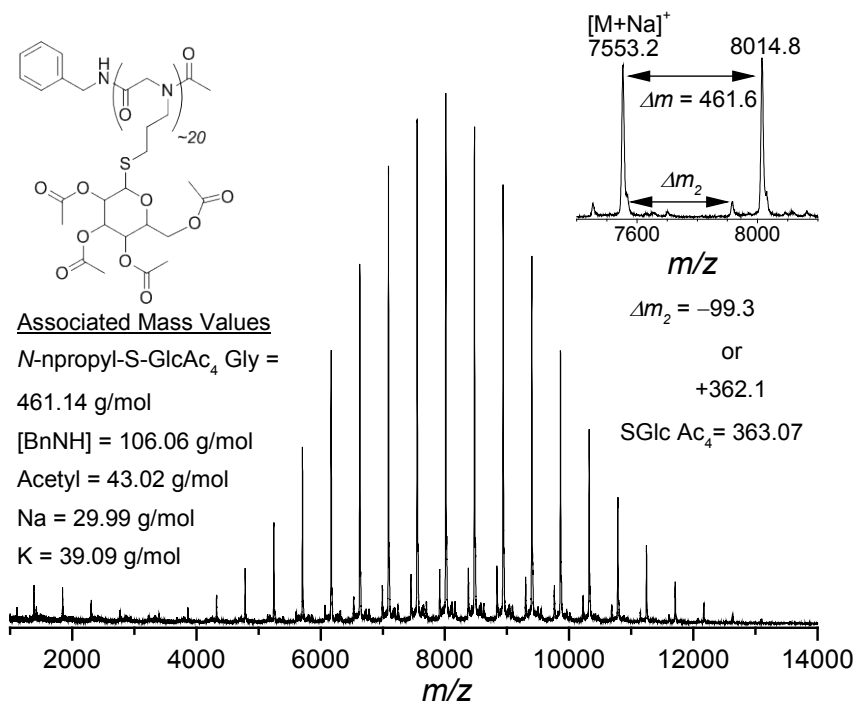


A55. FT-IR spectrum of post-modified 10k (AP182A) with HS-GlcAc neat (AP183B).

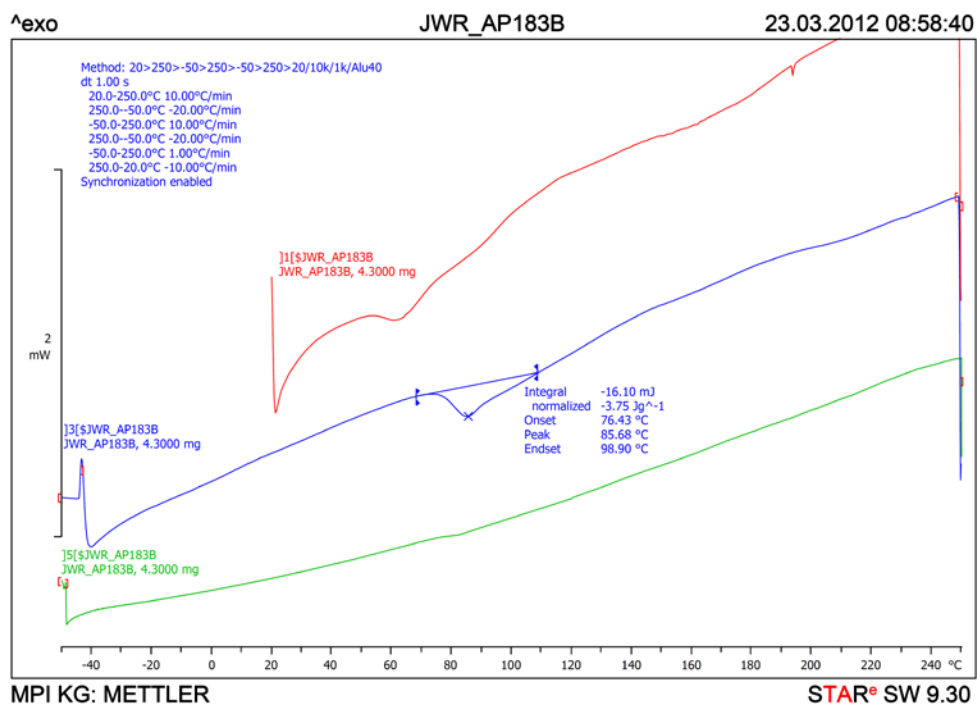


A56. SEC elugram (NMP, RI) of post-modified 10k (AP182A) with HS-GlcAc prepared in DMF (AP183B).

Appendix: Supporting Spectra

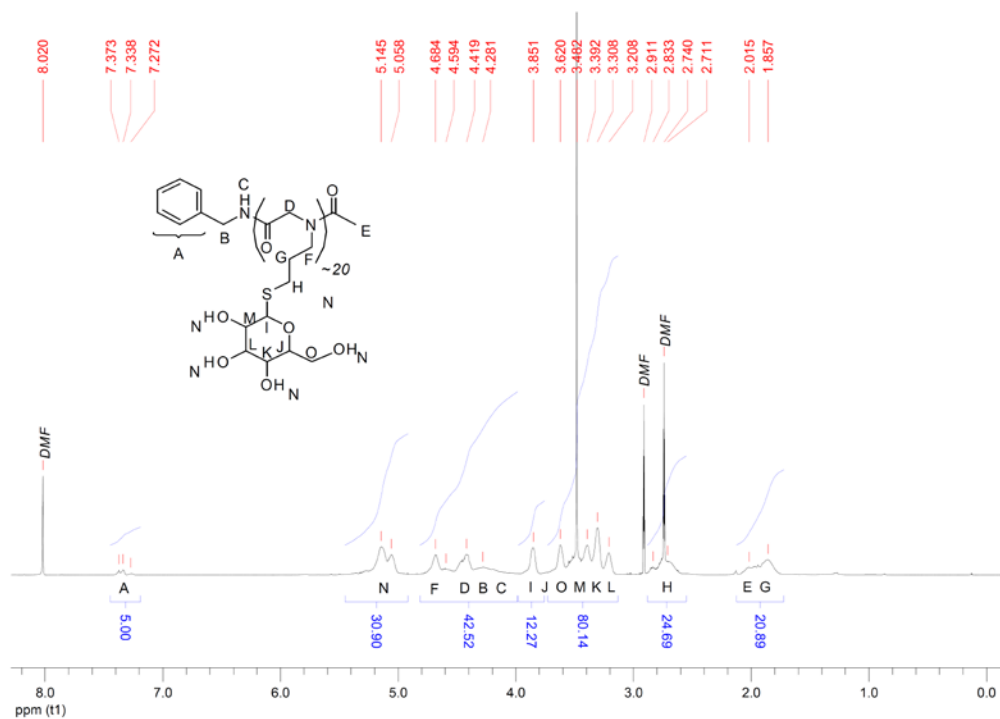


A57. MALDI-ToF MS (linear mode, DCTB/Na) of post-modified 10k (*AP182A*) with HS-GlcAc₄ (*AP183B*).

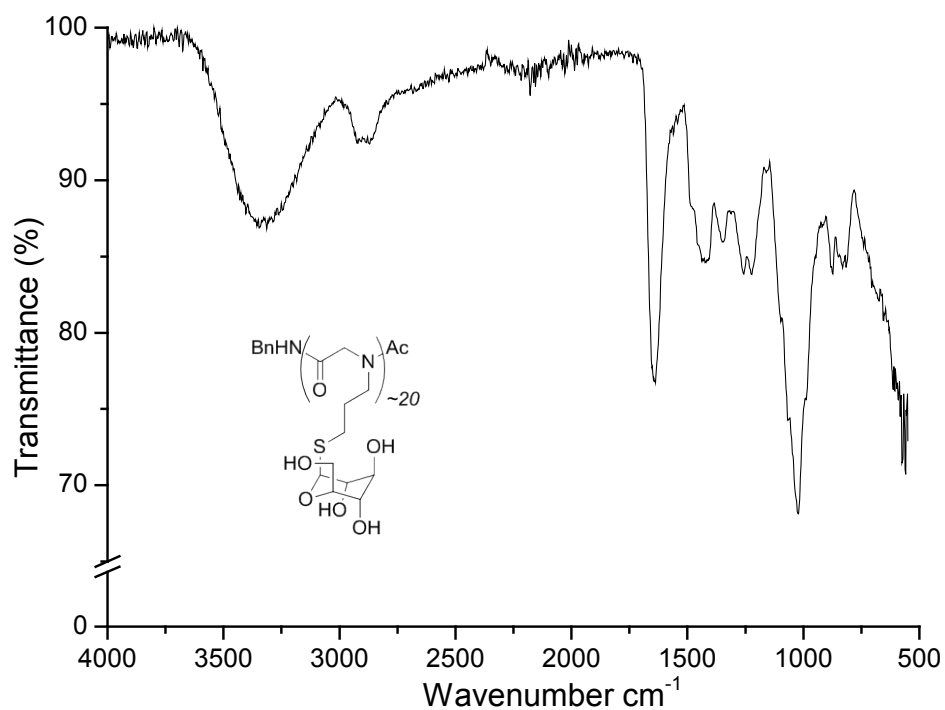


A58. DSC heating curves of post-modified 10k (*AP182A*) with HS-GlcAc₄ (10 K/min) (*AP183B*).

Appendix: Supporting Spectra

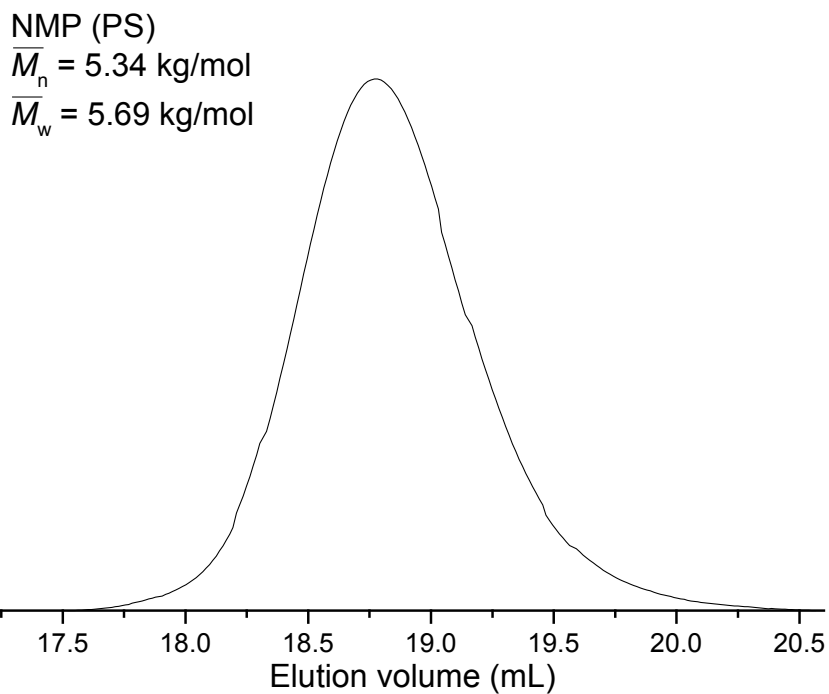


A59. ¹H-NMR spectrum of post-modified 10k (AP182A) with HS-Glc in DMF-d₇ (AP184A).

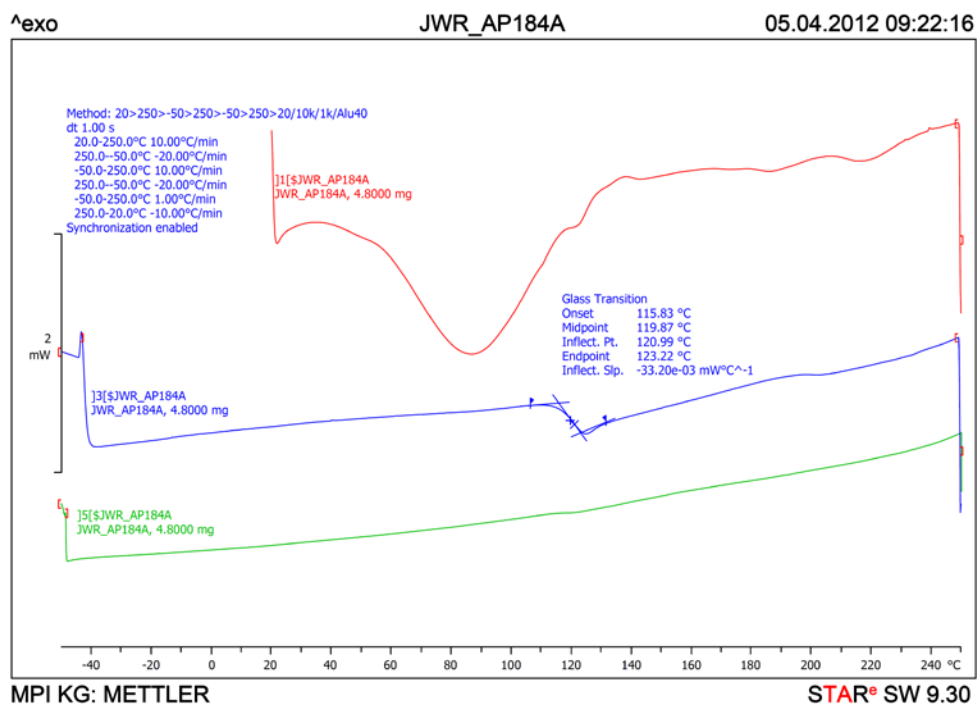


A60. FT-IR spectrum of post-modified 10k (AP182A) with HS-Glc neat (AP184A).

Appendix: Supporting Spectra

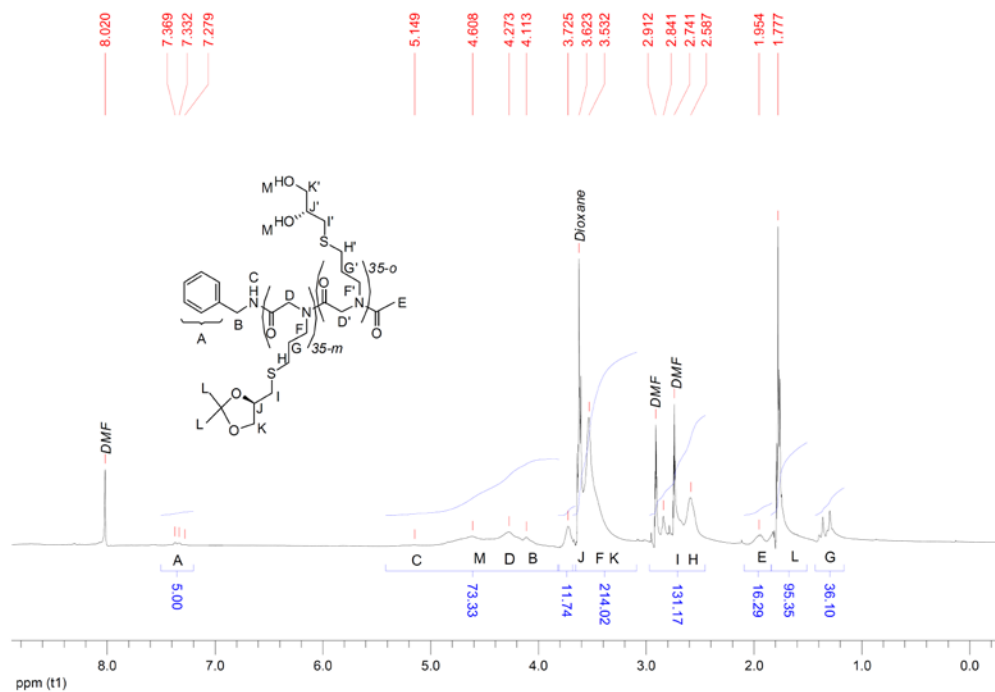


A61. SEC elugram (NMP, RI) of post-modified 10k (*AP182A*) with **HS-Glc** prepared in DMF (*AP184A*).

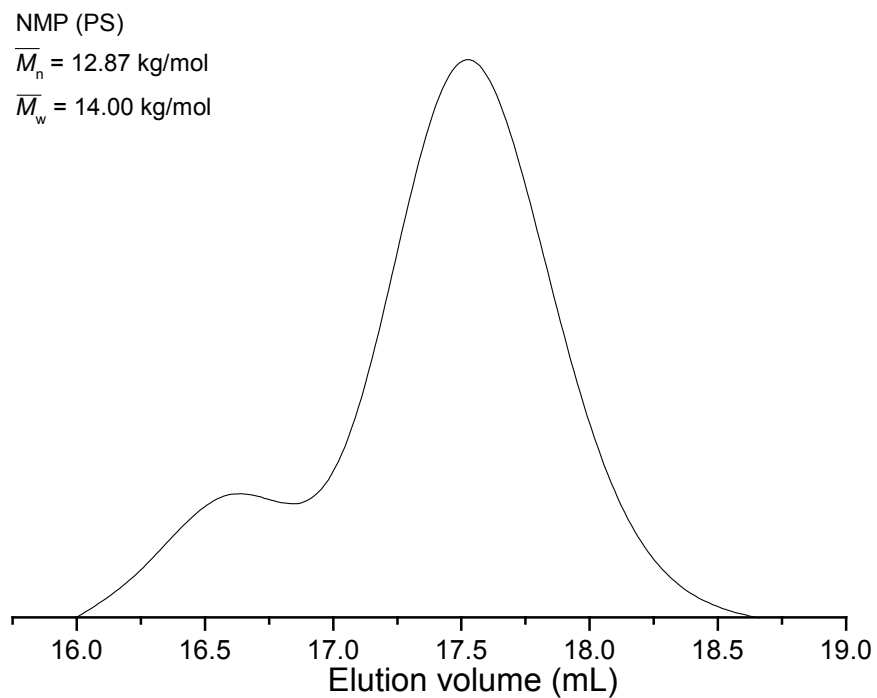


A62. DSC heating curves of post-modified 10k (*AP182A*) with **HS-Glc** neat (*AP184A*).

Appendix: Supporting Spectra

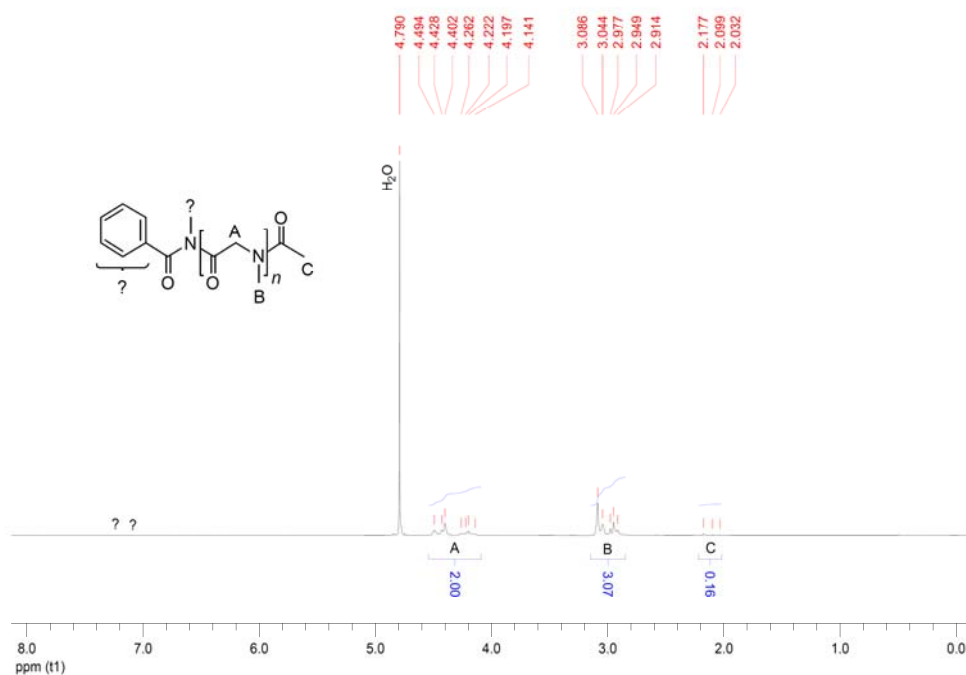


A63. ¹H-NMR spectrum of post-modified 10k (*BP25.50*) with **2R-thiol-glycerol(ketal)** in DMF-d₆ (**BP79.50**).



A64. SEC elugram (NMP, RI) of post-modified 10k (*BP25.50*) with **2R-thiol-glycerol(ketal)** prepared in DMF (**BP79.50**).

Appendix: Supporting Spectra

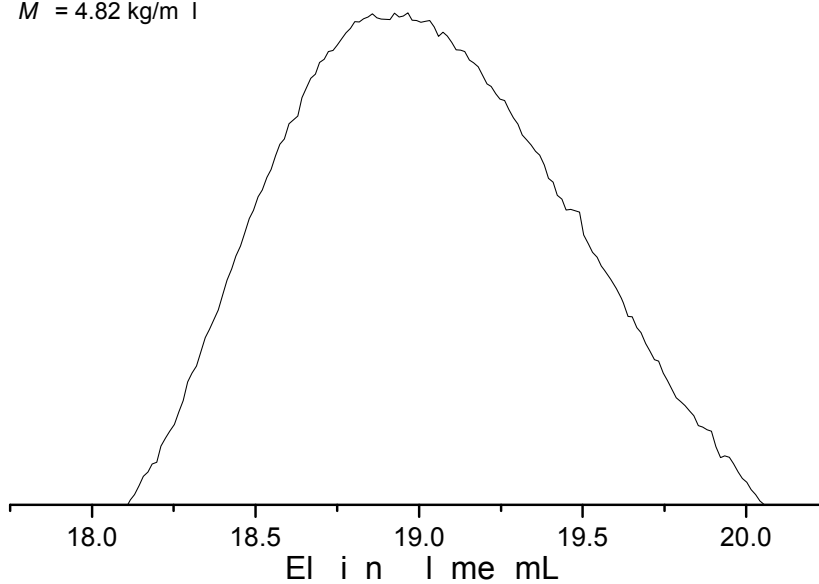


A65. ¹H-NMR spectrum of AP91 (PNMG) in D₂O.

NMP PS

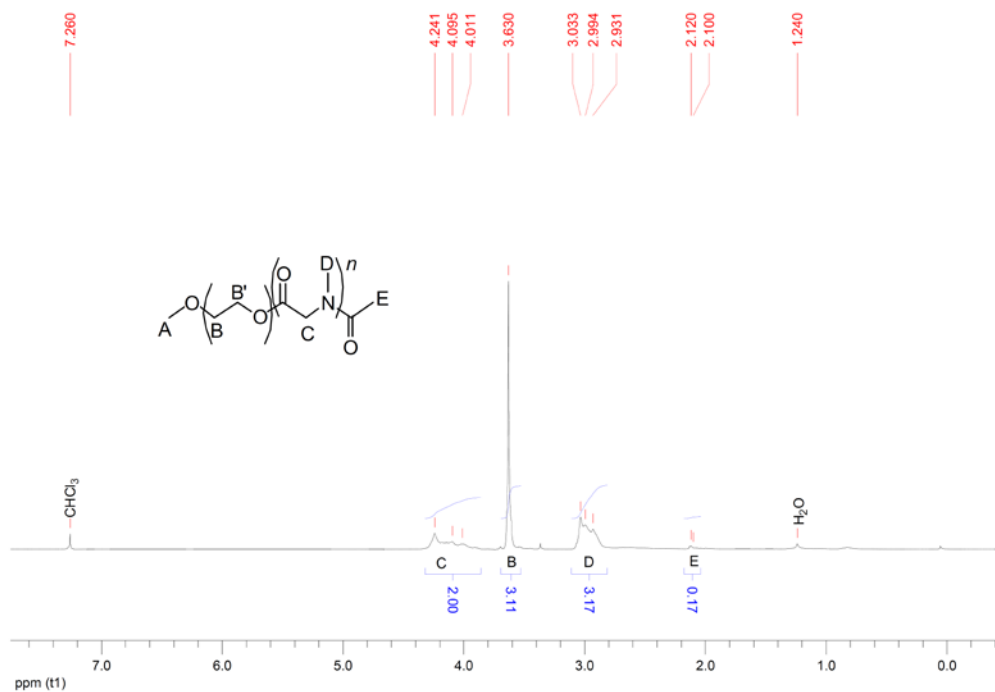
$\bar{M}_n = 4.02 \text{ kg/m l}$

$\bar{M} = 4.82 \text{ kg/m l}$



A66. SEC elugram (NMP, RI) of AP91 (PNMG).

Appendix: Supporting Spectra

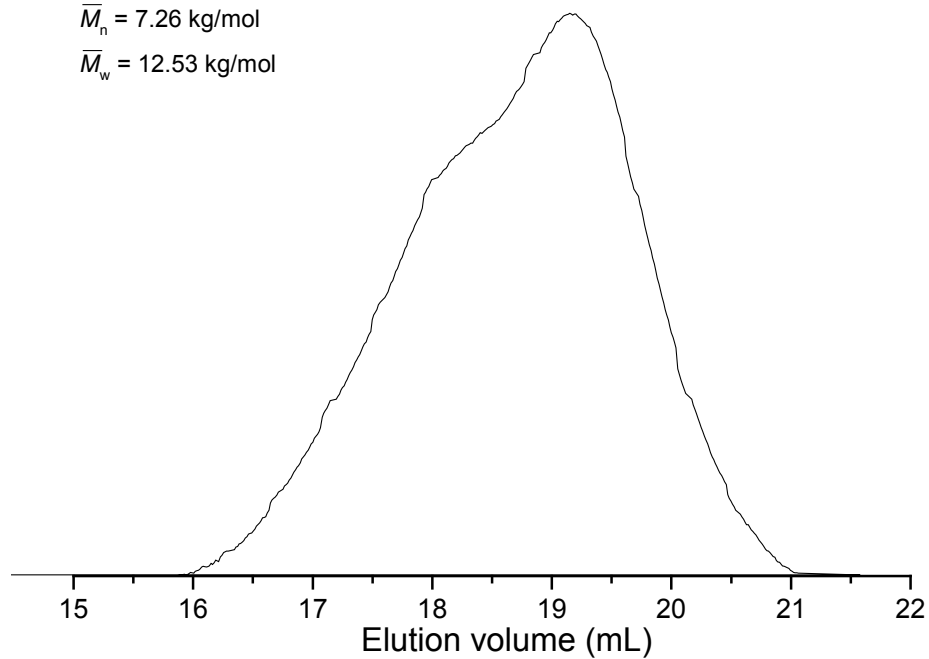


A67. ¹H-NMR spectrum of AP128 (PEO-b-PNMG) in CDCl₃.

NMP (PS)

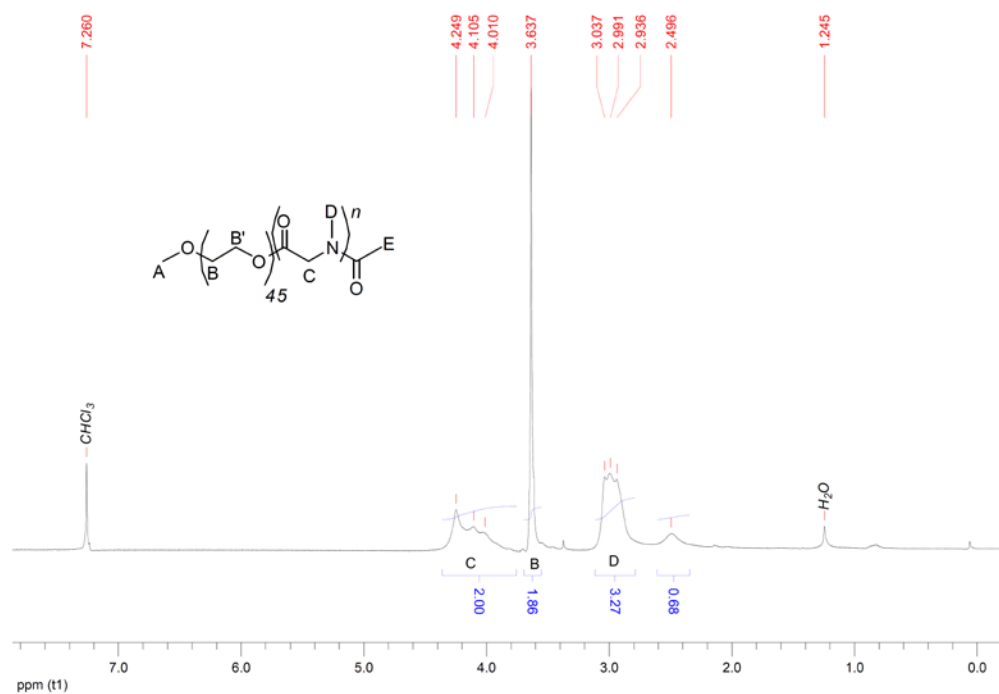
$\bar{M}_n = 7.26$ kg/mol

$\bar{M}_w = 12.53$ kg/mol

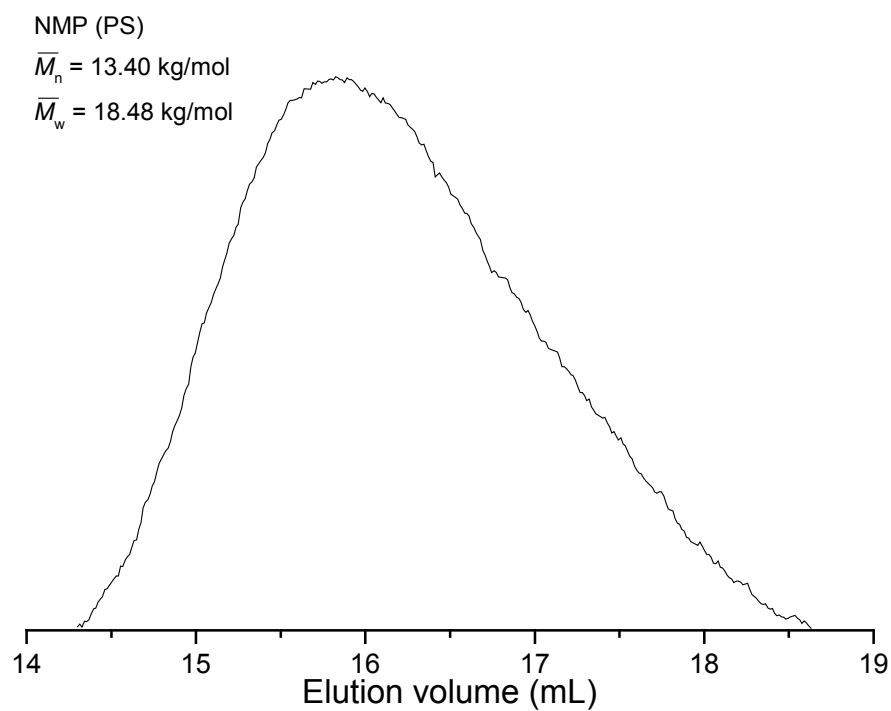


A68. SEC elugram (NMP, RI) of AP128 (PEO-b-PNMG).

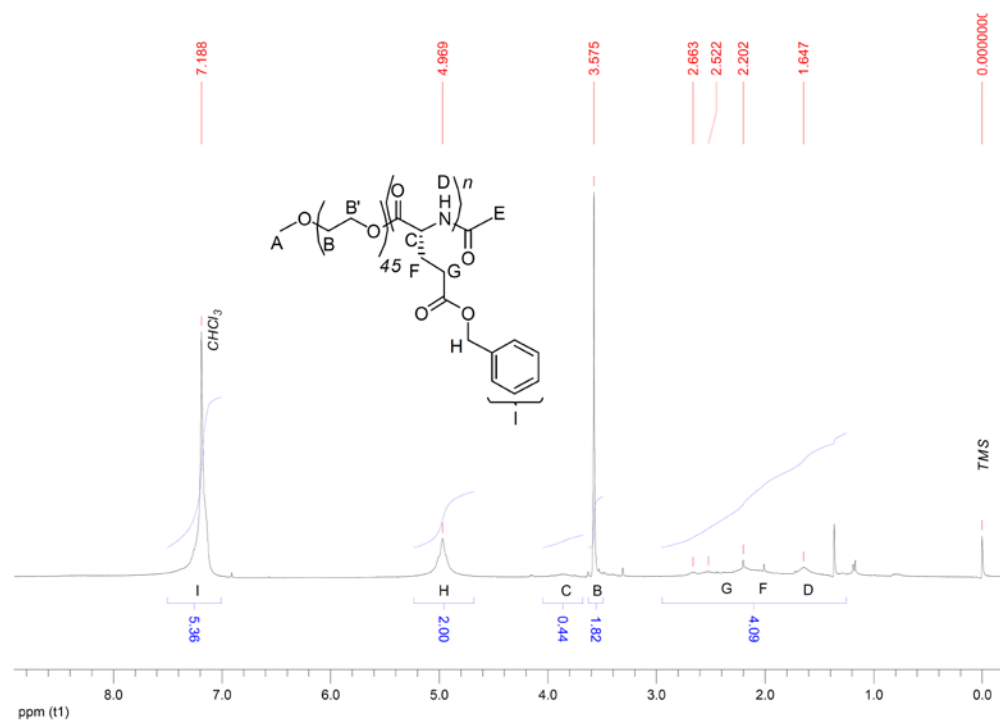
Appendix: Supporting Spectra



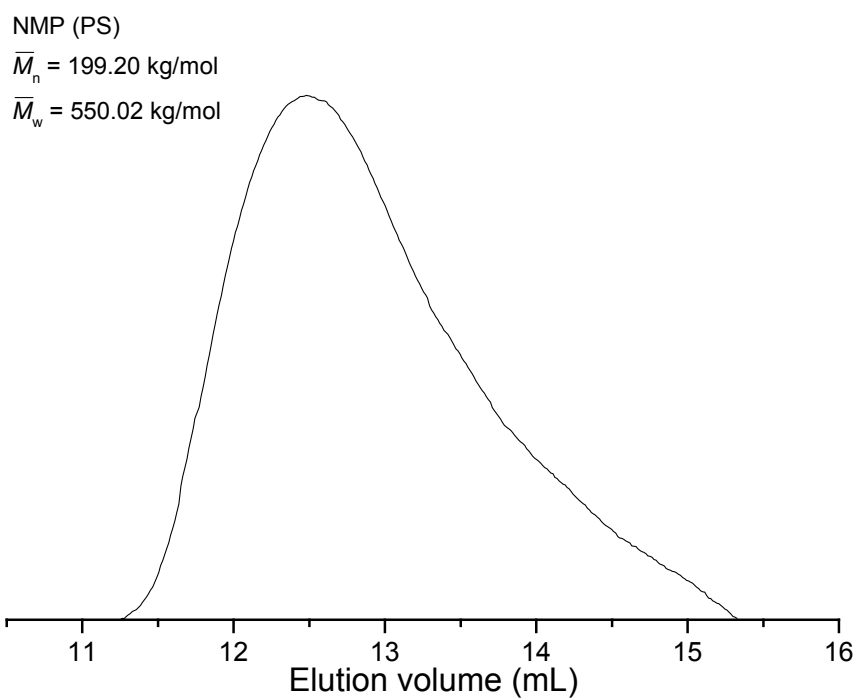
A69. $^1\text{H-NMR}$ spectrum of AP124 (PEO-b-PNMG; control B) in CDCl_3 .



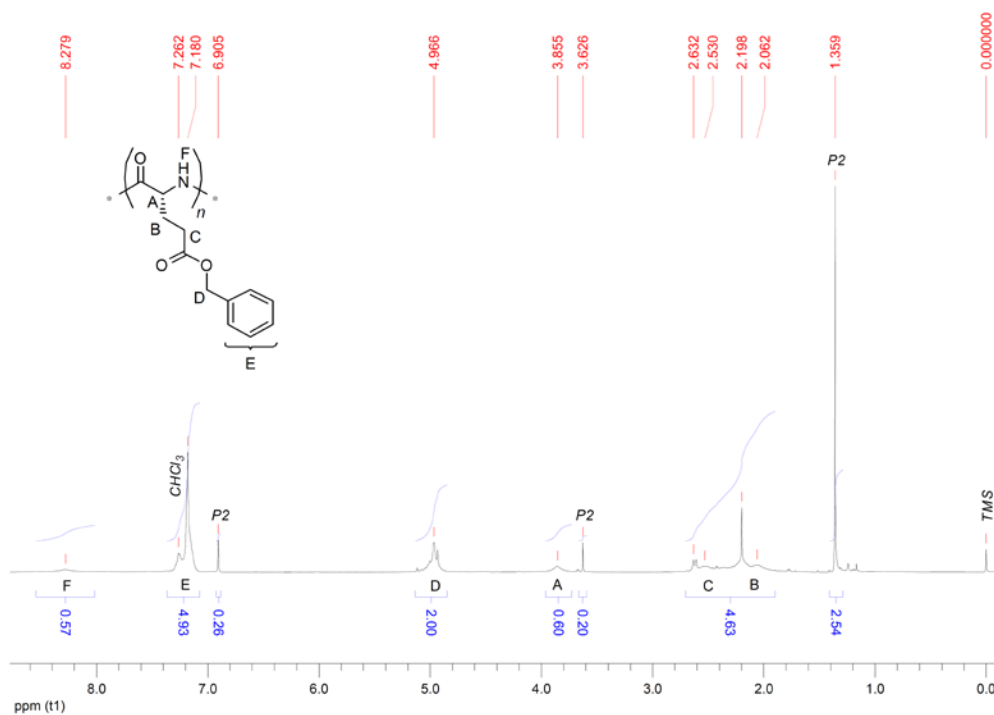
A70. SEC elugram (NMP, RI) of AP124 (PEO-b-PNMG; control B).



A71. ¹H-NMR spectrum of AP132 (PEO-b-PGlu) in CDCl₃.



A72. SEC elugram (NMP, RI) of AP132 (PEO-b-PGlu).

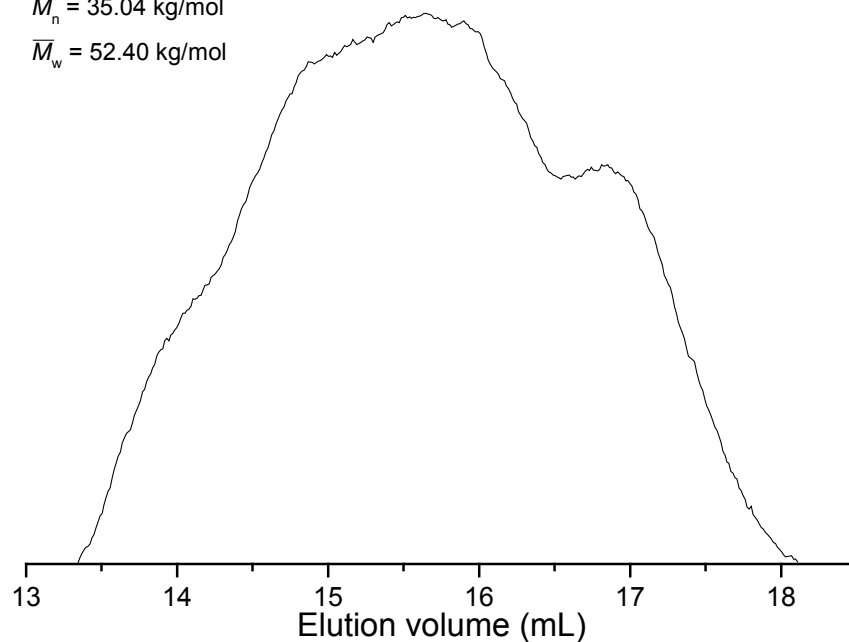


A73. 1H -NMR spectrum of AP133 (PGlu; control A) in $CDCl_3$.

NMP (PS)

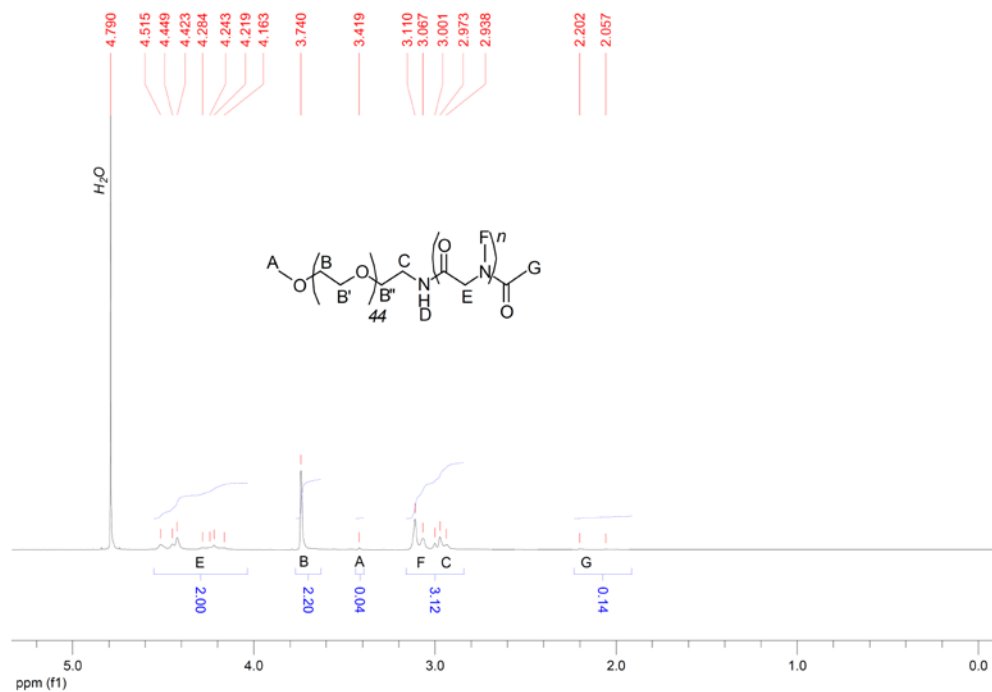
$\bar{M}_n = 35.04$ kg/mol

$\bar{M}_w = 52.40$ kg/mol



A74. SEC elugram (NMP, RI) of AP133 (PGlu; control A) prepared in THF.

Appendix: Supporting Spectra

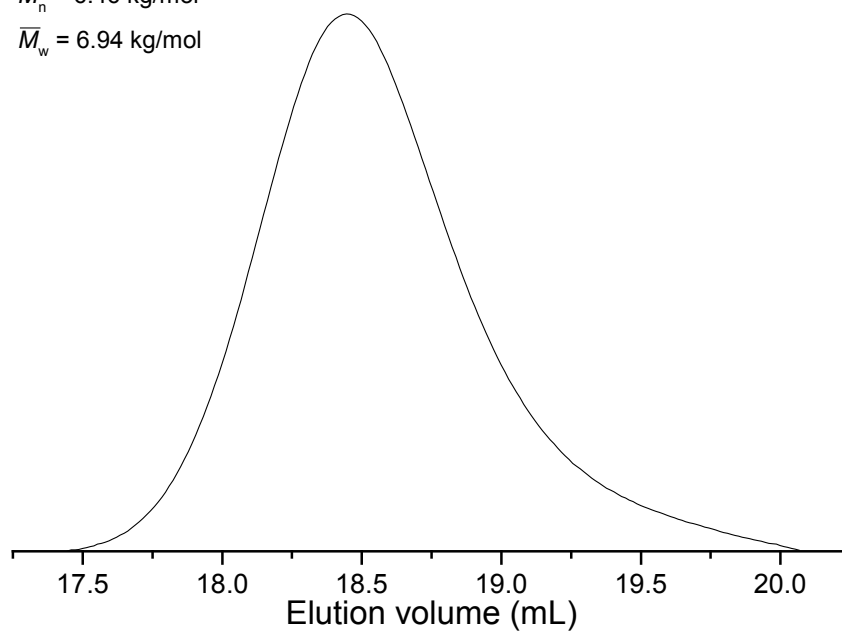


A75. ¹H-NMR spectrum of AP140 (PEONH-b-PNMG) in D₂O.

NMP (PS)

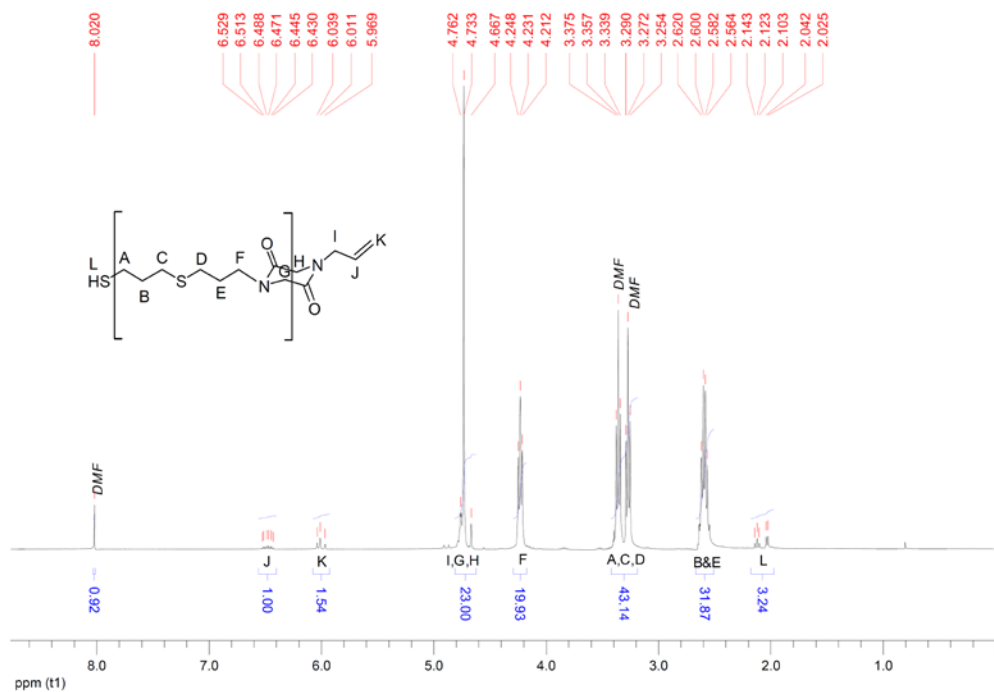
$\bar{M}_n = 6.46$ kg/mol

$\bar{M}_w = 6.94$ kg/mol

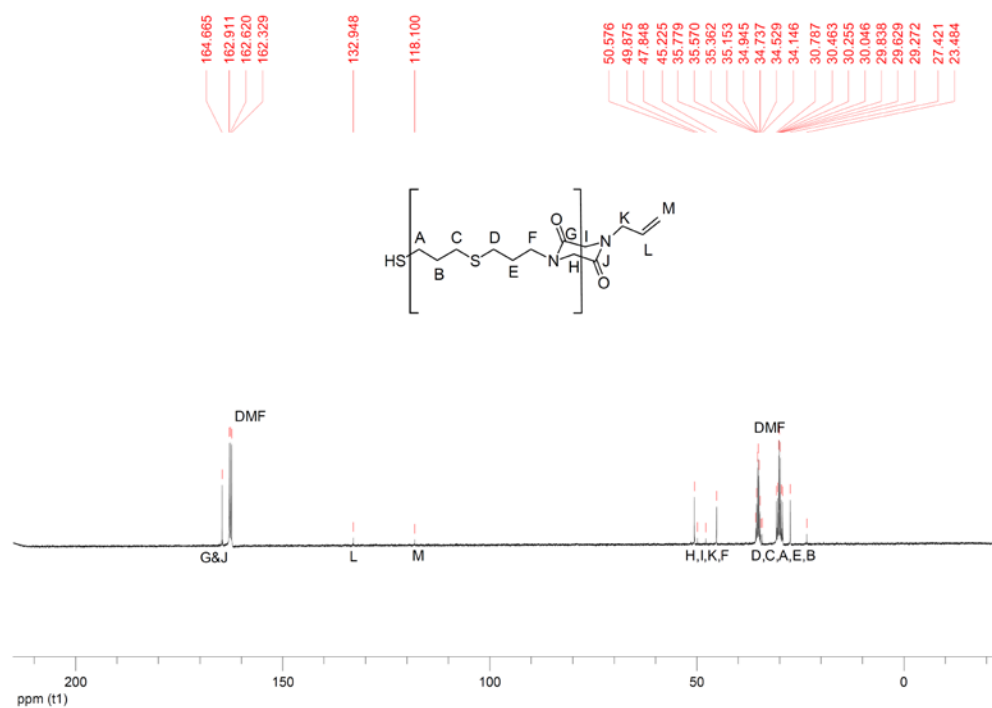


A76. SEC elugram (NMP, RI) of AP140 (PEONH-b-PNMG).

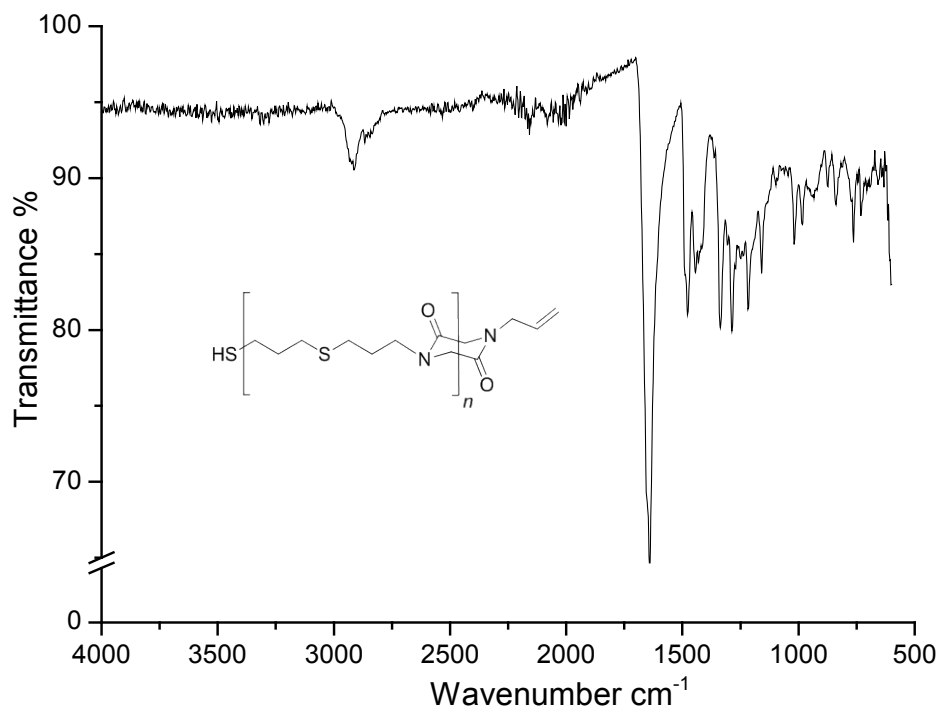
Appendix: Supporting Spectra



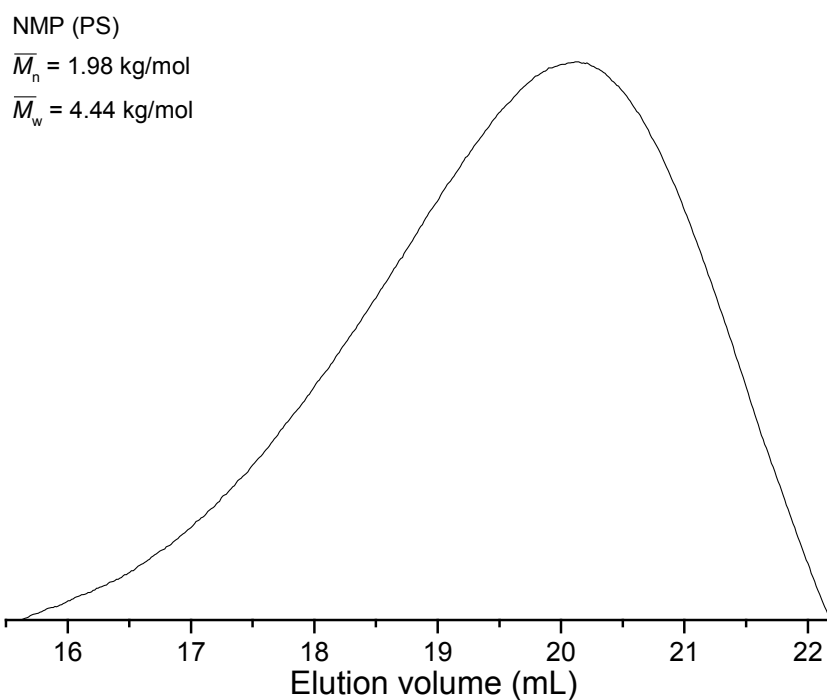
A77. $^1\text{H-NMR}$ spectrum of PDKP in DMF-d_7 .



A78. $^{13}\text{C-NMR}$ spectrum of PDKP in DMF-d_7 .

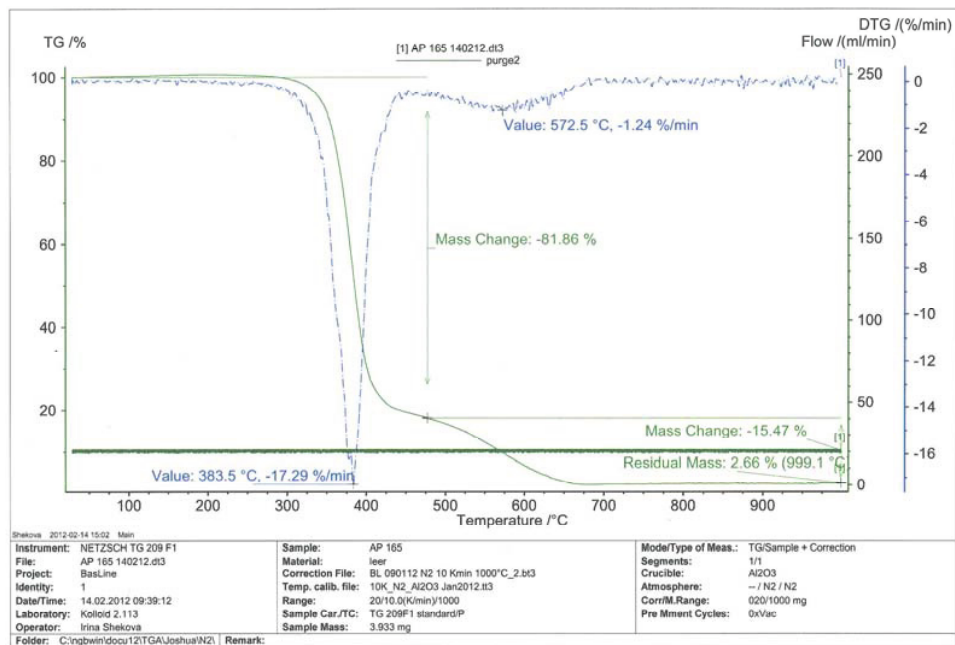


A79. FT-IR spectrum of **PDKP** neat.

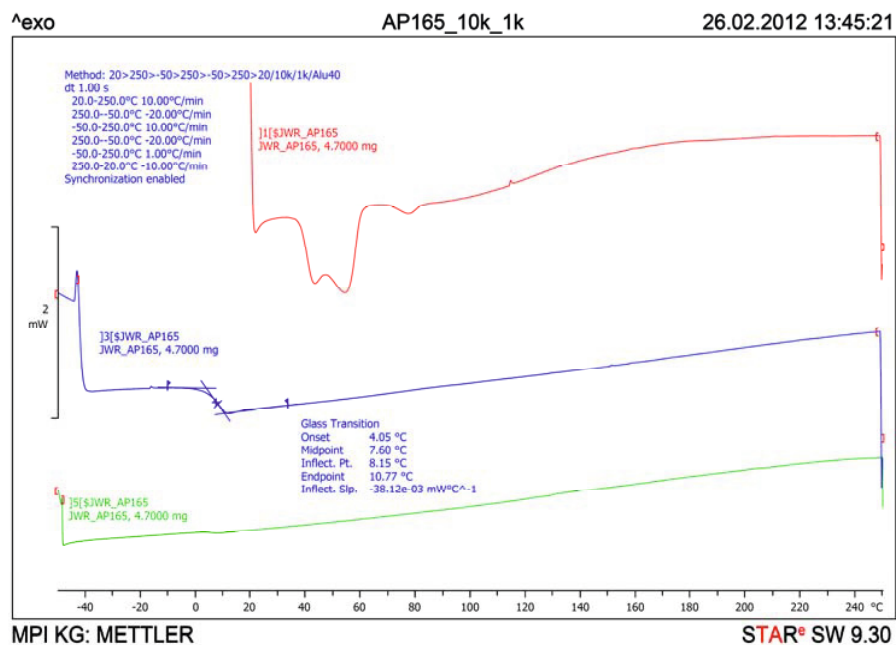


A80. SEC elugram (NMP, RI) of **PDKP** prepared in heated DMF.

Appendix: Supporting Spectra



A81. TGA thermogram of **PDKP** neat (20K/min).



A82. DSC heating curves of **PDKP** neat.